

Establishing biotechnological processes within the envisaged circular bioeconomy requires holistic approaches, including integration of all stages of process development. The presented thesis illustrates the integration of strain and process engineering using the example of producing the biosurfactant rhamnolipids with recombinant *Pseudomonas putida* KT2440.

When producing biosurfactants in aerated bioreactors, excessive foaming is process-hindering. To mitigate this challenge, an *in situ* liquid-liquid extraction was established by selecting a suitable, biocompatible extraction solvent in a multi-step strategy. Unraveling interactions of integrated up- and downstream processing resulted in the definition of a joint operational window for cultivation and extraction. Thereby, a foam-free fed-batch cultivation of rhamnolipid-producing *P. putida* KT2440 with integrated *in situ* extraction was established. Subsequently, different cultivation modes have been evaluated for enhanced production, and strategies for improved phase separation have been explored.

Host engineering was approached to further enhance the solvent tolerance of *P. putida* KT2440, thereby enabling the utilization of additional extraction solvents. *P. putida* KT2440 was adapted to tolerate 1-octanol, and reconstruction of tolerant strains enabled the production of rhamnolipids in the presence of 1-octanol. Another challenge is transient oxygen limitations in industrial fermentations, which *P. putida* KT2440 masters well without losing production capacity, highlighting its outstanding suitability for industrial-scale production processes.

Previous findings were applied to define an operational window to produce rhamnolipids with recombinant *P. putida* KT2440 in a custom-designed multiphase loop reactor, integrating cultivation and an *in situ* counter-current liquid-liquid extraction. Performance indicators compared well with two-liquid phase cultivations in stirred-tank reactors, emphasizing the robustness of *P. putida* KT2440 and serving as a proof of concept for the novel reactor type.

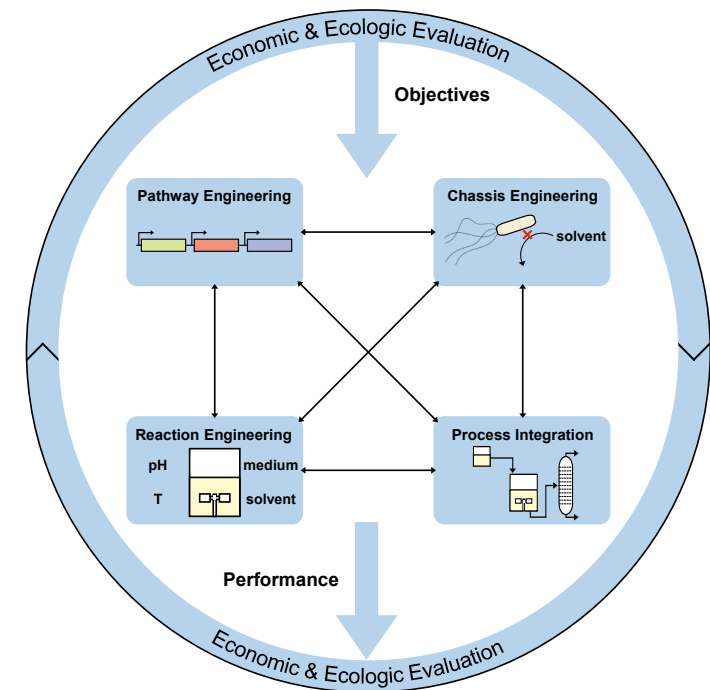
In conclusion, this thesis advocates integrated and interdisciplinary bioprocessing. While the specific outcomes of this thesis are related to the presented system, basic concepts can be extrapolated to other challenging cases in bioprocess development. Thereby, competitive industrial bioprocesses are promoted, contributing to establish the envisaged circular bioeconomy.

Philipp Demling

Integrated biochemical engineering: Strain and process engineering for the production of rhamnolipids

Integrated biochemical engineering:
Strain and process engineering for the production of rhamnolipids

Philipp Demling



ISBN 978-3-98555-005-0



Integrated biochemical engineering: Strain and process engineering for the production of rhamnolipids

Von der Fakultät für Mathematik, Informatik und Naturwissenschaften der
RWTH Aachen University zur Erlangung des akademischen Grades eines Doktors
der Ingenieurwissenschaften genehmigte Dissertation

vorgelegt von

M. Sc. Molekulare und Angewandte Biotechnologie
Philipp Demling

aus

Münster, Nordrhein-Westfalen, Deutschland

Berichter:

Univ.-Prof. Dr.-Ing. Lars M. Blank

Univ.-Prof. Dr.-Ing. Andreas Jupke

Tag der mündlichen Prüfung: 09.08.2021

Diese Dissertation ist auf den Internetseiten der Universitätsbibliothek verfügbar.

Bibliografische Information der Deutschen Nationalbibliothek

Die Deutsche Nationalbibliothek verzeichnet diese Publikation in der Deutschen Nationalbibliografie; detaillierte bibliografische Daten sind im Internet über <https://portal.dnb.de> abrufbar.

Philipp Demling:

Integrated biochemical engineering: Strain and process engineering for the production of rhamnolipids

1. Auflage, 2021

Gedruckt auf holz- und säurefreiem Papier, 100% chlorfrei gebleicht.

Apprimus Verlag, Aachen, 2021

Wissenschaftsverlag des Instituts für Industriekommunikation und Fachmedien
an der RWTH Aachen

Steinbachstr. 25, 52074 Aachen

Internet: www.apprimus-verlag.de, E-Mail: info@apprimus-verlag.de

Printed in Germany

ISBN 978-3-98555-005-0

Eidesstattliche Erklärung

Ich, Philipp Demling, erkläre hiermit, dass diese Dissertation und die darin dargelegten Inhalte die eigenen sind und selbstständig, als Ergebnis der eigenen originären Forschung, generiert wurden.

Hiermit erkläre ich an Eides statt

1. Diese Arbeit wurde vollständig oder größtenteils in der Phase als Doktorand dieser Fakultät und Universität angefertigt;
2. Sofern irgendein Bestandteil dieser Dissertation zuvor für einen akademischen Abschluss oder eine andere Qualifikation an dieser oder einer anderen Institution verwendet wurde, wurde dies klar angezeigt;
3. Wenn immer andere eigene oder Veröffentlichungen Dritter herangezogen wurden, wurden diese klar benannt;
4. Wenn aus anderen eigenen oder Veröffentlichungen Dritter zitiert wurde, wurde stets die Quelle hierfür angegeben. Diese Dissertation ist vollständig meine eigene Arbeit, mit der Ausnahme solcher Zitate;
5. Alle wesentlichen Quellen von Unterstützung wurden benannt;
6. Wenn immer ein Teil dieser Dissertation auf der Zusammenarbeit mit anderen basiert, wurde von mir klar gekennzeichnet, was von anderen und was von mir selbst erarbeitet wurde;
7. Ein Teil oder Teile dieser Arbeit wurden zuvor veröffentlicht und zwar in:

Demling P, von Campenhausen M, Grütering C, Tiso T, Jupke A, Blank LM. Selection of a recyclable *in situ* liquid-liquid extraction solvent for foam-free synthesis of rhamnolipids in a two-phase fermentation. *Green Chemistry* 2020, 22:8495-8510. DOI: 10.1039/D0GC02885A.¹

Demling P, Ankenbauer A, Klein B, Noack S, Tiso T, Takors R, Blank LM. *Pseudomonas putida* KT2440 endures temporary oxygen limitations. *Biotechnology & Bioengineering* 2021, 1-16. DOI: 10.1002/bit.27938.²

Aachen, 24.09.2021



Philipp Demling

¹ Reprinted (adapted) with permission from Green Chemistry. © The Royal Society of Chemistry 2020.

² Reprinted (adapted) with permission from Wiley & Sons. Open Access CC BY-NC-ND 4.0. © The Authors 2021.

Funding

The presented work was performed in the scope of the project “Integrated Biotransformation and Separation for the Production of Valuable Compounds in a Novel Multiphase Loop Reactor” (InBioSep), which was funded by the German Federal Ministry for Education and Research (BMBF, funding code 031B0350B).



Federal Ministry
of Education
and Research

Contributions

Biotechnology and bioprocess engineering are highly interdisciplinary research fields requiring extensive collaboration to successfully work on a common goal. Therefore, parts of this thesis include results, which have been obtained in close collaboration with others and which have been acquired with the support of supervised students. Contributions and assistance of others are detailed at the beginning of each chapter.

Further, this thesis is built upon a foundation of long-term acquired knowledge and experience built at the Institute of Applied Microbiology, RWTH Aachen University, which is gratefully acknowledged.

Danksagung

Zu Beginn möchte ich mich bei Prof. Dr.-Ing. Lars M. Blank für die Möglichkeit, meine Dissertation im Institut für Angewandte Mikrobiologie anfertigen zu können, und für die Übernahme der Erstbetreuung bedanken. Lars, vielen Dank für deine große Unterstützung in allen bisherigen Projekten, auch schon vor Beginn meiner Zeit als Doktorand. Dein Rat in wissenschaftlichen, aber auch persönlichen Dingen, deine Denkanstöße und deine Offenheit für neue Ideen schätze ich sehr und haben maßgeblich zum Gelingen des Projekts beigetragen. Ich freue mich, weiterhin mit dir am iAMB zusammenarbeiten zu dürfen.

Außerdem möchte ich Prof. Dr.-Ing. Andreas Jupke für die Übernahme der Zweitbetreuung und die hervorragende Koordination des Gesamtprojektes InBioSep danken.

Ein großer Dank gilt Till Tiso. Till, vielen Dank für deine Unterstützung als Arbeitsgruppenleiter und Mentor. Immer konnte ich mit Anliegen jeder Art zu dir kommen und du hast dir stets die Zeit genommen, mir zuzuhören, mir weiterzuhelfen, neue Impulse zu geben und alle möglichen Texte auch kurzfristig noch gegenzulesen. Ich schätze deine lockere Art und die angenehme Arbeitsatmosphäre, die du innerhalb deiner Gruppe etabliert hast.

In diesem Sinne möchte ich auch allen Betreuern und Mentoren danken, die über all die Jahre des Studiums und während der praktischen Ausbildung in diversen Laboren ihr Wissen mit mir geteilt haben und mir es ermöglicht haben, heute überhaupt in der Lage zu sein, diese Dissertation zu schreiben.

Außerordentlicher Dank gilt auch meinen InBioSep-Projektpartnern Lucia Brandt und Maximilian von Campenhausen. Es war mir immer eine Freude mit euch zusammenzuarbeiten. Besonders die beinahe tägliche Zusammenarbeit mit dir, Max, hat mir sehr viel Spaß bereitet und mich unglaublich bereichert. Neben unseren Konferenzreisen bleiben mir besonders auch zahlreiche gemeinsame Grillabende, der Sport und unsere legendären Tischtennisduelle in Erinnerung, die zur Entwicklung einer guten Freundschaft geführt haben.

Insbesondere allen Studierenden, die ich während meiner Zeit als Doktorand teils sogar mehrfach und stellenweisen zusammen mit Maximilian von Campenhausen betreuen durfte, möchte ich danken. Nadine Smandzich, Sven Kratel, Arne Zimmermann, Sarika Karri, Carolin Grütering, Greta Kleinert, Dominik Schaffeld, Florian Röck und Steffen Dietz, ihr habt maßgeblich zum Gelingen dieser Arbeit beigetragen. Die Zusammenarbeit hat mir immer Freude bereitet und mich auch persönlich bereichert. Vielen Dank für euren tatkräftigen Einsatz.

Im Zuge des Projektes möchte ich mich auch bei dem Bundesministerium für Bildung und Forschung (BMBF) und somit bei allen Steuerzahlern bedanken, die es ermöglichen, dass Forschung in diesem Rahmen möglich ist. Freie Forschung und daraus resultierende Innovation

Danksagung

ist essenziell für die Aufrechterhaltung und Weiterentwicklung unserer Gesellschaft, wie zurzeit besonders eindrücklich wird, und muss weiterhin umfassend unterstützt werden.

Des Weiteren möchte ich mich bei allen derzeitigen und ehemaligen Mitarbeitern und Studierenden des Instituts für Angewandte Mikrobiologie bedanken. Die Atmosphäre am iAMB ist unschlagbar und ich bin immer gerne zur Arbeit gekommen. Ihr alle habt mich in vielen unterschiedlichen Art und Weisen in wissenschaftlichen Fragen aber auch privat unterstützt. Speziell auch die Aktivitäten abseits der Arbeit machen das iAMB zu einem besonderen Ort großen Spaßes und Zusammenhalts. Ich freue mich, dass ich weiterhin bei euch bleiben darf. In diesem Zuge möchte ich mich speziell bei der Biotensid-Gruppe bedanken. Isabel Bator, Carl Blesken, Melanie Filbig, Tobias Karmainski, Bernd Leuchtle, Conrad Müller und Gina Welsing, mit euch hat die Arbeit an Schaum & Co. und besonders auch die Aktivitäten nach der Arbeit viel Spaß gemacht. Besonders bedanken möchte ich mich auch bei Sebastian Köbbing. Danke für deine Unterstützung und deine Ratschläge, Sebastian, vor allem bezüglich molekularbiologischer Fragen. Ich freue mich auf die nächste Dartsparte und das nächste Feierabendbier.

Mein größter Dank gilt jedoch meiner Familie. Mama und Papa, ihr habt mich von klein auf immer in all meinen Unterfangen unterstützt und mir Rückhalt gegeben. Ihr habt mir eine Bildung ermöglicht, von der die meisten Menschen nur träumen können, und dafür bin ich euch für immer dankbar. Christian, dir danke ich für deinen brüderlichen Beistand in allen Belangen und für die häufigen Diskussionen, die mich oft dazu bringen, Dinge aus einer anderen Perspektive zu betrachten. Auf dich ist Verlass und ich blicke sehr oft zu dir auf. Dir, Laura, möchte ich dafür danken, dass du immer für mich da bist. Meine Zeit als Doktorand war oft stressig, du hattest aber immer offenes Ohr und großes Verständnis. Danke für deinen Rückhalt und deine Motivation, ohne dich hätte ich es nicht geschafft.

“All men dream, but not equally. Those who dream by night in the dusty recesses of their minds, wake in the day to find that it was vanity: but the dreamers of the day are dangerous men, for they may act on their dreams with open eyes, to make them possible.”

- T.E. Lawrence -

Table of Contents

Summary	V
Zusammenfassung	VII
Nomenclature	IX
List of Figures	XV
List of Tables.....	XIX
1 General Introduction.....	1
1.1 The urgency to transfer to a circular bioeconomy	3
1.2 Industrial biotechnology as a major driver for the bioeconomy	4
1.3 Integration of process development stages in microbial biotechnology	5
1.4 Bioprocess intensification	8
1.4.1 Strategies for <i>in situ</i> product removal	9
1.4.2 <i>In situ</i> liquid-liquid extraction in the scope of bioprocess intensification	11
1.5 Integrated bioprocessing for the production of rhamnolipids	11
1.5.1 Biosurfactants	11
1.5.2 Rhamnolipids as prominent representatives of biosurfactants	12
1.5.3 Challenges in rhamnolipid production and remedial approaches	14
1.6 Scope and outline of this thesis.....	15
2 Materials & Methods	19
2.1 Chemicals.....	21
2.2 Bacterial strains and growth media.....	21
2.3 Plasmid and strain construction	21
2.4 Cultivation strategies.....	27
2.4.1 Strain propagation	27
2.4.2 Cultivations for characterizing the biocompatibility of solvents	28
2.4.3 Microtiter plate cultivations	28
2.4.4 Cultivations in STRs	29
2.4.5 Cultivations in a parallel fermentation system	31
2.4.6 Cultivations in the multiphase loop reactor.....	32
2.5 Adaptive laboratory evolution	33
2.6 Genome re-sequencing.....	34

Table of Contents

2.7	Construction of a solvent database	34
2.8	Extractions	35
2.8.1	Extraction efficiencies	35
2.8.2	pH-dependent extractions.....	35
2.8.3	Time-resolved extractions.....	35
2.8.4	Back-extractions.....	36
2.9	Phase separation.....	36
2.10	Catastrophic phase inversion	37
2.11	Analytical methods	37
2.11.1	Determination of bacterial growth	37
2.11.2	Metabolite quantification	37
2.11.3	Rhamnolipid quantification.....	38
2.11.4	Detection and quantification of 1-octanol.....	39
2.11.5	Untargeted proteomics	39
2.12	Data analysis	40
3	Results	43
3.1	Evaluation of <i>in situ</i> extraction solvents to robustly produce rhamnolipids in a two-liquid phase fermentation.....	45
3.1.1	Abstract	47
3.1.2	Introduction	47
3.1.3	Results	50
3.1.4	Discussion	63
3.1.5	Conclusion.....	66
3.2	Engineering of <i>Pseudomonas putida</i> KT2440 for enhanced solvent tolerance.....	69
3.2.1	Abstract	71
3.2.2	Introduction	71
3.2.3	Results	73
3.2.4	Discussion	84
3.2.5	Conclusion.....	87
3.3	Exploration of fed-batch cultivation strategies for the production of rhamnolipids.....	89
3.3.1	Abstract	91
3.3.2	Introduction	91

3.3.3	Results	93
3.3.4	Discussion	100
3.3.5	Conclusion.....	101
3.4	<i>Pseudomonas putida</i> KT2440 withstands repeated oxygen limitations	103
3.4.1	Abstract	105
3.4.2	Introduction	105
3.4.3	Results	108
3.4.4	Discussion	117
3.4.5	Conclusion.....	119
3.5	A novel multiphase loop reactor allows simultaneous production and <i>in situ</i> extraction of rhamnolipids	123
3.5.1	Abstract	125
3.5.2	Introduction	125
3.5.3	Results	128
3.5.4	Discussion	132
3.5.5	Conclusion.....	135
4	General Discussion & Outlook.....	137
4.1	Integrated design of holistic bioprocesses	139
4.2	Considerations for the scale-up of microbial production processes	141
4.3	Implementation of <i>in situ</i> product removal in bioprocesses	143
4.3.1	Challenges and opportunities for <i>in situ</i> extractions in biotechnological processes	143
4.4	Concluding remarks and outlook	144
	Appendix	148
	References	171
	Curriculum Vitae.....	200

Summary

Establishing biotechnological processes within the envisaged circular bioeconomy requires holistic approaches including an integration of all stages of process development. In this scope, the presented thesis illustrates the integration of strain and process engineering using the example of producing the biosurfactant rhamnolipids with recombinant *Pseudomonas putida* KT2440.

A process-hindering challenge during the production of biosurfactants in aerated bioreactors is excessive foaming. To mitigate this challenge, an *in situ* liquid-liquid extraction was established by selecting a suitable, biocompatible extraction solvent in a multi-step strategy, including the assessment of product recovery and solvent recycling. A refinement of cultivation parameters was required to enhance functionality of the extraction, in turn influencing the performance of the whole-cell biocatalyst. Unraveling interactions of integrated up- and downstream processing resulted in the definition of a joint operational window. Finally, a foam-free fed-batch cultivation of rhamnolipid-producing *P. putida* KT2440 with integrated *in situ* extraction was established. Subsequently, different cultivation modes have been evaluated for enhanced production, and strategies for improved phase separation have been explored.

As the microbial boundaries of the operational window are restricting process performance, host engineering was approached to enhance the solvent tolerance of *P. putida* KT2440, thereby enabling the utilization of additional extraction solvents. *P. putida* KT2440 was successfully adapted to tolerate high concentrations of 1-octanol. Genome re-sequencing and subsequent reverse genome engineering enabled the construction of tolerant strains capable of producing rhamnolipids in the presence of 1-octanol. Another challenge are transient oxygen limitations in industrial fermentations, which *P. putida* KT2440 masters well without losing production capacity, thereby highlighting its outstanding suitability for industrial-scale production processes.

Previous findings were considered to define an operational window to produce rhamnolipids with recombinant *P. putida* KT2440 in a custom-designed multiphase loop reactor, integrating cultivation and an *in situ* counter-current liquid-liquid extraction. Performance indicators compared well with previous two-liquid phase cultivations in stirred-tank reactors, emphasizing the robustness of *P. putida* KT2440 and serving as a proof of concept for the novel reactor type.

In conclusion, this thesis advocates integrated bioprocessing and the urgency for a holistic, interdisciplinary perspective on the overall process development. While the specific outcomes of this thesis are related to the presented system of producing rhamnolipids with recombinant *P. putida* KT2440, basic concepts and proposed solutions can be extrapolated to other challenging cases in bioprocess development. Thereby, competitive industrial bioprocesses are promoted, eventually contributing to establishing the envisaged circular bioeconomy.

Zusammenfassung

Um biotechnologischer Prozesse im Zuge der angestrebten zirkulären Bioökonomie zu etablieren, müssen ganzheitliche Ansätze verfolgt werden, die alle Stufen der Prozessentwicklung integriert. In diesem Rahmen veranschaulicht die vorgestellte Arbeit die Integration von Stamm- und Prozessentwicklung am Beispiel der Produktion der Biotensid-Klasse der Rhamnolipide mit rekombinantem *Pseudomonas putida* KT2440.

Starke Schaumbildung hindert die Prozessführung für die Produktion von Biotensiden in Bioreaktoren. Um diese Herausforderung zu umgehen, wurde eine *in situ* flüssig-flüssig-Extraktion etabliert, wofür ein geeignetes biokompatibles Lösungsmittel in einer mehrstufigen Auswahlstrategie identifiziert wurde. Diese Strategie schloss die weitere Produktrückgewinnung und das Lösungsmittelrecycling mit ein. Um die Funktionalität der Extraktion zu verbessern, wurden Kultivierungsparameter angepasst, was wiederum die Leistung des Ganzzell-Biokatalysators beeinflusste. Das Aufdecken von Wechselwirkungen der integrierten Up- und Downstream-Prozessschritte führte zur Definition eines Betriebsfensters, das eine schaumfreie Fed-Batch-Kultivierung von Rhamnolipid-produzierendem *P. putida* KT2440 mit integrierter *in situ* Extraktion erlaubte. Anschließend wurden verschiedene Kultivierungsmodi für eine gesteigerte Produktion evaluiert und Strategien für eine verbesserte Phasentrennung erarbeitet.

Da die Grenzen des Betriebsfensters durch den Ganzzell-Biokatalysator limitiert sind, wurden Methoden der Stammentwicklung genutzt, um die Lösungsmitteltoleranz von *P. putida* KT2440 zu erhöhen und damit die Verwendung zusätzlicher Extraktionsmittel zu ermöglichen. Hier wurde *P. putida* KT2440 erfolgreich dahingehend angepasst, hohe Konzentrationen von 1-Oktanol zu tolerieren. Nach Genom-Resequenzierung und anschließendes Reverse Genome Engineering wurden Stämme erzeugt, die Rhamnolipid-Produktion in der Gegenwart von 1-Oktanol ermöglichen. Des Weiteren wurde gezeigt, dass *P. putida* KT2440 vorübergehende, sich jedoch wiederholende Sauerstofflimitierungen überstehen kann, ohne dabei an Produktionskapazität einzubüßen. Dies unterstreicht seine herausragende Eignung für Produktionsprozesse im industriellen Maßstab.

Die erhobenen Erkenntnisse wurden verwendet, um ein Betriebsfenster für die Produktion von Rhamnolipiden in einem speziell entwickelten Mehrphasen-Schlaufenreaktor zu definieren, der die Kultivierung mit einer *in situ* flüssig-flüssig-Extraktion im Gegenstrom integriert. Die Leistungsindikatoren der durchgeführten Kultivierung waren vergleichbar mit denen der zweiphasigen Kultivierungen in Rührkesselreaktoren, was die Robustheit von *P. putida* KT2440 als Ganzzell-Biokatalysatoren unterstreicht und als Machbarkeitsnachweis für den neuartigen Reaktor dient.

Zusammenfassend zeigt diese Arbeit Aspekte der integrierten Bioprozessentwicklung und die Dringlichkeit einer ganzheitlichen, interdisziplinären Betrachtung für die gesamte Prozessentwicklung auf. Obwohl sich die Ergebnisse dieser Arbeit spezifisch auf das vorgestellte System zur Herstellung von Rhamnolipiden mit rekombinantem *P. putida* KT2440 beziehen, können die grundlegenden Konzepte und vorgeschlagenen Lösungsansätze auf anderer Bioprozesse übertragen werden. Dadurch wird die Entwicklung kompetitiver, industrieller Bioprozesse gefördert, die schlussendlich zur Etablierung der angestrebten zirkulären Bioökonomie beitragen.

Nomenclature

Abbreviations

Abbreviation	Description
3-HA	3-hydroxy alkanoate
AA	amino acid
abs	absolute value
AEC	adenylate energy charge
ADP	adenosine diphosphate
ALE	adaptive laboratory evolution
ALR	airlift reactor
AMP	adenosine monophosphate
ATP	adenosine triphosphate
aq	aqueous
BES	bioelectrochemical system
BMBF	German Federal Ministry for Education and Research
BS	backscatter
CAD	charged aerosol detector (HPLC)
CAD	computer-aided design
CER	carbon emission rate
CFD	computational fluid dynamics
COG	cluster of orthologous groups
CPI	catastrophic phase inversion
DNA	deoxyribonucleic acid
DOT	dissolved oxygen tension
DOT _d	dissolved oxygen tension in the downcomer
DOT _{PV}	process value of the dissolved oxygen tension
DOT _r	dissolved oxygen tension in the riser
DOT _{SP}	setpoint of the dissolved oxygen tension
DSMZ	German Collection of Microorganisms and Cell Cultures GmbH
DSP	downstream processing
dTDP	deoxythymidine diphosphate
EDTA	ethylenediaminetetraacetic acid
<i>e.g.</i>	<i>exempli gratia</i>

Abbreviation	Description
EU	European Union
FADH ₂	dihydroflavin adenine dinucleotide
G6P	glucose-6-phosphate
GC	gas chromatography
GLC	glucose
H	harvest
HAA	3-(3-hydroxyalkanoyloxy)alkanoic acid
HPLC	high-performance liquid chromatography
HV1	host-vector system safety level 1
iAMB	Institute of Applied Microbiology
<i>i.e.</i>	<i>id est</i>
InDel	Insertion and deletion
ISPR	<i>in situ</i> product removal
LB	lysogeny broth
LC	liquid chromatography
LCA	life cycle assessment
LLE	liquid-liquid extraction
MOPS	3-morpholino-propanesulphonic acid
MPLR	multiphase loop reactor
MS	mass spectrometry
MSM	mineral salts medium
MTP	microtiter plate
NADH	(reduced) nicotinamide adenine dinucleotide
OD ₆₀₀	optical density at a wavelength of 600 nm
org	organic
OTR	oxygen transfer rate
OUR	oxygen uptake rate
PCA	perchloric acid
PCR	polymerase chain reaction
PFR	plug-flow reactor
PHA	polyhydroxyalkanoates
PI	process intensification
PID (controller)	proportional-integral-derivative (controller)
ppGpp	guanosine tetraphosphate

Abbreviation	Description
(mono/di-)RL	(mono/di-)rhamnolipid
RI	refractive index
RND	Resistance-nodulation-division
SNP	single-nucleotide polymorphism
STR	stirred-tank reactor
TAE	tris-acetic acid EDTA buffer
TCS	two-component system
TEA	techno-economic assessment
TS	target sequence
USD	United States dollar
USP	upstream processing
WT	wild type

Symbols

Symbol	Description	Unit
a	volume-specific surface area	m^{-1}
A_r	area of the cross-section of the riser	m^2
A_d	area of the cross-section of the downcomer	m^2
Bo	Bodenstein number	-
BS	back scatter	a.u.
C	concentration	g L^{-1}
C_0	initial surfactant concentration	g L^{-1}
C_1	surfactant concentration after extraction	g L^{-1}
C^*	DO concentration at the gas-liquid phase boundary on the liquid side	mmol L^{-1}
C_L	DO concentration in the liquid bulk phase	mmol L^{-1}
d	diameter	mm
d_{cylinder}	inner diameter of the inner cylinder	mm
d_{vessel}	inner diameter of the vessel	mm
D_{MPLR}	inner diameter of the vessel of the MPLR	mm
D_r	inner diameter of the riser of the MPLR	mm
E	extraction efficiency	%
F	feed rate	mL min^{-1}
ε_G	gas hold-up	-

Symbol	Description	Unit
ε_{Gr}	gas hold-up in the riser	-
ε_{Gd}	gas hold-up in the downcomer	-
g	gravitational acceleration	$m\ s^{-2}$
h_c	height of coalescence (phase separation setup)	cm
h_d	height of dispersion (phase separation setup)	cm
h_L	height of the gas-free liquid (in the MPLR)	mm
h_w	height of withdrawal (phase separation setup)	cm
H_e	effective height of the MPLR	mm
H_{MPLR}	height of the MPLR	mm
H_B	height of the bottom compartment of the MPLR	mm
H_C	height of the cylinder of the MPLR	mm
k_{La}	volumetric oxygen transfer coefficient	h^{-1}
m	mass	g
μ	growth rate	h^{-1}
n	shaking frequency	min^{-1}
P	partition coefficient	-
p_h	headspace pressure	bar
Δp_g	difference in gravitational pressure	$kg\ m^{-1}\ s^{-2}$
$Peri$	perimeter of a well in MTPs with a specific geometry to the perimeter of a round well	[-]
ϕ	phase ratio	$mL_{org}\ mL_{aq}^{-1}$
Q_m	molar gas flow rate	$mol\ min^{-1}$
q_s	specific carbon uptake rate	$g\ g_x^{-1}\ h^{-1}$
R	universal gas constant	$kg\ m^2\ s^{-2}\ mol^{-1}\ K^{-1}$
ρ_d	average fluid density of the downcomer	$kg\ m^{-3}$
ρ_r	average fluid density of the riser	$kg\ m^{-3}$
ρ_L	average density of the non-aerated fluid	$kg\ m^{-3}$
Sh	Sherwood number	-
STY	space-time yield, productivity	$g\ L^{-1}\ h^{-1}$
t	(cultivation) time	
T	temperature	K
τ_d	residence time in the downcomer of the MPLR	s
τ_{PFR}	residence time in the PFR	s
U_G	superficial gas velocity	$m\ s^{-1}$

Symbol	Description	Unit
U_{Gr}	gas velocity in the riser	m s^{-1}
U_{Ld}	velocity of the continuous liquid phase in the downcomer	m s^{-1}
U_{Lr}	velocity of the continuous liquid phase in the riser	m s^{-1}
V	volume	m^3
V_{L}	filling volume (of MTPs)	μL
W_{d}	width of the downcomer	mm
x	biomass	g
$Y_{P/S}$	product yield	$\text{g}_{\text{product}} \text{g}_{\text{substrate}}^{-1}$
$Y_{X/S}$	biomass yield	$\text{g}_x \text{g}_{\text{substrate}}^{-1}$

List of Figures

Figure 1 Integrated stages of bioprocess development.	7
Figure 2 Definition of a joint operational window in bioprocess intensification.....	9
Figure 3 Representative structure of a rhamnolipid.	13
Figure 4 Schematic illustrations of the MPLR.....	33
Figure 5 Schematic setup of the experiment for phase separation.	36
Figure 6 Extraction efficiencies of 18 organic solvents for the extraction of rhamnolipids from fermentation broth at pH 6.5.....	51
Figure 7 Mean CO ₂ volume concentration in the headspace of shake flask cultivations of <i>P. putida</i> KT2440 in MSM with 3 g L ⁻¹ glucose in the presence of organic solvents.	53
Figure 8 Coalescence curves defined by the clear cut between the densely packed drop layer and the coherent phase of ethyl decanoate.	55
Figure 9 pH-dependency of rhamnolipid extraction with ethyl decanoate.	57
Figure 10 Back-extraction of rhamnolipids from loaded ethyl decanoate.	58
Figure 11 Extractive two-phase fermentation at standard conditions.	59
Figure 12 Production of rhamnolipids in extractive two-liquid phase fermentations and OUR- derived growth rates at different pH values.....	60
Figure 13 Production of rhamnolipids in a fed-batch fermentation with a foam-based pH reduction.	62
Figure 14 Sequential cultivation of <i>P. putida</i> KT2440 in absence and presence of 1-octanol to generate inheritable tolerance.	76
Figure 15 Cultivation of adapted <i>P. putida</i> KT2440 strains and the non-adapted wild-type <i>P. putida</i> KT2440 in the presence of 1-octanol.....	77
Figure 16 Qualitative solvent tolerance assay of adapted and engineered <i>P. putida</i> KT2440 strains with 16.7% (v/v) 1-octanol after 20 h of incubation.	80
Figure 17 Quantitative solvent tolerance assay of engineered and adapted strains.	81
Figure 18 Two-liquid phase cultivations of <i>P. putida</i> KT2440 PP_3453-P324R <i>rhlAB</i> and <i>P. putida</i> KT2440 PP_3454-P106R <i>rhlAB</i> in STRs with 1-octanol as the extractant.....	83
Figure 19 Production of rhamnolipids in a two-liquid phase fed-batch cultivation of <i>P. putida</i> KT2440 SK4 with a linearly increasing feeding profile.....	95

Figure 20 Production of rhamnolipids in a two-liquid phase fed-batch cultivation of <i>P. putida</i> KT2440 SK4 with a linearly increasing feeding profile and an adjusted composition of the feeding solution.	97
Figure 21 Ratio of HAAs to total surfactants produced by <i>P. putida</i> KT2440 SK4 in all performed fed-batch cultivations.	99
Figure 22 Catastrophic phase inversion after 20 h of settling. Ratios from 1:1 (v/v) to 1:7 (v/v) emulsion to excess ethyl decanoate were assessed.	100
Figure 23 Schematic illustrations of different scale-down cultivation setups to mimic large-scale inhomogeneities in lab-scale.	107
Figure 24 Backscatter signal throughout cultivations of <i>P. putida</i> KT2440 in microtiter plates at different intervals of oscillating agitation.	109
Figure 25 Cultivations of <i>P. putida</i> KT2440 at different intervals of oscillating aeration and agitation.	110
Figure 26 Comparison of cultivations of <i>P. putida</i> KT2440 SK4 at different intervals of oscillating aeration and agitation.	114
Figure 27 Relative differences in abundances of detected proteins in <i>P. putida</i> KT2440 subjected to oscillating DOT values compared to undisturbed control cultivations.	116
Figure 28 Dimensions of the MPLR.	128
Figure 29 Cultivation of <i>P. putida</i> KT2440 SK4 in the first generation MPLR.	129
Figure 30 Cultivation of <i>P. putida</i> KT2440 SK4 in the second generation MPLR with a redesigned aeration setup.	131
Figure 31 Extending the boundaries of the operational window imposed by the whole-cell biocatalyst <i>via</i> strain engineering.	140
Figure A1.1 Representative HPLC-CAD chromatogram for the separation and quantification of rhamnolipid congeners.	152
Figure A2.1 Time-resolved depletion of rhamnolipids in the aqueous phases.	153
Figure A2.2 Selected solvents after shaking for 4 h before centrifugation.	153
Figure A2.3 pH-dependency of rhamnolipid extraction with ethyl decanoate resolved for measured congeners.	154
Figure A2.4 Extractions of rhamnolipids at varying pH values.	155
Figure A2.5 List of physicochemical properties of solvent candidates.	159

Figure A3.1 Cultivation of <i>E. coli</i> DH5 α pBNT (left) and <i>E. coli</i> DH5 α pBNT- <i>ttgGHI</i> in the presence of 50% (v/v) <i>n</i> -hexane.	160
Figure A3.2 Growth of adapted and constructed <i>P. putida</i> KT2440 strains in absence of 1-octanol.	160
Figure A4.1 Growth of <i>P. putida</i> KT2440 at differing supplied trace element concentrations. .	161
Figure A5.1 Logarithmic backscatter signal over time of cultivations of <i>P. putida</i> KT2440 in microtiter plates at different intervals of oscillating agitation.	162
Figure A5.2 Close view of the DOT signal of an STR cultivation of <i>P. putida</i> KT2440 subjected to an oscillating agitation and aeration at an interval of 2 min.	163
Figure A5.3 Extracellular metabolites measured during cultivations of <i>P. putida</i> KT2440 at different intervals of oscillating aeration and agitation.	163
Figure A5.4 Batch cultivations of wild-type <i>P. putida</i> KT2440 at differing DOT _{SP} in a parallel cultivation device.	164
Figure A5.5 Extracellular metabolites measured during cultivations of <i>P. putida</i> KT2440 SK4 at different intervals of oscillating aeration and agitation.	164
Figure A6.1 Half-logarithmic plot of the OUR of <i>P. putida</i> KT2440 SK4 in the MPLR with the second generation of the aeration setup.	166

List of Tables

Table 1 Bacterial strains used and constructed in this study.....	25
Table 2 Thresholds and short explanations for performed solvent selection steps.	50
Table 3 Theoretical CO ₂ accumulation in the headspace of the shake flask with solvents compared to a cultivation without solvents and the corresponding characteristic of the interaction of solvent and microorganism.....	52
Table 4 Mutations in the genome of <i>P. putida</i> KT2440 introduced by ALE in the presence of 1-octanol.	78
Table 5 Growths rates and RL titers of shake flask cultures with different supplied trace element concentrations	96
Table 6 Performance indicators of fed-batch cultivations with different feeding strategies.....	98
Table 7 Performance indicators for cultivations of wild-type <i>P. putida</i> KT2440 in STRs at different conditions.	111
Table 8 Performance indicators for cultivations of <i>P. putida</i> KT2440 SK4 in STRs at different conditions.	115
Table 9 Performance indicators and key characteristics of the cultivation of <i>P. putida</i> KT2440 SK4 in different reactor types at current stages of bioprocess and reactor development.	135
Table A1.1 Stock solutions for MSM.	149
Table A1.2 Oligonucleotides used in PCRs.	150
Table A5.1 Significantly altered proteins of <i>P. putida</i> KT2440 subjected to 2 min intervals of oscillation compared to control cultivations at t_1 and t_2	148

Chapter 1

General Introduction

Contributions

This chapter was written by Philipp Demling and reviewed by Lars M. Blank.

1 General Introduction

1.1 The urgency to transfer to a circular bioeconomy

Within the last century, the exploitation of non-renewable fossil resources to generate platform chemicals for the production of fine chemicals, pharmaceuticals, and commodities such as plastics and fuels has led mankind to a critical turning point. The emission of greenhouse gases, most prominently carbon dioxide as a waste product from processing fossil resources and consuming petrochemically derived products, has been causing global warming. Critical consequences for the global ecosystem, *e.g.*, warming of oceans and water bodies, rising sea levels due to the melting of the polar ice caps, desertification, increased frequency of extreme weather anomalies, and ultimately mass extinction have been observed [1–5]. Although fossil resources are finite and thus could be depleted, technological advancement for identifying and exploiting new sources of fossil resources, some of them ironically claimed to be sustainable, will satisfy the demand in the foreseeable future [6, 7]. The demand is predicted to further increase due to a growing world population, however, at a reduced rate [8]. In turn, this causes the climate crisis with all its destructive consequences for the global ecosystem to be intensified, resulting in a shortage of arable and habitable land and, consequently, insecurities in food and water supply [9, 10]. Therefore, critical rethinking and intervention are urgently required to decrease the dependency on products derived from fossil resources [11].

An obvious solution to reduce the demand is limiting the continuous growth of the world population. Although the population in Europe and Asia is predicted to stagnate or decline within the next 30 years, the global population is presumed to grow at least until the end of the century [12]. As this period is too long to avoid irreversible consequences stemming from climate change, sustainable and resource-efficient solutions need to be developed and implemented immediately [13]. The awareness for sustainability has been rising among the population [14], raising pressure on governments to institute stricter regulations for carbon dioxide emission [15] and on companies to transit to ecologically friendly and sustainable production processes [16–18]. However, to truly reach long-term sustainability, global zero-waste resource cycles need to be established and maintained to impact climate change and potentially reverse global warming. Transitioning from a linear economy based on fossil resources to a circular bio-based economy, also referred to as bioeconomy, is crucial to establish closed carbon cycles [19]. In the bioeconomy, renewable resources are utilized to produce chemicals, fuels, and energy [20], which are currently derived from fossil resources, or respective alternatives to replace established production processes. Here, closed carbon cycles cause net-zero carbon emission processes, transforming society to be carbon-

neutral. Reaching this goal by 2050 was declared by the European Union (EU) within The European Green Deal and by other states [21], ultimately paving the way to limit global warming with all its consequences. However, a carbon-negative society might be required to limit or potentially reverse global warming [22].

1.2 Industrial biotechnology as a major driver for the bioeconomy

Industrial biotechnology is a crucial sector to establish the envisaged bioeconomy as carbon from renewable resources, such as biomass, carbon dioxide, and waste, can be used as a feedstock for bioconversions to produce desired, value-added compounds. Bioconversions are catalyzed by prokaryotes or eukaryotes as whole living or dead cells or by cell-free systems such as purified enzymes. In the last decades, substantial progress has been made for the targeted production of valuable compounds, and there is a growing number of promising cases in industrial biotechnology that are expected to be successfully implemented in the market within the next decade [23]. While this positive development is gaining momentum, products are typically highly specific, *i.e.*, pharmaceuticals and fine chemicals. Despite a few exceptions, like the production of ethanol [24] or amino acids such as L-lysine [25], hardly any biotechnological production processes for bulk chemicals or commodities have been able to compete with processes utilizing fossil resources due to several reasons. First, biotechnological production processes cannot compete economically with petrochemical processes in many cases [26]. This is mainly due to the comparably low price of fossil resources and optimized and depreciated production processes. However, with increasing costs for exploitation to satisfy the demand for fossil resources as well as stricter regulations on carbon dioxide emission (*e.g.*, carbon dioxide pricing in the EU and Germany) and, in turn, more cost-efficient biotechnological production, economic competitiveness might be reached relatively soon. Second, the comparably high complexity and dynamic nature of biological systems often result in a limited understanding of the whole-cell biocatalyst and the entire process, which can cause severe losses in productivity and performance, particularly during scale-up from laboratory to industrial scale [27]. Third, the downstream processing (DSP) of biotechnologically produced compounds is generally more complicated due to the high dilution of products and the complex composition of cultivation broth, including cells, cell debris, and byproducts [28]. Cost- and labor-intensive product recovery and purification are unprofitable unless the product has an accordingly high market price, which is usually not the case for bulk chemicals.

While the challenges to establish biotechnological production processes in industry to contribute to a circular bioeconomy are manifold, there are no alternatives to overcome the dependency on fossil resources. Innovative approaches and holistic perspectives, considering the overall production process already at primary stages of development, are required [29]. Thereby,

the transition of biotechnological approaches from research-focused laboratory scale to industrial applications will be achieved as famously demanded for synthetic biology as an integral part of biotechnology already in 2010 [30].

1.3 Integration of process development stages in microbial biotechnology

Microbial bioprocess development comprises several stages ranging from the molecular scale to large-scale production and eventually product recovery and formulation [29, 31]. Different stages are outlined, and crucial interactions are identified in the following paragraphs.

Initially, the demand for a novel compound or an alternative production route for established products is identified. Promising economic or ecologic advantageousness drives the identification and engineering of a metabolic pathway on multiple levels [32–34]. Here, genes encoding for enzymes that catalyze the desired reactions are designed, selected, and potentially modified to increase efficiency and alter the specificity of the enzymes [35]. By interconnecting functional DNA elements, such as promoters or regulatory sequences, the expression levels of genes can be altered [36]. Further modifications can be implemented at the translational level [37]. In recent years, the development of tools in metabolic engineering, synthetic biology, automation, and DNA synthesis have paved the way for rapid and more cost-effective pathway construction [38, 39].

To implement the production pathway, a whole-cell biocatalyst has to serve as a chassis. While the overall type of whole-cell biocatalyst needs to be carefully selected for a specific application, certain characteristics can be engineered, such as enhancing the solvent tolerance [40], modifying the cell surface [41], or restricting motility [42]. Furthermore, carbon fluxes can be re-routed [43], *e.g.*, by gene deletions, and the redox balance can be modified, both enhancing the production capacity of the chassis strain. Similar to metabolic pathway engineering, recent technological developments have accelerated strain engineering. Moreover, systems biology approaches, such as rapid whole-genome sequencing, high-throughput analysis of the transcriptome, proteomics, fluxomics, and metabolomics, enable data collection on multiple cellular levels [29, 34]. Acquired data are integrated into regulatory and metabolic networks organized in predictive and descriptive models, thereby allowing the generation of knowledge on a systems level [44].

Reaction engineering is required to exploit the production capacity of the whole-cell biocatalyst optimally. Here, the configuration of the whole-cell biocatalyst is defined, *i.e.*, if growing or resting cells are employed and if a pure, one-organism culture or a mixed co-culture is utilized [45]. Further, parameters for reaction conditions are defined, such as the pH value, temperature, aeration, and the composition of the cultivation medium. If beneficial, *in situ* product removal strategies for toxic or process-inhibiting products can be explored to push the limitation in maximally producible titers [46]. Suitable strategies to assess biocompatibility, *e.g.*, the toxicity

of an organic solvent in case of an *in situ* extraction, and the feasibility of the technical implementation are defined. While the construction of whole-cell biocatalysts is rapid nowadays, their characterization and the definition of optimal reaction parameters are considered as a bottleneck [47]. However, increasing automation and scalable cultivation devices allow a more reliable transition from multiplexed micro- and small-scale cultivation to production scale without the loss of performance [48–51].

Lastly, the fermentation process needs to be embedded in the process chain. This requires the definition of its mode of operation, *i.e.*, batch, fed-batch, continuous cultivation, or hybrid strategies [52, 53]. Further, the design and scale-up of the reactor need to be considered. Next to conventional stirred-tank reactors (STRs), other types of reactors are conceptualized and constructed, such as bubble columns, air lift reactors, and integrated systems like a multiphase loop reactor (MPLR), allowing *in situ* extraction [54–56]. For reactor design and scale-up, computational fluid dynamic (CFD) models are required to assess mixing, mass transfer, and trajectories of cells through different zones or compartments of the reactor [27]. Further, an efficient strategy for DSP needs to be designed to recover and formulate the product. Typically, DSP is comprised of a sequence of unit operations, varying in length and complexity depending on the product and the required purity, but eventually ending in product polishing and formulation [57, 58]. The operational windows of all process segments are defined and aligned to each other, and the overall process is optimized from an economic and ecologic perspective [28, 59].

What appears to be a linear approach for developing and establishing a bioprocess needs to have a circular and iterative character (Figure 1). Every stage of bioprocess development implies consequences for the other stages, displaying its high requirement for interaction, especially as people of different disciplines, namely biotechnology, chemical engineering, and economics, have to work hand in hand. While there are numerous interactions, selected ones are highlighted in the following paragraph.

Products and processing routes need to be identified, which have added value and have a chance to compete economically and ecologically with existing alternatives when introduced to the market. Here, tools such as techno-economic assessment (TEA) based on mass balances, the process scheme, and economic data, as well as life-cycle assessment (LCA) introducing ecological weighing factors, are applied [60–62]. These tools define objectives for the overall process, such as productivity, product titer, yields, robustness, selectivity, and product localization [29]. The defined objectives directly impact the design and conception of a molecular production pathway and the selection of a suitable chassis strain to meet the required objectives. Only the overlap in products of economic and ecologic interest and biotechnological feasibility can be considered attractive for production. Further, the metabolic pathway requires a suitable chassis to construct

an efficient whole-cell biocatalyst, heavily influencing reaction conditions and the mode of cultivation. Required resources and produced waste streams at cultivation can, in turn, have economically and ecologically unfavorable impacts, conflicting set objectives. Besides, the type of product, type of whole-cell biocatalyst, and type of upstream processing (USP) also have direct implications on the design of DSP, which typically accounts for a large fraction of the overall production costs due to usually high demands in energy and resources but depends on the type of product and purity [28]. A TEA can *a priori* assess if the highly diluted produced molecule can be recovered from the cultivation broth while still being economically and ecologically beneficial. Further, the necessary production volume can be determined with consequences for scaling or numbering the overall production process [26]. Concluding, for establishing a bioprocess with the most beneficial outcome, all disciplines have to constantly interact, be governed, and be monitored. Thereby, the acquired performance is validated to match the superordinated objectives, and adjustment and iteration can be prompted if required.

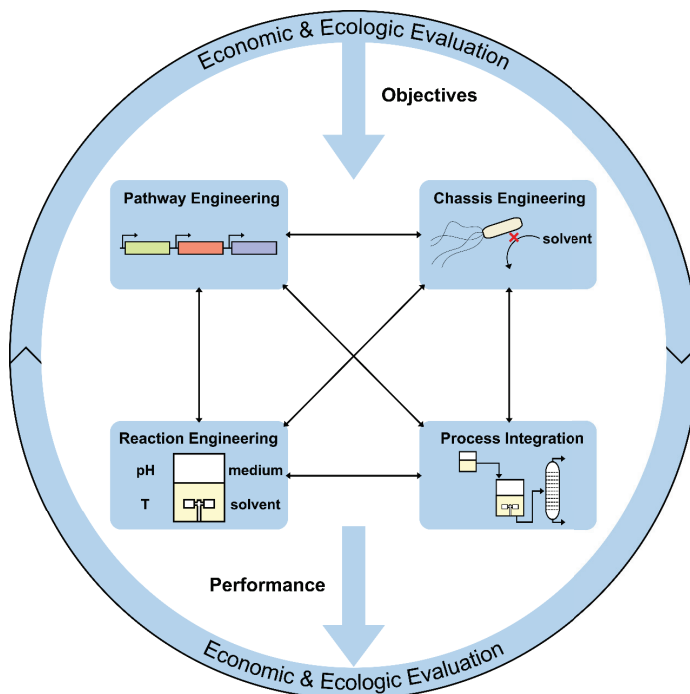


Figure 1 Integrated stages of bioprocess development. All stages comprising pathway engineering, chassis engineering, reaction engineering, and process integration need to be integrated and constantly re-evaluated for economic and ecologic efficiency. The overall process design requires iterative optimization to achieve the performance matching the objectives.

1.4 Bioprocess intensification

The concept of process intensification (PI) has been introduced into bioprocess development several decades ago but has attracted increasing attention in recent years. Remarkably, or perhaps even caused by its rising popularity and its resulting application to many fields, there is a lack of a clear definition of PI [63]. In a broader sense, PI is enhancing the efficiency of a process at a level ranging from transport phenomena and energy conversion on the molecular scale to the miniaturization and integration of apparatuses for unit operations to save time and space, to improve functionality, or to increase sustainability [63, 64]. For bioprocesses, Woodley [65] defined four complementary strategies for PI. The first two, (i) reactor compartmentalization and (ii) hybridization, are similar to their counterparts in traditional chemical engineering, although performed for different purposes. The other two, (iii) metabolic engineering and (iv) enzyme engineering, are unique to bioprocesses and can yield more degrees of freedom. Considering the mentioned definitions, holistic bioprocess development itself can be defined as PI.

The two PI strategies (i-ii) common to conventional chemical engineering are further introduced in a biotechnological setting. Here, integrating multiple unit operations, usually spatiotemporally separated, into a single stage of the process allows the unit operations to be performed simultaneously in one, optionally compartmented, apparatus [66]. Thereby, the efficiency of the overall process can be increased, ultimately making it economically more beneficial, as the production cycle can be shortened as well as the size of the production plant and ideally operational expenditures are reduced [67]. A drawback of these strategies is that all integrated unit operations have to be functional and efficient at the same conditions applied to the intensified stage of the process. Therefore, a joint operational window allowing optimal functionality has to be defined.

The definition of the operational window is driven by constraints in a multivariate parameter space of the single unit operations (Figure 2). Determining a joint operational window is not trivial and often requires trade-offs, especially if a microbial cultivation for producing a value-added compound is subject to be intensified [68]. Whole-cell biocatalysts often have narrow optima for different process parameters, such as pH value and temperature. Deviations from these optima might be possible within certain narrow limits. However, large deviations are typically detrimental to growth and production. As conditions of unit operations of chemical processes can be harsh in terms of temperature and pressure, matching the rather non-flexible boundaries of whole-cell biocatalysts might be challenging.

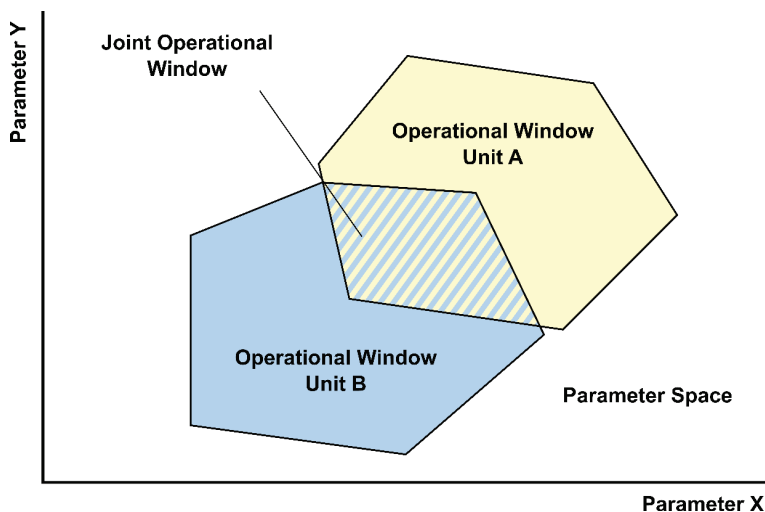


Figure 2 Definition of a joint operational window in bioprocess intensification. The operational window of each unit operation is multivariate and restricted by several parameters. For illustration, only two parameters are displayed, however, the operational window is defined in a parameter space. The joint operational window for the intensified bioprocess (shaded area) is defined by the intersection of the individual operational windows.

1.4.1 Strategies for *in situ* product removal

Despite the challenges, the integration of unit operations has been successfully applied in microbial bioprocesses. Thus, defining a joint operational window has been demonstrated to be feasible. A prominent example is the application of *in situ* product removal (ISPR) in fermentations. Depending on the physicochemical properties of the product, such as the molecular weight, volatility, hydrophobicity, charge, and reactivity, different types and strategies for ISPR have been explored [46, 69, 70]. The most common techniques are briefly described in the following paragraphs.

In situ liquid-liquid extraction (LLE) is one of the most extensively studied methods for ISPR in bioprocesses. Here, the product is extracted into a second liquid phase, driven by a concentration gradient. The partition coefficient, *i.e.*, the ratio of product concentrations in the two liquid phases, is used as a measure for the efficiency of extraction at given conditions [71]. In bioprocesses, LLEs have been most prominently implemented by the direct addition of an organic solvent exhibiting a miscibility gap to the aqueous cultivation broth. Few strategies for selecting a suitable solvent have been developed, targeting efficient extraction in terms of capacity and selectivity, simultaneously exhibiting no detrimental effects on the whole-cell biocatalysts [72, 73]. The latter has been identified as one of the most exclusive parameters in solvent selections for bioprocesses

due to the lack of biocompatibility of many solvents [74]. However, although case studies highlighted economic benefits [75, 76], holistic approaches and their implementations in industry are hardly reported. Another challenge is the emulsification occurring when the two liquid phases are in direct contact. However, membrane-supported approaches and other methods promise remediation [77]. Further, aqueous two-phase systems have been used in bioprocesses [78].

A product can be removed from the cultivation broth by evaporation. Here, the product needs to be more volatile than water, as water is the main component of a cultivation broth. Different technical implementations have been assessed, ranging from simple gas stripping [79, 80] to flash or vacuum fermentations [81, 82] and continuous product distillations with cell retention [83]. For gas stripping, the conventionally applied gas stream in aerated bioreactors can be used to recover the product. Although flash and vacuum fermentations can significantly enhance productivity [69, 76], these approaches appeared to be economically unfavorable. In contrast, continuous distillation with cell retention by centrifugation was previously successfully applied and transferred to industrial scale more than three decades ago [83].

Another method for ISPR is immobilization in the form of adsorption. Here, the product is adsorbed onto a resin, such as a polymeric matrix, and is thereby withdrawn from the cultivation broth. The characteristics and the type of the polymeric matrix need to be tailored to the product. In this regard, the interaction between the matrix and the product is most prominently based on hydrophobic or ionic interactions [69]. As the surface of the matrix is decisive for the capacity of product removal, mesoporous materials with engineered pore structures and functionalities have been applied [84, 85]. With higher capacity, the cost for applied material can be reduced, resulting in economic viability.

The molecular size of the product can be utilized for its separation in bioprocesses, similar to established methods in conventional DSP. Here, selective membranes allow the permeation of the product while retaining other components of the cultivation broth in the reactor compartment. The main driving force is either the concentration gradient of the product or the pressure gradient across the membrane [86]. The product needs to be removed from the downstream side of the membrane to maintain the gradient. Therefore, membranes are most effectively combined with other methods of ISPR, such as evaporation (resulting in pervaporation) and LLE (resulting in perstraction). Further, the introduction of a membrane either for selective permeation of the product or for cell retention prevents the direct contact of the whole-cell biocatalyst and the extractant, which is beneficial in terms of biocompatibility or biodegradability [70]. However, fouling and obstruction of the membrane need to be considered.

Other methods exploit the solubility and reactivity of the product for ISPR. Here, the product is precipitated or crystallized [87], or the solubility of the product is adjusted by reversible

complexation of the product. Precipitation can occur spontaneously if the product concentration exceeds the saturation concentration [87, 88] or is, among others, mediated electrochemically [89]. The complexation or other binding of the product involving a chemical reaction is referred to as reactive extraction [90, 91] and is typically combined with other ISPR techniques.

1.4.2 *In situ* liquid-liquid extraction in the scope of bioprocess intensification

Considering ISPR as a method for bioprocess intensification, the importance of holistic process perspectives and the definition of a common operational window as described in previous sections become obvious. Here, this is demonstrated at the example of *in situ* LLE for the recovery of a microbially produced compound.

By utilizing molecular biology, the whole-cell biocatalysts can be engineered to enhance production and tailor the strain to specific reaction conditions, here, the presence of an organic solvent. In turn, regarding reaction engineering, the solvent has to guarantee efficient extraction and likewise sufficient biocompatibility to sustain growth and production. Thus, the conditions for optimal extraction have to match cultivation conditions. Similarly, considerations for further DSP are required in early stages of process development to recover the product from the extractant efficiently. Further, the economic and ecologic impact of the used solvent has to be assessed. Concluding, all mentioned disciplines are dependent on each other for successfully implementing the most efficient production process.

1.5 Integrated bioprocessing for the production of rhamnolipids

This thesis focuses on the interactions of different stages of bioprocess development and aims to advocate holistic perspectives of bioprocess chains. Practically, this was demonstrated at the example of intensifying a biosurfactant production process with recombinant *Pseudomonas putida* KT2440 serving as the whole-cell biocatalyst. To fully comprehend the studied system, short introductions into the topics of *P. putida*, biosurfactants, and the challenges for production are given in the following paragraphs.

1.5.1 Biosurfactants

A group of products that have recently drawn increased attention for biotechnological production are biosurfactants as a replacement for conventional surfactants [92]. Surfactants are amphiphilic molecules and are therefore utilized in several commodities, such as cleaning agents, cosmetics, and food, due to their emulsifying properties. While conventional surfactants are based on fossil resources, typically requiring harsh conditions and elevated demands for energy for production [93], biosurfactants are produced from renewable feedstocks. Next to a replacement of

conventional surfactants, biosurfactants have distinct properties, which allow novel applications. Exemplary, as biosurfactants are typically biodegradable, they can be utilized in open environments, such as in agriculture and for remediation purposes, while having a smaller ecological footprint than their conventional counterparts [94]. Many other applications ranging from generic utilization in cleaning agents to oil recovery and highly specialized applications in medicine have been reported, which have been extensively described and reviewed [94, 95]. However, most proposed applications have not been established beyond the level of proof of concept or are predicted based on their physicochemical properties, with few exceptions, mainly in the detergent industry. Nevertheless, the economic interest in biosurfactants is rising, expressed by a generated revenue expected to increase from 4.5 billion USD in 2020 to 6.5 billion USD by 2027 [96]. However, due to the broad range of proposed applications and resulting requirements for the final product, the market price of biosurfactants is varying strongly.

Multiple microorganisms are capable of naturally producing biosurfactants [97]. The synthesis of biosurfactants typically gives the host an advantage in specific environments. For example, biosurfactants are used by its producer to make carbon sources, specifically hydrophobic hydrocarbons, accessible as a nutrient and energy source [98]. Depending on the microorganism and its specific environmental niche, different classes of biosurfactants have been discovered and classified in the groups of glycolipids, phospholipids, lipopeptides, as well as particulate and polymeric biosurfactants [97]. For biotechnological production, either the native producers are utilized, or metabolic production pathways are transferred to established chassis as reported by many studies [92]. In this thesis, the main focus is on the production of rhamnolipids (RLs). Therefore, a more detailed insight into this type of biosurfactant is given.

1.5.2 Rhamnolipids as prominent representatives of biosurfactants

Among biosurfactants, RLs are one of the most studied class of glycolipids [99]. As a surfactant, the molecular structure of RLs exhibits a hydrophilic and a hydrophobic moiety (Figure 3). The hydrophobic part typically comprises two β -hydroxy fatty acids, which are esterified by the acyltransferase RhIA to form a 3-(hydroxyalkanoxyloxy)alkanoic acid (HAA). The hydrophilic part is formed by the free or esterified carboxylic groups of the HAA, which can be enhanced by the fusion of rhamnose moieties catalyzed by the rhamnosyltransferases RhIB and RhIC [100]. The class of RLs itself covers more than 50 congeners [101]. Depending on the homolog of RhIA [102], the chain length and degree of saturation of the esterified β -hydroxy fatty acids can typically vary from 8 to 16 carbon atoms each [101], while chain lengths of up to 24 carbon atoms have been reported [103]. Further, the number of rhamnose moieties can vary from zero to two, depending on the synthesis of RhIB (adding the primary rhamnose moiety resulting

in a mono-RL) and RhIC (adding the secondary rhamnose moiety resulting in a di-RL). Additionally, other variants, such as RLs with one fatty acid chain or a double bond have been reported [102, 104].

RLs are highly promising to replace surfactants based on fossil resources as they can be efficiently produced by various microorganisms [102]. Its commercial interest has recently been highlighted by the successful introduction of a microbial RL production process by Evonik Industries AG and the subsequent application in commodities [105]. In previous studies, *Pseudomonas aeruginosa* has been used as the most common whole-cell biocatalyst for RL production. However, as *P. aeruginosa* is an opportunistic human pathogen, a transfer of the genetic cassette encoding enzymes responsible for RL production to non-pathogenic chassis strains has been adapted. In this thesis, recombinant *P. putida* KT2440, previously constructed and established to enable RL production [106, 107], has been used. In short, *P. putida* is regarded as a promising whole-cell biocatalyst for industrial applications due to several reasons. Its versatile metabolism allows great substrate flexibility [108, 109], and *P. putida* shows a robust phenotype at various environmental conditions. Its capability in regenerating redox cofactors [110, 111] results in high resistance against oxidative stress [112]. Detailed information on the mentioned characteristics and the application of *P. putida* for the production of various value-added compounds have been extensively reviewed [113–115], and relevant aspects are described in respective sections of this thesis.

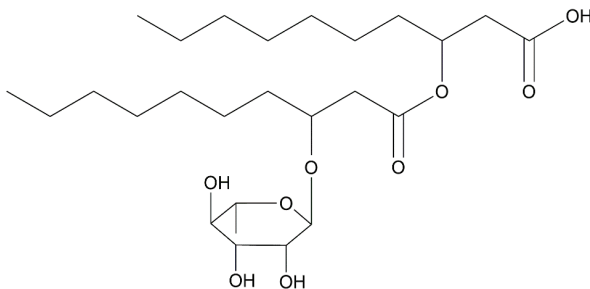


Figure 3 Representative structure of a rhamnolipid. The displayed RL is a mono-RL- C_{10} - C_{10} (one rhamnose moiety linked to a HAA with two carbon chains of 10 carbon atoms). Multiple different variants of RLs, so-called congeners, have been reported, varying in number of rhamnose moieties, carbon chain length, and saturation. This figure was previously published [125] and is reprinted with permission from Green Chemistry. Copyright The Royal Society of Chemistry 2020.

1.5.3 Challenges in rhamnolipid production and remedial approaches

The amphiphilic character of RLs is a desired trait for its application in multiple different products, as outlined above. However, the same characteristic imposes particular challenges for bioprocessing. The presence of RLs in the cultivation broth causes excessive foaming in conventional bioreactors due to the aeration and agitation applied to ensure sufficient oxygen transfer into the liquid for cellular respiration and to enable thorough mixing [116]. Titers in the lower range of mg L^{-1} of RLs in the cultivation broth already induce foaming at given conditions. This causes a rapid build-up of foam in the headspace of the reactor, eventually leading to an overflow of the reactor. The whole-cell biocatalyst is typically entrapped in the foam as it is physically equivalent to a particle in the liquid cultivation broth and attaches to the phase boundary due to hydrophobic regions of the cell surface [41, 117]. Therefore, the whole-cell biocatalyst is washed out of the reactor and is lost for catalyzing the reaction desired for production, resulting in an inefficient process.

To maintain efficiency, approaches for enabling bioprocessing were developed, which either can manage extensive foaming or prevent foaming in the first place. Intuitively, antifoaming agents have been added to the cultivations [118]. Although foam could be avoided and high titers of RLs were produced, a comparably high amount of antifoam was required. However, antifoam is typically expensive and has severe effects on the cultivation and particularly on DSP due to more complicated product recovery [119, 120]. Thus, the use of antifoam is regarded as economically unfavorable. In cultivations of *P. aeruginosa*, plant oil has been used as a substrate [121], simultaneously preventing foam formation. However, the same difficulties for DSP as described above occur.

Instead of preventing foam formation, the foam has been used as a method for ISPR. Here, the foam exits the reactor in a controlled manner and is subsequently fractionated [41, 122]. Promising approaches, *e.g.*, combined with integrated adsorption of RLs, have been established [117, 123]. However, the biocatalyst can still be washed out of the reactor as described above. Cell retention and cell recycling have been applied to mitigate the loss of whole-cell biocatalyst [117]. Further, Blesken *et al.* [41] engineered the cell surface to reduce the enrichment of *P. putida* KT2440 in the foam. While foam fractionation has been established as demonstrations of functionality in laboratory scale [124], a transferability to industrial-scale production is questionable. Another ISPR strategy could be the application of *in situ* liquid-liquid extraction, limiting the concentration of RLs in the cultivation broth below critical levels, thereby preventing foam formation.

The challenges to position renewable carbon-based chemicals in the market are specific to the respective product. Here, the challenges are outlined for RLs, for which their favorable traits cause difficulties in USP and DSP.

1.6 Scope and outline of this thesis

In the presented thesis, an integrated approach of USP and DSP development for the biochemical production of RLs with recombinant *P. putida* KT2440 as a whole-cell biocatalyst is pursued. USP development includes rational and untargeted strain engineering, the characterization of *P. putida* KT2440 to be suitable for industrial-scale production, and the development of novel fermentation and reactor concepts. Rather unconventional to common objectives in chassis design and metabolic engineering, strain engineering is here not mainly targeted to maximize product yields and titers, but it is process-guided, *i.e.*, the aim of strain engineering is to enable specific fermentation concepts. All approaches in USP development consider integrating DSP development and an overall process chain, with a focus on PI in a holistic perspective.

In Chapter 1, the thesis is embedded in the overall scope of the emerging bioeconomy. Strategies of integrated USP and DSP development and the intensification of fermentation processes are presented. In this regard, the concept of integrated and iterative adaptation of both the whole-cell biocatalyst and the reactor in the scope of holistic process development is introduced. As an exemplary holistic process development, the production of RLs with recombinant *P. putida* KT2440 is elucidated, building the structure of the presented thesis.

Chapter 2 details the experimental approaches, which have been performed to obtain and reproduce the results described in Chapter 3.

In Chapter 3.1, a methodology for selecting an *in situ* liquid-liquid extraction solvent for bioprocesses is presented and applied for a foam-free production of RLs in a two-liquid phase fermentation. A data-based selection preceded experimentally acquired performance parameters, such as extraction efficiency, biocompatibility, phase separation, and pH-dependency of extraction and back-extraction, to reduce the number of potentially suitable candidates, thus limiting the experimental effort to a reasonable level. The performance of the selected solvent was confirmed in laboratory-scale (fed-)batch fermentations, thereby defining a mutual operational window for integrated USP and DSP.

In Chapter 3.2, the approaches for both targeted and untargeted engineering of *P. putida* KT2440 to enhance its tolerance towards organic solvents, potentially used as extractants in two-liquid phase fermentations, are described. Targeted approaches included the expression of genes encoding for an efflux pump, a chaperone complex, and a cold-shock protein, all viewed as promising candidates for increasing or enabling solvent tolerance. Further, adaptive laboratory evolution (ALE) as an untargeted approach was applied to enhance tolerance to 1-octanol. Strains generated by introducing the unveiled point mutations into wild-type *P. putida* KT2440 *via* reverse

genome engineering were assessed for increased tolerance. The improved phenotypes of the strains were further characterized, and their capacities to produce RLs and 1-octanol were evaluated.

Chapter 3.3 further explores fed-batch cultivation strategies beyond the one developed in Chapter 3.1. The different feeding strategies comprise altering feeding profiles and compositions of the feeding solution. Their interactions with the implemented *in situ* extractions are evaluated. Further, catastrophic phase inversion (CPI) as a measure for breaking emulsions, particularly prominent in two-liquid phase fed-batch cultivations with high biomass titers, is assessed.

Chapter 3.4 focuses on the capability of *P. putida* KT2440, conventionally viewed as an obligate aerobic microorganism, to withstand repeated, short-term oxygen limitation. Thereby, it is assessed if the strain is suited for production in large-scale fermenters, in which gradients can occur due to non-ideal mixing, or in specialized compartmented reactors, such as the multiphase loop reactor described in the following chapter. Oscillation of dissolved oxygen tensions (DOTs) was induced across different cultivation scales and setups. Controlled scale-down experiments were performed to subject *P. putida* KT2440 to a defined duration of oxygen starvation, enabling comparison of growth at given conditions with well-aerated fermentations. Further, the impact of oscillating DOT values on the production of RLs was evaluated. First insights into coping mechanisms were gained by untargeted proteomics and the quantification of intracellular nucleotides.

In Chapter 3.5, the developed fermentation process for foam-free production of RLs is transferred from STRs to a novel multiphase loop reactor (MPLR). After the design and construction of the reactor, a first cultivation revealed that the installed aeration system could not satisfy the oxygen demand of the growing cells. Therefore, a redesigned, highly porous sparger enabling microbubble formation was constructed and integrated into the MPLR. A subsequent batch cultivation of RL-producing *P. putida* KT2440 could be supported until carbon depletion. Simultaneously, the implemented counter-current *in situ* LLE of RLs combined with specific bioprocess design prevented excessive foaming, and an *in situ* phase separation enabled continuous solvent recirculation. The newly established fermentation process was compared with STR cultivations of previous chapters.

In Chapter 4, the approaches for a holistic perspective on an integrated bioprocess design are discussed. Further considerations and general aspects of establishing microbial production processes in the industrial landscape to eventually contribute to the envisaged bioeconomy are presented.

Chapter 2

Materials & Methods

Partially published as

[125] Demling P, von Campenhausen M, Grütering C, Tiso T, Jupke A, Blank LM. 2020. Selection of a recyclable *in situ* liquid-liquid extraction solvent for foam-free synthesis of rhamnolipids in a two-phase fermentation. *Green Chemistry*. doi: 10.1039/D0GC02885A.

[Reprinted (adapted) with permission from Green Chemistry. © The Royal Society of Chemistry 2020]

[126] Demling P, Ankenbauer A, Klein B, Noack S, Tiso T, Takors R, Blank LM. 2021. *Pseudomonas putida* KT2440 endures temporary oxygen limitations. *Biotechnology & Bioengineering*. doi: 10.1002/bit.27938.

[Reprinted (adapted) with permission from Wiley & Sons. Open Access CC BY-NC-ND 4.0. © The Authors 2021]

Contributions

Maximilian von Campenhausen is the original author of the following subsections in the Material & Methods section of the published article [125]: “Extraction efficiencies” and “Phase separation”. Those sections have been included in this thesis, either in full or partially in an adapted form. Bianca Klein and Stephan Noack performed untargeted proteomics and provided technical details for this method, which is included in a compendious form. All other parts of this chapter were written by Philipp Demling and reviewed by Till Tiso and Lars M. Blank.

2 Materials & Methods

2.1 Chemicals

All chemicals used in this thesis were purchased from Sigma-Aldrich (St. Louis, MO, USA), Carl Roth (Karlsruhe, Germany), or Merck (Darmstadt, Germany).

2.2 Bacterial strains and growth media

All strains, which were used in this thesis are listed in Table 1. All constructed *Pseudomonas putida* KT2440 strains are based on the host-vector system safety level 1 (HV1) certified chassis strain *P. putida* KT2440 (DSMZ: 6125) [127–129].

For initial seed cultures, lysogeny broth (LB) was used (5 g L^{-1} yeast extract, 10 g L^{-1} tryptone, 2 g L^{-1} NaCl), whereas secondary seed cultures, characterization cultures, and production cultures were grown in a mineral salts medium (MSM) modified from Hartmans *et al.* [130] (10 g L^{-1} glucose, 11.64 g L^{-1} K_2HPO_4 , 4.89 g L^{-1} NaH_2PO_4 , 2 g L^{-1} $(\text{NH}_4)_2\text{SO}_4$, 0.1 g L^{-1} $\text{MgCl}_2 \cdot 6 \text{ H}_2\text{O}$, 10 mg L^{-1} EDTA, 2 mg L^{-1} $\text{ZnSO}_4 \cdot 7 \text{ H}_2\text{O}$, 1 mg L^{-1} $\text{CaCl}_2 \cdot 2 \text{ H}_2\text{O}$, 5 mg L^{-1} $\text{FeSO}_4 \cdot 7 \text{ H}_2\text{O}$, 0.2 mg L^{-1} $\text{Na}_2\text{MoO}_4 \cdot 2 \text{ H}_2\text{O}$, 0.2 mg L^{-1} $\text{CuSO}_4 \cdot 5 \text{ H}_2\text{O}$, 0.4 mg L^{-1} $\text{CoCl}_2 \cdot 6 \text{ H}_2\text{O}$, 1 mg L^{-1} $\text{MnCl}_2 \cdot 2 \text{ H}_2\text{O}$). Stock solutions for preparing the MSM are given in the Appendix A1, Table A1.1. The medium was highly buffered to counteract a decrease in the pH value due to gluconate production by *P. putida* KT2440. For batch and fed-batch bioreactor cultivations, during which the pH value can be controlled by acid or base addition, the phosphate buffer ($\text{K}_2\text{HPO}_4/\text{NaH}_2\text{PO}_4$) concentration was lowered threefold. For feeding, a concentrated and adjusted MSM was used (200 g L^{-1} glucose, 7.76 g L^{-1} K_2HPO_4 , 3.26 g L^{-1} NaH_2PO_4 , 40 g L^{-1} $(\text{NH}_4)_2\text{SO}_4$, 0.33 g L^{-1} $\text{MgCl}_2 \cdot 6 \text{ H}_2\text{O}$, 3 mg L^{-1} EDTA, 66 mg L^{-1} $\text{ZnSO}_4 \cdot 7 \text{ H}_2\text{O}$, 3.3 mg L^{-1} $\text{CaCl}_2 \cdot 2 \text{ H}_2\text{O}$, 16.5 mg L^{-1} $\text{FeSO}_4 \cdot 7 \text{ H}_2\text{O}$, 0.66 mg L^{-1} $\text{Na}_2\text{MoO}_4 \cdot 2 \text{ H}_2\text{O}$, 0.66 mg L^{-1} $\text{CuSO}_4 \cdot 5 \text{ H}_2\text{O}$, 1.32 mg L^{-1} $\text{CoCl}_2 \cdot 6 \text{ H}_2\text{O}$, 3.3 mg L^{-1} $\text{MnCl}_2 \cdot 2 \text{ H}_2\text{O}$, also modified from Hartmans *et al.* [130]). In Chapter 3.4, different feeding strategies are described, partially altering the feed compositions, which are detailed in the corresponding chapter.

If required, the media were supplemented with antibiotics in the concentrations of $50 \text{ } \mu\text{g L}^{-1}$ for kanamycin and $30 \text{ } \mu\text{g L}^{-1}$ for gentamycin. If *Escherichia coli* was cultivated in MSM, thiamine was added in a concentration of $10 \text{ } \mu\text{g L}^{-1}$.

2.3 Plasmid and strain construction

Plasmids and strains were mainly constructed to enhance the solvent tolerance of *P. putida* KT2440 to organic solvents. All strategies for plasmid construction and host strain engineering

were planned *a priori* and *in silico* with the software CloneManager 9 (SCI Ed Software LLC, Westminster, CO, USA). All generated strains and their respective parental strains are given in Table 1.

The construction of plasmids was designed with the NEBuilder Assembly online tool and subsequently performed with HiFi DNA Assembly (New England Biolabs, Ipswich, MA, USA) [131]. The DNA fragments for Gibson Assembly were amplified *via* polymerase chain reaction (PCR), applying the Q5 High Fidelity DNA Polymerase (New England Biolabs, Ipswich, MA, USA) and oligonucleotides with DNA overhangs, specifically annealing with the adjacent DNA fragments according to the NEBuilder Assembly online tool. All sequences of used oligonucleotides are listed in the Appendix A.1 (Table A1.2). Further, purified genomes (isolated with High Pure PCR Template Preparation Kit, Roche Holding, Basel, Switzerland) were used as template DNA for amplification. The genes encoding for the efflux pump TtgGHI were recovered from the genome of *Pseudomonas taiwanensis* VLB120, whereas the genes encoding for chaperone GroEL-GroES and the cold-shock protein CspA-II were amplified from the isolated genome of *P. putida* KT2440. Vectors, standardly linearized by restriction with XbaI (New England Biolabs, Ipswich, MA, USA) or occasionally amplified *via* PCR if necessary, were used in Gibson Assemblies for the construction of plasmids. Different types of plasmids were constructed to enable various expression levels and modi in the later host strain, depending on the expressed genes. In general, expression levels were chosen to be in a low range to minimize the additional burden on the cells. The low-copy vector pBT harbors the constitutive P_{lac} promotor [132], whereas pBNT harbors a salicylate-inducible promotor system *nagR/PnagAa* (based on Verhoef *et al.* [133]). Both vectors harbor a kanamycin selection cassette.

To construct the plasmids pBT-*groEL/groES* and pBT-*cspA-II*, the encoding DNA fragments were amplified with the primer pairs PD9/PD10 and PD13/PD14, respectively, and assembled with the PCR-amplified vector pBT.

Various expression systems were used to express the genes encoding for the efflux pump TtgGHI. Plasmid pBT-*ttgGHI* was constructed using linearized pBT vector and the genes *ttgGHI* amplified from the genome of *P. taiwanensis* VLB120 using oligonucleotide combination PD19/PD20. Further, a salicylate-inducible system was constructed by assembling the linearized pBNT vector with the *ttgGHI* coding sequence amplified with oligonucleotides PD21/PD22. In addition, the promotor system of pBNT was exchanged with varying constitutive promoters of different but generally low activities, which were previously developed and generously provided by Sebastian Köbbing (Institute of Applied Microbiology, RWTH Aachen University, Aachen, Germany, not published). The five promotor variants SPS_2.3_TCC_BCD2, SPS_2.8_ACC_BCD2, SPS_2.4_AAC_BCD2, SPS_2.5_TCG_BCD2, and

SPS_2.6_TAG_BCD2, listed from highest to lowest activity, have been introduced by amplifying respective nucleotide sequences from a promotor library with oligonucleotides SK1/SK2. For simplicity, only the first six characters of the promotors are given hereafter. Subsequently, the PCR-amplified, thus linearized pBNT vector lacking its original promotor (amplified with oligonucleotides PD23/PD24), the respective promotor sequences, and compatible DNA fragments encoding for TtgGHI (amplified with oligonucleotides PD25/PD26) were assembled by Gibson Assembly to construct all five variants of the plasmid collection pBNT-SPS2.X-*ttgGHI* (X represents the specific number and sequence of the promotor).

The constructed plasmids were transferred into either *E. coli* PIR2 or *E. coli* DH5 α by heat shock transformation as described by Hanahan [134], and resulting transformants were subsequently selected on LB agar plates supplemented with kanamycin. PCRs were performed using cell material lysed with 60% (v/v) alkaline polyethylene glycol adjusted to a pH value of 13 [135] as a template and the OneTaq polymerase (New England Biolabs, Ipswich, MA, USA) to verify the introduction of the plasmid with the correct size of the amplified region. Plasmids harboring inserts of the correct size were isolated with the Monarch Plasmid Miniprep Kit (New England Biolabs, Ipswich, MA, USA). The nucleotide sequences of regions of interest were in general verified by Sanger sequencing (Eurofins Genomics, Ebersberg, Germany). The respective plasmids were introduced individually into competent *P. putida* KT2440 cells *via* electroporation [136] performed in a cuvette with a gap size of 2 mm and a GenePulser XCell (Bio-Rad, Hercules, CA, USA) at 2.5 kV, 200 Ω , and 25 μ F. Subsequently, the obtained transformants were selected for antibiotic resistance and validated by colony PCR as described above.

The I-SceI-based genome editing method originally described by Martínez-García and de Lorenzo [133] was used for the targeted deletion of genes. Here, two target sequence (TS) regions spanning approximately the 500 bp up- and downstream of the region of interest in the genome of *P. putida* KT2440 were amplified. The fragments were incorporated into the pEMG vector *via* Gibson Assembly, and the resulting plasmid was introduced into *E. coli* PIR2 by heat shock transformation [134]. The resulting transformants were verified to carry a plasmid with an insert of the correct size by colony PCR. A positive clone was then used to transfer the plasmid into the *Pseudomonas* chassis strains *via* conjugational transfer. The protocol for triparental mating modified by Wynands *et al.* [137] was followed. First, the non-replicative pEMG plasmid was integrated into the genome of the *Pseudomonas* chassis *via* homologous recombination. Subsequently, the pEMG backbone was removed by introducing the I-SceI-harboring plasmid pSW-2 resulting in targeted restriction, thus forcing homologous recombination for the strain to survive. Kanamycin-sensitive clones were validated for the deletion of the targeted gene *via* colony PCR. Positive clones were sequentially cultivated in LB medium without antibiotics, causing the

cells to lose the pSW-2 plasmid, thus generating marker-free strains. The strains were once again validated for the targeted deletion using colony PCR for final confirmation.

The I-SceI-based genome editing method was additionally used to introduce targeted point mutations into the genome of the *Pseudomonas* chassis strains *P. putida* KT2440 and *P. putida* KT2440 3x Δ *fad*. Generally, the protocol described above was followed, apart from integrating the point mutation in the overhang sequences of the oligonucleotides generating the TS1 fragments amplified from the genome of *P. putida* KT2440 and used to construct the respective pEMG plasmids. The successful introduction of point mutations was verified by Sanger sequencing (Eurofins Genomics, Ebersberg, Germany).

Further, to reduce the copy number, a part of SPS2-*X-ttgGHI* variants was introduced into the genome of *P. putida* KT2440 at three different loci identified to result in varying expression levels [138]. Here, pEMG plasmids, which were generously provided by Sebastian Köbbing (Institute of Applied Microbiology, RWTH Aachen University, Aachen, Germany), harboring the respective SPS2-*X-ttgGHI* variants and specifically integrating into the genomic regions close to the genes encoding for PP_1738, PP_3808, and PP_4945 were chosen [138].

Constructed strains, which showed an increased solvent tolerance, were evaluated for their feasibility to produce value-added compounds. Rhamnolipid (RL) production was enabled by integrating the genes *rhlAB* from *Pseudomonas aeruginosa* PAO1 into the genome of chassis strains. The mini-Tn7 delivery transposon vector pSK02 [139] harboring the constitutive synthetic promoter P_{ffg} [140] and *rhlAB* was introduced into the chassis strains and integrated into the genome *via* transposition as previously described by Zobel *et al.* [141]. Correct integration was confirmed by colony PCR. To qualitatively assess the production capacity of obtained clones, the hemolytic activity of mono-RLs was utilized. Halos surrounding colonies incubated on a cetrimide-blood agar plate supplemented with 7.5% (v/v) sheep blood indicated productivity. To quantitatively determine the production capacity, several clones were cultivated in MSM, and the RL titer was quantified by high-performance liquid chromatography (HPLC) measurements after 24 h of incubation. Best performing producers were selected for further studies.

Alternatively, 1-octanol was chosen as a potential product synthesized by solvent tolerant strains. To enable production of 1-octanol from glucose as the sole carbon source, the plasmid pOCT04 generously provided by Till Tiso was introduced into several solvent tolerant strains *via* electroporation. The plasmid pOCT04 harbors the genes encoding for the *Anaerococcus tetradius* acyl-ACP thioesterase (Tes3), the *Mycobacterium marinum* carboxylic acid reductase (CAR), the *Bacillus subtilis* phosphopantetheinyl transferase (Sfp), and the *E. coli* aldehyde reductase (AHR), representing the whole pathway for 1-octanol production from octanoyl-ACP provided by the *de novo* fatty acid synthesis native to *P. putida* KT2440.

Table 1 Bacterial strains used and constructed in this study.

Strain	Characteristics	Reference or Source	iAMB strain #
<i>E. coli</i>			
DH5α	<i>supE44</i> , Δ <i>lacU169</i> (Φ 80 <i>lacZ</i> Δ <i>M15</i>), <i>hsdR17</i> (τ_K^- m_K^+), <i>recA1</i> , <i>endA1</i> , <i>thi-1</i> , <i>gyrA96</i> , <i>relA1</i>	[142]	2382
DH5α <i>λ</i> pir	<i>λ</i> pir lysogen of DH5α; host for <i>oriV</i> (R6K) vectors	[143]	2077
PIR2	F ⁺ , Δ <i>lacI69</i> , <i>rpoS</i> (<i>Am</i>), <i>robA1</i> , <i>creC510</i> , <i>hsdR514</i> , <i>endA</i> , <i>recA1 uidA</i> (Δ <i>MluI</i>): <i>pir</i> ; host for <i>oriV</i> (R6K) vectors	Thermo Fisher Scientific	3222
HB101 pRK2013	Sm ^R , <i>hsdR-M'</i> , <i>proA2</i> , <i>leuB6</i> , <i>thi-1</i> , <i>recA</i> ; harboring plasmid pRK2013: Km ^R , <i>oriV</i> (RK2/ColE1), <i>mob</i> ⁺ , <i>tra</i> ⁺	[144]	2037
DH5α pSW-2	DH5α harboring plasmid pSW-2: Gm ^R , <i>ori</i> RK2, <i>xyiS</i> , P _m → I-SceI (transcriptional fusion of I-SceI to P _m), tool for genomic deletion	[145]	2404
DH5α <i>λ</i> pir pEMG	DH5α <i>λ</i> pir harboring plasmid pEMG: Km ^R , <i>ori</i> R6K, <i>lacZα</i> with two flanking I-SceI sites	[145]	2075
DH5α <i>λ</i> pir pTNS1	DH5α <i>λ</i> pir harboring plasmid pTNS1: Ap ^R , <i>ori</i> R6K, <i>TnSABC+D</i> operon	[146]	3221
DH5α <i>λ</i> pir pSK02	DH5α <i>λ</i> pir harboring Tn7 delivery vector pSK02 (derived from pBG14f_80i_14f_80i_14g) for chromosomal integration of <i>rhlAB</i> genes from <i>P. aeruginosa</i> PA01	[139]	5234
PIR2 pOCT04	PIR2 harboring plasmid pOCT04 for 1-octanol synthesis: Km ^R , <i>oriT</i> , <i>tes3</i> , <i>car</i> , <i>sfp</i> , <i>ahr</i>	Till Tiso	5162
DH5α pBT	DH5α harboring plasmid pBT: Km ^R , P _{tac} (constitutive), <i>ori</i> pBBR1, expression vector	[132]	2049
DH5α pBNT	DH5α harboring plasmid pBNT: Km ^R , <i>nagR/PnagAa</i> (salicylate-inducible), expression vector	[133]	2047
DH5α pBT- <i>ttgGHI</i>	DH5α harboring plasmid pBT- <i>ttgGHI</i>	This study	6935
DH5α pBNT- <i>ttgGHI</i>	DH5α harboring plasmid pBNT- <i>ttgGHI</i>	This study	6936
DH5α pTn7-SPS_2.X_NNN_BCD2_msGFP	DH5α harboring pTn7 plasmids with promotor variants of the library with msGFP, combinations for 2.X_NNN: 2.3_TCC, 2.4_AAC, 2.5_TCG, 2.6_TAG, 2.8_ACC, promoters were amplified from the respective strain	Sebastian Köbbing (unpublished)	-
PIR2 pEMG_PP_1738_int	PIR2 harboring pEMG_PP_1738 for chromosomal integration at PP_1738 of <i>P. putida</i> KT2440	[138]	6558
PIR2 pEMG_PP_3808_int	PIR2 harboring pEMG_PP_1738 for chromosomal integration at PP_3808 of <i>P. putida</i> KT2440	[138]	6590
PIR2 pEMG_PP_4945_int	PIR2 harboring pEMG_PP_1738 for chromosomal integration at PP_4945 of <i>P. putida</i> KT2440	[138]	6578
<i>P. taiwanensis</i>			
VLB120	wild type	[147]	2060

Strain	Characteristics	Reference or Source	iAMB strain #
<i>P. putida</i>			
KT2440	wild type	[128]	2058
KT2440 SK4	<i>P. putida</i> KT2440 with <i>atrTn7::P_{trg}-rhlAB</i>	[148]	5252
KT2440 pBT- <i>groEL/groES</i>	<i>P. putida</i> KT2440 harboring plasmid pBT- <i>groEL/groES</i>	This study	6937
KT2440 pBT- <i>cspA-II</i>	<i>P. putida</i> KT2440 harboring plasmid pBT- <i>cspA-II</i>	This study	6938
KT2440 pBT- <i>ttgGHI</i>	<i>P. putida</i> KT2440 harboring plasmid pBT- <i>ttgGHI</i>	This study	6939
KT2440 pBNT- <i>ttgGHI</i>	<i>P. putida</i> KT2440 harboring plasmid pBNT- <i>ttgGHI</i>	This study	6940
KT2440 pBNT-SPS_2.3_TCC_BCD2_ <i>ttgGHI</i>	<i>P. putida</i> KT2440 harboring plasmid pBNT-SPS_2.3_TCC_BCD2_ <i>ttgGHI</i>	This study	6941
KT2440 pBNT-SPS_2.4_AAC_BCD2_ <i>ttgGHI</i>	<i>P. putida</i> KT2440 harboring plasmid pBNT-SPS_2.4_AAC_BCD2_ <i>ttgGHI</i>	This study	6942
KT2440 pBNT-SPS_2.5_TCG_BCD2_ <i>ttgGHI</i>	<i>P. putida</i> KT2440 harboring plasmid pBNT-SPS_2.5_TCG_BCD2_ <i>ttgGHI</i>	This study	6943
KT2440 pBNT-SPS_2.6_TAG_BCD2_ <i>ttgGHI</i>	<i>P. putida</i> KT2440 harboring plasmid pBNT-SPS_2.6_TAG_BCD2_ <i>ttgGHI</i>	This study	6944
KT2440 pBNT-SPS_2.8_ACC_BCD2_ <i>ttgGHI</i>	<i>P. putida</i> KT2440 harboring plasmid pBNT-SPS_2.8_ACC_BCD2_ <i>ttgGHI</i>	This study	6945
KT2440 SPS_2.3_PP_1738:: <i>ttgGHI</i>	<i>P. putida</i> KT2440 with chromosomally integrated SPS_2.3_TCC_BCD2_ <i>ttgGHI</i> at PP_1738	This study	6946
KT2440 SPS_2.4_PP_1738:: <i>ttgGHI</i>	<i>P. putida</i> KT2440 with chromosomally integrated SPS_2.4_AAC_BCD2_ <i>ttgGHI</i> at PP_1738	This study	6947
KT2440 SPS_2.5_PP_1738:: <i>ttgGHI</i>	<i>P. putida</i> KT2440 with chromosomally integrated SPS_2.5_TCG_BCD2_ <i>ttgGHI</i> at PP_1738	This study	6948
KT2440 SPS_2.6_PP_1738:: <i>ttgGHI</i>	<i>P. putida</i> KT2440 with chromosomally integrated SPS_2.6_TAG_BCD2_ <i>ttgGHI</i> at PP_1738	This study	6949
KT2440 SPS_2.8_PP_1738:: <i>ttgGHI</i>	<i>P. putida</i> KT2440 with chromosomally integrated SPS_2.8_ACC_BCD2_ <i>ttgGHI</i> at PP_1738	This study	6950
KT2440 SPS_2.4_PP_3808:: <i>ttgGHI</i>	<i>P. putida</i> KT2440 with chromosomally integrated SPS_2.4_AAC_BCD2_ <i>ttgGHI</i> at PP_3808	This study	6951
KT2440 SPS_2.5_PP_3808:: <i>ttgGHI</i>	<i>P. putida</i> KT2440 with chromosomally integrated SPS_2.5_TCG_BCD2_ <i>ttgGHI</i> at PP_3808	This study	6952
KT2440 SPS_2.8_PP_3808:: <i>ttgGHI</i>	<i>P. putida</i> KT2440 with chromosomally integrated SPS_2.8_ACC_BCD2_ <i>ttgGHI</i> at PP_3808	This study	6953
KT2440 SPS_2.3_PP_4945:: <i>ttgGHI</i>	<i>P. putida</i> KT2440 with chromosomally integrated SPS_2.3_TCC_BCD2_ <i>ttgGHI</i> at PP_4945	This study	6954
KT2440 RIS1	<i>P. putida</i> KT2440 recovered after cultivation stage 1 from replicate 1 from ALE to the presence of 1-octanol, no exposure to 1-octanol after stage 1	This study	-
KT2440 RIS4	<i>P. putida</i> KT2440 recovered after cultivation stage 4 from replicate 1 from ALE to the presence of 1-octanol	This study	6967

Strain	Characteristics	Reference or Source	iAMB strain #
KT2440 R2S4	<i>P. putida</i> KT2440 recovered after cultivation stage 4 from replicate 2 from ALE to the presence of 1-octanol	This study	6968
KT2440 R3S4	<i>P. putida</i> KT2440 recovered after cultivation stage 4 from replicate 3 from ALE to the presence of 1-octanol	This study	6969
KT2440 PP_3453-P324R	<i>P. putida</i> KT2440 with AA exchange P324R of PP_3453	This study	6770
KT2440 PP_3454-P106R	<i>P. putida</i> KT2440 with AA exchange P106R of PP_3454	This study	6771
KT2440 ΔPP_3453	<i>P. putida</i> KT2440 with deleted PP_3453	This study	6772
KT2440 ΔPP_3454	<i>P. putida</i> KT2440 with deleted PP_3454	This study	6773
KT2440 ΔPP_3453 ΔPP_3454	<i>P. putida</i> KT2440 with deleted PP_3453 and PP_3454	This study	6774
KT2440 PP_3453-P324R <i>rhlAB</i>	<i>P. putida</i> KT2440 PP_3453-P324R with <i>atrTn7::P_{flg}-rhlAB</i>	This study	6775
KT2440 PP_3454-P106R <i>rhlAB</i>	<i>P. putida</i> KT2440 PP_3454-P106R with <i>atrTn7::P_{flg}-rhlAB</i>	This study	6776
KT2440 pOCT04	<i>P. putida</i> KT2440 harboring pOCT04	Till Tiso	5168
KT2440 PP_3453-P324R pOCT04	<i>P. putida</i> KT2440 PP_3453-P324R with pOCT04	This study	-
KT2440 PP_3454-P106R pOCT04	<i>P. putida</i> KT2440 PP_3454-P106R with pOCT04	This study	-
KT2440 3Δ <i>fad</i> pOCT04	<i>P. putida</i> KT2440 3Δ <i>fad</i> with pOCT04	Till Tiso	-
KT2440 3Δ <i>fad</i> PP_3453- P324R pOCT04	<i>P. putida</i> KT2440 3Δ <i>fad</i> PP_3453-P324R with pOCT04	This study	-
KT2440 3Δ <i>fad</i> PP_3454- P106R pOCT04	<i>P. putida</i> KT2440 3Δ <i>fad</i> PP_3454-P106R with pOCT04	This study	-

Only final constructed strains, their parent strains, and strains utilized for their characteristics are presented. Transitional strains (e.g., for plasmid construction) are omitted if not used in characterization experiments.

2.4 Cultivation strategies

2.4.1 Strain propagation

A strict strain propagation protocol was followed for the characterization of strains or production cultures. In general, aliquots of cryopreserved strains (20% (v/v) glycerol, optical density (OD₆₀₀) of 5, -80 °C) were streaked onto agar plates and incubated at 30 °C for 24 h. Single colonies were picked to inoculate 5 mL LB medium incubated at 30 °C and 300 rpm in an orbital shaker (shaking diameter: 50 mm) for initial liquid seed cultures. At mid-exponential growth phase, appropriate volumes of the first seed culture were transferred to the second seed culture consisting of 50 mL MSM supplied with 10 g L⁻¹ glucose. The second seed culture was incubated at the same conditions as stated above and harvested for transfer into main cultures during the mid-exponential growth phase.

2.4.2 Cultivations for characterizing the biocompatibility of solvents

2.4.2.1 Qualitative assessment of the biocompatibility of organic solvents

The biocompatibility, indicated by the tolerance of wild-type and engineered strains to a specific solvent, was primarily assessed in simplistic cultivation setups to gain qualitative results. For this, 1 mL MSM inoculated with the respective strain to an OD₆₀₀ of 0.05 was overlaid with 200 μ L solvent in hangar tubes. The tubes were sealed air-tight to prevent evaporation of the solvent. Further, the glucose concentration of the MSM was set to 2 g L⁻¹ to avoid a complete consumption of the oxygen provided in the headspace of the tube (approximately 14 mL). The cultures were incubated at 30°C and a shaking frequency of 200 rpm for an indefinite time. Regularly, the cultures were inspected for developed turbidity, indicating growth.

2.4.2.2 Quantitative assessment of the biocompatibility of organic solvents

Strains qualitatively showing tolerance to solvents were cultivated in 50 mL MSM in presence of the respective solvent at fixed phase ratio ϕ of 1:25 (v/v) organic to aqueous phase in a three-neck 1.3 L shake flask. The cultures were incubated at 30°C and a shaking frequency of 150 rpm. As state-of-the-art methods for biomass quantification were not feasible due to the formation of stable emulsions, CO₂ production was used as an indicator for growth. CO₂ was measured in the headspace of shake flasks by BCP-CO₂ sensors, and the data was monitored with BlueVis (both BlueSens, Herten, Germany). The shake flask was closed to avoid any evaporation of the solvent. Additionally, custom-made reservoirs filled with 1 mL solvent were installed in the headspace to saturate the gaseous phase of the shake flask with the respective solvent. The maximal consumable glucose concentration in the medium was estimated to 6.3 g L⁻¹ based on the amount of available oxygen in the headspace of the shake flasks. For this, the assumptions of ideal gas law and pure combustion reaction were applied, neglecting biomass and potential product formation. The solvents may potentially be degraded and used as a carbon source resulting in further production of CO₂ after glucose depletion. To observe potential diauxic shifts, the glucose concentration was set to 3 g L⁻¹, well below the maximally consumable concentration estimated above.

Next to assessing the biocompatibility and biodegradation of solvents, the cultivation setup was used for adaptive laboratory evolution (ALE) described in Chapter 2.5.

2.4.3 Microtiter plate cultivations

2.4.3.1 Microtiter plate cultivations in the BioLector

Microtiter plate cultivations were performed in Round Well Plates (MTP-R48-B, m2p-labs, Baesweiler, Germany; sealing: Breathseal Sealer, Greiner Bio-One, Kremsmünster, Austria) and were controlled by the BioLector I (m2p-labs, Baesweiler, Germany). The filling volume of the

wells was set to 1 mL of MSM inoculated to an initial OD₆₀₀ of 0.05. The cultivation temperature was kept constant at 30 °C, and humidity control was activated to limit evaporation.

In Chapter 3.4, the impact of repeated temporary oxygen limitation on growth and production of *P. putida* KT2440 is described. To subject the cells to temporary but repetitive low dissolved oxygen tensions (DOTs), specialized shaking profiles were designed, as the maximal oxygen transfer rate (OTR_{max}) is dependent on the shaking frequency [149]. A shaking profile oscillating between 1,200 rpm and 200 rpm for specific time intervals was established by developing a script implemented in the respective backend setups of each run. According to the equation published by Lattermann *et al.* [150] (Appendix A.1, Equation 20) to estimate the OTR_{max} at different cultivation conditions, approximate OTR_{max} of 1.2 mmol L⁻¹ h⁻¹ and 60.0 mmol L⁻¹ h⁻¹ have been predicted for low and high shaking frequencies, respectively, thereby validating intended oscillations. Time intervals of high and low shaking frequencies were identical within one cultivation, *i.e.*, the duration of vigorously shaking was set equal to the duration of restricted shaking. Time intervals of 2 min, 4 min, and 6 min were tested and compared to a control cultivation constantly shaking at 1,200 rpm. Measurement intervals were synchronized with shaking intervals to record the backscatter as an online signal for biomass always at a shaking frequency of 1,200 rpm. Thereby, an erroneous signal caused by sedimented cells was avoided.

2.4.3.2 Microtiter plate cultivations in the Growth Profiler and System Duetz

For characterizing growth, the constructed strains and respective controls were cultivated in either 24- or 96-square deep-well microtiter plates (MTPs), which were incubated in the Growth Profiler 960 (EnzyScreen, Heemstede, Netherlands), allowing online monitoring of growth due to the transparent bottom of the plates. In general, cultures were inoculated to a starting OD₆₀₀ of 0.1 and subsequently incubated at 225 rpm and 30 °C. The green value, derived from image analysis of individual wells by the Growth Profiler Control Software v2_0_0, served as a measure for growth and was recorded by the detector every 30 min. Cultivations in the 24-well MTPs were performed at a filling volume of 1 mL MSM (10 g L⁻¹ glucose), whereas the filling volume of cultivations in 96-well MTPs was set to 0.2 mL MSM (10 g L⁻¹ glucose). Sandwich covers corresponding to the respective plates were used to seal the plates while still guaranteeing sufficient aeration [151].

If only final titers of produced RLs were determined, cultures in non-transparent deep-well MTPs were incubated at 300 rpm continuous shaking and 30 °C without online monitoring of biomass. The cultures were sampled after 24 h.

2.4.4 Cultivations in stirred-tank reactors

In general, batch and fed-batch cultivations performed in stirred tank reactors (STRs) were fully controlled by BioFlo120 units and DASware Control Software 5.5.0 (both Eppendorf, Jülich, Germany). The respective working volumes of MSM were inoculated with the second seed culture to an initial OD₆₀₀ of 0.2. The pH value was monitored with online pH probes (phferm, Hamilton Company, Bonaduz, Switzerland) and kept at the desired value by the automated addition of 4 M H₂SO₄ and 4 M KOH. The DOT value was surveilled with online probes (VisiFerm, Hamilton Company, Bonaduz, Switzerland). For all cultivations, the temperature was set to 30 °C. If applicable, O₂ and CO₂ concentrations in the exhaust gas were measured by BlueInOne Ferm Gas analyzers and monitored with BlueVis (both BlueSens GmbH, Herten, Germany). Cultures producing RLs were performed in two-liquid phase cultivations to enable an *in situ* extraction of RLs and thereby avoid extensive foaming. When wild-type *P. putida* KT2440 was cultivated, and thus no RLs were produced, no organic solvent was added to the bioreactor.

In Chapter 3.4, the effect of repeated oxygen starvation on the growth of wild-type *P. putida* KT2440 is described. The corresponding batch cultivations were performed in 3 L STRs (Eppendorf, Jülich, Germany) with a working volume of 2 L. The pH was kept constant at a value of 7. To induce oscillating DOT values throughout the cultivations, agitation and aeration were periodically altered between low (25 rpm, 0 L min⁻¹) and high (800 rpm, 2 L min⁻¹) setpoints. Intervals of high and low agitation and aeration rates were set to equal durations of 2 min or 4 min. Control cultivations were aerated and agitated constantly at high setpoints.

In Chapter 3.1, two-liquid phase fermentation processes were developed for the *in situ* extraction of RLs produced by *P. putida* KT2440 SK4. These cultivations were performed in 1.3 L STRs (Eppendorf, Jülich, Germany) with a working volume of 700 mL MSM overlaid with 100 mL ethyl decanoate. Cultivations were performed at different pH values of 6, 6.5, and 7 to assess its influence on *in situ* extraction, growth, and production. Once set, the pH value was kept constant during the respective cultivations. The DOT value was maintained at above 30 % by a cascaded agitation (400 - 1,000 rpm) to prevent oxygen limitation. The aeration rate was kept constant at 0.7 L min⁻¹.

Further, in Chapter 3.4, cultivations for assessing the influence of oscillating DOT values on RL production by *P. putida* KT2440 SK4 were performed. Here, the conditions for two-liquid phase cultivations were adjusted to 3 L STRs (Eppendorf, Jülich, Germany) with a working volume of 2 L MSM by adding 250 mL ethyl decanoate to avoid foaming. The interval of oscillating aeration and agitation, as described above for non-producing cultures, was set to 2 min. Continuously well-aerated and well-agitated cultivations were performed as a control. The pH was maintained at a value of 6.

Fed-batch cultivations as described in Chapter 3.1 and further developed in Chapter 3.3 were generally performed in 1.3 L STRs (Eppendorf, Jülich, Germany) with a reduced initial working volume of 400 mL MSM to allow the addition of feed solutions. As a second liquid phase for *in situ* extraction, 100 mL ethyl decanoate was added. The agitation was kept constant at 1,000 rpm, and the setpoint of the pH value was manually reduced when foam covered the surface of the cultivation broth. All other parameters were set as described for batch cultivations. The feeding strategy and the composition varied as these were subject for optimization and are thus described in the respective sections of Chapter 3.3. For the fed-batch cultivation in Chapter 3.1, a DOT-based feeding strategy was chosen. When the DOT signal increased, indicating a depletion of carbon source, the feeding pump was activated. At a DOT value of 70%, the pump rate was set to 12 mL h⁻¹ resulting in an addition of feed solution and a decrease of the DOT value. At a DOT value of 30%, feeding was stopped until the carbon source was once again depleted, and a DOT value of 70% was reached, thus initiating the feeding loop once again. A total of 247 mL concentrated feed solution, as described in Chapter 2.2, were added throughout the fermentation.

In Chapter 3.2, 1-octanol was used as a solvent for the *in situ* extraction of RLs produced by tolerant *P. putida* KT2440 with a production cassette integrated into the genome in batch cultivations. The cultivations were performed in 3 L STRs (Eppendorf, Jülich, Germany) with a working volume of 1.5 L MSM and 250 mL 1-octanol. Cascaded agitation (400 - 1,000 rpm) ensured a DOT value at above 30%, whereas the aeration rate was kept constant at 1.5 L min⁻¹. The pH was controlled at a value of 7. All other parameters were set as generally described above.

2.4.5 Cultivations in a parallel fermentation system

The DASbox 2.1 cultivation system (Eppendorf, Jülich, Germany) was used to assess the impact of different DOT values on the growth of *P. putida* KT2440. Single DASBox reactors with a filling volume of 200 mL of MSM (10 g L⁻¹ glucose) were inoculated to an initial OD₆₀₀ of 0.15. The temperature was kept constant at 30 °C, and the pH was controlled at a value of 7 by adding 2 M KOH and 4 M H₂SO₄. The initial agitation and the initial aeration rate were set to 400 rpm and 100 mL min⁻¹ (0.5 vvm), respectively. With increasing biomass and thus increasing oxygen demand, a cascade maintained constant DOT values above thresholds set to 60%, 30%, 15%, and 5%. The cascade was set up to first increase the agitation from 400 rpm at an output value of 0% to 1,200 rpm at an output value of 40% and the aeration rate from 100 mL min⁻¹ at an output of 40% to 200 mL min⁻¹ at an output of 100%. During the cultivation, it was observed that the cascade was not ideally set to maintain the DOT at a value 60% for the respective reactors. Thus, it was adjusted to an agitation of 1,800 rpm at an output value of 40%. This was done for all reactors to ensure comparability. Further, neither the factory-set proportional-integral-derivative (PID)

controller values nor well-tested PID controller values from previous cultivations in the BioFlo120 system at a scale of 1.5 L were suitable for both pH and DOT control, resulting in oscillations due to overdriving. Therefore, respective settings were adjusted during the fermentations.

2.4.6 Cultivations in the multiphase loop reactor

The multiphase loop reactor (MPLR) was developed based on a patent and succeeding simulations at the Chair of Fluid Process Engineering, RWTH Aachen University [54–56]. In short, the reactor is a modified air lift reactor (ALR). The inner compartment is delimited by a hanging cylinder inserted into a standard 5 L glass vessel (Eppendorf, Jülich, Germany) of a larger diameter ($d_{\text{cylinder}} = 144 \text{ mm}$, $d_{\text{vessel}} = 176 \text{ mm}$). The cylinder-ring gap defines the outer compartment, which is called the downcomer. When the inner compartment, named the riser, is aerated, a loop flow of a continuous fluid phase is induced. The fluid rises above the upper edge of the cylinder, enters the outer compartment, and flows into the riser at the bottom of the reactor. In the lower part of the downcomer, an organic solvent is dispersed and rises to the liquid surface due to a difference in density compared to the continuous aqueous phase. Therefore, a counter-current liquid-liquid extraction is established (Figure 4A).

Cultivations in the MPLR were designed by adapting previously established cultivation protocols for STRs. Besides the outer glass vessel (Eppendorf, Jülich Germany), all other parts of the MPLR (head plate, stand, sparger (air), disperser (solvent), inner cylinder and its mounting, cooling coil, sampling tube) were custom-made. The MPLR was operated at a filling volume of 4 L MSM (10 g L⁻¹ glucose), which was inoculated with RL producing *P. putida* KT2440 SK4 to an initial OD₆₀₀ of 0.2. The riser and the downcomer were each controlled by linked BioFlo110 control units (Eppendorf, Jülich, Germany), allowing individual control of either compartment of the reactor. Ethyl decanoate for the *in situ* extraction of RLs was dispersed at the bottom of the downcomer by applying a continuous flow rate of 10 mL min⁻¹ *via* an external peristaltic pump (Masterflex L/S Computer-Compatible Digital Drive, Cole-Parmer GmbH, Wertheim, Deutschland). A coherent solvent phase, which accumulated at the liquid surface, was withdrawn by another external peristaltic pump (Masterflex L/S Variable-Speed Drive, Cole-Parmer GmbH, Wertheim, Deutschland) operated at a flow rate of 20 mL min⁻¹. The pump was connected to a pipe with an outlet fixed in a settler compartment slightly above the liquid surface to maintain the filling volume at a constant level. A partially enlarged inner wall inhibited the loop flow to enter the settling zone, thereby establishing a turbulence-free compartment. An unstructured, stainless steel coalescer supported the coalescence of solvent droplets to allow the formation of a coherent solvent phase in the settling compartment (Figure 4B). The DOT was monitored in both compartments *via* invasive probes (VisiFerm, Hamilton Company, Bonaduz, Switzerland).

Likewise, the pH value was measured in both compartments (pherm, Hamilton Company, Bonaduz, Switzerland), and either value could be used as an input value to set the desired pH value by the addition of 4 M HCl and 4 M KOH *via* peristaltic pumps built in the BioFlo110 pump module. The pH value was lowered to enhance the RL extraction efficiency when foam accumulated and threatened to enter the settler compartment. The riser was aerated at specific rates, set by a thermal mass flow controller (EL Flow Select F-201CV-20K-AGD-00-V, Bronkhorst Deutschland Nord GmbH, Kamen, Netherlands) and converted to volumes in the range of 0 - 20 L min⁻¹ of air. Aeration rates were adjusted to enable a sufficiently high DOT value for microbial growth during the cultivation. The temperature was kept constant at 30 °C. Concentrations of O₂ and CO₂ in the exhaust gas were measured by a BlueVary unit and monitored by BlueVis (both BlueSens GmbH, Herten, Germany).

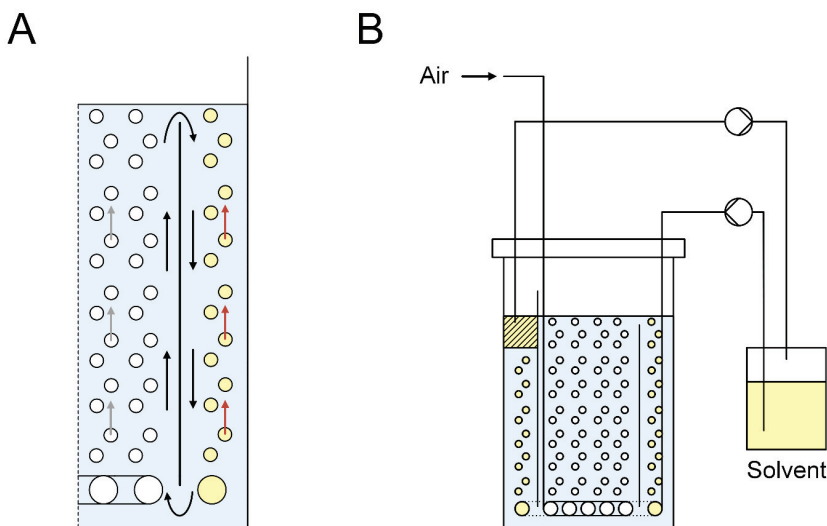


Figure 4 Schematic illustrations of the MPLR. (A) Half cross-section of the MPLR with flow patterns of the continuous aqueous phase (blue background, black arrows), the dispersed gaseous phase (white circles, grey arrows), and the dispersed organic phase (yellow circles, red arrows). Large white circles at the bottom display the air sparger and the solvent disperser, small white circles in the riser represent air bubbles. (B) Installation of the MPLR, including solvent recirculation (shaded area represents the settler compartment with coalescer) and aeration. Further installations such as DOT, pH, and temperature probes, cooling coil, heating jacket, sampling device, and exhaust gas monitoring are not displayed to avoid clarity.

2.5 Adaptive laboratory evolution

Wild-type *P. putida* KT2440 was adapted to 1-octanol by repeatedly subjecting the strain to the solvent during cultivation. In general, the same experimental setup, including media composition, solvent fraction, solvent reservoirs, and CO₂ sensors, as described for the quantitative

biocompatibility assessment in Chapter 2.4.2.2, was applied. In contrast to conventional ALE strategies, gradually increasing the selective pressure over the cultivation cycle, the strain was exposed to unaltered concentrations of 1-octanol only in every second cultivation cycle. Thus, the cultivation conditions alternated between absence and presence of the selective pressure. This strategy, previously described by Eng *et al.* [152], was applied to investigate if a potential adaptation is inheritable, even if the selective pressure is removed for several cell divisions. As conventional methods for biomass quantification were not feasible due to the formation of emulsions in the presence of 1-octanol, the CO₂ volume fraction in the headspace was used as a measure for growth. The initial cultivation cycle, during which no selective pressure was applied, was inoculated to an OD₆₀₀ of 0.01. Thereafter, 1 mL of the respective culture was transferred to a clean shake flask to inoculate the next cultivation cycle at a threshold fraction of 3% CO₂ (v/v). After each cultivation cycle, the strain was cryopreserved for subsequent analysis. The ALE was performed in three independent cultivations and was terminated after four cultivation cycles.

2.6 Genome re-sequencing

To identify mutations in the genome of *P. putida* KT2440 strains, which were subjected to ALE enhancing tolerance to 1-octanol, genomic re-sequencing was performed on all strains recovered after the fourth cultivation cycle and the initially applied wild-type strain for comparison. Genomic DNA was isolated from cells of 5 mL LB cultures with the High Pure PCR Template Preparation Kit (Roche, Basel, Switzerland). Sequencing using Illumina technology as paired-end reads of 100 base pairs as well as single nucleotide polymorphism and insertion and deletion (SNP/InDel) calling was performed by CeGaT GmbH (Tübingen, Germany). The reference was mapped against the database with BWA-mem Version 0.7.17-cegat [153]. SNPs and InDels were analyzed with SnpEff (version 4.3t build 2017-11-24) [154].

2.7 Construction of a solvent database

Data for organic solvents of different types exhibiting various physicochemical properties were collected and listed in a data spreadsheet. The list encompasses properties relevant for extraction processes, such as density, solubility in water at room temperature, and the boiling point at ambient pressure. Additionally, the octanol/water partition coefficient ($\log P$) as an indicator for biocompatibility [74, 155] and flash points for assessing fire hazards of the solvents were listed. Further, the Health Score developed for the CHEM21 solvent selection guide [156] was included. Primary data sources were ChemSpider (Royal Society of Chemistry, London, UK), PubChem (National Center for Biotechnology Information, Rockville Pike, USA), and the manufacturer's documentation depending on data availability.

2.8 Extractions

2.8.1 Extraction efficiencies

As part of the reductive, multi-step solvent selection described in Chapter 3.1, the efficiency of solvent candidates for the extraction of RLs was tested in cell-free cultivation broth generated from shake flask cultivations of *P. putida* KT2440 SK4 and subsequent centrifugation (14,000 g, 10 min). Solvents were saturated with distilled water overnight in a tempered shaker (Thermo Shaker MHR 23, Hettich Benelux BV, Geldermalsen, Netherlands) at 30 °C and 600 rpm to minimize changes of concentrations due to cross-solubility of the solvent with water. Two-liquid phase systems in fixed phase ratios ϕ of 1:4 (v/v) organic solvent to cultivation broth (pH 6.5) were shaken at 99 rpm in an overhead shaker (Intelli-Mixer RM-2L, ELMi Ltd. laboratory equipment, Riga, Latvia) for 4 h. As the temperature for optimal growth and production for *P. putida* KT2440 was previously determined to be at 30 °C [157] and the solvents were assessed for *in situ* extractions, all extraction experiments were conducted at 30 °C. Samples were taken from the aqueous phase to quantify the RL concentration after extraction (C_i), thus determining the reduction of RL concentration relative to the initial RL concentration (C_0) and the corresponding partition coefficient P in regard to the phase ratio ϕ (refer to Equation 1 and 2, Chapter 2.12).

2.8.2 pH-dependent extractions

In Chapter 3.1, the influence of the pH value of the cultivation broth on the efficiency of RL extraction was assessed. Here, the pH values of the cultivation broths were adjusted to seven different values in the range of pH 3.3 to pH 10 by adding respective amounts of 1 M NaOH or 1 M HCl. Fixed phase ratios ϕ of 1:4 (v/v) organic solvent to cultivation broth were incubated at 30 °C and 1,400 rpm horizontal shaking (HLC Cooling-ThermoMixer MKR13, DITABIS AG, Pforzheim, Germany) for 4 h. Samples were taken from the aqueous and the organic phase for RL quantification.

2.8.3 Time-resolved extractions

Extractions were monitored over time to assess the duration needed to reach equilibria. Multiple extractions at a phase ratio ϕ of 1:4 (v/v) organic solvent to cultivation broth and incubated at 30 °C and 1,400 rpm horizontal shaking (HLC Cooling-ThermoMixer MKR13, DITABIS AG, Pforzheim, Germany) were performed. At specific time intervals, a subset of extractions was interrupted by short centrifugation (15 s, 21,300 g) to separate the liquid phases. Quickly, samples from both phases were drawn to determine RL concentrations. Durations of extraction ranged from 15 s to 30 min. The time-resolved extractions were performed with two exemplary solvents, 1-decanol and ethyl decanoate.

2.8.4 Back-extractions

To recover extracted RLs from the solvents, back-extractions at varying pH values were performed. Double-distilled water was buffered using tris acetic acid EDTA (TAE, 40 mM Tris, 20 mM acetic acid, 1 mM EDTA) and adjusted with 1 M NaOH and 1 M HCl to respective pH values in the range of 4.8 to 11.75. TAE was chosen as the buffer as it showed compatibility with analytical methods in the relevant concentrations. Fixed phase ratios ϕ of 1:1 (v/v) organic solvent enriched with RLs to pH-adjusted double-distilled water were incubated at 30 °C and 1,400 rpm horizontal shaking (HLC Cooling-ThermoMixer MKR13, DITABIS AG, Pforzheim, Germany) for 4 h. Samples were taken from the aqueous and organic phases for RL quantification.

2.9 Phase separation

The phase separation was studied in a vertical cylinder filled with 100 mL cultivation broth containing *P. putida* KT2440 SK4 and RLs. A custom-made plate disperser (18 evenly distributed holes, $d = 1$ mm) inserted at the bottom of the cylinder (designated height h_d of ~5.4 cm) was connected to a peristaltic pump (501U, Watson-Marlow, Marlow, UK) to disperse the solvent. Withdrawing the coherent solvent phase at a height h_w of 4.5 cm enabled recirculation at 211 mL min⁻¹ (Figure 5). The height of top-most not coalesced droplet (h_c), starting with the first droplet reaching the phase boundary ($t = 0$ s, $h = 0$ cm), was recorded and plotted similarly to the decay of the batch dispersion of Hartland and Jeelani (1987) [158] but shows the advancement of a non-coalescing dispersion over time until steady state is reached. A stainless-steel mesh was used as a coalescer to optionally enhance coalescence.

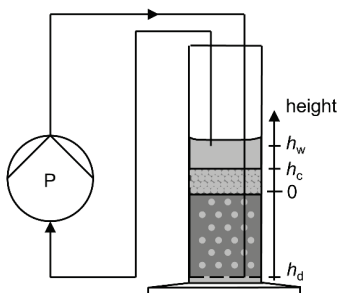


Figure 5 Schematic setup of the experiment for phase separation. The peristaltic pump (P) disperses the solvent at height h_d . The droplets coalesce at height h_c to a coherent phase being withdrawn at height h_w . This figure was originally designed by Maximilian von Campenhausen, was previously published [125], and is reprinted with permission from Green Chemistry. Copyright The Royal Society of Chemistry 2020.

2.10 Catastrophic phase inversion

Catastrophic phase inversion (CPI) was performed as a proof of concept to break stable emulsions of an organic solvent and cultivation broth, containing cells, cell fragments, RLs. Defined volumes of excess solvent were added to the emulsion and incubated at 100 rpm overhead shaking at room temperature for approximately 1 h before allowing the system to settle for 20 h. Ratios of emulsion to excess solvent ranged from 1:1 (v/v) to 1:7 (v/v).

2.11 Analytical methods

2.11.1 Determination of bacterial growth

The optical density of liquid cultures was measured at 600 nm using Ultrospec 10 cell density meter (Biochrom, Cambridge, UK). Further, cell dry weight was quantified by centrifuging 1 mL of sampled fermentation broth at 21,300 g and 4 °C for 5 min (Centrifuge 5430 R, Eppendorf, Jülich, Germany). The supernatant was discarded, and the cells were washed by resuspending the pellet in 1 mL deionized water. After another centrifugation, the cell suspension was transferred to pre-dried and pre-weighed glass vials and incubated at 80 °C. Dried samples were weighed to determine the cell dry weight. Linear regression was applied to determine growth rates. For weighing, a precise micro balance was used (NewClassic MF MS105DU, Mettler Toledo, Gießen, Germany; error: 0.015 mg). Per point of time and per biological replicate, four technical replicates were measured. Evaluation of this method revealed an error of approximately 15% for biomass titers $< 0.2 \text{ g L}^{-1}$, which was reduced to $< 5\%$ for biomass titers of $> 0.5 \text{ g L}^{-1}$, considering biological and technical replicates.

2.11.2 Metabolite quantification

Cell-free supernatants of samples of liquid cultures were generated by centrifugation (21,000 g, 3 min). Routinely, substrates and intermediates in culture supernatants, namely glucose, gluconate, and 2-ketogluconate, were quantified using a DIONEX UltiMate 3000 High Performance Liquid Chromatography (HPLC) System (DIONEX UltiMate 3000 composed of pump module LPG-3400SD, autosampler WPS-3000 (RS), and the column oven TCC-3000 (RS), all Thermo Fisher Scientific Thermo Scientific, Germany) with an ISERA Metab AAC $300 \times 7.8 \text{ mm}$ separation column (particle size: 10 μm , ISERA GmbH, Düren, Germany). The coupled DIONEX UltiMate 3000 Variable Wavelength Detector was set to 210 nm, and additionally a refractive index (RI) detector SHODEX RI-101 (Showa Denko Europe GmbH, Germany) was used. Glucose and 2-ketogluconate were quantified using the signals of the Variable Wavelength Detector, whereas gluconate was quantified *via* the signal from the RI detector.

Elution was performed with 5 mM H₂SO₄ at a flow rate of 0.6 mL min⁻¹ at 40 °C. The volume of the injected sample was set to 10 µL.

For glucose quantification performed in Chapter 3.1, an enzymatic assay automated on a liquid handling platform (4BioCompact, 4BioCell GmbH & Co. KG, Bielefeld, Germany) was used. The system was calibrated with defined glucose solutions ranging from 0.1 g L⁻¹ to 4 g L⁻¹. For measurements out of range, the liquid handling platform automatically diluted the respective samples and repeated the assay. Before quantification, the aqueous samples were centrifuged (21,000 g, 3 min) to remove cells.

2.11.3 Rhamnolipid quantification

For RL quantification, reversed-phase HPLC-CAD (DIONEX UltiMate 3000 composed of pump module LPG-3400SD, autosampler WPS-3000 (RS), and the column oven TCC-3000 (RS) with a Corona Veo Charged Aerosol Detector (CAD), all Thermo Fisher Scientific, Waltham, USA; NUCLEODUR C18 Gravity 150 x 4.6 mm separation column, particle size: 3 µm, Macherey-Nagel GmbH & Co. KG, Düren, Germany) was used. A continuous nitrogen flow for the CAD was maintained by the nitrogen generator Parker Balston NitroVap-1LV (Parker Hannifin GmbH, Kaarst, Germany).

The employed method was described previously [139]. A gradient elution with two buffers, (A) acetonitrile and (B) 0.2% (v/v) formic acid in double-distilled, purified water, was run over a 15 min measurement interval. Initial conditions were set to 70% buffer A and 30% buffer B, which remained unaltered for 1 min. Over an 8 min linear incline, the fraction of buffer A was increased to 80%, followed by a 1 min linear incline, enhancing the fraction of buffer A to 100%, kept constant for 1 min. Subsequently, initial conditions were restored within 1.5 min and retained until the end of the measurement interval. The flow rate and the column oven temperature were kept constant at 1 mL min⁻¹ and 40 °C, respectively. The volume of injected sample was set to 5 µL. The method enabled the detection and quantification of four HAA congeners and four mono-RL congeners (Appendix A.1, Figure A1.1).

Before sample preparation, the pH value of aqueous samples was adjusted to 7 with 1 M KOH or 1 M HCl, if necessary, to avoid quantification bias. Equal volumes of acetonitrile were added to aqueous samples for protein precipitation. After mixing and incubation at 4 °C for more than 4 h, the samples were centrifuged (21,000 g, 3 min) and filtered (Phenex RC syringe filters, pore size: 0.2 µm, *d* = 4 mm, Phenomenex, Torrance, USA). For solvent samples, the organic phase was evaporated at 20 mbar (abs), 60 °C, and 1,400 rpm (ScanSpeed 40 attached to ScanVac Coolsafe 110-4, both Labogene ApS, Lyngø, Denmark, and Chemistry Hybrid Pump RC 6,

vacuubrand GmbH + Co. KG, Wertheim, Germany) and dry residuals were resolved in appropriate volumes of a 50% acetonitrile - double distilled water solution before filtering.

2.11.4 Detection and quantification of 1-octanol

Samples from production cultures were centrifuged to remove cells (12,000 g, 5 min), and 900 μL of the cell-free supernatant were extracted with 450 μL hexane at thorough mixing (Intelli-Mixer RM-2, 63 rpm, 15 min). Another centrifugation enhanced phase separation at the conditions described above. For derivatization, 20 μL MTBSTFA were mixed with 100 μL of the organic phase and incubated at 65 °C for 1.5 h.

Detection of 1-octanol was performed *via* gas chromatography coupled to mass spectrometry (GC-MS) on a Trace GC Ultra coupled to a ISQ single quadrupole mass spectrometer (both Thermo Scientific, Waltham, MA, USA). Analyte separation was performed with a VF-5ms capillary column (30 m length, 0.25 μm inner diameter, 0.25 μm film thickness, Agilent Technologies Inc., Santa Clara, CA, USA) at a constant carrier gas flow of 1 mL min^{-1} helium. A sample volume of 1 μL was injected (AI/AS 1310 autosampler, Thermo Scientific, Waltham, MA, USA) and the inlet temperature was set to 200 °C. A split ratio of 1:10 was chosen. The column temperature was initially kept at 100 °C for 2.5 min, then increased at a rate of 20 $^{\circ}\text{C min}^{-1}$ to 250 °C, followed by an increase of 50 $^{\circ}\text{C min}^{-1}$ to 320 °C, at which it was held for 5 min. The transfer line and ion source temperatures were set to 280 °C and 300 °C, respectively. Ions were generated by electron impact ionization at 70 eV.

2.11.5 Untargeted proteomics

Samples were drawn as technical duplicates from each STR cultivations of *P. putida* KT2440 SK4 at the different applied conditions performed in biological duplicates. The control cultures were sampled at $t_1 = 7.6$ h, whereas the cultures subjected to 2 min oscillations were sampled at $t_1 = 7.6$ h and again at $t_2 = 11.9$ h, shortly before glucose depletion. Ten mL of cultivation broth were sampled in pre-chilled (-20 °C) reaction tubes, subsequently centrifuged (5,000 g, 10 min, 4 °C), and washed with 0.9% NaCl (4 °C). Cell pellets were rapidly cooled in liquid nitrogen and stored at -20 °C until further analysis.

The cell pellets were suspended in lysis buffer containing 50 mM potassium phosphate buffer (pH 8.0), 2 mM EDTA, 2 mM 1,4-dithiothreitol, and supplemented with cOMplete protease inhibitor cocktail (1697 498, Roche Applied Science, Basel, Switzerland). Cell suspensions were disrupted in a Precellys System (Bertin Instruments, Montigny-le Bretonneux France) using 0.1-0.2 mm glass beads plus two glass beads with 5 mm diameter for 30 s at maximum frequency was repeated twice. The supernatant containing protein fractions were collected and stored at -20 °C until further analysis. Concentrations of proteins in crude extracts were measured using a Bradford

assay (B6916, Sigma Aldrich, USA) with bovine serum albumin as a standard. According to previously described methods [159], the resulting crude extracts were applied for untargeted LC-MS/MS measurements. Briefly, a maximum of 50 μL of the crude extracts (up to 100 μg total protein) were used for tryptic digestion. Crude extracts were digested with 1 μg trypsin in a total volume of 100 μL for 5 h at 42 $^{\circ}\text{C}$ (T7575, Sigma Aldrich). Peptide solutions were diluted 1:2 with MilliQ H_2O (Millipore, Merck KGaA) before LC-MS/MS measurements.

With injected sample volumes of 10 μL , protein amounts of up to 5.0 μg were applied. Peptide mixtures were separated by reversed-phase HPLC (Infinity 1260 HPLC, Agilent Technologies; column at 21 $^{\circ}\text{C}$: 150 \times 2.1 mm Ascentis Express Peptide ES-C18 2.7 μm (53307-U, Sigma Aldrich); equilibration: 3% B (12 min); gradient B: 3-40% (70 min), 40% (8 min), 40-60% (1 min), 60% (10 min); flow: 0.2 mL min^{-1} ; A: 0.1% (v/v) formic acid, B: acetonitrile + 0.1% (v/v) formic acid) prior to ESI-MS-TOF (Q-ToF 6600 mass spectrometer, Sciex, Darmstadt, Germany) measurements. The TripleTOF6600 was operated at following parameters: curtain gas: 35, ion source gas 1: 50, ion source gas 2: 50, ion spray voltage: 5500, temperature: 450, declustering potential: 120. The variable width Q1 windows were monitored in a non-scheduled manner during the elution under the above-specified parameters. SWATH window width was calculated with SWATH Variable Window Calculator_V1.0. The autosampler was set to ± 6 $^{\circ}\text{C}$. Data acquisition and peak integration were performed using the software PeakView 2.1 (Sciex), while proteins were identified with the software ProteinPilot 5.1 (Sciex). Marker View software (Sciex) was used for t-test analysis.

2.12 Data analysis

Quantified data were analyzed to enable comparison across different cultivation systems and modes according to equations described in the following.

The extraction efficiency E was calculated according to Equation 1:

$$E = \frac{C_0 - C_1}{C_0} \cdot 100\% \quad (1)$$

with C_0 referring to the concentration before extraction and C_1 referring to the concentration after extraction.

The partition coefficient P was calculated according to Equation 2:

$$P = \frac{C_0 - C_1}{C_1 \cdot \phi} \quad (2)$$

with ϕ representing the volumetric phase ratio of organic to aqueous phase.

The total mass of produced RLs was calculated according to Equation 3:

$$m_{RL,total} = C_{RL,aq} \cdot V_{aq} + C_{RL,org} \cdot V_{org} \quad (3)$$

with $m_{RL,total}$ being the total mass of produced RLs, $C_{RL,aq}$ and $C_{RL,org}$ representing the RL concentrations in the aqueous and the organic phase, respectively, and V_{aq} and V_{org} representing the volumes of the aqueous and the organic phase, respectively.

The product yield $Y_{P/S}$ was calculated according to Equation 4:

$$Y_{P/S} = \frac{m_{RL,total}}{m_{GLC,total}} = \frac{C_{RL,aq} \cdot V_{aq} + C_{RL,org} \cdot V_{org}}{C_{GLC,aq} \cdot V_{aq}} \quad (4)$$

with $m_{GLC,total}$ representing the total mass of glucose either supplied in the batch phase or fed during the feeding phase.

The biomass yield $Y_{X/S}$ was calculated according to Equation 5:

$$Y_{X/S} = \frac{x}{m_{GLC,total}} \quad (5)$$

with x being the produced biomass.

The space-time-yield, or productivity, STY was calculated according to Equation 6:

$$STY = \frac{m_{RL,total}}{V_{aq} \cdot t} = \frac{C_{RL,aq} \cdot V_{aq} + C_{RL,org} \cdot V_{org}}{V_{aq} \cdot t} \quad (6)$$

with t representing the time of cultivation. As the productivity was calculated over the entire cultivation, or separate for batch and fed-batch phases, t either corresponds to the end of the cultivation, the point of time at the start of feeding, or the difference of the prior two points of time.

Growth rates, the increase of oxygen uptake rate (OUR), and the specific glucose uptake were derived *via* linear regression. Errors denote the standard deviation for sample sizes of $n \geq 2$ or the minimal and maximal values for sample sizes of $n = 2$.

Chapter 3

Results

Chapter 3.1

Evaluation of *in situ* extraction solvents to robustly produce rhamnolipids in a two-liquid phase fermentation

Partially published as

[125] Demling P, von Campenhausen M, Grütering C, Tiso T, Jupke A, Blank LM. 2020. Selection of a recyclable *in situ* liquid-liquid extraction solvent for foam-free synthesis of rhamnolipids in a two-phase fermentation. *Green Chemistry*. doi: 10.1039/D0GC02885A.

[Reprinted (adapted) with permission from Green Chemistry. Copyright The Royal Society of Chemistry 2020]

Contributions

Philipp Demling conducted all experiments and analytics, in part jointly with others. Maximilian von Campenhausen co-conducted the property-based solvent screening, extractions, back-extractions, and studies regarding the solvent settling behavior to equal parts. Carolin Grütering co-performed biological experiments, extractions, back-extractions, and analytics. Philipp Demling and Maximilian von Campenhausen equally contributed to writing the original published article, which is integrated in this chapter. Maximilian von Campenhausen is the original author of the following sections of the published article: “Introduction”, “A primary selection based on physicochemical properties eliminates inapt solvent candidates”, “Extraction efficiencies and flash points further reduce the number of solvent candidates”, and “Coalescer accelerates phase separation”. Those sections have been included in this thesis, either in full or partially in an adapted and compendious form for complete comprehension. Philipp Demling originally wrote all other sections. Till Tiso and Lars M. Blank reviewed the chapter.

3.1 Evaluation of *in situ* extraction solvents to robustly produce rhamnolipids in a two-liquid phase fermentation

3.1.1 Abstract

Excessive foaming causes instabilities in fermentation processes, particularly when producing biosurfactants, which can be overcome by intensifying the fermentation *via in situ* product recovery. A reductive, multi-step approach for selecting organic solvents for an *in situ* liquid-liquid extraction of rhamnolipids produced by recombinant *Pseudomonas putida* KT2440 was developed. 1) A database consisting of physicochemical parameters for 183 solvents was composed, allowing a pre-selection by setting respective thresholds. 2) The number of solvents was reduced by evaluating their extraction efficiencies regarding rhamnolipids in cell-free cultivation broth and their impact on the growth of *P. putida* KT2440. 3) The most promising solvent was characterized regarding phase separation, pH-dependency of the extraction, and applicability of back-extraction for product recovery and solvent regeneration. The overall performance was assessed in two-liquid phase (fed-)batch fermentations in lab-scale stirred-tank reactors. The solvent selection approach revealed ethyl decanoate to be a highly suitable and sustainable solvent for the *in situ* liquid-liquid extraction of rhamnolipids. During the final two-liquid phase fed-batch fermentation, 30 g L⁻¹ produced rhamnolipids accumulated in the organic phase. Integrating extraction and increasing the partition coefficient by moderately lowering the pH value prevented foaming during fermentation, thus resolving the initial process instability. Rapid phase separation and back-extractability allowed product recovery and solvent recycling. The here presented reductive, multi-step solvent selection approach was successfully applied to establish a two-liquid phase fermentation producing rhamnolipids by engineered *P. putida* KT2440, resolving the foaming challenge. The approach can serve as a blueprint for selecting solvents for *in situ* liquid-liquid extractions in bioprocesses.

3.1.2 Introduction

The envisaged bioeconomy requires replacements for petrochemically derived chemicals. Promising alternatives for surfactants are rhamnolipids (RLs), produced mainly by bacteria from the *Pseudomonas* genus [99]. The class of rhamnolipids encompasses a high diversity of molecular structures as congeners vary in the number of rhamnose moieties (zero to two) as well as chain length and saturation of the alkanic acid residues [101]. These biosurfactants have potential applications, *e.g.*, in detergents, food, remediation of oil-polluted sites, medicine/pharmacology, plant protection, and agriculture. Specific congeners of RLs might have additional, innovative applications, which have to be fully explored and exploited [160]. Because *P. aeruginosa*, the most

prominent producer of RLs [100, 161], is an opportunistic human pathogen, RL production using recombinant, non-pathogenic *P. putida* KT2440 was established [106, 107]. Further information on biosurfactants and RLs is given in the General Introduction (Chapter 1).

A central challenge in the production of surfactants in bioreactors is excessive foaming, even at small product concentrations, caused by the aeration required to continuously provide oxygen for cellular respiration. Microorganisms accumulate in the foam, resulting in a substantial loss of the biocatalyst. Although antifoam has been applied to prevent foaming at high concentrations of biosurfactants [118], it is not only complicating downstream processing (DSP) [119, 120] but is also costly as large amounts are required. Therefore, innovative process alternatives as the integration of *in situ* product removal (ISPR) like foam fractionation [41, 122, 123, 162] are advantageous for the biotechnological production of surfactants but pose challenges when transferred to large-scale production due to challenging scalability [124]. The implementation of *in situ* liquid-liquid extraction might be a promising alternative. Here, a liquid organic phase exhibiting a miscibility gap with the aqueous fermentation broth is added to the system. The product transfers into the organic phase, lowering the surfactant concentration in the fermentation broth and thus prevents foaming. Previously, ethyl acetate was favored for the *ex situ* extraction of RLs from cultivation broth [148, 163].

In situ liquid-liquid extractions have been applied in different setups for biotechnological production processes to resolve product inhibitions. A typical setup is spatially separating production and extraction by coupling the fermenter compartment to an extraction compartment removing, e.g., lactic acid [164], gibberellic acid [165], butanol [166], and itaconic acid [167]. An industrial ready process was evaluated by DSM Biotech GmbH, Jülich (Germany), and DSM, Geleen (Netherlands) to produce L-phenylalanine [168]. The sequential coupling of fermentation and liquid-liquid extraction allows independent optimization of respective process parameters like dissolved oxygen, shear stress, temperature, or pH value. However, as the fermentation broth is circulated through the compartments, a change of parameters causes the production host to encounter repeatedly changing environments perturbing its metabolism, which can result in an impaired production or even cell death [169, 170]. Although submerged membranes can retain the organisms in the fermenter compartment, such a setup requires additional equipment with increased investment and maintenance cost due to biofouling of the membrane [86, 171].

Fermentation and *in situ* liquid-liquid product extraction in a single compartment, i.e., two-liquid phase fermentation, were investigated for many catalyst/product pairs overcoming the drawbacks described above. Examples for two-liquid phase fermentations are the production of phenol [172], *p*-hydroxysterene [173], 3-methyl-1-butanol [174, 175], ethanol [176], and pullulan [177]. In an approach for the epoxidation of styrene, the toxic substrate was supplied *via* an organic

phase, simultaneously serving as an extractant for the equally toxic product [178, 179], even predicting an economic advantage compared to conventional chemical production processes [75]. Publications on *in situ* liquid-liquid extractions for industrial fermentations are rare. However, *e.g.*, Isobionics (Geleen, Netherlands) owns a patent for two-liquid phase fermentation to produce isoprenoids [180]. In contrast to coupled extractions, the operational window for two-liquid phase fermentations is defined by combining the respective operational windows for fermentation and liquid-liquid extraction. Hence the freedom of design and operation is reduced. Challenging operational constraints can cause detrimental effects on fermentation and extraction performance. Examples are underperformance of whole-cell biocatalysts due to toxicity of the extractants or unfavorable surface properties of organisms, resulting in poor phase separation, interphase formation, or high viscosity [181, 182]. These interactions depend on the choice of solvent and its physical properties. Thus, a comprehensive screening of solvents regarding specifications of the fermentation is indispensable.

Previous solvent screenings for two-liquid phase fermentations consisted mainly of comparing the extraction efficiencies and biocompatibilities of only up to 25 solvents [76, 183–187], probably not to exceed a feasible number of experiments. However, since there are hundreds of solvent candidates, finding a highly suitable but simultaneously sustainable and safe solvent for the respective application might be accidental and based on available chemicals. The chemical industry uses model-based predictions of liquid-liquid equilibria [188], enabling an *in silico* screening of large numbers of solvents for their partition coefficients. While this approach is complicated to transfer to fermentations, some physicochemical properties of the solvent can be considered to evaluate the compatibility for the envisioned two-liquid phase fermentation. Therefore, a first reduction of the number of potential solvent candidates can be performed by screening a database for physicochemical properties in a predefined property target space [72, 189].

In this chapter, 183 organic solvents were evaluated for liquid-liquid *in situ* extraction of RLs in a multi-step, reductive selection approach. First, a data-based screening of physicochemical and economic properties led to a reduced number of solvent candidates, further limited by thresholds for experimentally determined partition coefficients, biocompatibility, and biodegradation by *P. putida* KT2440, simultaneously favoring solvents posing low risk to the user. In more detail, characteristics of the most promising solvent, including phase separation behavior and pH-dependency of the (back-)extraction for product and solvent recovery, were determined. The performance of the final organic solvent was evaluated in two-liquid phase fermentations using stirred-tank reactors (STRs).

3.1.3 Results

3.1.3.1 Reductive multi-step solvent selection

A primary selection based on physicochemical properties eliminates inapt solvent candidates

The large quantity of organic solvents potentially used as *in situ* extractants in two-liquid phase fermentations requires a pre-selection of the most promising candidates to keep the experimental efforts for detailed characterization within reasonable limits. Here, a theoretical approach based on solvent properties gathered in a database was used to limit the number of potential candidates.

Data for properties of 183 potential organic solvent candidates, selected based on solvents applied as extractants in bioprocesses in literature, were gathered (Appendix A.2, Figure A2.5). Properties include the octanol/water partition coefficient ($\log P$) and low solubility in water, favoring the selection of biocompatible and recyclable solvents. The Health Score, developed within the solvent selection guide by Prat *et al.* [156, 190] in the scope of the CHEM21 project, was used as a measure for toxicity to humans. Further, exhibiting a miscibility gap with water and being fluid at standard conditions were regarded as prerequisites for a solvent to be included. A primary and a secondary threshold were defined by knowledge-based assumptions for each property (Table 2).

Table 2 Thresholds and short explanations for performed solvent selection steps.

Property	Thresholds (classification)		Reason
	Primary threshold ('Suitable')	Secondary threshold ('Limited')	
Density	$\leq 880 \text{ g L}^{-1}$	$\leq 920 \text{ g L}^{-1}$	Sufficient difference in density to the aqueous phase for gravimetric separation
Boiling point	$\geq 100 \text{ }^{\circ}\text{C}$	$\geq 80 \text{ }^{\circ}\text{C}$	Limit the loss of solvent to the gaseous phase
Solubility in water	$\leq 0.3 \text{ g L}^{-1}$	$\leq 0.5 \text{ g L}^{-1}$	Limit the loss of solvent to the aqueous phase
$\log P$	4	3.5	Preselection for biocompatibility of the solvent
Price ^a	$\leq 100 \text{ €}/100 \text{ mL}$	$\leq 120 \text{ €}/100 \text{ mL}$	Economically affordable range
Toxicity	Health Score ^b ≤ 2	Health Score ^b ≤ 4	Limit toxic hazards for operators
Flash point			Flash points above $100 \text{ }^{\circ}\text{C}$ avoid reaching flammability thresholds of applied solvents in aqueous fermentation systems ^c

^a Prices are here regarded as market prices for laboratory use. Market prices for bulk sizes are substantially lower.

^b According to Prat *et al.* [156].

^c Solvents have been examined until solvent selection steps were conducted, for which protection against fire hazards could not be guaranteed using available laboratory equipment.

The thresholds of each property allowed a classification of the solvents as ‘not suitable’ (infringing at least one secondary threshold of any property), ‘limited’ (infringing at least one primary threshold of any property), or ‘suitable’ (infringing no threshold) for application as an *in situ* extraction solvent. Classified as ‘not suitable’ were 153 (83.6%) of the initially listed solvents, including ethyl acetate, previously favored as an *ex situ* extractant for RLs [148, 163]. Regarded as ‘limited’ were 12 solvent candidates (6.6%). The remaining 18 solvents (9.8%) were classified as ‘suitable’ and advanced in the subsequent selection stage.

Extraction efficiencies and flash points further reduce the number of solvent candidates

The selected 18 solvents were assessed for their capability to extract RLs from cell-free fermentation broth. The solvents extracted RLs with an efficiency of 18.9% to 99.8%, translating to partition coefficients ranging from 0.93 for *n*-hexadecane to 2,530 for 1-decanol for the ratio of organic to aqueous phase of 1:4 (v/v) (Figure 6). A threshold value of 8 was chosen for a minimal partition coefficient to select economically and ecologically advantageous solvents as less solvent is required with increased partition coefficients. For two representative solvents (1-decanol and ethyl decanoate), a time-resolved extraction was performed to validate the assumption of reaching

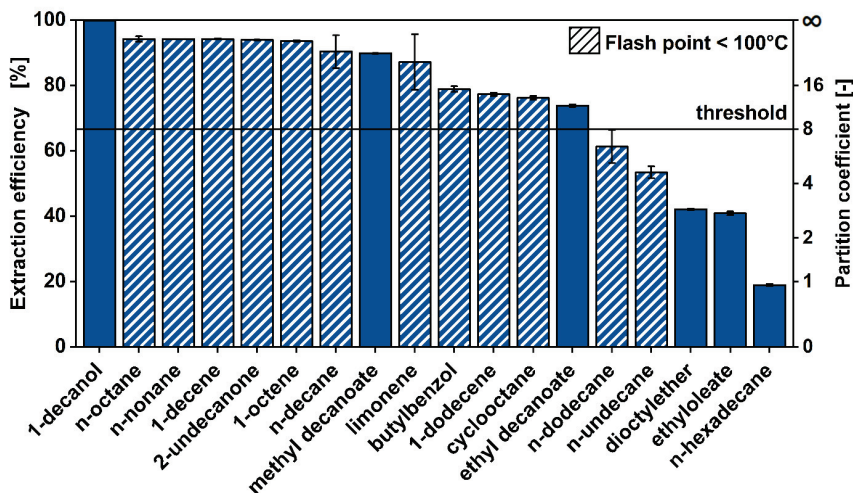


Figure 6 Extraction efficiencies of 18 organic solvents for the extraction of rhamnolipids from fermentation broth at pH 6.5. The extraction efficiency was determined from the remaining RLs in the aqueous phase after extraction relative to non-extracted cultivation broth. The black horizontal line marks the threshold for the partition coefficient of 8. Error bars represent the maximum and minimum values of measurements from two independent experiments. The figure was originally designed by Maximilian von Campenhausen. This figure was originally designed by Maximilian von Campenhausen, was previously published [125], and is reprinted with permission from Green Chemistry. Copyright The Royal Society of Chemistry 2020.

equilibrium within 4 h (Appendix A.2, Figure A2.1). The flash point as a measure for flammability was introduced as another threshold to balance the performance of the solvent with the effort for introducing appropriate measures for protection against fire hazards [156, 191]. Only solvents with a flash point higher than 100 °C were further considered in the succeeding selection stages to avoid safety hazards or the requirement of laboratory equipment complying with fire safety regulations (refer to Table 2). Thereby, the number of solvent candidates was reduced to three (1-decanol, methyl decanoate, and ethyl decanoate), fulfilling the criteria of a partition coefficient above 8 and a minimum flash point of 100 °C.

Ethyl decanoate shows high biocompatibility and negligible biodegradability

In the initial screening based on the physicochemical properties of the solvents, $\log P$ was regarded as an estimation for biocompatibility. 1-Decanol, methyl decanoate, and ethyl decanoate were further investigated by monitoring the accumulation of CO₂ in the headspace of a closed shake flask when the cells were cultivated in the presence of the respective solvent. As state-of-the-art methods for biomass determination were not feasible due to the formation of stable emulsions in the presence of solvents, the CO₂ accumulation served as a measure for growth.

The influence of the respective solvent on the growth of the cells can be determined regarding the deviation of CO₂ volume concentrations in the headspace of shake flasks with solvent from a solvent-free cultivation (Table 3). Conclusions on the biocompatibility of the solvent in the presence of a preferred carbon source (here glucose) and the ability to degrade the solvent after depletion of the preferred carbon source can be drawn. Additional to the listed effects, the solvent can cause a prolonged initial adaptation phase of the microorganism.

Table 3 Theoretical CO₂ accumulation in the headspace of the shake flask with solvents compared to a cultivation without solvents and the corresponding characteristic of the interaction of solvent and microorganism.

Before depletion of preferred carbon source			After depletion of preferred carbon source		
	Development of CO ₂ accumulation	Impact on cell growth		Development of CO ₂ accumulation	Impact on cell metabolism
I	None	Solvent is bacteriocidal	A	None	Solvent is not metabolized
II	Lower rate	Negative impact of solvent on growth but not bacteriocidal	B	Delayed	Adjustment of metabolism to solvent as carbon source
III	Same rate	No impact of solvent on growth	C	Immediate	Instant metabolism of solvent as carbon source

The rate of CO₂ accumulation in the headspace of shake flasks in the presence of methyl decanoate ($0.42 \pm 0.01 \text{ h}^{-1}$) and ethyl decanoate ($0.44 \pm 0.01 \text{ h}^{-1}$) was similar to the rate of the control cultivation ($0.44 \pm 0.01 \text{ h}^{-1}$) until glucose was depleted (Figure 7). The comparable CO₂ accumulation rates indicate high compatibility of the solvents to *P. putida* KT2440 SK4 as growth

was not impaired. In contrast, the rate of CO₂ accumulation in the presence of 1-decanol ($0.35 \pm 0.01 \text{ h}^{-1}$) is lowered compared to the control, suggesting impeded growth. This is not entirely in agreement with log *P* values as an indicator for biocompatibility. While ethyl decanoate has the highest log *P* (4.71) of the tested solvents, the log *P* of 1-decanol (4.57) is higher than the one of methyl decanoate (4.41) and should thus be less biocompatible. However, membrane interactions due to the cross-solubility of the solvent indicated by log *P* is not the only described phenomenon for solvent toxicity to microorganisms as thoroughly reviewed by Ramos *et al.* [192] and Heipieper *et al.* [193]. In this regard, more solvent-tolerant *P. putida* strains like *P. putida* S12 or *P. putida* DOT-T1E could serve as production hosts allowing the use of more disruptive solvents as extractants [31]. Here, increased precautions to meet higher safety levels of the strains may need to be considered. Alternatively, solvent tolerance can be increased by strain engineering, as reviewed by Mukhopadhyay *et al.* [40] and also approached in this thesis in Chapter 3.2.

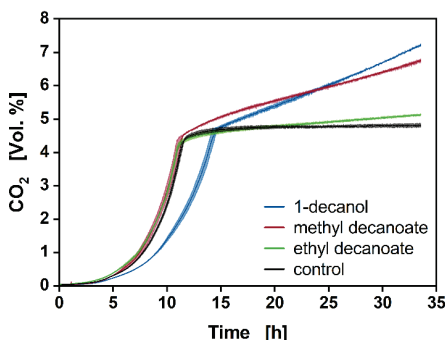


Figure 7 Mean CO₂ volume concentration in the headspace of shake flask cultivations of *P. putida* KT2440 in MSM with 3 g L⁻¹ glucose in the presence of organic solvents. 1-decanol (blue), methyl decanoate (red), ethyl decanoate (green), control in the absence of solvent (black). Shaded areas represent the range of measurements from two independent experiments. Data associated with this figure were partially obtained from Carolin Grüttering's Internship Report [194]. This figure was previously published [125] and is reprinted with permission from Green Chemistry. Copyright The Royal Society of Chemistry 2020.

After glucose depletion, displayed by a sudden decrease in CO₂ accumulation rate at a CO₂ volume concentration of around 4.5%, the volume concentrations for the cultures with added methyl decanoate and 1-decanol increased at moderate rates ($0.09 \pm 0.00 \text{ h}^{-1}$ and $0.14 \pm 0.01 \text{ h}^{-1}$, respectively) without delay. In comparison, CO₂ accumulated at a lower rate for the cultures with added ethyl decanoate ($0.02 \pm 0.01 \text{ h}^{-1}$). This indicates a high metabolism rate of 1-decanol and methyl decanoate by *P. putida* KT2440 SK4. Ethyl decanoate, however, cannot be used as a carbon- and energy source as efficiently as indicated by a slow increase of the CO₂ volume concentration after glucose depletion. According to the categories mentioned in Table 3, 1-decanol can be classified as II C, methyl decanoate as III C, and ethyl decanoate as III B. The ideal *in situ*

extraction solvent should neither impede cell growth nor be degraded. The results suggest ethyl decanoate to be closest to an ideal *in situ* extraction solvent.

3.1.3.2 Characterization of the selected solvent

Ethyl decanoate was selected as the most promising of the tested solvents for the *in situ* extraction of RLs. In addition to the physical properties evaluated above, ethyl decanoate has several advantages regarding work safety, economics, and cost-effectiveness. It does not have any hazardous classification, and due to the high flash point, no additional measures for fire hazard protection need to be established. It occurs as a fermentation ester in wine production [195, 196] and is used as a food additive [197]. It can be produced without using petrochemical raw material by the esterification of the natural products ethanol and decanoate [198]. The prior can be produced biotechnologically and the latter can be purified from coconut or palm oil [199]. Regarding an industrial application, the non-purified mixture of esters derived from ethanol and fatty acids from plant oil as well as other commercially available solvent mixtures could potentially be used for *in situ* RL extraction to lower overall process costs. However, due to intermolecular interactions, their respective performances need to be confirmed. Detailed characteristics crucial for applying ethyl decanoate (Merck, Darmstadt, Germany; purity $\geq 98\%$) for *in situ* extractions of RLs were further investigated.

Coalescer accelerates phase separation

Another crucial solvent-specific property is its rapid separation from the aqueous phase, particularly if it is intended to be removed continuously, as envisaged for the multiphase loop reactor (MPLR). RLs produced by *P. aeruginosa* have been shown to influence coalescence [200]. The experiments for extraction efficiency described earlier in this chapter revealed qualitative differences in settling behavior (Appendix A.2, Figure A2.2), *e.g.*, based on molecular weights (alkenes) and most prominently functional groups (ethyl decanoate). The settling behavior and phase separation of ethyl decanoate were further evaluated in specifically designed experiments, in which the solvent was continuously dispersed through the cultivation broth and recirculated. The influence of components of the cultivation broth was determined by performing a control with purified water. In all cases, a layer of densely packed solvent droplets formed in between the coherent aqueous and solvent phases. The height of the top-most solvent droplet was recorded over time (Figure 8A).

The top-most solvent droplet in the system with pure water as the aqueous phase reached a height of 0.5 cm after 15 s and did not alter until the end of the experiment, thus reaching steady-state. In contrast, using cultivation broth as the aqueous phase, the top-most solvent droplets reached a larger height more rapidly, leading to an abortion of the experiment as the outlet for

solvent recirculation at 4.5 cm was approached by the solvent droplet after 103 s. This emphasizes the high impact of the composition of the aqueous phase on the settling behavior, which is negatively influenced by the presence of cells, RLs, and proteins. To potentially enhance coalescence, a stainless-steel mesh serving as a coalescer was installed. As soon as solvent droplets got in contact with the mesh, a collapse of the droplets was observed. However, due to its inhomogeneous packing, droplets could enter the coalescer before reaching steady-state, which was robustly maintained in a single long-time experiment, enabling the recirculation of coherent solvent for 14 h (Figure 8B).

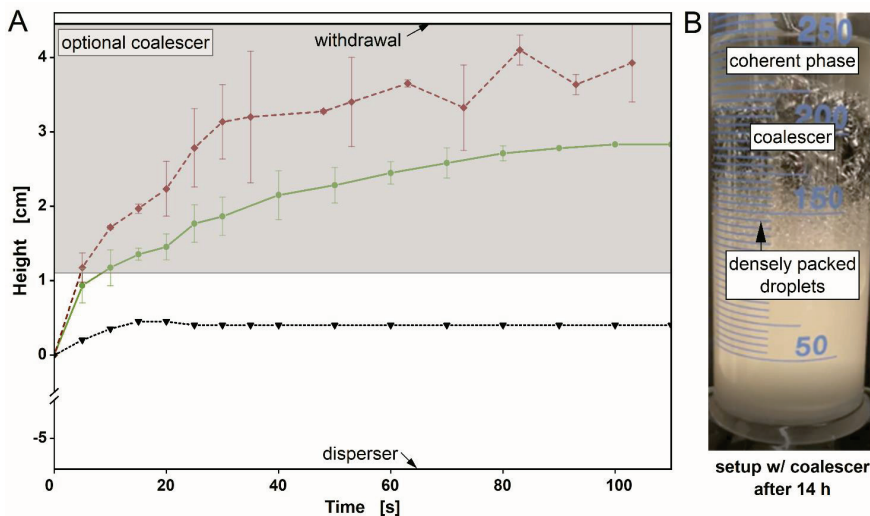


Figure 8 Coalescence curves defined by the clear cut between the densely packed drop layer and the coherent phase of ethyl decanoate. Coalescence curves for two-phase systems of (A) ethyl decanoate - water (black) and ethyl decanoate - fermentation broth without (red) and with coalescer (green) until 110 s and (B) the system with coalescer after 14 h are shown. The grey shaded area represents the location of the optional coalescer. Error bars represent standard deviations from the mean of measurements from three independent experiments. This figure was originally designed by Maximilian von Campenhausen, was previously published [125], and is reprinted with permission from Green Chemistry. Copyright The Royal Society of Chemistry 2020.

A successful transfer of the phase separation to a running fermentation process is highly dependent on the operational conditions. In the phase separation experiment, a narrow drop-size distribution could be observed. However, this is not the case in fermentation concepts using agitation, such as present in STRs with Rushton turbines commonly installed for bacterial cultures, as high shear forces are induced. These cause a small Sauter mean diameter and a broad drop size distribution of the second liquid phase [201], and the formed emulsion is stabilized by the presence of RLs due to their surface-active characteristic [202]. Although beneficial for extraction efficiency due to a high surface-to-volume ratio, the emulsion tends to separate less rapidly [203].

Nevertheless, continuous two-liquid phase fermentations have been conducted in STRs [175, 204]. For two-liquid phase STR cultivations described in this thesis, the solvent was not removed continuously, but phase separation was achieved by centrifugation. However, regarding the operation of the MPLR described in Chapter 3.5, the concept of introducing a coalescer in a solvent settling compartment was readopted.

Extraction of rhamnolipids with ethyl decanoate is dependent on pH

The dissociated form of molecules with carboxylic groups dissolves easily in water, whereas the protonated form can pass interfaces into organic phases. This principle for pH-dependent extraction has been described and modeled, *e.g.*, for carboxylic acids [205], to which the produced RLs are similar as they exhibit a carboxyl group. In accordance, the pH value was previously shown to impact the extraction of RLs with ethyl acetate as an organic solvent [163]. However, as determined in the preliminary selection based on physicochemical properties, ethyl acetate does not meet the requirements for being applied as an *in situ* extraction solvent in bioprocesses.

In detail, the pH-dependency was investigated for the extraction with ethyl decanoate in a broad pH range with a focus on the physiologically feasible range (pH 6 - 8) for *P. putida* KT2440. The experiments confirmed that the equilibrium concentrations of RL in the respective phases are dependent on the pH value (Figure 9A). At acidic conditions, the RLs were almost exclusively present in the organic phase. In contrast, at alkaline pH values, a shift of the partition coefficient below 4 at the respective phase ratio of 1:4 (v/v) was observed (Figure 9B). Considering different congeners, the pH value for reaching an inversion of the partition coefficient for HAAs in favor of the aqueous phase was shifted to a more alkaline pH value in comparison to mono-RLs (Appendix A.2, Figure A2.3). However, as the percentage of mono-RLs in the extracted fermentation broth was 80 % of the total amount of RLs, the sum of all HAA and mono-RL congeners was used as a measure for extraction.

The transitional range, in which an inversion of the partition coefficient is reached, roughly spans from pH 6 to pH 8. Thus, the pK_A -value of the RLs is located around neutral pH. In contrast, pK_A -values for RLs produced by *P. aeruginosa* determined by potentiometry and spectroscopic approaches range from 4.28 to 5.50 [206]. However, the congener composition influences the pK_A as indicated when considering the different congeners individually (Appendix A.2, Figure A2.3).

RLs are amphiphilic molecules, *i.e.*, they exhibit highly hydrophilic and hydrophobic regions. Therefore, they tend to accumulate at interfaces [207] or form micelles in bulk phases [208]. Since the presence of the RLs in respective phases depends on the pH value, their overall affinity changes most likely by the dissociation degree of the carboxylic group enabling the RLs to pass the phase boundary.

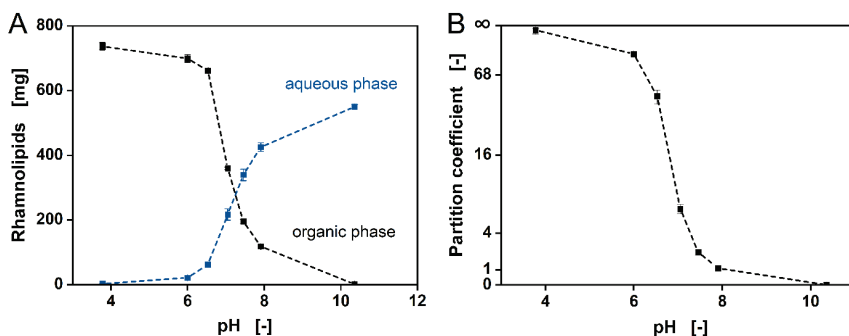


Figure 9 pH-dependency of rhamnolipid extraction with ethyl decanoate. (A) RL amount in the coherent ethyl decanoate (black) and aqueous (blue) phase at different pH values, and (B) respective partition coefficients for extraction from the aqueous phase to the organic phase. Error bars represent standard deviations from the mean of measurements from three independent experiments. This figure was previously published [125] and is reprinted with permission from Green Chemistry. Copyright The Royal Society of Chemistry 2020.

Generally, at higher pH values, more interphase was visible. As RL concentrations could only be measured in the coherent phases, the product entrapped in the interphase was not quantified, explaining the inconsistent total mass of RLs at different pH values. Thus, the partition coefficient was calculated from the ratio of concentrations quantified in the coherent phases. The accumulation of RLs in the interphase was previously identified as one of the main reasons for the loss of product [209]. As the interphase formation is strongly dependent on the pH value and proteins typically present in the fermentation broth, precipitation of the proteins can prevent interphase formation and overcome product loss. However, this is not feasible for an *in situ* extraction as protein precipitation cannot be applied during fermentation. Nevertheless, the recovery of RLs from the interphase should be considered for a higher overall yield of the process.

For comparison, the same pH-dependent extraction experiments were conducted with 1-decanol and methyl decanoate. No pH-dependency of the extraction was observed for 1-decanol, whereas the distribution of RLs when extracting with methyl decanoate was less sensitive to pH-shifts compared to extraction with ethyl decanoate (Appendix A.2, Figure A2.4). Therefore, the pH-dependency of RL extraction cannot be assumed universally but depends on the solvent.

Efficient recovery of rhamnolipids and solvent is enabled by pH-shift

Although often not regarded in studies for two-liquid phase fermentations, subsequent product recovery from the organic phase after *in situ* extraction has to be considered, as it economically and ecologically affects the overall process. Here, a thermal separation is not applicable as unreasonable amounts of energy would be required due to the high boiling point of ethyl decanoate (241.5 °C) at normal pressure. Therefore, back-extraction as a non-thermal recovery operation was assessed for pH values ranging from 4.8 to 11.75.

In general, the back-extraction showed similar results compared to the initial extraction as it was strongly influenced by the pH value (Figure 10). While the bulk of the RLs remained in the organic phase at acidic pH values, the partition coefficient shifted to a minimum, close to zero, at only slightly alkaline pH values. Therefore, the RLs can be recovered from ethyl decanoate, allowing the reuse of the solvent for further extractions. Concerning interphase formation, similar phenomena could be observed as described above for extracting RLs from the aqueous phase. Considering process design, the high sensitivity to pH values proposes back-extraction of RLs as the product recovery operation subsequent to *in situ* extraction.

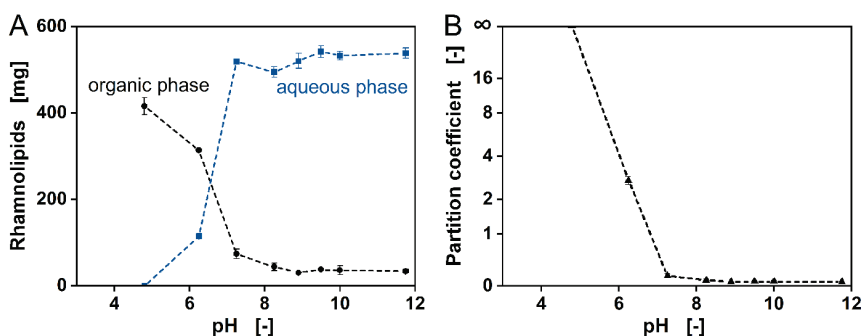


Figure 10 Back-extraction of rhamnolipids from loaded ethyl decanoate. (A) RL amount in coherent ethyl decanoate (black) and aqueous (blue) phase at different pH values, and (B) respective partition coefficients for back-extraction from the organic phase to the aqueous phase. Error bars represent standard deviations from the mean of measurements from three independent experiments. This figure was previously published [125] and is reprinted with permission from Green Chemistry. Copyright The Royal Society of Chemistry 2020.

3.1.3.3 Application in two-liquid phase fermentations

Ethyl decanoate was identified as the most promising solvent candidate for *in situ* RL extraction. The favorable characteristics were validated in two-phase fermentations in stirred-tank bioreactors.

Ethyl decanoate can prevent foaming in two-liquid phase fermentations

First, fermentations were conducted without *in situ* extraction. Notably, the fermentations started to foam excessively at an RL concentration of merely 18.5 mg L^{-1} shortly after inoculation. Foaming could only be controlled by the addition of large amounts of antifoam. In contrast, in the two-liquid phase batch fermentation at a pH value of 7, the addition of ethyl decanoate initially prevented foaming (Figure 11), thus enabling cultivation for a short time. However, to cultivate longer than 3.8 h, again, extensive amounts ($> 40 \text{ mL}$) of anti-foaming agent (Antifoam 204, Sigma-Aldrich) had to be added. The addition of antifoam resulted in unprecise RL quantifications as indicated by enlarged error bars. Moreover, due to high costs and increased efforts in further

DSP, the addition of large amounts of antifoam is not recommended [119, 120] and was not further considered.

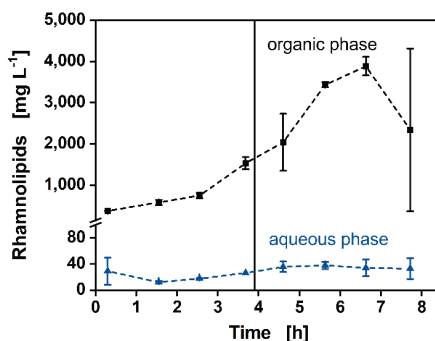


Figure 11 Extractive two-phase fermentation at standard conditions. *P. putida* KT2440 SK4 were cultivated in 700 mL MSM and in the presence of 100 mL ethyl decanoate. The pH was maintained at a value of 7. Data for rhamnolipid concentrations in the organic phase (blue triangles) and the aqueous phase (black squares) are shown. The black vertical line marks the time foaming occurred and the addition of anti-foaming agent. Error bars represent the maximum and minimum values of measurements from two independent experiments. Data associated with this figure were partially obtained from Carolin Grütering's Internship Report [194]. This figure was previously published [125] and is reprinted with permission from Green Chemistry. Copyright The Royal Society of Chemistry 2020.

Foam-free fermentations prolonged by reducing the pH value

The addition of ethyl decanoate enabled fermentations in STRs at reference conditions. However, the duration of the fermentation was not prolonged enough resulting in low RL concentrations at the time of foaming. As a strong dependency of the extraction efficiency on the pH value in cell-free fermentation broth was observed, its feasibility was attempted to be transferred to *in situ* extractions in the presence of *P. putida* KT2440 SK4. Here, the impact of a lowered pH on cell growth and productivity was assessed by comparing the previous batch fermentations at a pH value of 7 (standard condition) with fermentations at pH values of 6.5 and 6. The fermentations were terminated when excessive foaming occurred, or glucose was depleted.

As shown above, at pH 7, the fermentation started to foam excessively 3.8 h after inoculation. Here, about 1.5 g L_{org}⁻¹ RLs accumulated in the organic phase, and 26 mg L_{aq}⁻¹ remained in the aqueous phase. By reducing the pH value to 6.5, foaming caused the fermentation to be terminated after 6.1 h, during which 3.2 g L_{org}⁻¹ RLs were extracted into the organic phase, and 38 mg L_{aq}⁻¹ remained in the aqueous phase. At a pH value of 6, no foaming occurred, and 10 g L⁻¹ glucose was depleted within 10.8 h resulting in 6.8 g L_{org}⁻¹ RLs present in the organic phase and about 84 mg L_{aq}⁻¹ in the aqueous phase translating to a yield of 0.106 g_{RL} g_{GLC}⁻¹ (Figure 12A). After glucose depletion, cells did not show any respiratory activity, indicating an immediate metabolization of ethyl decanoate without adaptation to be infeasible for *P. putida* KT2440 SK4 at the given conditions. Therefore, the characteristics determined in the biocompatibility and

biodegradation assay are transferable to fermentations in STRs. Remarkably, comparing the cultivations, the RL concentrations in the aqueous phases differed at the time foaming occurred. Higher concentrations at lower pH values indicate a direct impact on the foaming characteristics of RLs, which has been suggested previously [210]. Here, the undissociated RLs might have a less amphiphilic character at lower pH values resulting in a lower tendency towards foaming. The ratio of produced RLs was composed of approximately 20% HAAs and 80% mono-RLs, which did not alter throughout all fermentations.

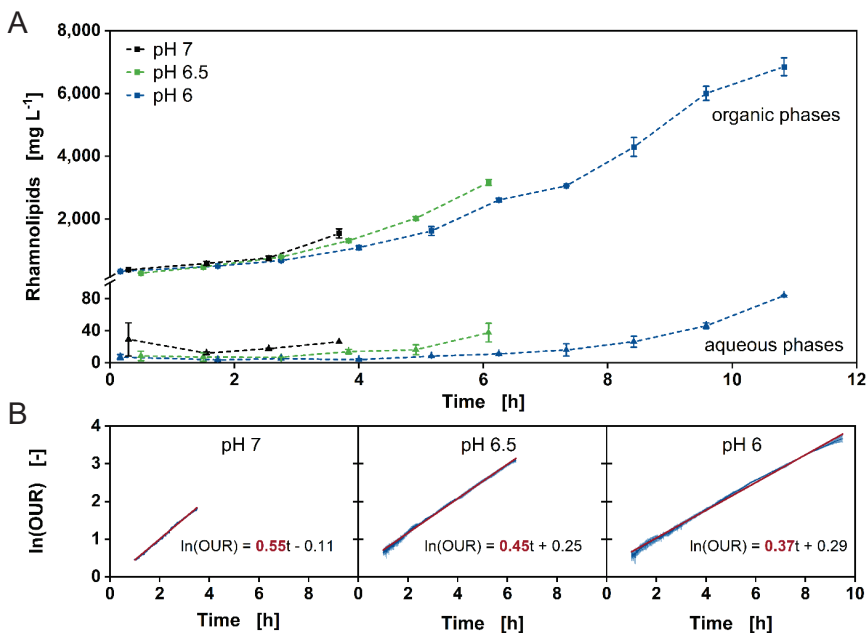


Figure 12 Production of rhamnolipids in extractive two-liquid phase fermentations and OUR-derived growth rates at different pH values. *P. putida* KT2440 SK4 were cultivated in 700 mL MSM with 10 g L^{-1} and in the presence of 100 mL ethyl decanoate. The pH was maintained at 7, 6.5, and 6. Cultivation was terminated when foaming occurred. (A) RL titers over the course of the fermentations at pH 7 (black), pH 6.5 (green), and pH 6 (blue) in organic (square) and aqueous (triangle) phases. (B) Determination of OUR-derived growth rates at respective pH values. Fermentations were terminated when foaming occurred. Error bars or borders of shaded areas represent maximum and minimum values of measurements from two independent experiments. Data associated with this figure were partially obtained from Carolin Grütering's Master Thesis [211]. This figure was previously published [125] and is reprinted with permission from Green Chemistry. Copyright The Royal Society of Chemistry 2020.

Since optical density measurements or the determination of the cell dry weight were not possible due to the formation of stable emulsions, the oxygen uptake rate (OUR) was used to estimate growth rates. Assuming an equal oxygen demand for each cell at each point of time and exponential growth, the slope of the logarithmic OUR over time represents the growth rate (Figure 12B). The cultivations at pH 7 showed an OUR-derived growth rate of 0.55 h^{-1} , which agrees with

published growth rates of *P. putida* KT2440 on glucose as the sole carbon and energy source in the absence of a solvent [212, 213]. Therefore, it can be concluded that ethyl decanoate is not detrimental to the viability of *P. putida* KT2440 SK4, confirming its biocompatibility. At lowered pH values of 6.5 and 6, the OUR-derived growth rates decreased to 0.45 h^{-1} and 0.37 h^{-1} , respectively, which can be attributed to the limited acidic stress response of *P. putida* KT2440 [108] and indicates non-optimal conditions for the production strain. However, the determined growth rates are still sufficiently high for efficient fermentation. Therefore, decreasing the pH value was shown to be an efficient measure for enhanced extraction of RLs and thus foam prevention in two-liquid phase fermentations. Although a reduced pH value has a negative effect on the whole-cell biocatalyst, a good overall performance for producing RLs could be maintained.

Gradual pH reduction prevents foaming at optimal growth in fed-batch fermentation

As a lowered pH is disadvantageous for growth but prevents foaming, a two-liquid phase fermentation strategy with foam-dependent reduction of the pH value was developed, ensuring optimal cultivation conditions for the longest possible duration. Here, the initial pH value was set to 7 and was gradually reduced every time the surface of the fermentation broth was covered with foam. pH-shifts in the course of fermentations are common, however, usually focused on influencing the metabolism of the whole-cell biocatalyst for higher production [88, 214–216] rather than on establishing fermentation stability *via* ISPR. The previous fermentations demonstrated that foaming could be prevented entirely at a pH value of 6, a phase ratio of 1:7 (v/v) organic to aqueous phase and 10 g L^{-1} glucose. Here, the initial aqueous phase was reduced to 400 mL resulting in a ratio of 1:4 (v/v) organic to aqueous phase to enable the addition of feed solution after the initial 10 g L^{-1} glucose had been depleted. Thus, over time, the phase ratio decreased to 1:7 (v/v) organic to aqueous phase.

After initial glucose depletion after 8.6 h, a DOT-controlled feeding was applied to enable fermentation at glucose-limited conditions, except when starting the feed. Throughout the fermentation, the bulk of the produced RLs was extracted by ethyl decanoate. While the concentration of RLs in the organic phase increased over time until the end of the cultivation, the concentration in the aqueous phase remained between $1.2 \text{ g L}_{\text{aq}}^{-1}$ and $1.5 \text{ g L}_{\text{aq}}^{-1}$ after approximately 15 h (Figure 13). The pH value had to be reduced in shorter time intervals at the beginning of the cultivation, whereas only one reduction was necessary after the start of the feed, although the bulk of RLs was produced in fed-batch mode. At depletion of the feeding solution, final titers of $29.6 \text{ g L}_{\text{org}}^{-1}$ RLs in the organic phase and $1.2 \text{ g L}_{\text{aq}}^{-1}$ RLs in the aqueous phase were achieved, corresponding to 3.8 g produced RLs within 33.2 h (volumetric productivity of $0.16 \text{ g L}^{-1} \text{ h}^{-1}$). A total of 52.7 g glucose was converted at this point, translating to a yield of $0.072 \text{ g}_{\text{RL}} \text{ g}_{\text{GLC}}^{-1}$. Both performance indicators compare well with the study of Blesken *et al.* [41]

while exceeding those of Anic *et al.*[123] and Beuker *et al.*[122], all producing RLs from glucose using recombinant *P. putida* KT2440 and integrating *in situ* RL recovery by foam fractionation, partially coupled to adsorption. The yield of the batch phase, *i.e.*, before the start of the feed, is increased by 11% to $0.118 \text{ g}_{\text{RL}} \text{ g}_{\text{GLC}}^{-1}$ compared to the yield of the batch fermentation at a constant pH value of 6 ($0.106 \text{ g}_{\text{RL}} \text{ g}_{\text{GLC}}^{-1}$), indicating a beneficial effect of the foam-dependent pH-reduction. The pH value had to be lowered to a minimum of 6.2 to prevent foaming. Therefore, the pH-dependency for RL extraction with ethyl decanoate shown *in vitro* could be successfully transferred to fermentations, as a moderate pH-shift was sufficient for foam prevention. In particular, the pH value represents an easily controllable parameter in fermentation processes, which is standardly assessed and maintained in state-of-the-art fermentations. Thus, no extraordinary technical effort as required for foam fractionation or foam recycling is necessary, allowing better scalability. Increasing the phase ratio by adding more solvent or implementing fermentation concepts with integrated continuous solvent circulation [54, 204] could enable foam prevention even at elevated pH values, thus potentially improving the yield even further.

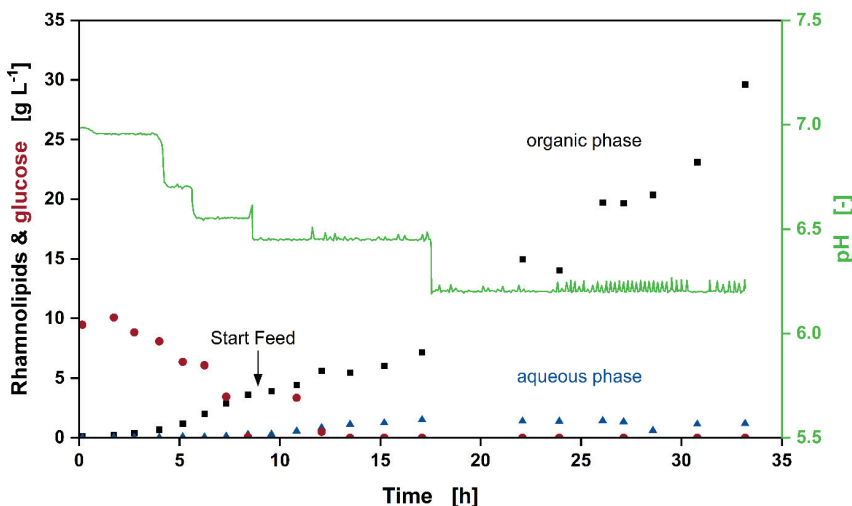


Figure 13 Production of rhamnolipids in a fed-batch fermentation with a foam-based pH reduction. *P. putida* KT2440 SK4 was cultivated in the presence of 100 mL ethyl decanoate serving as the extractant. The 400 mL MSM for the initial batch cultivation was supplemented with 10 g L^{-1} glucose, while the 247 mL feeding solution was concentrated MSM supplemented with 200 g L^{-1} glucose. Feeding was controlled by the DOT value, with a setpoint for feed start at DOT = 70% and feed stop at DOT = 30%. The pH value was manually reduced when foaming occurred. RL titers in the organic (black squares) and the aqueous phase (blue triangles), glucose concentrations (red circles) as well as the pH profile (green line) are shown. Data associated with this figure were partially obtained from Carolin Grütering's Master Thesis [211]. This figure was previously published [125] and is reprinted with permission from Green Chemistry. Copyright The Royal Society of Chemistry 2020.

3.1.4 Discussion

In this chapter, a multi-step, reductive solvent selection approach for *in situ* liquid-liquid extractions in bioprocesses was developed and applied. Ethyl decanoate was identified as highly suitable for *in situ* extraction of RLs produced by recombinant *P. putida* KT2440, thus preventing foaming during fermentation. A holistic process assessment considering the solvent characteristics and the resulting implications for the solvent selection approach are discussed in the following paragraphs.

3.1.4.1 Holistic process assessment regarding solvent characteristics is crucial

In general, processes cannot be designed only considering a single unit operation because conditions resulting in favorable performance indicators for one unit operation might be disadvantageous for others. Especially in process intensifications, where unit operations are often not separated spatiotemporally, potentially contrary effects need to be assessed carefully. For two-liquid phase fermentations, this encompasses the interactions of fermentation, extraction, and further operations for product recovery.

In the presented case of selecting an extraction solvent to recover RLs from the fermentation broth *in situ*, a sole assessment of the partition coefficient and the flash point, ensuring safe processing regarding flammability, would favor selecting 1-decanol over ethyl decanoate. However, these performance indicators do not assess solvent regeneration. As DSP is typically responsible for the majority of the overall process costs [57] and solvent wastage is environmentally critical [217], a careful assessment early in process development is inevitable. Rectification is commonly applied for solvent regeneration after extraction. However, a premise for its application is a reasonably low boiling point to avoid excessive use of energy. Generally, solvents exhibiting low boiling points typically are low in molecular size. Contrarily, solvents exhibiting high flash points necessary for safe operation are high in molecular size. Even if measures for protection against fire hazards can be taken, the application of solvents of small molecular size often conflicts with lower biocompatibility due to an increased solubility in the aqueous fermentation broth expressed in a low $\log P$ [218]. Both solvent candidates for *in situ* RL extraction, 1-decanol and ethyl decanoate, exhibit high boiling points at ambient pressure. Therefore, rectification is economically and ecologically not suitable for further recovery. The energy required for rectification results in an unfavorable Environmental Score according to the CHEM21 solvent selection guide by Prat *et al.* [156] and caused Rosinha Grundtvig *et al.* [72] to rate both solvents as ‘problematic’ for their application as extractants.

In this thesis, back-extraction by pH-shift as an operation to recover RLs from the extraction solvent as an alternative to rectification is presented, thus bypassing the requirement of a low

boiling point. For back-extraction, ecologic and economic evaluation parameters are the amounts of applied acids and bases as well as the produced salts to adjust the pH value, usually further treated as waste [58]. The partition coefficient of RLs in a 1-decanol-water system was shown not to be dependent on the pH value. In contrast, in an ethyl decanoate-water system, the partition coefficient could be entirely inverted by shifting the pH value solely by one unit from neutral to acidic or alkaline. While the pH value during fermentation needs to be slightly acidic to prevent foaming but still allow sufficient growth and production, its shift into the alkaline milieu for back-extraction requires only small amounts of base and is thus ecologically and economically favorable. Further, back-extraction as recovery operation regenerates the solvent for reuse, thus minimizing its wastage, which was viewed as an exclusion criterion by Najmi *et al.* [219] for using solvents for biosurfactant recovery. Therefore, the feasibility of applying back-extraction to recover RLs strongly favors ethyl decanoate over 1-decanol.

Contrary to an evaluation solely based on the partition coefficient, ethyl decanoate clearly outcompetes 1-decanol to be applied as a sustainable extractant for RLs in an overall process consideration. This supports the importance of a holistic process assessment, which, among others, has previously been highlighted by Kampwerth *et al.* [220], evaluating the overall solvent performance in a model comprised of extraction and subsequent recovery by rectification.

3.1.4.2 The reductive multi-step approach enables efficient solvent selection

In the scope of a holistic process evaluation, the solvent for a two-liquid phase fermentation is of central importance. To decide on a suitable solvent, many solvent parameters have to be considered. Here, a selection approach based on thermodynamic models is advantageous as many solvents can be evaluated for specific applications without experimental effort. In studies by Scheffczyk *et al.* [221] and Kruber *et al.* [222], more than 4,600 solvents were considered to extract γ -valerolactone from an aqueous phase based on the prediction of thermodynamic properties. Solvents were identified, reducing the total annual cost by more than 50% compared to a benchmark solvent. Although the studies aim for product removal from fermentation broths, they considered a binary component system. However, the complex and undefined nature of fermentation broths might lead to inaccurate predictions of the models as thermodynamic interactions of different metabolites, salts, proteins, and cells influence the extraction performance. This conflict is reflected in simulations by Birajdar *et al.* [223], who could qualitatively predict partition coefficients for sequential extraction of 2,3-butanediol from fermentation broth. However, quantitative results could only be obtained after implementing adapted parameters based on experimental data. While the fermentation broth can be clarified before a sequential extraction, *e.g.*, by precipitation and centrifugation, potentially increasing the prediction accuracy of the

binary component models, this is not suitable for *in situ* extractions. Additionally, the system is dynamic, as the composition of the broth changes throughout the fermentation.

Next to evaluations of solvents by thermodynamic models, several guides have been published, which base the solvent selection on physicochemical properties [156, 217, 224–228]. While these mainly regard solvent usage in the chemical industry, Rosinha Grundtvig *et al.* [72] focused on solvent applications in bioprocesses. This screening of organic solvents based on the CHEM21 solvent selection guide [156] addresses environment, health, and safety challenges in early selection stages. Further, Rosinha Grundtvig *et al.* [72] state the vital necessity to experimentally evaluate pre-selected solvents, as the actual suitability of the solvent for the process is dependent on the characteristics of the overall system, including interactions of the organism, the product, and the solvent. However, the experimental effort necessary to collect data increases with the number of considered solvents, rapidly reaching such efforts where time and resources invested outweigh the benefit of selecting the superior extraction solvent.

In accordance, a reductive, multi-step solvent selection approach is proposed here. This approach aims to consider many solvents and nevertheless examine critical parameters in detail by combining theoretical and experimental approaches. After a preceding selection based on physicochemical properties retaining an experimentally manageable number of solvents, further selection steps are structured in ascending order of experimental effort. The eventually chosen solvent is further characterized in detailed experiments, which consider the overall system, and finally tested in fermentations.

Next to focusing on physicochemical properties of the solvents in the data-based preselection, sustainable and low-hazardous solvents are favored. Equal to the approach by Rosinha Grundtvig *et al.*, we used the Health Score of the CHEM21 solvent selection guide, but in contrast, adjusted the safety and environmental considerations to the studied system. In the presented approach, especially the strong influence of the boiling point on the rating was attenuated to account for solvent recovery methods other than rectification such as back-extraction.

A disadvantage of the reductive approach could be the requirement of potential iterative loops for adjusting primarily chosen thresholds to prevent the exclusion of all solvents due to underperformance. In this case, primary thresholds would need to be adjusted by considering solvent candidates classified here as ‘Limited’ in the data-based screening.

In contrast to other published guides, the feasibility of the proposed selection approach is demonstrated here by successfully applying the selected solvent, ethyl decanoate, in an *in situ* extraction of RLs produced by recombinant *P. putida* KT2440 in laboratory-scale STRs. However, it cannot be surely claimed that ethyl decanoate is the best solvent in terms of overall cost and efficiency for the envisioned process. Due to the reductive nature of the selection, a solvent

performing better overall might have been excluded in early stages based on a single rated property. Nevertheless, ethyl decanoate was highly suitable as its application could not only resolve the initial objective of overcoming the process instability due to extensive foaming, but the pH-dependent partition coefficient also enables efficient product recovery and sustainable solvent reuse. Further, ethyl decanoate poses little risk in handling due to its low hazardousness.

The list of solvent candidates and their respective physicochemical properties is published as open access (<https://git.rwth-aachen.de/campenhausem/list-of-solvents>) to enable a transfer of the approach to other solvent selections, specifically in the field of bioprocessing. The user can edit, extend, and refine the solvent list, as completeness is not claimed. Additionally, the thresholds for the physicochemical properties chosen here have to be adapted for particular applications.

3.1.5 Conclusion

In this chapter, a reductive, multi-step approach for selecting *in situ* liquid-liquid extraction solvents in the field of bioprocessing was developed. Particularly, its applicability by establishing a two-liquid phase fermentation for the foam-free production of RLs was demonstrated. Although customized to the fermentation and product system, the presented approach will facilitate other solvent selections. Its reductive multi-step character minimizes experimental effort while still enabling the selection of highly efficient and sustainable solvents for bioprocesses until a theoretical, truly holistic methodology is available.

Chapter 3.2

Engineering of *Pseudomonas putida* KT2440 for enhanced solvent tolerance

Contributions

Plasmids and strains were designed, constructed, and characterized by Philipp Demling (all), supported by Greta Kleinert (genomic integration of point mutations), Arne Zimmermann (plasmid-based expression and genomic integration of *tigGHI* encoding for an efflux pump and plasmid-based expression of *groEL-groES* encoding for a chaperone complex), and Sarika Karri (plasmid-based expression of *cspA-II* encoding for a cold-shock protein). ALE experiments were performed by Philipp Demling and Arne Zimmermann. Philipp Demling and Greta Kleinert performed STR cultivations for rhamnolipid production. Sebastian Köbbing is gratefully acknowledged for the provision of specific genetic constructs. The manuscript is in preparation. The chapter was written by Philipp Demling and reviewed by Till Tiso.

3.2 Engineering of *Pseudomonas putida* KT2440 for enhanced solvent tolerance

3.2.1 Abstract

As *Pseudomonas putida* KT2440 has a versatile carbon metabolism, the consumption of the value-added product is a recurring challenge in bioprocesses catalyzed by the strain. *In situ* product removal and especially *in situ* product extraction by adding an organic solvent is promising to provide remedy. Compared to other *P. putida* strains, *P. putida* KT2440 is regarded as solvent-sensitive but has a number of advantages, including a documented biological safety categorization. In this chapter, *P. putida* KT2440 is engineered to increase its solvent tolerance to enable the use of a broader range of organic solvents as extractants, particularly for rhamnolipid recovery in the scope of this thesis. While rational strain engineering did not yield desired phenotypes, adaptive laboratory evolution as an untargeted approach enabled tolerance to 1-octanol. Preliminary results additionally indicated an enhanced tolerance to *n*-pentane. Re-sequencing of the genome of adapted strains revealed several point mutations, which were in part shown to cause the tolerant phenotype by their individual introduction into the genome of the wild-type strain. Engineered *P. putida* KT2440 strains tolerant to 1-octanol were assessed in terms of rhamnolipid production capacity in a two-liquid phase fermentation with 1-octanol serving as the extractant. Although the strains were able to produce rhamnolipids, production was delayed. However, excessive foaming, originally causing severe instabilities during the fermentation, could be avoided. Lastly, the capability of generated strains to produce 1-octanol - the original stressor itself - was estimated. Preliminary results indicated minor 1-octanol production.

3.2.2 Introduction

Microbial production of hydrocarbons and related oxygenates has been in the focus of synthetic biology and metabolic engineering as efficient production could reduce or even replace the use of petrochemically derived hydrocarbons [229, 230]. Particularly, several efforts have been made to produce alternative fuels, replacing conventional propellants, or drop-in compounds, which are admixed to established fuels for partial substitution [231–234]. Further, there is an increased interest to apply organic solvents in two-liquid phase fermentation processes for the *in situ* extraction of products [46]. In particular, applying *in situ* product removal (ISPR) in fermentation processes for the production of toxic compounds, which inhibit the whole-cell biocatalysts above lethal concentrations [73], or for resolving process instabilities such as excessive foaming [125] (also refer to Chapter 3.1) is promising. Nevertheless, the application or production of many hydrocarbons and related oxygenates in fermentation processes is restricted as many are toxic to whole-cell biocatalysts used for production [235], even at low concentrations.

Although tolerant strains have been isolated and engineered to produce compounds such as (*S*)-styrene oxide [178, 236], phenol [42, 137, 172], and *n*-octanol [237], in cases, more severe restrictions due to increased biological safety levels have to be complied with. In a complementary approach, whole-cell biocatalysts, which are not or sparsely endowed with tolerances to solvent-like organic compounds naturally, are engineered to enhance specific or general tolerances.

Several rational approaches for strain engineering have been performed as thoroughly reviewed by Mukhopadhyay [40] and Dunlop [238]. Generally, genetic constructs responsible for solvent-defense mechanisms in tolerant strains were transferred to preferred chassis for whole-cell biocatalysts. These defense mechanisms include solvent extrusion *via* efflux pumps, elevated stress responses, *e.g.* supporting protein refolding, membrane modifications, and excess energy production [192, 239]. Particularly, the expression of solvent-specific efflux pumps non-native to the host chassis [240, 241] and the overproduction of chaperones for assisted protein folding or supported protein production [242, 243] have been of interest and are highlighted in this chapter.

Efflux pumps, particularly RND (Resistance-Nodulation-Division) family efflux transporters, are regarded as highly efficient for conferring tolerance to Gram-negative bacteria [239]. The structure of RND efflux pumps, consisting of an inner membrane protein for solvent extrusion to the periplasm, an outer membrane protein channeling the periplasm to the cell's exterior, and a stabilizing protein, allows the cell to actively extrude components from the cytosol to the exterior utilizing the proton-motive force [244]. In solvent-tolerant pseudomonads, such as *P. putida* DOT-T1E, *P. putida* S12, or *P. taiwanensis* VLB120, three RND efflux pumps (TtgABC, TtgDEF, and TtgGHI, the latter named SrpABC in *P. putida* S12) have been identified to be synergistically responsible for conferring tolerance to specific aromatics and other hydrocarbons or related oxygenates [245]. While TtgABC and TtgDEF are encoded in the core genome of the mentioned strains, *ttgGHI* is located on a native mega-plasmid [42]. *P. putida* KT2440 lacks the mega-plasmid and therefore the TtgGHI efflux pump, which is regarded as one of the main reasons for its diminished solvent tolerance [246]. Likewise, deletion of *srpABC* in *P. putida* S12 severely reduced solvent tolerance (among others to 1-octanol), which could be restored by reintroducing plasmids harboring *srpABC* [247].

In contrast to solvent-tolerant strains, *P. putida* KT2440 reacts to solvent stress by activating a comparably higher number of chaperones [248, 249]. Among these activated chaperones, CspA-II was identified to support protein synthesis, and the GroEL-GroES complex or homologs (also called HSP10 and HSP60) have been shown to be induced in response to solvents by assisting protein refolding in several bacterial species [250, 251].

Alternatives to rational engineering approaches for enhancing the solvent tolerance of whole-cell biocatalysts are non-targeted approaches. In this regard, adaptive laboratory evolution (ALE)

has been widely applied in many studies recently, enhancing tolerance to several toxic compounds in different microorganisms or increasing growth rates on comparably unfavorable substrates [152, 252–254]. During ALE, the microorganism is serially cultivated in the presence of a stressor to select for favorable mutations that allow adaptation to the selective pressure, which is typically increased regularly throughout the series of cultivations, leading to the development of variants of the parent strain with an improved phenotype at given conditions. Regarding organic solvents as stressors, among others, *E. coli* tolerant to *n*-butanol [255] and ethanol [256] and *P. putida* KT2440 tolerant to ethanol [257], have been developed, underlining the potential of ALE complementary to rational chassis engineering.

In this chapter, *P. putida* KT2440 was engineered to enhance tolerance to organic solvents. Rational approaches focused on overproducing the non-native efflux pump TtgGHI, the chaperone complex GroEL-GroES, and the cold-shock protein CspA-II, the latter two being native to *P. putida* KT2440. Further, *P. putida* KT2440 was subjected to ALE to generate tolerance to 1-octanol. Strains, which were able to tolerate 1-octanol, were recovered, and their genomes were re-sequenced to unveil potential mutations conveying tolerance. Selected mutations were reintroduced into the genome of wild-type *P. putida* KT2440. The resulting strains were tested for tolerance to several solvents, and ultimately, the tolerant strains were used as chassis for the production of RLs and 1-octanol.

3.2.3 Results

3.2.3.1 Synthesis of the efflux pump TtgGHI, the chaperone complex GroELS, and the cold-shock protein CspA-II in *P. putida* KT2440 did not yield tolerant phenotypes

The genes encoding for the efflux pump TtgGHI were introduced into *P. putida* KT2440 in multiple contexts. The transcription levels and triggers were adjusted by using promotor constructs for constitutive and inducible transcription. Further, different promotor sequences characterized to result in varying strengths of transcription were tested. In addition, resulting promoter/genes combinations were integrated at different genomic loci characterized to influence transcription. Since the production of large, recombinant protein complexes such as TtgGHI can result in a high metabolic burden for the cell [258], particularly low transcription levels were targeted. Next to TtgGHI, the genes encoding for the chaperone complex GroEL-GroES and the cold-shock protein CspA-II were overexpressed in *P. putida* KT2440. Here, the expression of the genes was plasmid-based and constitutive to enable an overproduction of the proteins native to *P. putida* KT2440.

Although most of the genetic variants for the expression of *ttgGHI* were successfully constructed, theoretically resulting in strains with different expression levels, none of the constructed *P. putida* KT2440 strains showed a phenotype of enhanced solvent tolerance.

Potentially, although targeted to be low, expression levels might have been too high. As TtgGHI spans across the inner and outer membrane of the cell, an overproduction might result in membrane disruption. Even when no stressor in form of an organic solvent was present, growth of the constructed strains was hampered, and plasmids harboring incomplete genetic insert were often detected, indicating that the plasmid was toxic for the cell. Further, the high energy demand for production and functionality of the efflux pump might have been a limiting factor. In contrast, the strain *E. coli* DH5 α pBNT-*ttgGHI*, originally a transitional strain for plasmid construction, showed tolerance to up to 50% (v/v) *n*-hexane by growing in multiple replicates of the qualitative solvent tolerance assay. *E. coli* DH5 α pBNT cultivated at the same conditions as a control was not tolerant to *n*-hexane (Appendix A.3, Figure A3.1). A potential low basal expression of *ttgGHI* might have occurred, producing the efflux pump in a suitable amount to confer tolerance without drastically decreasing the fitness of the cells. This is supported by *E. coli* DH5 α pBNT-*ttgGHI* showing tolerance to *n*-hexane, even when the culture was not supplemented with salicylate as the inducer. When subjected to other selected organic solvents, such as 1-octanol and cyclohexane, *E. coli* DH5 α pBNT-*ttgGHI* was not able to grow. Thus, the conferred tolerance is likely specific to *n*-hexane or potentially a limited number of organic solvents. However, the tolerant phenotype of *E. coli* DH5 α pBNT-*ttgGHI* indicates the functionality of the efflux pump. This agrees with literature, as the expression of *srpABC* of *P. putida* S12, homolog to *ttgGHI* in *P. taiwanensis* VLB120, in *E. coli* has been shown to confer tolerance to multiple solvents, including *n*-hexane, although only validated for a concentration of 1% (v/v) [259].

The overexpression of neither *groEL-groES* nor *cspA-II* conferred tolerance to solvents at high concentrations. Again, the expression levels might not have been optimal for *P. putida* KT2440. Although the functionality of CspA-II is, in contrast to GroEL-GroES [260], not dependent on chemical energy sources [261], its synthesis is. If the proteins were produced on a level that burdened the cells too strongly, less energy would be available for other mechanisms generating solvent tolerance.

As rational strain engineering did not yield the desired phenotypes, alternative approaches for generating tolerance to organic solvents were considered.

3.2.3.2 *P. putida* KT2440 adapts to generate inheritable tolerance to 1-octanol

An alternative, non-targeted approach to generate tolerance of *P. putida* KT2440 to 1-octanol was pursued by subjecting the cells to solvent stress, thus enforcing their adaptation for survival. 1-Octanol was chosen as a stressor as it was eliminated in the solvent selection in the step of screening physicochemical properties due to its comparatively low log *P* (3.00), thus was not regarded as biocompatible. However, the molecularly related 1-decanol showed high efficiency

for extracting RLs (refer to Chapter 3.1 and [125]). In a sequenced cultivation strategy, cells were cultivated in mineral salts medium (MSM) with glucose as a carbon source, alternatingly in absence or presence of the stressor 1-octanol to select for inheritable adaptations. Due to the formation of stable emulsions interfering with conventional methods to monitor biomass, the CO₂ volume concentration in the headspace of shake flasks served as a measure for growth.

In the first cultivation stage, no 1-octanol was present, and expectedly, all three replicates showed an exponential increase in CO₂ concentration after a short lag phase (Figure 14A-C, S1). After transferring part of the cells to MSM supplemented with a volume fraction of 1:25 (v/v) 1-octanol, no increase in CO₂ concentration was observable for 45 - 65 h, depending on the replicate, followed by an exponential increase, which indicated growth (S2). Removing the selective pressure in the subsequent cultivation stage (S3) resulted in a similar development of CO₂ concentration over time as exhibited in the first cultivation stage (S1) when likewise, no 1-octanol was present. When the cells were again exposed to 1-octanol in the fourth stage of the cultivation sequence (S4), the development of CO₂ concentrations differed from the primary exposure, as no stagnation was observed. In contrast, an immediate exponential increase was detected, indicating immediate growth in the presence of 1-octanol. Therefore, the adaptation, which occurred in S2, was inheritable and not detrimental to the overall fitness as the cells did not have to readapt to the presence of 1-octanol in S4, although the selective pressure was removed for several generations in between the cultivations (S3). Remarkably, the adaptation could be enforced in all three independent replicates by applying the selective pressure one time, thus indicating *P. putida* KT2440 to either have a robust cellular mechanism for building tolerance to 1-octanol, or to require only slight genomic modifications.

Further, comparing the exponential rates of increasing CO₂ concentrations indicates a generally higher growth rate for all replicates when 1-octanol was not present (Figure 14D, S1, S3). Considering cultivation stages in the presence of 1-octanol, improved rates of exponentially increasing CO₂ concentrations were recorded when subjecting the cells to 1-octanol for the second time (compare S2 to S4). This indicates the potential for further increasing the fitness by multiple exposures to 1-octanol as in a conventional ALE strategy targeting an improved growth rate. However, this often coincides with an increased uptake and conversion of the stressor [253, 262], which was not desired in this case. Rather, 1-octanol was targeted as a potential *in situ* extraction solvent in fermentation processes, and thus should not be consumed by *P. putida* KT2440. Notably, a change in the rate of increasing CO₂ concentrations (Figure 14B, S4; Figure 14C, S2) coincided with interrupting the shaker to retrieve one of the other cultures, which indicates a vital requirement for oxygen and thus energy to maintain solvent tolerance.

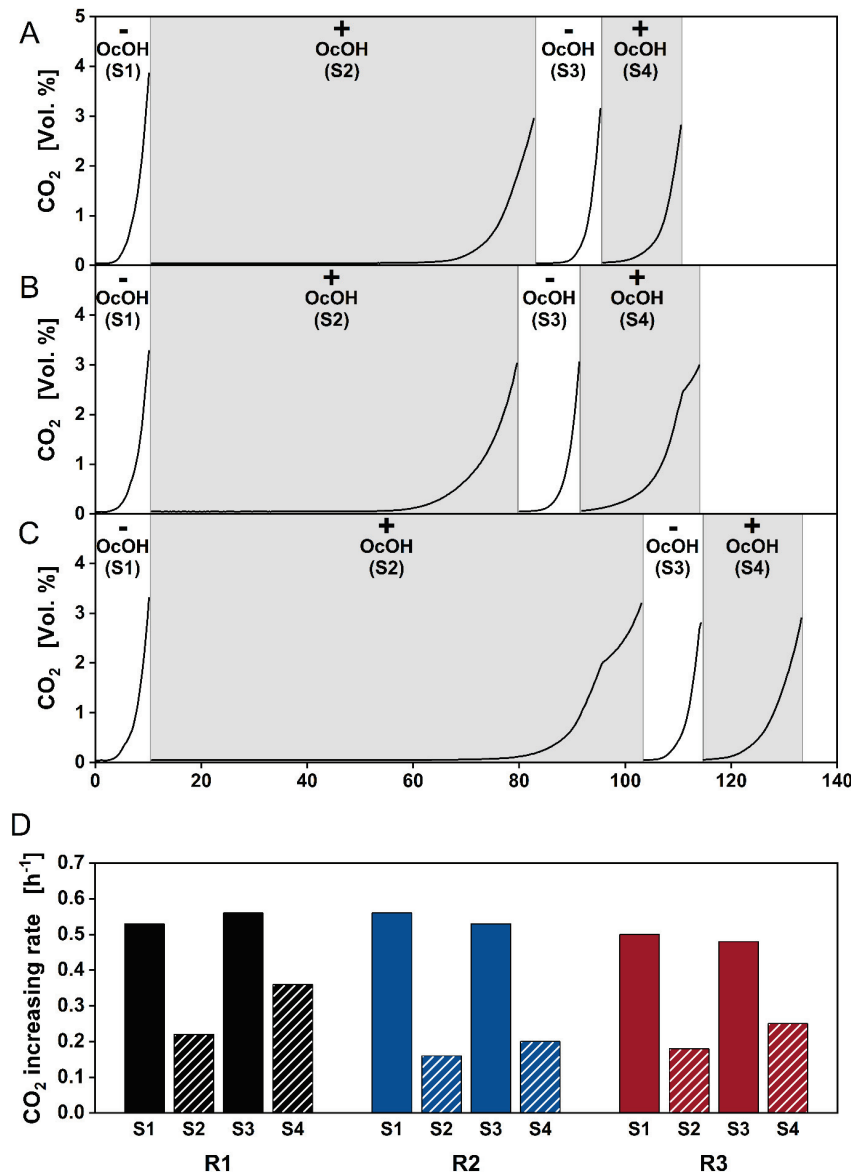


Figure 14 Sequential cultivation of *P. putida* KT2440 in absence and presence of 1-octanol to select for inheritable tolerance. *P. putida* KT2440 was cultivated in fresh MSM supplemented with 3 g L⁻¹ glucose (A-C) Independent replicates R1-R3. Light and shaded areas represent absence and presence of 1-octanol, respectively. OcOH = 1-octanol. (D) Rates of increasing CO₂ concentrations derived *via* linear regression. R# denotes the replicate, S# denotes the cultivation stage. Data associated to this figure were taken from Arne Zimmermann's Master Thesis [263].

All strains of respective cultivation stages (S1-S4) were cryopreserved for further characterization. To remove excessive 1-octanol, strains were recovered by cultivating the cryopreserved cells on solid LB agar plates and subsequently in liquid LB medium for secondary cryopreservation. Cells from the latter cultivation were again tested for tolerance to 1-octanol (Figure 15). Remarkably, even after removing 1-octanol as a selective pressure for several cultivation passages and thus multiple cell generations, *P. putida* KT2440 R#S4 from all three replicates showed immediate or slightly delayed growth once re-exposed to 1-octanol, indicating a robustly inherited tolerance. In contrast, non-adapted wild-type *P. putida* KT2440 did not show immediate tolerance but again adapted after an extensive incubation time.

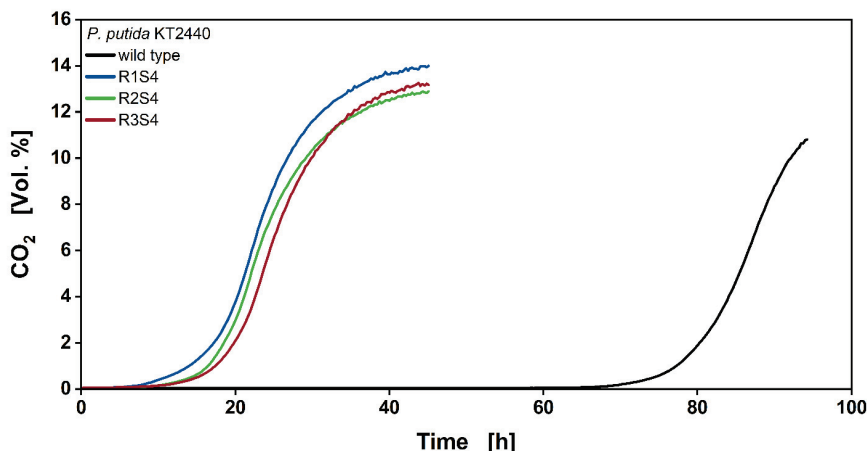


Figure 15 Cultivation of adapted *P. putida* KT2440 strains and the non-adapted wild-type *P. putida* KT2440 in the presence of 1-octanol. The MSM was supplemented with 2 g L⁻¹ glucose. All adapted strains were recovered from stage 4 of the ALE cultivation and processed for cryopreservation. Blue - replicate 1 stage 4 (R1S4), green - replicate 2 stage 4 (R2S4), red - replicate 3 stage 4 (R3S4), black - non-adapted wild-type strain. Data associated to this figure were partially taken from Arne Zimmermann's Master Thesis [263].

3.2.3.3 Genomic re-sequencing reveals potential tolerance-enhancing mutations

Genomes of evolved *P. putida* KT2440 strains originating from all S4-stages of the sequential ALE cultivations and one strain recovered after stage S1, serving as a non-adapted control, were sequenced and mapped to a reference genome of *P. putida* KT2440 (NC_00294) [264]. The differences between the non-adapted control strain and evolved strains were compared by setting a threshold value of 90% changed allele frequency regarding the reference genome (Table 4).

Table 4 Mutations in the genome of *P. putida* KT2440 introduced by ALE in the presence of 1-octanol.

Genomic position	Allele frequency of sequenced strain ^{a)}				Genetic change	Type/Influence	Protein ^{b)}
	R1S1 (control)	R1S4	R2S4	R3S4			
3212870	0	0.98	0	0	CA → C	Intergenic deletion	Upstream of <i>mexCD-oprJ</i> and <i>nfxB</i>
3913108	0	0	1.00	0	G → C	AA exchange (P324R)	PP_3453
3914470	0	0	0	1.00	G → C	AA exchange (P106R)	PP_3454
4586033	0	0.95	0.95	0	C → CG	Intergenic insertion	Downstream of PP_4063 and PP_4061

^{a)} R# refers to replicate, S# refers to the stage of the ALE cultivation after which the strain was recovered.

^{b)} According to the genomic annotation of *P. putida* KT2440 deposited at pseudomonas.com

All *P. putida* KT2440 strains, which were adapted to tolerate 1-octanol, exhibited genetic alterations compared to the non-adapted wild-type strain (R1S1). Although adapted individually, mutations in the same regions of the genomes and related genes were revealed.

In the genome of the adapted strain *P. putida* KT2440 R1S4 a mutation in the intergenic region between and upstream of *mexCD-oprJ* and *nfxB*, the latter encoding for the associated transcription regulator on the antisense strand, was detected. MexCD-OprJ is annotated as an efflux pump, which has been shown to be involved in conferring tolerance to antimicrobial agents [265, 266] and the organic solvents *n*-hexane and *p*-xylene [267] in *P. aeruginosa*.

Both *P. putida* KT2440 R2S4 and *P. putida* KT2440 R3S4 exhibited point mutations in either PP_3453 or PP_3454. The successive genes PP_3453 and PP_3454 are annotated as encoding for a signal-transducing, membrane-bound histidine kinase (also annotated as RstB) and its cognate transcription regulator (conceivably RstA), respectively [264], therefore composing a two-component signal transduction system (TCS). Those TCSs enable cells to react to environmental stimuli recognized by the membrane-bound histidine kinases, which specifically phosphorylate their cognate response regulators, in turn altering the transcription of target genes [268]. Point mutations potentially enable crosstalk between different TCSs. Here, both revealed point mutations lead to amino acid exchanges from proline to arginine. As proline is highly relevant to the structure of proteins [269], an altered function or potentially a loss of function is probable. The independent occurrence of mutations in the TCSs in two replicates of the ALE cultivation strongly supports their relevance in gaining tolerance to 1-octanol. Further, the point mutation in PP_3454 of *P. putida* KT2440 R3S4 was the only one detected in the whole genome, thus underlining its relevance.

Lastly, an intergenic insertion of a single nucleotide was detected in the genomes of *P. putida* KT2440 R1S4 and *P. putida* KT2440 R2S4 downstream of PP_4061 and PP_4063. The latter encodes for a long-chain fatty acid-CoA ligase, potentially having consequences for the composition of the cytoplasmatic membrane if expressed differently [270]. However, it remains unclear if this mutation influences the solvent tolerance of the cells as it did not occur as the only detected mutation in the genome, but always in combination with other mutations.

To characterize the impact of the single point mutations on tolerance to 1-octanol independently, they were introduced into the genome of wild-type *P. putida* KT2440. This chapter focused on the intragenic mutations in PP_3453 and PP_3454, as they appeared to be most relevant.

3.2.3.4 Introduction of identified mutations confers tolerance to 1-octanol

The mutations in the genes encoding for PP_3453 and PP_3454 revealed by genomic re-sequencing of evolved strains were introduced into wild-type *P. putida* KT2440 via the I-SceI-based genome editing methodology [145], resulting in strains *P. putida* KT2440 PP_3453-P324R and *P. putida* KT2440 PP_3454-P106R. Further, as the mutations were predicted to have a major influence on the structure of the proteins, individual single deletion strains and the corresponding double deletion strain were constructed, generating strains *P. putida* KT2440 Δ PP_3453, *P. putida* KT2440 Δ PP_3454, and *P. putida* KT2440 Δ PP_3453 Δ PP_3454. If both strains harboring single point mutations and the deletion strains showed the same phenotype regarding tolerance to 1-octanol, a loss of function by disruption of the PP_3453/PP_3454 TCS could be assumed. The constructed strains were characterized in terms of fitness in the absence and presence of 1-octanol.

First, the strains were cultivated in the absence of 1-octanol to determine if the insertion of the mutations or the deletion of PP_3453 and PP_3454 had a general influence on the growth behavior. Neither the point mutations nor the deletions generally altered the growth of the respective strains as similar growth curves compared to *P. putida* KT2440 were recorded (Appendix A.3, Figure A3.2). Although slight differences in initial lag phases and progressions of the curves were detected, all strains showed robust and comparable growth at standard conditions. Therefore, the modifications in the genomes of the respective strains did not influence their fitness.

Further, the constructed strains were qualitatively assessed for tolerance to 1-octanol by overlaying inoculated cultivation media with 16.7% (v/v) of the solvent before incubation. Wild-type *P. putida* KT2440 and the strains, which were obtained from ALE, served as controls. After 20 h of incubation, the cultures of *P. putida* KT2440 PP_3453-P324R and *P. putida* KT2440 PP_3454-P106R and the cultures of adapted strains showed turbidity as a distinct sign for growth (Figure 16). Notably, for cultivations of adapted or engineered strains harboring a mutation either

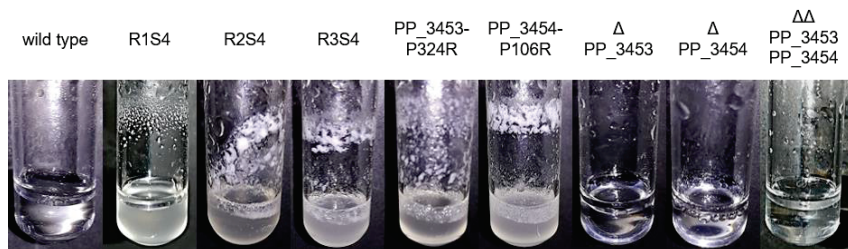


Figure 16 Qualitative solvent tolerance assay of adapted and engineered *P. putida* KT2440 strains with 16.7% (v/v) 1-octanol after 20 h of incubation. Strains were grown in 1 mL MSM supplemented with 2 g L⁻¹ glucose. R# denotes the replicate of the ALE. S# denotes the cultivation stage of the ALE. Turbidity indicates growth. Pictures were partially taken from Greta Kleinert's Bachelor Thesis [271].

in PP_3453 or PP_3454, crud formation was observed, indicating high levels of stress during growth. In contrast, cultures of the wild type and all deletion strains remained transparent, thus no apparent increase in biomass was observed. After 48 h of incubation, the wild-type strain had adapted to 1-octanol and was able to grow as indicated by distinct turbidity. Finally, after a total of 72 h of incubation, all deletion strains showed signs of growth. Consequently, the single point mutations introduced into PP_3453 and PP_3454 are gain-of-function mutations as the strains are immediately tolerant to 1-octanol in contrast to the phenotype of the deletion strains. The latter are still able to adapt to the presence of 1-octanol after a long period of incubation. Thus, *P. putida* KT2440 appears to be able to gain tolerance through multiple mechanisms and does not have to rely on PP_3453 and PP_3454 exclusively. This flexibility is consistent with the results obtained from genomic re-sequencing since the strain *P. putida* KT2440 R1S4 harbored mutations in neither PP_3453 nor PP_3454 but had acquired a tolerant phenotype during ALE, nevertheless. However, as wild-type *P. putida* KT2440 adapted substantially faster than the deletion strains, a preferred or more efficient adaptation mechanism *via* a modified PP_3453/PP_3454 TCS can be assumed.

Strains assessed qualitatively for solvent tolerance (engineered, adapted, and wild-type *P. putida* KT2440) were further evaluated in a quantitative assay for solvent tolerance. Here, as in the ALE cultivation, the CO₂ concentration in the headspace was monitored as a measure for growth in the presence of a volume fraction of 1:25 (v/v) 1-octanol.

Engineered strains *P. putida* KT2440 PP_3453-P324R and *P. putida* KT2440 PP_3454-P106R showed a similar growth behavior as the adapted strains *P. putida* KT2440 R2S4 and *P. putida* KT2440 R3S4, all harboring mutations in PP_3453 and PP_3454 (Figure 17). Although the strains remained in short lag phases of approximately 5-7 h, the CO₂ signal indicated exponential growth thereafter. In contrast, the wild-type strain required approximately 50 h to adapt to the presence of 1-octanol before growing, similarly as observed in the ALE cultivation.

Further, all deletion strains showed an increasing CO₂ concentration only after 80 h (Δ PP_3454, Δ PP_3453 Δ PP_3454) or not at all within 95 h (Δ PP_3453). The delayed growth supports the hypothesis that the PP_3453/PP_3454 TCS is not implicitly required for *P. putida* KT2440 to develop tolerance to 1-octanol, but adaptation occurs more rapidly if it is present. Therefore, the observations from the qualitative assay were confirmed. Further, the CO₂ concentrations of all cultivations reached maximum values of 11-13 vol. % when reaching stationary phase. Although it has been shown that solvent tolerant *P. putida* strains adjust their metabolism to satisfy an increased demand of energy for enhanced cellular maintenance processes in the presence of low log *P* organic solvents resulting in increased respiration [213], the molar amount of carbon in the headspace exceeds the amount of carbon provided by 3 g L⁻¹ glucose supplied in the medium. Therefore, *P. putida* KT2440 must have metabolized 1-octanol. Remarkably, no diauxic shift indicating a sequential metabolization of the two carbon sources could be observed, indicating their simultaneous utilization. *P. putida* strains have a versatile metabolism and are thereby able to use several different carbon sources [272]. Although not reported for *P. putida* KT2440, the closely related but more solvent tolerant strain *P. putida* S12 is able to degrade and utilize 1-octanol [172].

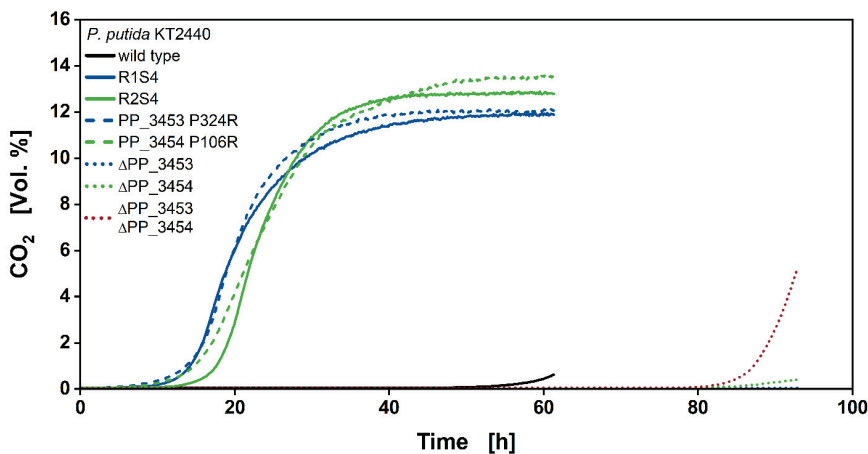


Figure 17 Quantitative solvent tolerance assay of engineered and adapted strains. A volume of 4 mL 1-octanol was added to 50 mL MSM supplemented with 3 g L⁻¹ glucose. The color represents the alteration (either point mutation or deletion) of the gene: Blue - PP_3453, green - PP_3454, red - both PP_3453 and PP_3454, black - no alteration. The pattern of the line denotes the strain type: Solid - strains obtained from ALE or the non-adapted wild-type, dash - reintroduced point mutation, dot - deletion. Data associated to this figure were taken from Greta Kleinert's Bachelor Thesis [271].

Concluding, two of the mutations revealed by genome re-sequencing conferred tolerance to 1-octanol if reintroduced into the genome of *P. putida* KT2440 resulting in strains capable of growing in the presence of a second liquid phase of 1-octanol. Further, preliminary results of assessing the tolerance to solvents other than 1-octanol indicated an increased tolerance of strains harboring point mutations in the PP_3453/PP_3454 TCS to *n*-pentane.

3.2.3.5 Engineered strains allow the use of 1-octanol as an extractant in fermentations

The two strains, *P. putida* KT2440 PP_3453-P324R and *P. putida* KT2440 PP_3454-P106R, which showed tolerance to 1-octanol after introducing the point mutations into the genome of *P. putida* KT2440, were assessed as chassis strains for RL production in two-liquid phase fermentations with 1-octanol as an extractant. The genes *rhlAB* enabling mono-RL production under the control of a strong constitutive promotor were integrated into the genome of the respective chassis strain, resulting in *P. putida* KT2440 PP_3453-P324R *rhlAB* and *P. putida* KT2440 PP_3454-P106R *rhlAB*.

First, a cultivation in the absence of 1-octanol was performed to assess if the strains were still capable of RL production at a capacity comparable to the standardly used producer strain *P. putida* KT2440 SK4 [148] at optimal conditions. After 24 h of incubation, the RL titers (approximately 1 g L^{-1}) of some cultivations inoculated with cells originating from single colonies of the respective strains were in the same range as the titer produced by the benchmark production strain *P. putida* KT2440 SK4. Cryopreserved cultures from productive clones were selected for two-liquid phase cultivations with 1-octanol as an extractant.

In two-liquid phase cultivations in stirred-tank reactors (STRs), 250 mL 1-octanol was added to 1.5 L minimal medium, resulting in a ratio of 1-octanol to cultivation broth of 1:6 (v/v). Due to the formation of stable emulsions, the O_2 and CO_2 concentrations indicating the level of respiration served as an estimate for growth. In contrast to previous cultivations for quantitatively assessing biocompatibility, extensive lag phases of 46 h and 56 h for *P. putida* KT2440 PP_3454-P106R *rhlAB* and *P. putida* KT2440 PP_3453-P324R *rhlAB*, respectively, were recorded (Figure 18A). However, both strains entered exponential growth at maximum rates of 0.21 h^{-1} and 0.24 h^{-1} , derived from linear regression of the oxygen uptake rate (OUR), thereafter. Both cultivations reached a comparable OUR_{max} of $20.9 \text{ mmol L}^{-1} \text{ h}^{-1}$ and $21.5 \text{ mmol L}^{-1} \text{ h}^{-1}$. The carbon emission rate (CER) values of both cultivations were constantly lower than the OUR values, resulting in a respiratory quotient (RQ) < 1 , which suggests a co-metabolization of glucose and 1-octanol. Again, no distinct diauxic shift was detected in the exhaust gas signals. As large amounts of carbon were present in the reactors in the form of 1-octanol, another nutrient besides carbon probably became limiting during the cultivation, as indicated by the sudden decrease of cellular respiration.

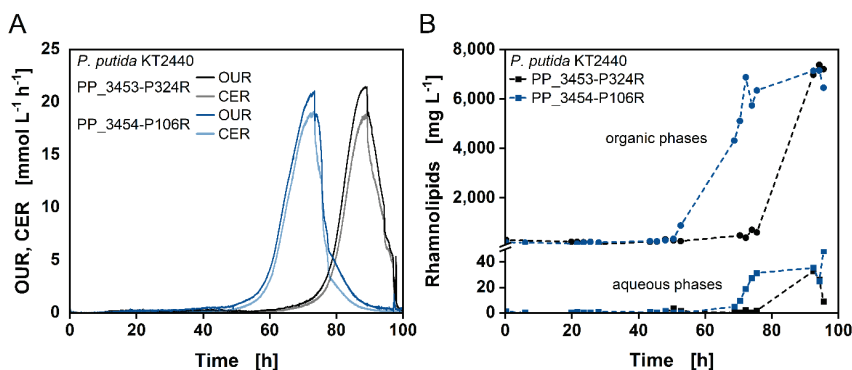


Figure 18 Two-liquid phase cultivations of *P. putida* KT2440 PP_3453-P324R *rhlAB* and *P. putida* KT2440 PP_3454-P106R *rhlAB* in STRs with 1-octanol as the extractant. The strains were cultivated in 1.5 L MSM supplemented with 10 g L⁻¹ glucose and in the presence of 250 mL 1-octanol. The agitation rate was cascaded to maintain a DOT \geq 30%. (A) Oxygen uptake rates (OUR) and carbon emission rates (CER). (B) Rhamnolipid concentrations in 1-octanol phases (dot) and aqueous phases (squares). *P. putida* KT2440 PP_3453-P324R *rhlAB* (black) and *P. putida* KT2440 PP_3454-P106R *rhlAB* (blue). ‘*rhlAB*’ is omitted in legends for conciseness. Data associated to this figure were taken from Greta Kleinert’s Bachelor Thesis [271].

Despite the long lag phase, both *P. putida* KT2440 PP_3454-P106R *rhlAB* and *P. putida* KT2440 PP_3453-P324R *rhlAB* were able to produce RLs once the strains entered exponential growth (Figure 18B). The bulk of the produced RLs was extracted *in situ* resulting in maximum titers of 7.4 g L_{org}⁻¹ for *P. putida* KT2440 PP_3454-P106R *rhlAB* and 7.2 g L_{org}⁻¹ for *P. putida* KT2440 PP_3453-P324R *rhlAB* in the respective 1-octanol phases, while less than 50 mg L_{aq}⁻¹ remained in the aqueous phases. A maximum RL partition coefficient of 284 was achieved, demonstrating a high extraction efficiency. Due to the implementation of the *in situ* extraction, no excessive foaming occurred during the entire cultivation. Thus, the initial instability during the microbial production of RLs could be resolved. Considering the applied glucose, a product yield of 0.14 g_{RL} g_{GLC}⁻¹ was reached. In comparison with the reference production strain, *P. putida* KT2440 SK4 (refer to Chapters 3.1 and 3.4), the product yield was enhanced by 0.02 g_{RL} g_{GLC}⁻¹, potentially indicating utilization of 1-octanol as a secondary carbon source. Further, only low productivity was achieved due to the extensive lag phase.

In conclusion, 1-octanol could be applied as an extractant in two-liquid phase cultivations in lab-scale STRs. The *in situ* extraction of RL resolved the challenge of foaming. However, although strains exhibiting tolerant phenotypes in small-scale assays were deployed, an extensive span for adaptation to the conditions in the STRs was required, resulting in low productivities.

3.2.3.6 Production of 1-octanol

In addition to the production of RLs, tolerant chassis strains were evaluated for the production capacity of 1-octanol. To enable 1-octanol biosynthesis, the plasmid pOCT04 was introduced into *P. putida* KT2440 PP_3453-P324R and *P. putida* KT2440 PP_3454-P106R. Further, all three homologs of *fadD* were deleted to increase the supply of fatty acids [273, 274] as precursors for 1-octanol synthesis by avoiding β -oxidation. Combined chassis strains of the individual point mutations and the *fadD* deletions were generated.

Preliminary results showed a production of 1-octanol from glucose by *P. putida* KT2440 3 Δ *fad* PP_3454-P106R pOCT04. However, only trace amounts of 1-octanol were detected at the beginning of the exponential growth phase. As observed during the quantitative biocompatibility assays, *P. putida* KT2440 is able to co-metabolize 1-octanol simultaneously to glucose. Thus, the product might have been consumed by the cells. Further strain engineering, such as deleting genes encoding for alcohol dehydrogenases, which are responsible for the initial oxidation of 1-octanol, and process engineering by implementing an ISPR strategy into the cultivation will be pursued.

3.2.4 Discussion

In this chapter, *P. putida* KT2440 was engineered to acquire a phenotype with enhanced solvent tolerance. Several cases of rational engineering approaches have previously led to chassis strains with desired phenotypes regarding solvent tolerance or bioreactor cultivations, which served as a basis for constructing more efficient whole-cell biocatalysts [40, 42, 275, 276]. Here, a rational approach did not yield desired phenotypes. In fact, taking a similar approach to rationally engineer the solvent tolerance, Wynands *et al.* [42] integrated the efflux pump TtgGHI into the core genome of streamlined *P. taiwanensis* VLB120. While the tolerance to 4-ethylphenol could be enhanced, the integration of TtgGHI negatively affected the tolerance to phenol. These results underline the high substrate specificity of the efflux pump and the burden it places on the cell when not functional regarding the applied solvent. In this chapter, the tolerance to linear hydrocarbons and their oxygenates, which potentially are no suitable substrates for TtgGHI, were focused on. Further, as addressed above, the energy expenses to synthesize and operate the pump are high, especially if unfavorable amounts are produced. Thereby, available energy is deducted from other solvent defense mechanisms, which are usually highly energy-demanding themselves [192]. Additionally, the volume fractions of up to 50% (v/v) of applied solvents tested in this chapter were set to be comparably large for the solvent to form a second liquid phase. Here, additional physical effects, such as the attachment of the cells at the phase boundary, might play a role in solvent tolerance.

While rational approaches did not yield desired phenotypes, *P. putida* KT2440 acquired tolerance to 1-octanol by ALE. Two of the acquired mutations, both located in the genes encoding for a TCS, could be reintroduced into the genome of the wild-type strain individually, resulting in tolerance to 1-octanol. Although occasionally annotated as the RstA/RstB TCS in the genomic sequence of *P. putida* KT2440 (PP_3453 as RstB and PP_3454 as PP_RstA), the amino acid sequences only have identities of approximately 31% for RstB and 47% for RstA in comparison with the well-studied and mechanistically resolved system of *Klebsiella pneumonia* [277]. Research on the RstA/RstB TCS has been focused on (opportunistic) pathogens such as *K. pneumonia* [278, 279], enterohemorrhagic *E. coli* [280], and *Vibrio alginolyticus* [281], identifying its role in virulence, antibiotic resistance, motility, adhesion, biofilm formation, and membrane integrity. Further, the RstA/RstB TCS was shown to interact with other TCSs such as PhoPQ [278], and the introduction of mutations led to enhanced cross-talk between multiple TCSs [268]. Although it remains unclear if the PP_3453/PP_3454 TCS can be regarded as functionally equal to the RstA/RstB TCS of other species, its detection of environmental changes through the membrane-bound histidine kinase and the subsequent trigger of cellular response mechanisms *via* the phosphorylated transcription response regulator can be assumed. Remarkably, in response to 1-octanol, single mutations causing an amino acid exchange from proline to arginine in either of the two components resulted in a tolerant phenotype. Although the mentioned amino acid exchanges replacing proline should substantially affect the protein structures [269], a loss of function could be excluded as deletion strains did not show the tolerant phenotype. The point mutations could have resulted in unspecific crosstalk between the PP_3453/PP_3454 TCS and other TCSs by PP_3453 phosphorylating different response regulators or PP_3454 enhancing or repressing the transcription of genes other than natively targeted. Recently, the solvent tolerance of mega-plasmid cured *P. putida* S12 has been restored by ALE [282]. A point mutation in genes encoding the GacA/GacS TCS was detected, however, identified as a loss-of-function mutation. Nevertheless, this highlights the importance of TCSs in response to organic solvents, as they typically influence the regulation and expression of several genes. While extensive crud formation during cultivations was observed, indicating an altered biofilm formation and thus agreeing with mentioned studies on the RstA/RstB TCS [281], the altered expression of genes targeted by the mutated PP_3453/PP_3454 TCS has not been determined yet. Transcriptomic studies will reveal up- or downregulated expressions of target genes and further elucidate the cellular mechanism of the acquired solvent-tolerant phenotype.

The tolerant chassis strains were further engineered to enable the production of RLs, ultimately in a two-liquid phase fermentation using 1-octanol as the extractant. Although production and efficient *in situ* extraction could be established, the strains needed extensive adaptation before

growing and producing. This conflicts with previous tolerance assays, in which the chassis strains showed immediate tolerance to 1-octanol. However, in the two-liquid phase cultivation in the STR, the volume fraction of the solvent was increased to 1:6 (v/v), highly exceeding volume fractions of 1:25 (v/v) applied previously. Additionally, in contrast to the shaken cultivation in the ALE and subsequent solvent tolerance assays, thorough mixing by stirring caused the mean Sauter diameter of the solvent droplets to decrease substantially and the drops to be dispersed in the entire aqueous phase, thus causing an increased surface-to-volume ratio. As the cells are known to attach to solvent droplets if their cell surface is hydrophobic [283], increased and direct exposure to the solvent might have occurred, representing an additional toxicity mechanism [284, 285]. Engineering the hydrophobicity of the cell surface as described by Blesken *et al.* [41] might result in less direct contact between the cells and the solvent. Further, as the oxygen demand of the cells is not high at the beginning of the cultivation, the agitation could be reduced and gradually increased when needed, thus reducing dispersion and consequently the surface-to-volume ratio. Applying these altered bioprocessing parameters might resemble the conditions in the shake flask, originally used for adaptation, more closely.

In addition to the differing cultivation setups, RLs were produced, potentially influencing the toxic effect of the solvent on the *P. putida* chassis. On the one hand, biosurfactants such as RLs cause a further reduction of the mean Sauter diameter of the solvent droplets due to their surface activity [286], thus enhancing the effect described in the previous paragraph. On the other hand, RLs are known to integrate into the membrane of *P. putida* KT2440 and, hence, change its composition and integrity [287, 288]. As membrane integrity is a crucial mechanism of organisms to counteract solvent toxicity [192], the production of RLs might be disadvantageous for establishing a tolerant phenotype. However, as both *P. putida* KT2440 PP_3453-P324R *rhlAB* and *P. putida* KT2440 PP_3454-P106R *rhlAB* were able to grow and produce RLs eventually, the cells managed to adapt to the changed conditions once again, highlighting the enormous flexibility of *P. putida*. Reducing the time required for adaptation will be targeted in the future.

Developing a whole-cell biocatalyst, which is tolerant to a solvent usually toxic to most microorganisms, can lead to a substantial advantage in bioprocessing. Next to the application of the solvent as an extractant, the used equipment does not have to be sterilized before the cultivation as non-tolerant microorganisms will be inactivated by the solvent. Not requiring strictly sterile environments decreases energy usage due to the omitted prior autoclavation and reduces the need for equipment such as filters to supply sterile aeration. Overall, the bioprocess can thereby be economically more favorable. However, the costs for the solvent and its recovery or disposal have to be considered.

3.2.5 Conclusion

In this chapter, *P. putida* KT2440 strains exhibiting phenotypes tolerant to 1-octanol were acquired through ALE and could be successfully re-engineered by integrating the detected mutations into the genome of wild-type *P. putida* KT2440. The acquired strains can serve as a chassis for the development of *P. putida* KT2440 as a whole-cell biocatalyst, encountering solvent stress. However, further development is required for establishing immediate tolerance to 1-octanol in two-liquid phase fermentations in STRs. Although 1-octanol was shown to be a highly efficient extractant for RLs, at this point, it could not compete with the beneficial characteristics of ethyl decanoate, the preferred organic solvent of the solvent selection described in Chapter 3.1. Particularly, the apparent reduction in growth rate when encountering non-ideal aeration as observed in the ALE experiment by halting the shaker could be of concern when cells encounter non-ideally mixed zones of industrial-scale STRs or the non-aerated downcomer of the multiphase loop reactor described in Chapter 3.5. Thus, in the following chapters, ethyl decanoate has been selected as the extractant of choice.

Chapter 3.3

Exploration of fed-batch cultivation strategies for the production of rhamnolipids

Contributions

Philipp Demling performed all fermentations and associated analytics, supported by Carolin Grütering.

Philipp Demling wrote the chapter, which was reviewed by Till Tiso.

3.3 Exploration of fed-batch cultivation strategies for the production of rhamnolipids

3.3.1 Abstract

The foam-free production of rhamnolipids was established by implementing an *in situ* liquid-liquid extraction as described in Chapter 3.1, and a glucose-limited and dissolved oxygen tension-controlled fed-batch cultivation was performed, resulting in a pseudo-linear feeding profile. In this chapter, a different feeding profile with a linear increase of the feeding rate over time and an adapted composition of the feeding solution were assessed to further explore the design of an efficient feeding strategy. While the linear feeding strategy with the original composition of the feeding solution did not result in improved performance indicators, increasing the concentration of trace elements in the feeding solution by six-fold led to a higher overall productivity of rhamnolipids ($0.23 \text{ g L}^{-1} \text{ h}^{-1}$). However, the extraction efficiency was reduced, presumably due to a substantially increased ionic strength of the cultivation medium after feeding. Further, as enhanced emulsification with increasing biomass and rhamnolipid titers was observed, catastrophic phase inversion was explored as a measure for breaking the emulsion. Phase separation could be achieved by adding solvent in a ratio of 1:2 (v/v) emulsion to solvent. However, a distinct separation without clouding of the organic phase was only present at phase ratios of 1:6 (v/v) and above. Concluding, valuable insights for establishing two-liquid phase fed-batch cultivations for the production of rhamnolipids and catastrophic phase inversion as a succeeding downstream processing unit operation were gained.

3.3.2 Introduction

The three main modes of operation for biotechnological fermentation processes are batch, fed-batch, and continuous mode, which exhibit different advantages and disadvantages. While performing a batch cultivation, during which no cultivation media is added to or withdrawn from the reactor, is simple from a technical perspective, the operator cannot control substrate or product concentrations during the cultivation [289]. Further, reactor downtimes between batch fermentations needed for maintenance, cleaning, and sterilization can be economically unfavorable [290]. In contrast, a continuous cultivation can be operated for long durations, and the operator can control substrate, product, and biomass concentrations as well as the growth rate by adjusting the volumetric flow rate, thereby maximizing efficiency, especially in the case of substrate or product inhibitions. However, the technical effort is considerable compared to batch fermentations. The requirement to actively add and remove culture medium to the reactor is critical in terms of risking contaminations and long cultivations might promote genetic variation [52, 289]. The fed-

batch mode, *i.e.*, only growth media is added to the reactor but not withdrawn, combines some of the advantages of the prior two cultivation modes. The technical effort is reasonable, and the risk of contamination is comparably low. While product and biomass accumulate during the cultivation, the substrate concentration can be controlled by a suitable feeding strategy [291]. Although the process duration is limited by the reactor size, the feed rate, and the initial filling volume, fed-batch cultivations typically are advantageous in terms of productivity [292–294].

Although progress has been made in recent years, the challenges involving continuous bioprocessing impede its implementation in industrial biotechnology in many cases [53]. Next to batch cultivations, the fed-batch cultivation mode has prevailed due to its high efficiency, moderate risk, and reduced environmental impact due to reduced waste production [295]. Multiple cases of successful implementation and optimization of industrial-scale fed-batch bioprocesses have been reported, *e.g.*, for the production of amino acids, penicillin, enzymes, and biomass itself [296]. However, fed-batch cultivations exhibit an increased complexity compared to batch cultivations. Additional variables such as initial and final volume, the feeding profile, the feed composition, feed initiation, and others are subject to optimization [292]. All parameters have to be specified for a single production process and tailored to the respective whole-cell biocatalyst to avoid detrimental effects, *e.g.*, due to over-feeding or undersupply, all driven by maximizing performance indicators for production. To determine a beneficial operational window, ideally, iterative rounds of computationally aided cultivation and dynamic optimization cycles are required [297–299].

Previously, applying a fed-batch strategy was suggested to be beneficial for rhamnolipid (RL) production [118, 300]. Further, the two-liquid phase fed-batch cultivation as described in Chapter 3.1 revealed an efficient production and *in situ* extraction of RLs, thereby avoiding excessive foaming. The applied fed-batch strategy in Chapter 3.1 was based on the dissolved oxygen tension (DOT) signal as a measure for the present carbon source, thereby triggering feeding periods. This DOT-controlled fed-batch can be assigned to the category of ‘feed-back controlled strategies’, which rely on online process values [301]. Next to the DOT value, other values such as the glucose concentration, pH, or biomass concentration can be utilized to trigger and control feeding [215]. In contrast, ‘non-feed-back controlled strategies’ can be applied for fed-batch cultivations. Here, the feed rate is predefined by a control function, most commonly of constant, linearly increasing, or exponentially increasing nature [292]. Further, in advanced bioprocesses, mixed feeding strategies can be implemented, *e.g.*, transitioning from an exponential feed to a linear based on specific characteristics or stages of the cultivations [292, 302]. In this regard, multiple different feeding solutions can be added to the reactor in certain stages of the cultivation or simultaneously at differing rates [303]. To avoid a rapid increase in filling volume and consequentially a short

duration of the cultivation process, feeding solutions are often highly concentrated. Beneficial concentrations ranging from 10- to 15-fold increase compared to the initial batch medium have been reported [304]. However, an excessive increase of media components bears the risk of precipitation, which should be avoided to maintain defined cultivation conditions.

In two-liquid phase cultivations with an organic solvent used as an extractant, the formation of emulsions can occur, especially at high biomass titers typical in later stages of fed-batch cultivations and if surfactants are present [305]. The formation of emulsions is detrimental since it strongly conflicts with the concept of *in situ* product removal by extraction. The product cannot be recovered from the organic phase if the phases cannot be separated. There are several methods for breaking emulsions, among others ultracentrifugation [306], phase inversion by a temperature shift and salt addition [307], and supercritical CO₂-assisted phase separation [308]. A comparably efficient but straightforward approach is the catastrophic phase inversion (CPI), which alters the emulsion from oil-in-water to water-in-oil by adding excessive organic solvent. It can be applied to form or break emulsions [309–311]. CPI has been successfully applied for breaking emulsions originating from bioprocesses previously [312, 313] and might be promising for the present system consisting of cultivation broth, ethyl decanoate, RLs, cells, and potentially cell debris.

In this chapter, linearly increasing feed rates and an inferred adjustment of the composition of the feeding solution for the production of RLs in a two-liquid phase fed-batch cultivation are explored. The performance indicators of the cultivations regarding production caused by the different feeding profiles are compared with the DOT-controlled two-liquid phase fed-batch fermentation presented in Chapter 3.1. Further, CPI is assessed as a unit operation for breaking formed emulsions.

3.3.3 Results

In Chapter 3.1, a two-liquid phase fed-batch fermentation strategy was developed, allowing long-term foam-free production of RLs. Here, a DOT-based feeding profile was chosen, *i.e.*, a rising DOT value indicating the depletion of the carbon source triggered feeding, leading to a glucose-limited fed-batch cultivation. To allow functionality, the DOT value was not adjusted by other process variables, such as agitation and aeration, which remained constant. The filling volume can be approximated to

$$V(t) = V(0) \quad \text{for } t < t_{fs} \quad (7)$$

$$V(t - t_{fs}) = 7.14(t - t_{fs}) + V(0) \quad \text{for } t > t_{fs} \quad (8)$$

and the feed rate can be regarded as pseudo-constant approximated to

$$V(t - t_{fs})' = F = 7.14 \quad (9)$$

where $V(t)$ is the filling volume over time, $V(0)$ the initial filling volume, t_{fs} the point of time when feeding was started, and $V(t)' = F$ the feed rate, assuming that sample withdrawal and the addition of acid and base are compensating. Detailed results are presented in Chapter 3.1, but a comparison of all approached fed-batch strategies is given at the end of this chapter (Table 6).

Different feeding strategies were explored in this chapter, with the DOT-based two-liquid phase fed-batch serving as a reference. In contrast to the reference, feeding profiles independent of online process values, such as the DOT value, were focused on.

3.3.3.1 Linearly increasing feed rate leads to similar performance compared to the reference

First, a feeding profile with a linearly increasing feed rate was chosen, which can be described as

$$V(t) = V(0) \quad \text{for } t < t_{fs} \quad (10)$$

$$V(t - t_{fs}) = 0.66(t - t_{fs})^2 + 6.82(t - t_{fs}) + V(0) \quad \text{for } t > t_{fs} \quad (11)$$

and

$$V(t - t_{fs})' = F = 1.32(t - t_{fs}) + 6.82 \quad (12)$$

As the feeding profile was independent of process variables, the agitation was cascaded from 400 rpm to 1,200 rpm to ensure a DOT value of $\geq 30\%$ to prevent oxygen limitation. The manual reduction of the pH value to prevent foaming by enhancing the extraction efficiency was performed according to the DOT-based two-liquid phase fed-batch cultivation.

After the initial batch phase, the feed was started at a cultivation time of 7.6 h shortly before glucose depletion to avoid carbon starvation and potential cell lysis (Figure 19). After 24.5 h of cultivation (16.8 h after the start of feeding), the entire feeding solution was added to the STR. All glucose supplied by the feed was depleted after 26.5 h as indicated by a sudden decrease of agitation due to a lower demand of oxygen caused by a reverted cascade to maintain a DOT value of $\geq 30\%$, and an increase of the DOT thereafter. The discrepancy of the end of the feed and carbon depletion indicates that not glucose but rather another media component was limiting for the cells. A pulse of trace element solution at 25.1 h resulted in an increasing agitation rate triggered by the DOT-based cascade and thus caused by a higher demand in oxygen by the cells, which indicated a component of the trace element solution to be limiting.

At the end of the cultivation, a RL titer of $24.5 \text{ g L}_{\text{org}}^{-1}$ was present in the organic phase, whereas $0.84 \text{ g L}_{\text{aq}}^{-1}$ remained in the aqueous phase. A reduction of the pH to a value of 6.3 was sufficient to avoid foaming. The titers in the different phases translate to a total production of 3 g RLs and a product yield of $0.05 \text{ g}_{\text{RL}} \text{ g}_{\text{GLC}}^{-1}$ as well as a productivity of $0.17 \text{ g L}^{-1} \text{ h}^{-1}$.

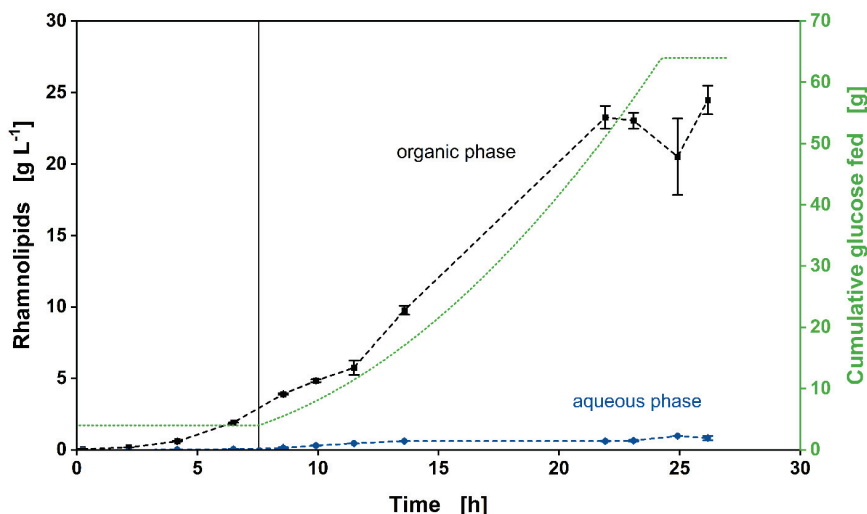


Figure 19 Production of rhamnolipids in a two-liquid phase fed-batch cultivation of *P. putida* KT2440 SK4 with a linearly increasing feeding profile. In the batch phase, the cultivation was conducted MSM supplemented with 10 g L⁻¹ glucose. The total amount of converted glucose at the end of the cultivation was 64g. RL titers in the organic phase (black squares) and in the aqueous phase (blue circles) and the cumulatively glucose fed (green dots) are presented. The black horizontal line denotes the start of feeding. Error bars represent maximal and minimal values of two independent experiments. Data associated to this figure were taken from Carolin Grütering's Master Thesis [211].

3.3.3.2 Trace element concentration influences growth rate

The fed-batch cultivation with a linearly increasing feed rate revealed a suboptimal ratio of components in the feeding solution as an increased respiratory activity was observed when adding trace elements in the final stage of the cultivation. Here, the concentration of trace elements in relation to the supplied carbon in the feeding solution was reduced six-fold compared to the mineral salts medium (MSM) used during batch cultivations. To assess the effect of the trace element concentration on growth and production, the trace element concentrations were altered between 8.3% and 100% of the original MSM and utilized to cultivate *P. putida* KT2440 SK4 in shake flasks.

The cultivations with differing trace element solutions revealed a decrease in maximal growth rate with less supplied trace elements ranging from 0.30 h⁻¹ for 8.3% to 0.42 h⁻¹ for 100% supplemented trace element solution (Table 5 and Appendix A.4, Figure A4.1). Therefore, it is assumed that the supplied concentration of trace elements in the feeding solution corresponding to 16.7% of the original concentration in the MSM was not sufficient to support unrestricted growth. The low growth rates compared to the STR cultivations might be due to the lack of pH control. Further, samples were drawn after 24 h to assess RL titers. Remarkably, titers differed only

insignificantly, indicating a progressive production and potentially growth after terminating the measurement of optical densities after 9.4 h.

Concluding, the reduction of trace element concentrations resulted in a diminished performance of *P. putida* KT2440, thus suggesting a modification of the composition of the feed solution for a succeeding fed-batch cultivation.

Table 5 Growth rates and RL titers of shake flask cultures with different supplied trace element concentrations.

Trace element concentration ^{a)}	8.3%	31.3%	54.2%	77.1%	100%
Maximal growth rate [h ⁻¹]	0.30 ± 0.01	0.34 ± 0.02	0.36 ± 0.01	0.40 ± 0.01	0.42 ± 0.01
RL titer [g L ⁻¹] ^{b)}	0.48 ± 0.01	0.57 ± 0.10	0.49 ± 0.01	0.48 ± 0.01	0.49 ± 0.01

^{a)} In percent of the standardly used concentration in MSM (refer to Chapter 2.2 and Appendix A.1, Table A1.1).

^{b)} After 24 h of cultivation.

3.3.3.3 An adjusted feed composition increases productivity

As the trace element concentration in the medium was shown to influence the growth rate of *P. putida* KT2440 the comparably low concentrations of trace elements in the feeding solution were increased to 100% of the original batch MSM in relation to the supplemented glucose. In the subsequent two-liquid phase fed-batch cultivations, a similar strategy as previously was applied by selecting a linearly increasing feed rate with slight adjustments. The feeding profile can be described as

$$V(t) = V(0) \quad \text{for } t < t_{fs} \quad (13)$$

$$V(t - t_{fs}) = 0.76(t - t_{fs})^2 + 4.5(t - t_{fs}) + V(0) \quad \text{for } t > t_{fs} \quad (14)$$

and

$$V(t - t_{fs})' = F = 1.52(t - t_{fs}) + 4.5 \quad (15)$$

As the feeding profile is independent of process values, the same conditions as for the previous fed-batch cultivation with linearly increasing feed were applied, including a gradual decrease of the pH value to avoid foaming when necessary.

After 7.7 h, the batch phase terminated shortly before carbon depletion, and the feeding was started. Within 25.2 h, the entire feeding solution was added to the reactor. Shortly thereafter, the carbon source was depleted, as indicated by a reduction of the agitation rate due to a revision of the DOT-controlled cascade and a subsequent increase in DOT values. As the respiratory activity of the cells terminated shortly after the addition of the feeding solution in contrast to the prior cultivation with a non-adapted feeding solution, a carbon limitation can be assumed. Therefore, the six-fold increase of trace element concentrations resolved the previously occurring limitation not originating from carbon. However, the overall concentration of salts in the feeding solution

was high, resulting in slight precipitation of components in the tubing. This is not desired since it is unknown which salts or complexes precipitated and were thus not fed to the reactor, resulting in an undefined system. Therefore, the composition of the feeding solution needs to be improved further.

During the cultivation, a total of 64 g glucose was converted, and produced RLs were enriched in the organic phase (Figure 20). The highest titer of RLs in the organic phase was measured to $21.8 \text{ g L}_{\text{org}}^{-1}$ at 22 h of cultivation, thus before the feeding was terminated, and decreased statistically insignificantly to $19.9 \text{ g L}_{\text{org}}^{-1}$. However, thereafter the titer in the aqueous phase increased from $1.5 \text{ g L}_{\text{aq}}^{-1}$ to $3 \text{ g L}_{\text{aq}}^{-1}$, resulting in a reduction of the partition coefficient. This is potentially due to a high ionic strength of the aqueous phase, which has been reported previously to influence the solubility of RLs [314, 315] and thereby the extraction efficiency in the present case. The produced RLs in both phases correlate to a product yield of $0.064 \text{ g}_{\text{RL}} \text{ g}_{\text{GLC}}^{-1}$ and a productivity of $0.23 \text{ g L}^{-1} \text{ h}^{-1}$, thereby indicating an improvement to the cultivation with a linearly increasing feed rate and a non-adapted feeding solution. However, there is a strong requirement for further optimization.

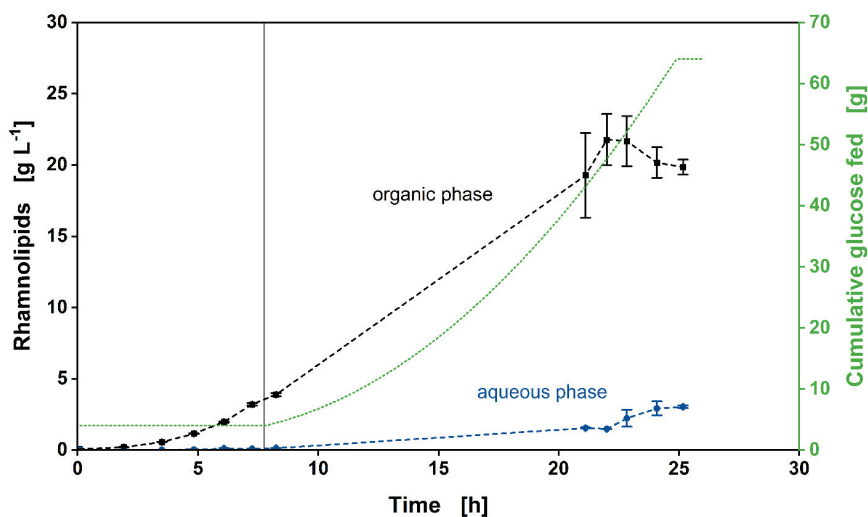


Figure 20 Production of rhamnolipids in a two-liquid phase fed-batch cultivation of *P. putida* KT2440 SK4 with a linearly increasing feeding profile and an adjusted composition of the feeding solution. In the batch phase, the cultivation was conducted MSM supplemented with 10 g L^{-1} glucose. The total amount of converted glucose at the end of the cultivation was 64 g. RL titers in the organic phase (black squares) and in the aqueous phase (blue circles) and the cumulatively glucose fed (green dots) are presented. The black horizontal line denotes the start of feeding. Error bars represent maximal and minimal values of two independent experiments. Data associated to this figure were taken from Carolin Grütering's Master Thesis [211].

3.3.3.4 Comparison of fed-batch strategies indicates enhanced rhamnolipid production at glucose limitation

Comparing different performance indicators allows to draw further conclusions about the different fed-batch cultivation strategies (Table 6). While the highest RL titer in the organic phase was measured for the DOT-controlled pseudo-linear feeding strategy (Chapter 3.1), the highest total amount of RLs was produced in the cultivation with a linearly increasing feed rate and adjusted feed composition. However, in the latter a large amount of RLs remained in the aqueous phase resulting in an overall titer of 4.1 g L^{-1} , potentially due to an increased ionic strength of the cultivation broth causing a reduced partition coefficient and thus a decreased extraction efficiency. Further, comparing the total amounts of produced RLs is misleading as the supplied amount of glucose differed between the DOT-controlled feeding strategy and the other approaches, thus comparing product yields and productivities is more appropriate. While the highest product yield was achieved at DOT-controlled feeding, the highest productivity was reached for the strategy with linearly increasing feeding rate and adjusted feed composition. Both performed better than the strategy with linearly increasing feeding rate and original feed composition, indicating that production is increased at strict glucose limitation.

Table 6 Performance indicators of fed-batch cultivations with different feeding strategies.

Performance indicator	DOT-controlled (pseudo-linear rate) ^{b)}	Linearly increasing rate	Linearly increasing rate + adjusted feed
Highest RL titer (org) [g L^{-1}]	29.6	24.5	19.9
Highest RL titer (aq) [g L^{-1}]	1.2	0.8	3.0
Total RLs [g] ^{a)}	3.8	3.0	4.1
Product yield [$\text{g}_{\text{RL}} \text{g}_{\text{GLC}}^{-1}$]	0.072	0.047	0.064
Productivity [$\text{g L}^{-1} \text{h}^{-1}$]	0.16	0.16	0.23

^{a)} Different amounts of glucose have been applied, thereby influencing maximal amount of product. 52.7 g glucose for DOT-controlled fed-batch and 64 g glucose for others.

^{b)} Results of this cultivation were described in Chapter 3.1.

Remarkably, the congener composition changed in all cultivations with increasing duration (Figure 21). While the ratio of HAAs to the total amount of surfactants, being the sum of HAAs and mono-RLs, converged to approximately 20% during batch phases, the ratio doubled to up to 40% during the cultivation with the feeding profile with a linearly increasing feed and a non-adapted composition of the feeding solution, before decreasing to approximately 30% shortly before glucose depletion. In contrast, the glucose-limited cultivations increase steadily towards a ratio of 30%. The difference can potentially be due to a consumption and thus an overall reduction of HAAs at glucose limitation, as observed previously [41]. Further, the increasing ratio of HAAs in all cultures could be explained by a bottleneck for the cell in providing activated rhamnose, in turn indicating the lack of sufficient energy equivalents. Moreover, as cells are more likely to lyse

with increasing duration of cultivation, potentially more HAAs could have been released from the cells before a rhamnose moiety was transferred. However, all hypotheses need further validation.

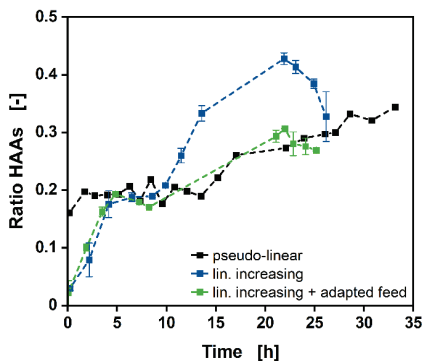


Figure 21 Ratio of HAAs to total surfactants produced by *P. putida* KT2440 SK4 in all performed fed-batch cultivations. The surfactants present in both the organic and the aqueous phases are considered. Black squares - DOT-controlled fed-batch with pseudo-linearly increasing feed rate, blue squares - linearly increasing feed rate, green squares - linearly increasing feed rate and adjusted composition of the feeding solution. Error bars represent maximal and minimal values of two independent experiments. Data associated to this figure were taken from Carolin Grütering's Master Thesis [211].

3.3.3.5 Catastrophic phase inversion breaks emulsions

Increased RL and biomass titers produced during fed-batch cultivations led to the formation of emulsions, which were challenging to separate. Especially in the late stages of the cultivations, during which cell lysis can be assumed to a certain extent, released proteins and cell fragments were predicted to hinder phase separation. While in small-scale, the emulsion in samples could be broken by intensive centrifugation, resulting in sufficient phase separation for sample preparation, this might not be feasible for large volumes as occurring in large-scale cultivations.

A suitable measure to break emulsion resulting from two-liquid phase cultivations could be CPI. The feasibility of its application for the present emulsion of cultivation broth, ethyl decanoate, RLs, and *P. putida* KT2440 cells, as well as their fragments, has been assessed. Emulsions from fed-batch STR cultivations have been suspended in different volumes of excess ethyl decanoate. After allowing the system to settle, the phase separation was qualitatively assessed. While the addition of equal volumes of ethyl decanoate did not result in phase separation, two phases can be observed at ratios of 1:2 (v/v) and lower (Figure 22). Distinct phase separations with little to no clouding of the organic phase occurred at ratios of 1:6 (v/v) and 1:7 (v/v). Thus, CPI can be used to achieve phase separation. However, compared to the volume of emulsion, the volume of excess solvent is substantial.

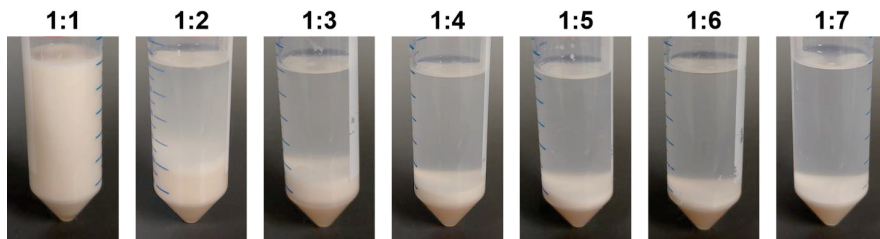


Figure 22 Catastrophic phase inversion after 20 h of settling. Ratios from 1:1 (v/v) to 1:7 (v/v) emulsion to excess ethyl decanoate were assessed. Emulsions were obtained from fed-batch cultivations exhibiting an exponential feed. Due to the angled view and the refraction the aqueous phase appears higher than it is but allows to differentiate between distinct and indistinct phase boundaries. Pictures were taken from Carolin Grütering's Master Thesis [211].

3.3.4 Discussion

In this chapter, different feeding strategies, including feeding profiles and feed composition, have been explored. Further, CPI has been evaluated for breaking the emulsions composed of cultivation broth, ethyl decanoate, RLs, cells, and cell fragments.

The application of different feeding strategies has revealed that *P. putida* KT2440 SK4 shows an increased performance in productivity and product yield when cultivated at glucose limitation. Both feeding strategies resulting in glucose limitation outperformed the linearly increasing feed rate with non-adjusted feeding solution, for which the cultivation continued for 2 h after the depletion of the feed, indicating an excess of carbon source. Only little has been reported regarding increased productivity of RLs by recombinant *P. putida* KT2440 at glucose limitation. Hypothetically, an increased RL production at glucose limitation could be due to a strategy of the cells to make additional carbon sources accessible, e.g., by emulsifying oil, which is usually barely soluble in water. However, limitations in nutrients other than carbon have been shown to be beneficial for RL production as well [106, 316]. Preliminary results obtained from fed-batch cultivations with an exponentially increasing feed rate support the finding of an increased RL production at glucose limitation. Here, overfeeding resulted in glucose in high excess but comparably low RL titers. However, further data, including glucose concentrations of samples, are required. Glucose concentrations could not be measured at this point due to interferences with analytics.

In general, the feeding strategies applied in this chapter have only been superficially developed. Further parameters, including feed composition, feeding rate, filling volumes, feed start, and others, need to be examined and put into relation [292]. Ideally, an optimization approach is computationally supported for model development [292, 317], and the cultivations are conducted in high throughput to obtain large amounts of data more rapidly [318]. This approach

allows successful developments of fed-batch production processes [50, 319] and should be applicable in the presented case as well. However, the presence of an organic phase further increases complexity due to additional parameters, such as phase ratio, emulsification, and dependent parameters like the pH value.

CPI as a simple and effective method for breaking the produced emulsion has been evaluated. In fact, the simple addition of excess ethyl decanoate has caused phase separation starting already at ratios of 1:2 (v/v) emulsion to ethyl decanoate. However, distinct phase separation without clouding of the organic phase required higher phase ratios. The increased solvent usage is not ideal as it is ecologically and economically critical [72, 320] due to potential unfavorable environmental characteristics and increased costs for supply and waste management. However, as described in Chapter 3.1, ethyl decanoate is regarded as environmentally friendly and can be produced independently from fossil resources [194]. In the case of RL production, ethyl decanoate can be recovered *via* back-extraction, allowing reuse. Further, a distinct phase separation can potentially be achieved at higher phase ratios, thus at less solvent utilization, by an additional subsequent unit operation, such as centrifugation, or by influencing separation kinetics by adding salts or altering the temperature [307]. Combinatory approaches should be assessed for the presented system.

3.3.5 Conclusion

Different fed-batch strategies for the production of RLs were explored, providing first insights into promising approaches. Fed-batch cultivations will be limited in application in the MPLR, which is described in Chapter 3.5 and for which an operational window is defined throughout this thesis, as the filling volume is a critical parameter for fluid dynamics in the reactor. However, performing fed-batch fermentations has prevailed in industrial biotechnology due to high efficiencies. Therefore, the gained insights might support the development of an industrial fed-batch fermentation. However, only superficial estimates have been achieved. Thus, there is a requirement for optimization.

Chapter 3.4

Pseudomonas putida KT2440 withstands repeated oxygen limitations

Partially published as

[126] Demling P, Ankenbauer A, Klein B, Noack S, Tiso T, Takors R, Blank LM. 2021. *Pseudomonas putida* KT2440 endures temporary oxygen limitations. *Biotechnology & Bioengineering*. doi: 10.1002/bit.27938.

[Reprinted (adapted) with permission from Wiley & Sons. Open Access CC BY-NC-ND 4.0. © The Authors 2021]

Contributions

Philipp Demling performed all MTP and STR batch cultivations, the latter in part supported by Florian Röck, including corresponding analytics. The STR-PFR cultivations were jointly conducted at the Institute of Biochemical Engineering, University of Stuttgart, by Philipp Demling and Andreas Ankenbauer, supported by Lorenzo Favilli. Analytics for STR-PFR cultivations were performed by Andreas Ankenbauer. Detailed descriptions of the STR-PFR cultivations and corresponding data will be published in the Doctoral Thesis of Andreas Ankenbauer and in the submitted article shortly. Relative quantitative proteomics and preliminary data processing were conducted at the Institute of Bio- and Geosciences (IBG-1), Forschungszentrum Jülich by Bianca Klein and Stephan Noack. Corresponding results were analyzed and interpreted by Philipp Demling.

This chapter was written by Philipp Demling. In the submitted article, the passages containing results and respective conclusions obtained from the STR-PFR cultivations have been authored by Andreas Ankenbauer. For consistency and complete understanding, these passages are partially included in a compendious form in the sections “*Pseudomonas putida* withstands repeated dual oxygen and glucose limitations” and “Discussion” of this chapter. Till Tiso and Lars M. Blank reviewed this chapter.

3.4 *Pseudomonas putida* KT2440 withstands repeated oxygen limitations

3.4.1 Abstract

The obligate aerobic nature of *Pseudomonas putida*, one of the most prominent whole-cell biocatalysts emerging for industrial bioprocesses, questions its ability to be cultivated in large-scale bioreactors, which exhibit zones of low dissolved oxygen tension. *P. putida* KT2440 was repeatedly subjected to temporary oxygen limitations in scale-down approaches to assess the effect on growth and an exemplary production of rhamnolipids. At those conditions, the growth and production of *P. putida* KT2440 were decelerated compared to well-aerated reference cultivations, but remarkably, final biomass and rhamnolipid titers were similar. The robust growth behavior was confirmed across different cultivation systems, media compositions, and laboratories, even when *P. putida* KT2440 was repeatedly exposed to dual carbon and oxygen starvation. Quantification of the nucleotides ATP, ADP, and AMP revealed a decrease of intracellular ATP concentrations with increasing duration of oxygen starvation, which can, however, be restored when resupplied with oxygen. Only minor changes in the proteome were detected when cells encountered oscillations in dissolved oxygen tensions. Concluding, *P. putida* KT2440 appears to be able to cope with repeated oxygen limitations as they occur in large-scale bioreactors, affirming its outstanding suitability as a whole-cell biocatalyst for industrial-scale bioprocesses and its suitability for cultivation in the multiphase loop reactor.

3.4.2 Introduction

Recently, *Pseudomonas putida* has emerged as a promising host for industrial bioprocesses [113–115, 321]. Its versatile carbon metabolism allows the usage of different carbon sources [322, 323], potentially contributing to valorize waste streams for the production of value-added compounds in the scope of an envisioned circular bioeconomy. Prominent examples are the production of rhamnolipids (RLs) from xylose [139] and the upcycling of plastic waste [324] using recombinant *P. putida* as a whole-cell biocatalyst. Further, *P. putida* has been shown to flexibly respond to several environmental perturbations like oxidative stress [325] and, most prominently, tolerating high concentrations of toxic substances such as organic solvents [239, 326, 327]. This ability allows the application of an organic solvent phase, *e.g.*, in process intensification by *in situ* extractions [172, 125].

P. putida KT2440 is considered the most suitable candidate among pseudomonads for industrial applications due to its host-vector system safety level 1 (HV1) status [129], facilitating accreditations for production processes. Further, the ability of *P. putida* KT2440 to withstand industrial-scale stress conditions in terms of fluctuations in carbon availability has recently been

demonstrated [321], indicating its potential to cope with nutrient gradients and local limitations due to non-ideal mixing, typically occurring in large-scale fermenters [169, 328]. In this regard, recent computational fluid dynamic simulations predict mean residence times up to 76 s for bacterial cells in low glucose or low oxygen regimes inside a 300 L pilot-scale bioreactor [329]. Therefore, zones within the fermenter exhibiting low oxygen concentrations pose a potential drawback to establish industrial-scale fermentations, particularly with obligate aerobic organisms such as *P. putida* KT2440. Further, in the scope of recent advances in bioreactor design, specialized apparatuses have emerged, which exhibit intentionally non-aerated compartments, leading to reactor zones with low oxygen availability [55, 56]. As inhomogeneous mixing hardly occurs in laboratory-scale fermentations, specialized scale-down reactors have been developed to intentionally induce ambient perturbations [328, 330, 331]. Considering oxygen, many studies have focused on mimicking gradients and transitions using model organisms [332, 333] like *E. coli* [334] or other industrially relevant microorganisms like *Corynebacterium glutamicum* [170, 335, 336] in scale-down reactors. However, the yeasts *Pichia pastoris* [337] and *Yarrowia lipolytica* [338–340] have been the only studied microorganisms regarded as being obligate aerobic.

Several efforts have been made to engineer *P. putida* KT2440 to be capable of either anaerobic fermentation or anaerobic respiration [341–343]. While survival was successfully demonstrated, growth or the production of value-added compounds could not be sustained. In the absence of oxygen, only bioelectrochemical systems (BES) could enable production [344–346]. Recently, a proof of concept for RL production in an oxygen-limited BES was reported [347]. Applying *in silico* approaches, Kampers *et al.* [348] identified several limitations for establishing anaerobic metabolism, and a derived strategy for rational strain engineering enabled *P. putida* KT2440 to grow under micro-oxic conditions. However, for a fully anaerobic metabolism, further extensive strain engineering has been predicted [349].

As oxygen concentrations in industrial-scale fermenters are typically fluctuating and subject to gradients, it is proposed that introducing a fully anaerobic metabolism into *P. putida* KT2440 is not stringently required, but rather its ability to cope with altering conditions needs to be evaluated and potentially enhanced. Thus, in this study, we assess the ability of *P. putida* KT2440 to endure temporary oxygen limitations. Different scale-down approaches, ranging from disturbed cultivations in microtiter plates (MTP) to cultivations in stirred-tank reactors (STR) and a defined compartmented reactor composed of an STR coupled to a non-aerated plug-flow reactor (PFR), are used to mimic industrial-scale reactor inhomogeneities in terms of oxygen availability to evaluate its effect on the growth of *P. putida* KT2440 (Figure 23). Additionally, the influence of repeated oxygen limitations on the production of secondary metabolites, here at the example of RLs, by a recombinant *P. putida* KT2440 is assessed.

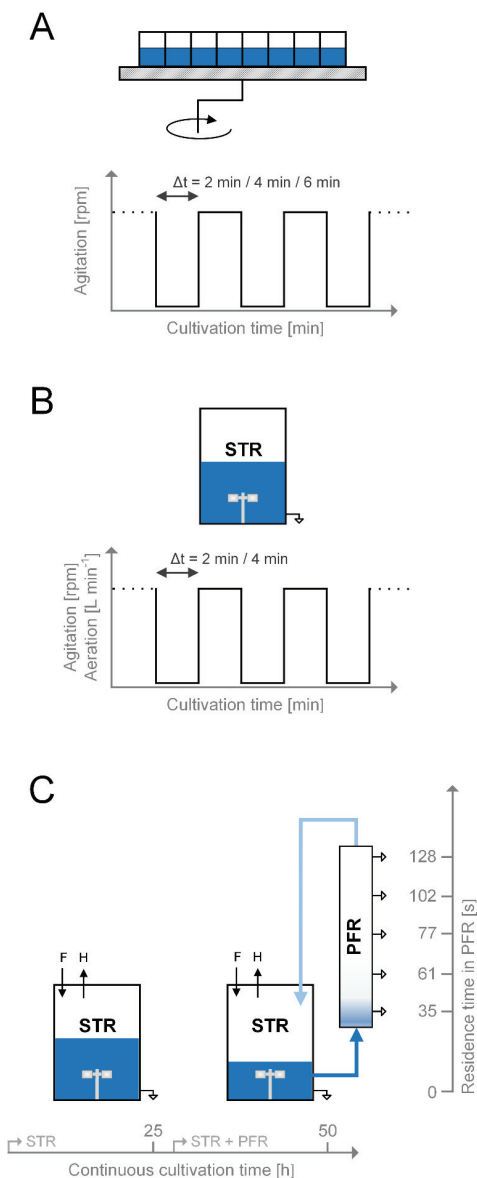


Figure 23 Schematic illustrations of different scale-down cultivation setups to mimic large-scale inhomogeneities in lab-scale. (A) MTP cultivations with oscillating shaking intervals. (B) STR cultivations with oscillating agitation and aeration. (C) A STR operated as glucose-limited chemostat with continuous medium feed [F] and harvest [H] served as reference condition after reaching steady-state after five residence times. By connecting the PFR with the STR, dual substrate starvation by glucose and oxygen was applied. The STR and the five ports of the PFR were sampled simultaneously after further five residence times. (C) has originally been designed by Andreas Ankenbauer.

3.4.3 Results

3.4.3.1 Periodic oxygen limitation leads to reduced growth rates in microtiter plate cultivations

Microtiter plate cultivations were performed to assess the influence of alternating shaking frequencies and a resulting oscillation of the oxygen transfer rate (OTR) on the growth behavior of wild-type *P. putida* KT2440. Shaking intervals of 2 min, 4 min, and 6 min at 200 rpm and 1,200 rpm were compared to a culture continuously shaken at 1,200 rpm.

Online backscatter signals revealed prolongations of the cultivation time until the stationary phase was reached when the culture was subjected to oscillation (Figure 24). While the continuously shaken culture entered stationary phase after 13 h, the cultivation time of the oscillating cultures was extended to 20.8 h, 21.2 h, and 21.5 h for the intervals of 2 min, 4 min, and 6 min, respectively. Although all durations of cultivations differ significantly (all p-values < 0.05), the growth retardation was only minorly influenced by increased durations of shaking intervals but primarily by the presence of oscillation itself. This is also reflected in the calculated growth rates during exponential phases of each set of cultivations. The maximal growth rates were determined in the latter part of the cultivations at backscatter signals (BS) > 100 to avoid technical bias (Appendix A.5, Figure A5.1). Obtained maximal growth rates for the control cultivations ($\mu_{\text{ctrl}} = 0.70 \pm 0.01 \text{ h}^{-1}$) were approximately 2.6-fold higher compared to growth rates of all cultures subjected to oscillation ($\mu_{\text{osc}} = 0.27 \pm 0.03 \text{ h}^{-1}$). Only transient phases of exponential growth could be determined, especially for the oscillating cultures, potentially indicating an oxygen limitation. However, although maximal backscatter signals of all cultivation conditions differed significantly (p-values < 0.05), generally similar values for all oscillations ($\text{BS}_{\text{max}, 2\text{min}} = 683 \pm 12 \text{ a.u.}$, $\text{BS}_{\text{max}, 4\text{min}} = 707 \pm 7 \text{ a.u.}$, $\text{BS}_{\text{max}, 6\text{min}} = 728 \pm 14 \text{ a.u.}$) were reached, being only slightly lower than the maximal backscatter signal of the continuously shaken control cultivations ($\text{BS}_{\text{max}, \text{ctrl}} = 770 \pm 25 \text{ a.u.}$). Therefore, a decelerated growth but similar final biomass titers were concluded when *P. putida* KT2440 was subjected to oscillating OTRs.

The cultivations in microtiter scale were influenced when subjected to oscillations in shaking frequencies leading to alternating maximal oxygen transfer rates (OTR_{max}). In the described cultivations, only the online backscatter signal was accessible, thus there was no information about the dissolved oxygen tension (DOT) values at different shaking frequencies. Microtiter plates with integrated DOT optodes [350] could have given estimates. However, DOT signals respond to the oscillation in a delayed manner, and measurements could not have been synchronized to the shaking intervals. In addition, a shaken culture in microtiter-scale needs validation to be comparable to cultivations in STRs [351]. To gain more detailed information on the performance

of *P. putida* KT2440 at oscillating oxygen availability, STR cultivations allowing access to several on- and offline signals were performed. Here, potential metabolic shifts indicated by stagnating increase in backscatter signal during the cultivations in MTPs can be elucidated by performing sampling and metabolite quantification during STR cultivations.

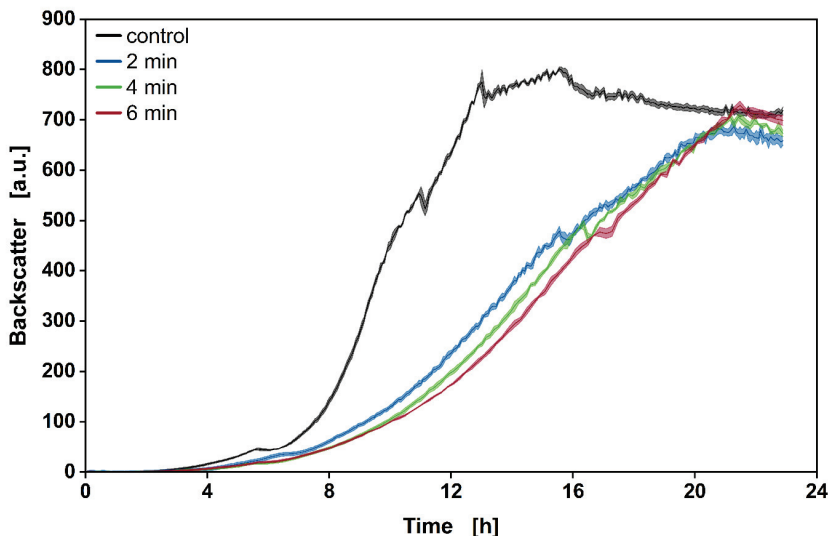


Figure 24 Backscatter signal throughout cultivations of *P. putida* KT2440 in microtiter plates at different intervals of oscillating agitation. A control cultivation, which was continuously shaken at 1,200 rpm (black), is compared to alternating shaking frequencies of 1,200 rpm and 200 rpm at intervals of 2 min (blue), 4 min (green), and 6 min (red). a.u. = arbitrary units. Shaded areas represent the standard deviation of measurements from five independent experiments.

3.4.3.2 Oscillation of dissolved oxygen tension decelerates growth in STRs

For a more detailed characterization of the effects a temporary and repeated shortage of oxygen availability has on *P. putida* KT2440, STR cultivations were performed. Repeated oxygen limitation during STR cultivations was induced by oscillating aeration and agitation between high and low setpoints. Here, intervals of 2 min and 4 min were investigated.

The duration until carbon source depletion was prolonged for both oscillating cultures compared to the control as indicated by a steep increase of the DOT signals and the measured substrate concentrations at sampling points (Figure 25A-C). All carbon in the control culture was consumed within 8.7 h, whereas the carbon source in the oscillating cultures with 2 min and 4 min of oscillation was depleted after 12.8 h and 13.6 h, respectively. The prolonged duration is reflected in the specific carbon uptake rates q_S (Table 7). While the difference in cultivation time between well-aerated and oscillating conditions was significant (4.1 h and 4.9 h), increasing the

interval of oscillations from 2 min to 4 min prolonged the duration of the cultivations only minorly (0.8 h). Dissolved oxygen was temporally depleted in either oscillation interval as indicated by the DOT values at low setpoints approaching 0 %. However, the culture subjected to 4 min of oscillation experienced temporal oxygen depletion earlier and over a more extended period. For comprehension, Figure 3A-C shows the minimal and maximal values of the DOT and a shaded range, in which DOT values oscillated. Additionally, Figure A5.2 in Appendix A.5 depicts a close view of a section of Figure 25B to exemplarily illustrate obtained oscillations of the DOT. The biomass signals reflected the differences in time of cultivations between undisturbed and oscillating cultures. Maximal biomass titers are similar, independent of cultivation conditions ($C_{X,\max,\text{ctrl}} = 3.36 \pm 0.02 \text{ g L}^{-1}$, $C_{X,\max,2\text{min}} = 3.39 \pm 0.09 \text{ g L}^{-1}$, $C_{X,\max,4\text{min}} = 3.29 \pm 0.02 \text{ g L}^{-1}$), but were reached after different durations of cultivation, coinciding with the depletion of carbon source.

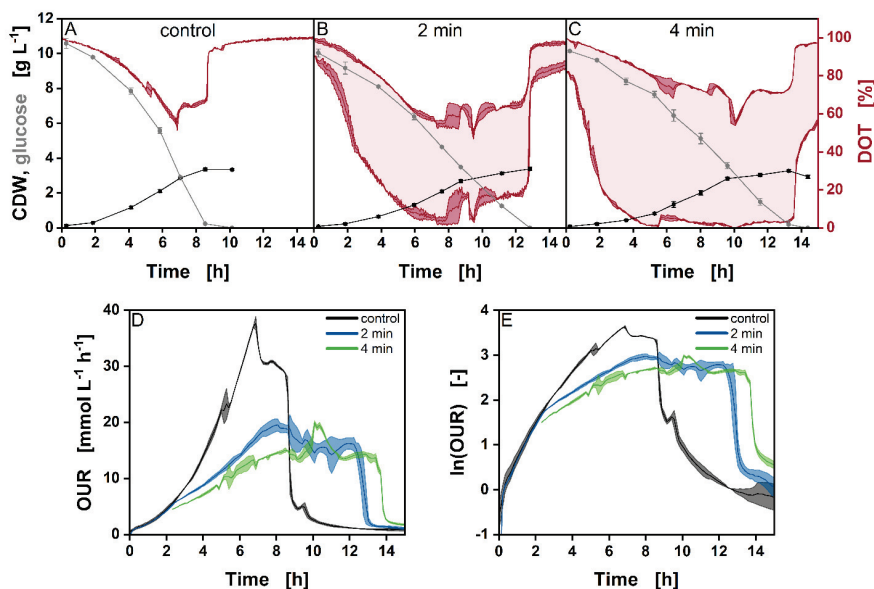


Figure 25 Cultivations of *P. putida* KT2440 at different intervals of oscillating aeration and agitation. (A-C) CDW (black squares), glucose (grey dots), and DOT (red line) over the cultivation time for (A) well-aerated control cultivations, (B) 2 min intervals of oscillation, and (C) 4 min intervals of oscillation. The solid red lines represent minima and maxima of DOT values, the light red shaded area represents the range of DOT values induced by oscillation. (D) Oxygen uptake rates and (E) the respective half-logarithmic plot for the control cultivations (black line), 2 min intervals of oscillation (blue line), and 4 min intervals of oscillation (green line). Error bars and darkly shaded areas represent errors derived from two independent experiments.

Assuming an equal demand of oxygen for each cell, thus a linear correlation between growth and oxygen uptake rate (OUR), the OUR indicated a more complex growth behavior than could be derived from the sampled biomass, especially when oscillation was induced (Figure 25D). As measurement intervals of the exhaust gas sensors and their response times did not match oscillation intervals, a moving average of the OUR is depicted, causing the signals not to appear oscillating. While the OUR of the well-aerated control cultivation and the oscillation at an interval of 2 min proceeded similarly up to a cultivation time of 2.3 h (data for the 4 min oscillation not available up to a cultivation time of 2.2 h), the signals diverged afterward as the increase in OUR of oscillating cultures decelerated. Linear regression of the OUR signals (Figure 25E) between 2.3 h and 5.1 h revealed the slope of the OUR to be reduced by approximately two-fold at either oscillation (Table 7), correlating with decreased growth rates of the respective cultures. Peaks and plateaus in the OUR indicate the co-metabolization of gluconate and 2-ketogluconate formed from glucose. The short stagnation of the OTR at 5 h of the control cultivation, which could also be observed in online backscatter signals of the previous cultivation in MTPs, coincided with a co-metabolization of 2-ketogluconate (refer to Appendix A.5, Figure A5.3). Notably, while maximal concentrations of gluconate are similar across all cultivations, the maximal concentrations of 2-ketogluconate increased with extended intervals of oscillation (Table 7 and Appendix A.5, Figure A5.3). The latter indicates limitations in providing NADH as the cells can circumvent the NADH-dependent ATP synthesis by generating electrons from the oxidation of gluconate to 2-ketogluconate. Integration of the OUR, starting from 2.3 h until carbon was depleted, revealed a comparable demand for oxygen, independent of disturbance (O_2 consumed, control = 140.4 ± 1.0 mmol L⁻¹, O_2 consumed, 2min = 143.6 ± 2.8 mmol L⁻¹, O_2 consumed, 4min = 139.1 ± 3.9 mmol L⁻¹).

In general, the results obtained from MTP cultivations could be confirmed. *P. putida* KT2440 grows at a reduced rate at oscillating oxygen availability, but final biomass titers at complete carbon depletion remain unaltered.

Table 7 Performance indicators for cultivations of wild-type *P. putida* KT2440 in STRs at different conditions.

Condition ^{a)}	m(lnOUR) ^{b)} [h ⁻¹]	qs ^{c)} [g g ⁻¹ h ⁻¹]	Y _{X/S} ^{d)} [g _X g ⁻¹]	Gluconate ^{e)} [g L ⁻¹]	2-Ketogluconate ^{e)} [g L ⁻¹]
Control	0.50 ± 0.02	0.65 ± 0.01	0.32 ± 0.01	0.39 ± 0.00	0.50 ± 0.07
2 min	0.27 ± 0.01	0.49 ± 0.02	0.33 ± 0.02	0.45 ± 0.01	0.67 ± 0.02
4 min	0.26 ± 0.01	0.45 ± 0.01	0.30 ± 0.00	0.40 ± 0.03	0.89 ± 0.12

^{a)} Control represents the well-aerated culture, 2 min and 4 min the respective intervals of aeration and non-aeration.

^{b)} Rates were derived *via* linear regression from OUR signals from 2.3 h to 5.1 h and correlate to growth rates.

^{c)} Specific glucose uptake rates were calculated *via* linear regression over the first 8 h of cultivation.

^{d)} Biomass yields were calculated from the maximal cell dry weight and the used substrate.

^{e)} Data represents maximal values occurring over the entire cultivation.

3.4.3.3 *Pseudomonas putida* withstands repeated dual oxygen and glucose limitation

Results from cultivations of *P. putida* KT2440 in an STR-PFR scale-down setup facing dual glucose and oxygen limitation in the PFR compartment are summarized in the following. In the STR-PFR cultivation, only part of the population encounters oxygen and glucose limitations. This setup mimics the conditions occurring in the multiphase loop reactor (MPLR) as described in Chapter 3.5 and industrial-scale bioreactors more closely, compared to oscillations of the DOT value in STRs, which subject the entire culture to temporary oxygen limitations simultaneously.

First, the STR was operated as a glucose-limited chemostat at a dilution rate of 0.2 h^{-1} to obtain reference characteristics after reaching steady-state conditions. Remarkably, although the DOT was set to a comparably low value of 5%, growth characteristics were similar to previous studies, in which a DOT of $> 20\%$ was maintained [321]. This was confirmed in a parallel cultivation device (DASbox, Eppendorf, Jülich, Germany), operating six small-scale reactors at different DOT values. Here, although DOT values as low as 5% were maintained, no significant differences in the growth behavior of *P. putida* KT2440 were detected (Appendix A.5, Figure A5.4).

By connecting the non-aerated PFR and ensuring oxygen and glucose depletion at the entrance and exit of the PFR, *P. putida* KT2440 was subjected to a dual limitation for the duration of its residence time in the PFR ($\tau_{\text{PFR}} = 2.6 \text{ min}$). After allowing the system to regain steady-state, samples were drawn from both the STR port and five PFR ports simultaneously to unravel both long- and short-time effects of the dual limitation. In short, most physiological parameters for a long-term response (cell dry weight, OUR, CER, glucose uptake rate) did not alter compared to the reference conditions, indicating that *P. putida* KT2440 could maintain a growth rate of 0.2 h^{-1} . Only a change in the adenylate energy charge (AEC) was observed, as it decreased from 0.84 ± 0.05 to 0.69 ± 0.15 , but not significantly ($p\text{-value} > 0.05$). Regarding short-term responses, ATP concentrations substantially reduced from 5.16 ± 1.56 (STR) to $2.21 \pm 0.24 \mu\text{mol gX}^{-1}$ (exit of the PFR) while *P. putida* KT2440 resided in the PFR. In contrast, AMP concentrations increased from 1.94 ± 1.39 (STR) to $5.63 \pm 0.55 \mu\text{mol gX}^{-1}$ (exit of the PFR), resulting in a reduced AEC of 0.32 ± 0.01 . Further, the levels of the stringent response alarmone ppGpp increased from $0.16 \pm 0.03 \mu\text{mol gX}^{-1}$ to $1.45 \pm 0.24 \mu\text{mol gX}^{-1}$ when facing dual starvation.

Concluding, substantial short-time responses were detected, as the AEC could not be maintained, and the stringent response was triggered, both being signs of severe stress at the instated dual starvation. However, *P. putida* KT2440 could fully recover when recirculated back to the STR, thereby maintaining robust growth characteristics over the entire long-term cultivation.

3.4.3.4 Exemplary production of rhamnolipids results in unaltered final titers at oscillating DOT values

The effect of oxygen limitation on the production capacity of *P. putida* KT2440 was also assessed, with RLs serving as an exemplary product. For this, *P. putida* KT2440 SK4, previously engineered to enable RL synthesis [148], was cultivated in STRs, again subjected to oscillating aeration and agitation. Besides, ethyl decanoate was added to the cultivation broth as an *in situ* extractant, and the pH value was set to 6 to avoid severe foaming. Both the effect of ethyl decanoate and the lowered pH value on growth and production have been described previously [125].

Similar to the STR cultivations performed with wild-type *P. putida* KT2440, the duration of the cultivation until depletion of the carbon source was prolonged at oscillating oxygen availability as indicated by the sudden increase of the DOT signal and the offline measurements of glucose (Figure 26A+B). However, the prolongation of cultivations was lowered to 1.5 h compared to cultivations of the wild-type *P. putida* KT2440 (4.1 h prolongation at 2 min oscillation intervals), where no organic solvent as a second liquid phase was present. Further, the DOT signal of the cultivation at oscillating conditions did not reach values as low as the culture of wild-type *P. putida* KT2440. As the addition of organic solvents has been proven beneficial for enhancing the mass transfer coefficient of oxygen in emulsified two-liquid phase fermentations [77], the added ethyl decanoate might have resulted in increased oxygen availability and an attenuated oscillation. Here, with increasing RLs and biomass concentrations throughout the cultivation, the extent of this effect would be highly dynamic, depending on different proposed mechanisms. Besides, the presence of surfactants itself affects the mass transfer, which is highly dependent on the type of surfactant and its concentration [352]. Further, the lowered pH value was shown to reduce growth rates of *P. putida* KT2440 [125]. Thus, the oxygen demand of the cells is lower over time compared to the wild type, in turn potentially resulting in a higher DOT value. In addition, it is questionable how much of the measured oxygen is available for the microorganisms as oxygen dissolved in ethyl decanoate might be inaccessible, but the average of DOT values in both phases was measured by the optical probe.

While gluconate accumulated similarly at both cultivation conditions for RL production, nearly no 2-ketogluconate was detected (Table 8 and Appendix A.5, Figure A5.5). This might be due to a higher demand for glucose-6-phosphate (G6P) required to produce activated dTDP-L-rhamnose, which is transferred to 3-(3-hydroxyalkanoyloxy)alkanoic acids (HAAs) by the rhamnosyltransferase RhIB to form mono-RLs. Previously, the carbon flux *via* the rhamnose pathway was revealed to be increased by 300% in an RL-producing *P. putida* KT2440 compared to the wild type, thus creating the mentioned demand [353]. The presence of ethyl decanoate severely impeded the determination of biomass concentration *via* gravimetry or spectroscopy.

Therefore, exhaust gas measurements were used as it correlates to biomass and growth. Whereas the OUR of the non-oscillating cultivation generally revealed an exponential incline between approximately 1.7 h and 8 h (Table 8), a two-staged growth behavior was observed for *P. putida* KT2440 SK4 subjected to oscillations. Between cultivation times of approximately 1.7 h and 5.1 h, the OUR of the cultures exhibited an exponential incline. However, growth appears to be linear thereafter (Figure 26C+D), indicating a limitation. Similar to the cultivation of wild-type *P. putida* KT2440, integration of the OUR led to comparable demands of oxygen until the carbon source was depleted (O_2 consumed, control = 120.7 mmol L⁻¹, O_2 consumed, 2 min = 123.4 ± 0.6 mmol L⁻¹).

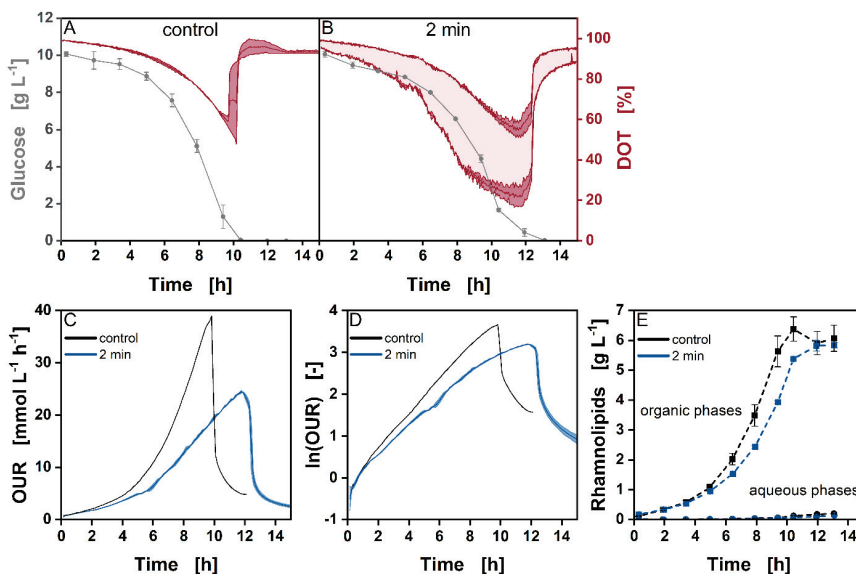


Figure 26 Comparison of cultivations of *P. putida* KT2440 SK4 at different intervals of oscillating aeration and agitation. (A-B) Glucose (grey dots) and DOT value (red line) over the cultivation time for (A) well-aerated control cultivations and (B) 2 min intervals of oscillation. The solid red lines represent averages of minima and maxima of DOT values. The light red shaded area represents the range of DOT values induced by oscillation. (C-D) Oxygen uptake rates and the respective half-logarithmic plot for the control cultivations (black line) and 2 min intervals of oscillation (blue line). (E) Average rhamnolipid titers in aqueous and organic phases for the control (black dashed lines) and 2 min intervals of oscillation (blue dashed lines). Error bars and darkly shaded areas represent errors derived from two independent experiments. For the control cultivation, only one exhaust gas measurement was recorded. Data associated to this figure were partially taken from Florian Röck's Internship Report [354].

The bulk of produced RLs was extracted into the organic phases (Figure 26E). Comparing titers of the two cultivation conditions, the same temporal offset as recorded in the exhaust gas data was observed. Despite slower production in the cultivation subjected to oscillations, maximum titers were comparable, thus indicating no significant adverse effects of repeated oxygen

limitations on the product yield, but rather on the space-time yield (Table 8), agreeing with the prolonged cultivation time until depletion of the carbon source.

Concluding, the cultivations of *P. putida* KT2440 SK4 in STRs showed that oscillating DOT values do not influence the strain's capacity to produce RLs, but result in reduced rates. While this was explicitly studied for producing RLs, it remains questionable if it can be generalized for any production of secondary metabolites with recombinant *P. putida* KT2440.

Table 8 Performance indicators for cultivations of *P. putida* KT2440 SK4 in STRs at different conditions.

Condition ^{a)}	m(lnOUR) ^{b)} [h ⁻¹]	Y _{P/S} ^{c)} [g _{RL} g ⁻¹]	STY ^{d)} [g _{RL} g ⁻¹]	Gluconate ^{e)} [g L ⁻¹]	2-Ketogluconate ^{e)} [g L ⁻¹]
Control	0.42	0.12 ± 0.01	0.11 ± 0.01	0.85 ± 0.01	0.01 ± 0.00
2 min	0.35 ± 0.01	0.11 ± 0.00	0.09 ± 0.00	0.79 ± 0.01	0.02 ± 0.00

^{a)} Control represents the continuously aerated culture, 2 min intervals of aeration and non-aeration.

^{b)} Slopes were derived *via* linear regression from OUR signals from 1 h to 5.1 h and reflect growth rates.

^{c)} Product yields were calculated from the maximal RL concentrations in the organic phase and the aqueous phase normalized by their respective volumes and the used substrate.

^{d)} Space-time yields were calculated from the maximal RL concentrations in the organic phase and in the aqueous phase normalized by their respective volumes and the time.

^{e)} Data represents maximal values occurring over the entire cultivation.

3.4.3.5 *Pseudomonas putida* KT2440 subjected to DOT oscillations alters proteome only minorly

Untargeted proteomics was used to compare samples from the STR cultivations of *P. putida* KT2440 SK4 at the different applied conditions to gain information about intracellular responses to oscillating DOT values. The continuously aerated cultures were sampled once at $t_1 = 7.6$ h, whereas the cultures subjected to oscillations were sampled at $t_1 = 7.6$ h and again at $t_2 = 11.9$ h, shortly before glucose depletion. Only proteins whose abundances were significantly altered at least two-fold (p -value < 0.05) when subjected to oscillations were considered.

The synthesis of only a minor number of proteins was up- or downregulated in cells cultivated at oscillating conditions (Figure 27A+B). Seven proteins were at least twofold more abundant, and seven proteins were reduced at least twofold compared to the control. In total, this accounts for only about 2 % of all 691 detected proteins. At t_2 , this ratio was even further reduced to 0.6 % (one upregulated and three downregulated). The relatively low overall alteration indicates that *P. putida* KT2440 does not majorly alter its proteome but can cope with oscillating oxygen availability using its existing set of proteins. When grouping the proteins of changed abundance according to the clusters of orthologous groups (COG) database [355] retrieved with eggnog 5.0.0, predominantly proteins of the COG C “Energy production and conversion” were less abundant. In contrast, mainly proteins associated with COG L “Replication, recombination, and repair” were synthesized at least twofold higher than in the control (Figure 27C).

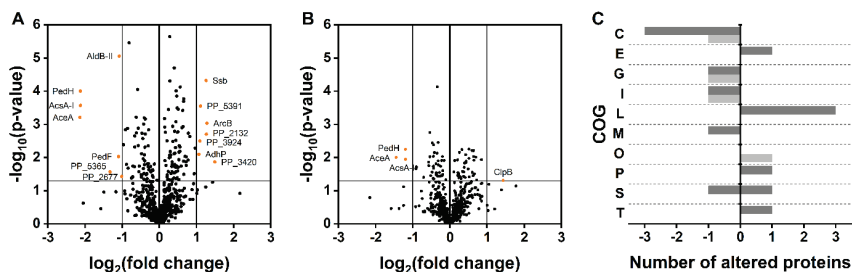


Figure 27 Relative differences in abundances of detected proteins in *P. putida* KT2440 subjected to oscillating DOT values compared to undisturbed control cultivations. (A) Volcano plot to determine significantly altered proteins at t₁. Cut-off values were set to a log₂ fold change of 1 and a p-value of 0.05. Orange data points represent proteins of significantly altered abundance. (B) Analog to (A) for t₂. (C) Grouping of altered proteins according to COGs, which were retrieved via eggno3 5.0.0, for t₁ (dark grey bars) and t₂ (light grey bars). Positive x-values represent the number of proteins with increased abundance, while negative numbers represent the number of proteins with reduced abundance. COGs: C - Energy production and conversion, E - Amino acid transport and metabolism, G - Carbohydrate transport and metabolism, I - Lipid transport and metabolism, L - Replication, recombination, and repair, M - Cell wall/membrane/envelope biogenesis, O - Post-translational modification, protein turnover, and chaperones, P - Inorganic ion transport and metabolism, S - Unknown function, T - Signal transduction mechanism. Proteins and corresponding information are listed in Appendix A.5, Table A5.1.

The protein exhibiting the most severe downregulated synthesis at t₁ and t₂ was the isocitrate lyase (AceA, PP_4116), indicating downregulation of the glyoxylate shunt and lower carbon flux through the TCA cycle. The upregulated synthesis of proteins related to replication, recombination, and repair, chaperones, or stress response (PP_0625, chaperone protein ClpB (t₂ only); PP_0485, single-stranded DNA-binding protein; PP_2132, universal stress protein; PP_3420, sensor histidine kinase (all t₁ only)) indicates stress for *P. putida* KT2440 at oscillation.

Further, proteomics data showed a downregulated synthesis of the acetyl-CoA synthase AcsA-I (PP_4487) and several proteins from the ped cluster (PP_2675, cytochrome c oxidase PedF; PP_2677, hypothetical protein; PP_2679, PQQ-dependent alcohol dehydrogenase PedH; and PP_2680, aldehyde dehydrogenase AldB-II) as well as an upregulated synthesis of the alcohol dehydrogenase AdhP (PP_3839). A change in levels of alcohol dehydrogenases indicates the presence of alcohols, which could potentially be attributed to impurities of the applied ethyl decanoate ($\geq 98\%$ purity) or its de-esterification by *P. putida* KT2440 resulting in ethanol and decanoate. However, ethyl decanoate from the same stock was used in both the control and the oscillating cultivation. We previously showed that *P. putida* KT2440 cannot use ethyl decanoate as a carbon source in the presence of glucose or directly after glucose depletion [125]. Further, metabolism of ethanol would require the activity of the acetyl-CoA synthase to generate acetyl-CoA from acetate. However, we observed a downregulated expression of *acsA-I*, which would result in an accumulation of acetate. Neither acetate nor ethanol were detected in the supernatant.

3.4.4 Discussion

3.4.4.1 *Pseudomonas putida* KT2440 endures temporary oxygen limitations

In this chapter, the influence of temporary oxygen deprivation on the growth of the obligate aerobic *P. putida* KT2440 was assessed across different cultivation systems and scales, ranging from microtiter to lab-scale reactors simulating large-scale fermenters. In batch cultivations at all scales, the growth behavior appeared to follow a similar pattern. When oxygen was temporarily limited, the growth rate of the cells decreased and transitioned into linear growth, leading to prolonged cultivation times until carbon source depletion compared to well-aerated cultures. However, final biomass titers were comparable. As this phenotype was consistent throughout MTP and STR cultivations, the presented approach of implementing oscillating shaking frequencies to cause repeated oxygen shortage could be applied in similar future studies for estimations on growth behavior before running scale-down experiments in more complex setups. Remarkably, the length of oscillating intervals did not seem to substantially impact the length of cultivation as studied for MTP and STR cultivations for wild-type *P. putida* KT2440. Rather the occurrence of oscillation caused the observed effect. This might be due to the equal durations of aeration and non-aeration within each periodic cycle. However, preliminary results from STR cultivations with unequal durations of each condition showed similar effects. Randomized durations might give different results and could be more accurate in simulating the transient conditions cells encounter due to their trajectory through large-scale reactors [356, 357]. At repeated exposure to dual oxygen and glucose limitations in the STR-PFR cultivations, *P. putida* KT2440 maintained the set growth rate of 0.2 h^{-1} after the PFR was connected. In a previous study, *P. putida* reached similar yields in biomass and showed an accelerated DNA replication when subjected to a critical low DOT value of 1.5% [358]. In contrast, it was previously demonstrated that final biomass titers of *P. putida* strains were reduced when subjected to a strict oxygen limitation induced by low but constant agitation [359, 360]. As we observed similar final biomass titers in this study, it can be inferred that *P. putida* KT2440 can rapidly recover from oxygen starvation when resupplied with oxygen. Its robust growth performance highlights the ability of *P. putida* to cope with various stress situations due to its versatile metabolism [361]. Further, the RL titers produced at oscillating conditions were comparable to those of well-aerated control cultivations, but space-time yields were decreased. Therefore, *P. putida* KT2440 is well suited for large-scale production processes exhibiting gradients in oxygen concentrations, however, at reduced productivity. Advantageously, in contrast to whole-cell biocatalysts capable of fermenting, no undesired byproducts are produced, except for gluconate and 2-ketogluconate, which are in turn metabolized and reused as a carbon source by *P. putida* KT2440. Thereby, carbon efficiency might be enhanced, and downstream

processing might be facilitated. It needs to be validated if these conclusions can be transferred to production processes for products other than RLs.

3.4.4.2 Intracellular mechanisms for coping with repeated oxygen starvation remain ambiguous

While growth and production are robust, the distinct intracellular mechanisms for coping with repeated oxygen limitations remain ambiguous. Previously, when encountering sole carbon limitation, *P. putida* KT2440 was shown to generate energy equivalents from intracellularly accumulated 3-hydroxyalkanoates (3-HA) [321]. Further, a transcriptomic upregulation of genes encoding for enzymes involved in amino acid and glycogen catabolism was observed at glucose limitation. Contrary, an inability of *P. putida* KT2440 to balance its energy demand when subjected to dual carbon and oxygen limitation was detected. The resulting decrease in energy charge from 0.7 to less than 0.4 lies well below energy charges of 0.7 or higher reported for growing *P. putida* [362, 363]. Assumably, the lack of oxygen stalls the electron transport in the respiratory chain, consequently preventing the oxidation of the energy equivalents NADH and FADH₂. As a result, failing to maintain a proton gradient compromises the functionality of the ATP synthase. Correspondingly, a decrease in intracellular ATP levels and an accumulation of AMP during dual oxygen and glucose limitation was observed. Moreover, levels of the stringent response alarmone ppGpp, a central signaling molecule for stress caused by starvation [364, 365] were elevated. Accordingly, increased levels in ppGpp were reported for *E. coli* [366] and *P. putida* [321] at glucose limitation.

In proteomics studies, an altered abundance of only a minor number of proteins was detected. The synthesis of the isocitrate lyase was downregulated when *P. putida* KT2440 encountered oscillating DOT values. Previously, it has been shown that a deletion of the isocitrate lyase resulted in an increased polyhydroxyalkanoates (PHA) production, assumed to cause a lower carbon flux through the tricarboxylic acid cycle, thus increasing the pool of acetyl-CoA potentially used for PHA synthesis [367]. *P. putida* KT2440 is known to produce PHA when encountering stress caused by changing environmental conditions, *e.g.*, repeated carbon starvation or transition to nitrogen starvation [321, 368]. A higher abundance of proteins associated with stress response was detected, but it is unknown if stress caused by oxygen limitation or oscillating oxygen availability induces PHA production, which was not quantified in this chapter. In this case, a likewise increase of RL titers could be expected as 3-hydroxyalkanoate (3-HA) is the precursor for both PHA and RLs. However, the recorded data show no change in RL titer when cells were subjected to oscillations.

Moreover, the proteomics studies revealed a downregulated synthesis of several proteins encoded within the ped cluster. Recently, proteins of the ped cluster have been reported to be involved in the oxidation of alcohols by *P. putida* KT2440 [257, 369, 370]. Subsequently, using cytochrome c, electrons are transferred to the cytochrome c oxidase (PP_2675, PedF), which was also less abundant here, in turn reducing O₂ as part of the respiratory electron transfer chain [371, 372]. The downregulation of the ped can thus be reasoned with the temporary low abundance of molecular oxygen, impeding the functionality of PedF and potentially the PQQ biosynthesis pathway, which requires molecular oxygen itself. As the regulation of the whole cluster seems to be multi-leveled and interconnected [257, 369], similar expression levels of individual genes of the cluster might be caused by the same trigger, such as limited availability of molecular oxygen. The higher abundance of NAD⁺-dependent AdhP indicates its function as a complementary alcohol dehydrogenase, which might be favored over PedH at a shortage of NADH, which is suggested by the increasing 2-ketogluconate concentrations in the cultivations of wild-type *P. putida* KT2440. In fact, deletion of both *pedH* and *adhP* caused *P. putida* KT2440 to lose its ability to metabolize short-chain alcohols, while single deletion strains retained functionality [369]. However, if altered abundances of proteins of the ped cluster and AdhP are solely due to oscillating DOT values or if the presence of an organic solvent triggers their synthesis in the first place, remains unclear.

In general, the presented data suggests that *P. putida* KT2440 can cope with repeated oxygen starvation at the cost of its energy charge but can partially restore it when oxygen becomes available again without majorly altering its proteome. Further studies on the transcriptome and proteome combined with the quantification of PHAs need to be conducted to elucidate the intracellular coping mechanisms in more detail.

3.4.5 Conclusion

Oxygen starvation zones accompanied by other substrate gradients caused by mixing inhomogeneities are likely to occur in industrial-scale bioreactors. In this chapter, the ability of *P. putida* KT2440, classified as an obligate aerobic microorganism, to withstand temporary oxygen limitations, even at simultaneous carbon starvation, is demonstrated. The growth performance of the wild-type strain is not affected significantly by repeated exposure to oxygen starvation. Remarkably, this was confirmed in different scales and cultivation systems, different cultivation media, and different laboratories. Moreover, the RL producing strain accumulated similar product titers during oxygen oscillation compared to the well-aerated reference process. As both growth and production are robust when cells are subjected to temporary oxygen starvation, the suitability of *P. putida* KT2440 for industrial-scale production processes was affirmed.

The results of this chapter have several implications for the operation of the MPLR, which is described in Chapter 3.5. Although classified as obligate aerobic, *P. putida* KT2440 is able to withstand repeated short-time oxygen starvation and can produce at given conditions. However, the residence time in the downcomer (τ_d) should not exceed several minutes and should be uniform, thus the loop flow needs to be similar in all parts of the reactor. Further, the presence of solvent can have conflicting impacts. On the one hand, the solvent could attenuate the oscillations experienced by cells following the loop flow as oxygen can be delivered by saturated solvent. On the other hand, repeated oxygen starvation causes ATP levels to decrease, potentially causing the cell to be unable to maintain energy-intensive solvent defense mechanisms. However, the selected solvent, ethyl decanoate, did not appear to stress the cells in biocompatibility assays.

Chapter 3.5

A novel multiphase loop reactor allows simultaneous production and *in situ* extraction of rhamnolipids

Contributions

Philipp Demling and Maximilian von Campenhausen jointly developed, constructed, and improved the MPLR, supported by Tammo Schöler, with Maximilian von Campenhausen focusing on fluid process engineering and Philipp Demling focusing on bioprocess engineering. The CAD results presented in Figure 28 were obtained from Maximilian von Campenhausen. Specific details regarding the reactor characterization will be presented in the Doctoral Thesis of Maximilian von Campenhausen. Philipp Demling and Maximilian von Campenhausen jointly performed cultivations in the MPLR, supported by Steffen Dietz. All analytics were done by Philipp Demling. Patrick Bongartz and Alexander Scheele constructed the redesigned aeration setup. This chapter was written by Philipp Demling and reviewed by Till Tiso.

3.5 A novel multiphase loop reactor allows simultaneous production and *in situ* extraction of rhamnolipids

3.5.1 Abstract

A novel multiphase loop reactor was developed and constructed, allowing a counter-current *in situ* extraction of value-added compounds produced in a microbial cultivation. Here, developed cultivation strategies for the integrated production and *in situ* recovery of rhamnolipids described in the previous chapters were transferred to the multiphase loop reactor. A first cultivation revealed that a custom-made metal ring sparger could not satisfy the oxygen demand of the cells, which were limited in oxygen approximately 3 h after inoculation. The short duration of the cultivation resulted in low estimated biomass titers and marginal rhamnolipid production while only a small amount of the carbon source was converted. Exchanging the ring sparger with a highly porous poly(2-propenamide) sparger resulted in sufficient aeration to meet the oxygen demand of *Pseudomonas putida* KT2440 SK4 until the end of the cultivation when 10 g L⁻¹ glucose were depleted. Reducing the pH value increased the extraction efficiency, as described in Chapter 3.1, allowing to avoid excessive foaming. A total of 3.6 g L⁻¹ rhamnolipids accumulated in ethyl decanoate, serving as the organic solvent phase, while only minor amounts of rhamnolipids remained in the aqueous phase. The novel multiphase loop reactor could be operated robustly, achieving sufficient phase separation and thereby continuous removal and recirculation of ethyl decanoate for a major part of the cultivation. Finally, performance indicators, such as product yield and productivity, revealed the efficiency of the cultivation in the multiphase loop reactor to be comparable to cultivations described in previous chapters. Overall, the successful operation of the multiphase loop reactor demonstrated the technical feasibility of the novel approach.

3.5.2 Introduction

In previous chapters, fermentation strategies for the foam-free production of rhamnolipids (RLs) with *Pseudomonas putida* KT2440 SK4 were developed by integrating an *in situ* liquid-liquid extraction in stirred-tank reactors (STRs). However, extensive agitation in the STRs needed for the introduction of energy to achieve sufficient mixing and a high gas-liquid mass transfer to supply the cells with oxygen resulted in the formation of emulsions, especially with increasing biomass and RL titers. Phase separations could be achieved by centrifugation or gravitational phase separation subsequent to catastrophic phase inversion (CPI), however, requiring an interruption or termination of the fermentation process. A continuous removal of the emulsion during the fermentation would lead to a loss of whole-cell biocatalyst attached at the phase boundary, thus reducing the efficiency of the fermentation process [373]. Continuous removal,

recovery, and recirculation of a coherent solvent phase require a reactor setup exhibiting less and homogeneous shear forces. As a result, larger and more homogenous solvent droplets facilitate faster coalescence.

A reactor type characterized by a rather homogenous energy dissipation and, thus, no focal point of shear forces, is the airlift reactor (ALR) [374, 375]. Agitation is solely based on the introduction of a gaseous stream. Therefore, no impellers or other moving installations are required, resulting in a rather simple structure. The ALR is regarded as advantageous in terms of energy efficiency, *i.e.*, mass transfer rates per energy input, and thus energy input per amount of product compared to STRs [374, 376, 377]. In contrast to bubble column reactors, not the entire reactor, but only a single compartment is aerated (riser) [378]. The higher gas hold-up in the riser results in a reduction of the average fluid density compared to the non-aerated compartment (downcomer) and creates a pressure gradient between the compartments if interconnected [379]. Thus,

$$\frac{\Delta p_g}{gH_e} = \rho_d - \rho_r = (\varepsilon_{Gr} - \varepsilon_{Gd})\rho_L \quad (16)$$

with Δp_g being the difference in gravitational pressure between downcomer and riser, g being the gravitational acceleration, H_e being the effective height of the cylinder separating riser and downcomer, ρ_d , ρ_r , and ρ_L being the average fluid densities of the downcomer, the riser, and the non-aerated fluid, respectively, and ε_{Gr} and ε_{Gd} being the gas hold-ups in the riser and downcomer. Consequentially, a loop flow is induced [380]. The difference in gas hold-up is dependent on the superficial gas velocity in the riser U_{Gr} , which is, in turn proportional to the molar gas flow rate Q_m (Appendix A.6, Equation 20). Therefore, the aeration rate is the most crucial parameter for operating an ALR [374, 381]. Further, the specific fluid dynamics are highly dependent on multiple geometrical parameters of the reactor, such as the ratio between the cross-sections of riser and downcomer and the height-to-diameter ratio of the reactor [380, 382].

ALRs have been constructed in different setups and with varying characteristics [374, 383]. The most widely used reactor is the internal loop reactor, in which both compartments are located in the same vessel but separated by internal cylindrical installations or flat sheets. Depending on the location of aeration, both inner and outer, or left and right compartments, respectively, can serve as the riser. In addition, the two compartments can be separated as in external loop reactors. Further, multiple variations of the two main reactor types have been constructed, *e.g.*, by introducing baffled [384], undulated [385], or perforated compartment boundaries [386, 387], installing flow promoters [388], static mixers [389] or moving impellers [390], hybridizing with packed- or moving-bed reactors [391, 392], pressurized reactors [393], or even interconnecting

multiple ALRs in built-in cascades [394, 395], each influencing fluid dynamics and reinforcing specific beneficial traits of the ALR.

In biotechnology, ALRs have been used in multiple setups for different purposes for more than 50 years [396, 397], with a peak interest presumably in the 1990s. Many fermentation processes using whole-cell biocatalyst to produce, *e.g.*, antibiotics [376], proteins [398], and hydrocarbons [399], among numerous others, and reaction concepts with immobilized enzymes, *e.g.*, to convert sugars [400] have been developed. Further, ALRs have been used in biofilm-driven waste water treatment [401]. These and multiple other applications have been reviewed extensively [381, 383].

The multiphase loop reactor (MPLR) previously developed, simulated, and patented [54–56] is based on the operational principle of an airlift reactor with an internal loop. Besides, extractant in form of an organic solvent is dispersed at the bottom of the downcomer. As the solvent is less dense than the aqueous phase, the solvent drops rise against the aqueous flow, thus establishing a counter-current *in situ* liquid-liquid extraction (LLE). Due to the low shear force and homogenous flow, solvent drops are not further dispersed and form a coherent solvent phase at the liquid surface, which can be removed continuously. As described in Chapter 3.1, an *in situ* LLE combined with distinct operational process parameters of the fermentation can prevent foaming. Further, operational limits regarding the endurance of temporary oxygen limitation by *P. putida* KT2440 have been defined in Chapter 3.4.

In biotechnological production processes, only few approaches for *in situ* product removal (ISPR) have been applied in ALRs. Mihal' *et al.* installed a membrane-supported extraction in the downcomer of an ALR to remove 2-phenylethanol produced by *S. cerevisiae* [399], whereas other approaches for the ISPR of lactic acid [402] and lipases [403] relied on the addition of resins for adsorption. An *in situ* LLE with direct contact of the two liquid phases has not been reported for ALRs. In contrast, continuous removal of a solvent phase from an operating STR has been conducted, however, at the cost of thorough agitation or with special installations to allow phase separation [78, 175, 204].

In this chapter, previous findings have been applied to construct and operate the MPLR to enable the foam-free production of RLs with *P. putida* KT2440 SK4 by introducing a counter-current *in situ* LLE. In contrast to two-liquid phase STR cultivations, phase separation could be performed within the reactor, enabling the extractant to be removed and recirculated continuously. After modifications in aeration and phase separations, a batch cultivation could be performed, which was compared to the two-liquid phase STR cultivations in terms of performance.

3.5.3 Results

3.5.3.1 Construction and installation of the multiphase loop reactor

The MPLR was built according to an *in silico* model with geometrical parameters (Figure 28). Computational fluid dynamics (CFD) simulations have estimated the resulting flow pattern in advance. All installations, including the cylinder (3 mm wall thickness) dividing riser and downcomer and the head plate, have been custom-made and constructed with stainless steel (1.4404, 316L), whereas the outer 5 L glass vessel was purchased (Eppendorf, Hamburg, Germany). The downcomer and the riser were monitored *via* a temperature sensor as well as a pH and dissolved oxygen tension (DOT) probe each and controlled *via* two linked BioFlo110 control units. The implementation of thermal mass-flow controllers allowed aeration at defined rates. Further, the counter-current *in situ* LLE was established by integrating two peristaltic pumps, a solvent disperser, and a solvent reservoir flask, allowing the introduction of solvent at the bottom of the downcomer and its withdrawal from the settler compartment. The settler compartment was geometrically designed to allow efficient phase separation by including an unstructured, stainless steel mesh serving as a coalescer. Temperature control was achieved by installing a cooling coil and a heating blanket. Further, the concentrations of oxygen and carbon dioxide in the exhaust gas were measured by installing respective sensors. Additional details of the MPLR and cultivation conditions are given in Chapter 2.4.6.

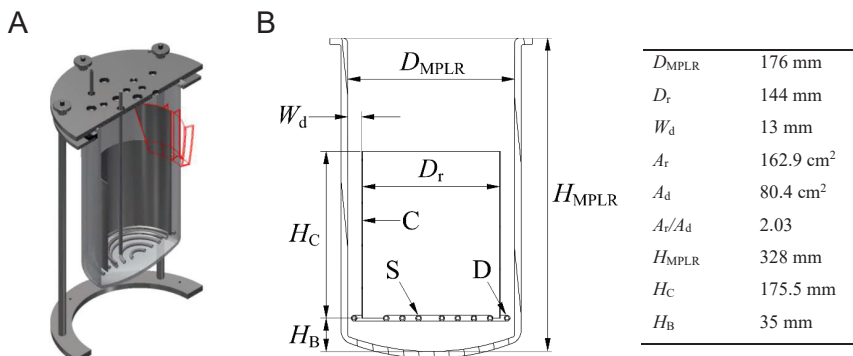


Figure 28 Dimensions of the MPLR. (A) Cross-section of a CAD-model of the MPLR. The red lines represent the settler compartment. Gratefully provided by Maximilian von Campenhausen. (B) Technical drawing of the MPLR and dimensions. D_{MPLR} - diameter of the MPLR, D_r - diameter of the riser, W_d - width of the downcomer, A_r - horizontal area of the riser, A_d - horizontal area of the downcomer, H_{MPLR} - height of the MPLR, H_C - height of the cylinder, H_B - height of the bottom compartment below the riser, C - cylinder separating riser and downcomer, S - sparger (gas), D - disperser (solvent).

3.5.3.2 Cultivation with a custom-made metal ring sparger results in oxygen limitation

After constructing and installing the MPLR, *P. putida* KT2440 SK4 was cultivated to assess the performance of the initial reactor design under production conditions. Produced RLs were extracted *in situ* by applying ethyl decanoate as a second liquid phase based on the results obtained in Chapter 3.1. In contrast to previous two-liquid phase cultivations in STRs, coherent organic phase was constantly removed from the settlement compartment and transferred to a solvent reservoir flask before recirculated to the reactor.

After inoculation, the DOT value rapidly decreased in both the riser and the downcomer, indicating an oxygen uptake rate (OUR) by the cells, which could not be sufficiently matched by the oxygen transfer rate (OTR) *via* aeration (Figure 29A). Increasing the aeration rate to 6 L min⁻¹ (1.5 vvm) 78 min after inoculation only temporarily increased the DOT value, before declining again, eventually resulting in a complete oxygen depletion after 160 min in the downcomer and 210 min in the riser. The biomass concentration could not be measured due to the presence of ethyl decanoate. However, as RL production is coupled to growth and exponential growth can be assumed only when no oxygen limitation occurred, a low increase in biomass and low RL titers can be expected. Thus, the installed aeration setup could not provide oxygen in amounts sufficient to enable an efficient cultivation and thus low conversion of the supplied carbon source.

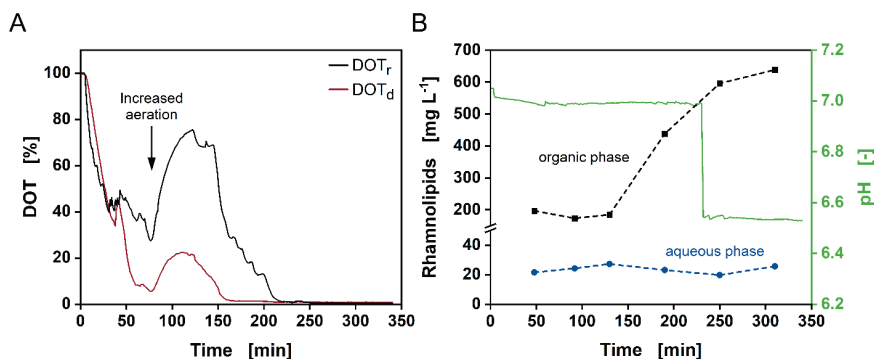


Figure 29 Cultivation of *P. putida* KT2440 SK4 in the first generation MPLR. *P. putida* KT2440 SK4 was cultivated in 4 L MSM supplemented with 10 g L⁻¹ glucose and in the presence of 1 L ethyl decanoate, which was continuously recirculated from a reservoir flask to the reactor and returned by withdrawing a coherent phase from the settlement compartment. (A) Dissolved oxygen tensions in the riser (DOT_r, black line) and the downcomer (DOT_d, blue line). The arrow denotes an increase of aeration rate from 4 L min⁻¹ to 6 L min⁻¹. (B) RL titers in the organic phase (black squares) and in the aqueous phase (blue circles) and the pH (green line). Data associated to this figure were partially taken from Steffen Dietz's Internship Report [404].

RL titers reached $638 \text{ mg L}_{\text{org}}^{-1}$ in the ethyl decanoate phase while titers in the aqueous phase remained below $30 \text{ mg L}_{\text{aq}}^{-1}$, translating to an amount of 0.82 g RLs and a product yield of $0.02 \text{ g}_{\text{RL}} \text{ g}_{\text{GLC}}^{-1}$ when regarding unused glucose as wasted (Figure 29B). Despite the low RL titer, the pH value had to be adjusted from 7 to 6.5 after 230 min to avoid excessive foaming. The decrease of pH value resulted in an increased extraction efficiency as reflected by the increase of the RL partition coefficient from approximately 8 to 26.

Overall, the ring sparger did not allow sufficient aeration for cultivating *P. putida* KT2440 SK4 to produce RLs in the MPLR. A redesign of the aeration setup needed to be considered.

3.5.3.3 A redesign of the aeration setup increased the OTR substantially and enabled a batch cultivation with efficient RL production

As the metal ring sparger could not satisfy the oxygen demand of *P. putida* KT2440 SK4 to enable growth and production, the aeration system was redesigned. The bubbles generated by the metal ring sparger were large in diameter (4 - 10 mm) and exhibited a non-uniform distribution. Thus, the surface-to-volume ratio was comparably low, resulting in a low volumetric gas transfer coefficient (k_{La}). Replacing the metal ring sparger with a custom-made, highly porous, spiral poly(2-propenamide) sparger allowed the dispersion of bubbles with small diameters (0.5 - 2 mm), enhancing the k_{La} by 2-3-fold, with respect to the aeration rate. Further, the solvent reservoir flask was actively aerated to remove co-extracted CO_2 and saturate the solvent with oxygen. Thereby, the solvent can serve as a vector for enhanced mass transfer of dissolved gasses [405, 406].

When using the redesigned sparger in a cultivation, the DOT values did not decrease to critical levels in either compartment directly after inoculation despite the comparably low aeration rate of 2.2 L h^{-1} (0.54 vvm). Instead, the DOT values transcended into a gradual decline typical for exponentially growing cultures (Figure 30A). After 5.8 h, the aeration rate was increased to maintain a DOT value in the riser (DOT_{r}) of $\geq 50\%$. At this time, dissolved oxygen had been depleted in the downcomer for approximately 20 min. Remarkably, after enhancing the aeration rate, the DOT value in the downcomer (DOT_{d}) increased by more than the DOT_{r} value, indicating a stronger loop flow and an enhanced mixing. During the cultivation, the aeration rate was increased several times to a maximal value of 9 L min^{-1} (approximately 2.2 vvm) to maintain a DOT_{r} value of $\geq 50\%$. However, this did not prevent a total depletion of oxygen in the downcomer starting at 11.5 h. A steep increase of both DOT signals indicated the depletion of the carbon source after 12.8 h, confirmed by glucose, gluconate, and 2-ketogluconate measurements (Figure 30B). Similar to previous cultivations (refer to Chapter 3.4), low concentrations of gluconate accumulated but mainly were consumed by the end of the cultivation, whereas only trace amounts of 2-ketogluconate were produced.

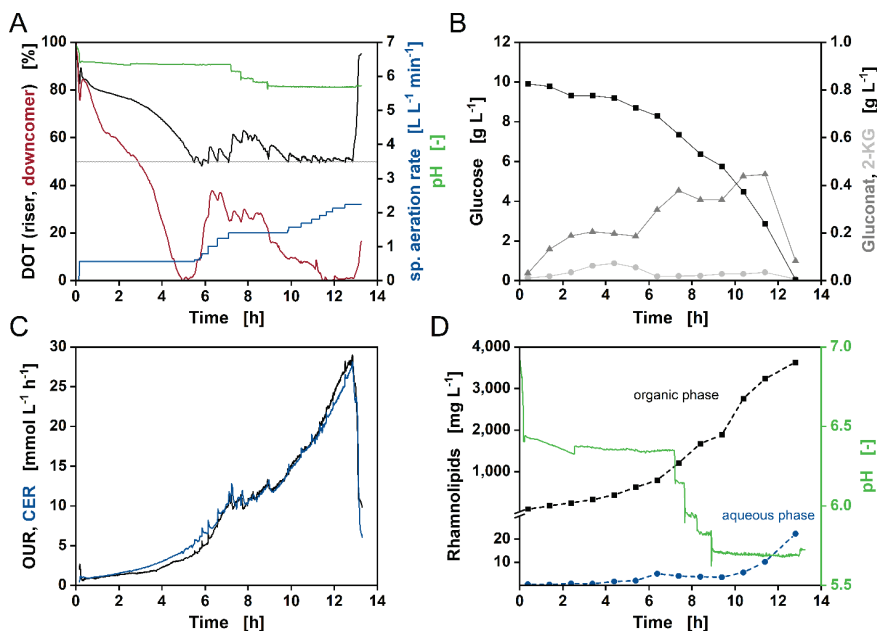


Figure 30 Cultivation of *P. putida* KT2440 SK4 in the second generation MPLR with a redesigned aeration setup. (A) Dissolved oxygen tensions in the riser (DOT_r, black line) and the downcomer (DOT_d, red line), the specific aeration rate (blue line), and the pH value (green line). The grey line denotes the targeted DOT_r. (B) Glucose (black squares), gluconate (dark grey triangles), and 2-ketogluconate (2-KG, light grey circles) concentrations. (C) Oxygen uptake rate (OUR, black line) and carbon emission rate (CER, blue line). (D) Rhamnolipid titers in the organic phase (black squares) and in the aqueous phase (blue circles) and the pH value (green line).

Analogous to the two-liquid phase cultivations in STRs, the pH value was gradually reduced to avoid foaming. Shortly after inoculation, the pH was set to 6.5, but had to be decreased to a minimal value of 5.7 during the cultivation. While foaming could be prevented, the decrease of the pH had a negative effect on the growth of *P. putida* KT2440 SK4. Although biomass could not be measured directly due to the presence of ethyl decanoate, the OUR and the CER stagnated shortly after the addition of HCl, indicating a non-increasing respiratory activity, thus no growth (Figure 30C). However, the cells could recover and resume exponential growth thereafter. The change of operational parameters is also reflected in the slope of the OUR, derived *via* linear regression, which correlates to the growth rate when exponential growth is assumed (Appendix A.6, Figure A6.1). At initial conditions, a slope of 0.3 h⁻¹ was reached, which substantially increased to 0.62 h⁻¹ when the aeration was enhanced. After adding acid, the slope was reduced close to zero, however recovering to 0.24 h⁻¹ thereafter. A better mixing and a more homogeneous supply of oxygen can be assumed after an enhanced aeration, resulting in an increased slope. The stagnation due to acid addition can be related to biological phenomena, since the pH value diverged

from the optimal range for *P. putida* KT2440 SK4, as already discussed in Chapter 3.1 [152]. Potentially, local gradients of pH values developed after the acid was added, which could be due to the lower turbulence and therefore increased mixing times compared to conventional STRs.

During the cultivation, RL titers in both the organic and the aqueous phase increased, demonstrating efficient production (Figure 30D). While the RL titer in the aqueous phase could be maintained below $25 \text{ mg L}_{\text{aq}}^{-1}$, thereby avoiding foam formation, RL accumulated in the organic phase indicating efficient extraction and resulting in a titer of more than $3.6 \text{ g L}_{\text{org}}^{-1}$ at glucose depletion. The titers translate to a product yield of $0.11 \text{ g}_{\text{RL}} \text{ g}_{\text{GLC}}^{-1}$, comparable to product yields obtained in previous two-liquid phase fermentations.

A coherent phase of ethyl decanoate could be withdrawn for most of the cultivation as the solvent drops coalesced in the settlement compartment. However, with increasing RL and biomass titers, the drops became smaller and more stable, hindering coalescence. Further, an increased loop flow of the aqueous phase in the downcomer due to an enhanced aeration amplified flooding of solvent drops into the more turbulent riser. The thereby dispersed drops resulted in a partial formation of an emulsion and deteriorated phase separation, causing the withdrawal of small amounts of the aqueous phase toward the end of the cultivation. Nevertheless, the reservoir flask contained mostly ethyl decanoate when the cultivation was terminated, and the present aqueous phase could be removed by centrifugation.

In general, the functionality of the MPLR could be demonstrated by the cultivation of *P. putida* KT2440 SK4, resulting in efficient production and *in situ* extraction of RLs.

3.5.4 Discussion

In this chapter, a proof of concept for the functionality of the MPLR is presented as a successful production and *in situ* extraction of RLs could be demonstrated. Performance indicators of the fermentation process are comparable to two-liquid phase STR cultivations as described in Chapters 3.1 and 3.3. Different aspects of the joint development of the MPLR and the operational parameters of the bioprocess are discussed in the following.

3.5.4.1 Type and rate of aeration are essential for performance in the MPLR

Two different types of spargers for aeration have been tested in this chapter. The metal ring sparger dispersing large bubbles ($d \approx 4 - 10 \text{ mm}$) could not supply sufficient oxygen to enable long-term cultivation in contrast to the highly porous poly(2-propenamide) sparger. The smaller bubbles ($d \approx 0.5 - 2 \text{ mm}$) produced by the latter resulted in an elevated OTR, as it is dependent on the volumetric gas transfer coefficient k_{La} , which is enhanced with an increased volume-specific surface area of the gas bubbles a

$$OTR = k_L a \cdot (C^* - C_L) \quad (17)$$

with C^* being the DO concentration at the phase boundary on the liquid side and C_L being the DO concentration in the liquid bulk phase. C^* equals the saturated DOT. Large bubbles generally result in a higher superficial gas velocity U_G and thus a lower gas hold-up ε_G , further reducing the OTR as

$$a = 6 \cdot \frac{\varepsilon_G}{d_b(1 - \varepsilon_G)} \quad (18)$$

with d_b being the average bubble diameter [374]. In contrast, large bubbles did not maintain a spherical or elliptical form when using the metal ring sparger but were deformed due to the drag on the bubble, causing a reduced superficial gas velocity U_G and thus a higher gas hold-up ε_G . The effect of bubble deformation on the superficial gas velocity and the gas hold-up has been described, among others, by Clift *et al.* [407] and Jamialahmadi *et al.* [408], identifying transitional changes for superficial gas velocities due to bubble deformation at the range of bubble diameters present in the MPLR. While producing microbubbles was clearly advantageous for obtaining a higher OTR, the effect of the bubble size and form especially in the presence of ionic media components and surfactants [409] needs to be investigated for full characterization of the MPLR. The novel feature of the MPLR, the *in situ* LLE in the downcomer, is similarly influenced by described parameters but additionally solvent drops experience the resistance of the aqueous phase in the downcomer, which is enhanced by the velocity of the aqueous phase U_{Ld} . The proportionalities of

$$U_{Ld} \propto U_{Lr} \propto U_{Gr} \propto Q_m \quad (19)$$

(refer to Appendix A.6, Equation 21) emphasize the importance of the aeration rate on both the extraction efficiency and supply of oxygen in both compartments. This implies that the aeration rate needs to be chosen carefully to avoid flooding of solvent drops if the counter-flow of the aqueous phase in the downcomer is too high.

The steeper increase of the DOT_d, which was observed when the aeration rate was enhanced during the second cultivation, results from the larger pressure gradient between riser and downcomer due to an enhanced gas hold-up in the riser [379]. Thus, an increased circulation velocity caused shorter mixing times. The gas hold-up depends on the aeration rate and the reactor geometry, such as the ratio of the cross-sectional areas of riser and downcomer, and fluid properties determined by the media composition in fermentations. A detailed characterization of the mentioned and additional aspects of fluid dynamics in the MPLR will be performed, among others, including the determination of axial dispersion in relation to the bulk movement of the liquid

described Bodenstein number Bo , essentially stating if ideal mixing ($Bo < 0.1$) or a plug flow ($Bo > 20$) is present at given conditions [383, 410]. Moreover, the Sherwood number Sh describing the convective-to-diffusive mass transfer ratio, here applied for extraction, will be determined.

Further, the influence of media components, RLs, and biomass on oxygen transfer and extraction efficiency at different operational parameters needs to be evaluated. Especially the RLs as surfactants are predicted to impact both the oxygen transfer and extraction efficiency as they attach to the surface of the air bubbles and solvent drops, thereby immobilizing the surface and resulting in a reduced mass transfer [352]. Further, due to their ascension, an inhomogeneous distribution of the RLs on the surface create gradients in surface tension (described as the Marangoni effect [411, 412]), in turn inducing a fluid flow from low to high surface tensions, which influences the circulation, shape, trajectory, and velocity of the bubbles and drops [413]. In addition, RL and biomass titers as well as other media components constantly alter during the cultivation of *P. putida* KT2440 SK4, resulting in a highly dynamic system, which might be challenging to describe mathematically in its entirety.

3.5.4.2 The MPLR supports the cultivation of *P. putida* KT2440 SK4 and continuous *in situ* extraction of rhamnolipids

Operating the MPLR, a batch cultivation could be performed, converting the entire supplied glucose. Performance indicators were comparable with those of two-liquid phase STR cultivations (Table 9) described in Chapter 3.1. The lower productivity and the prolonged time needed to convert the provided glucose are due to the non-optimal addition of acid and the lower overall pH value to avoid foaming, which will be the primary subject of optimization. Further, the cells repeatedly encountered low DOT values when circulating through the downcomer. The oscillation could have lowered productivity, similarly as observed for oscillating cultivations described in Chapter 3.4. However, average residence times in the downcomer were estimated to be in the range of lower single-digit seconds, as the velocity of the loop flow was comparably high. The improved phase separation in the MPLR compared to the two-liquid phase STR cultivations can enable continuous cultivations when the formation of an emulsion can be further prevented by modifying the settlement compartment. The continuous solvent removal is highly advantageous compared to two-liquid phase cultivations in STRs, which cannot be operated in continuous mode due to the increased local shear forces induced by the impeller, leading to stronger emulsification [414]. However, the increasing concentration of RLs and a change in media composition during the second cultivation in the MPLR led to a declining efficiency in phase separation toward the end of the cultivation. While media components have crucial effects on coalescence [415], assumably little can be improved by media optimization as RLs are the main driver for hindering coalescence.

In contrast, a redesign of the inserted coalescer in the settlement region, *e.g.*, by replacing or alternating the steel mesh with a plastic structure exhibiting a hydrophobic surface, is promising to enhance coalescence of the organic phase by altered wetting properties and thus phase separation [416]. Further, the coalescence could be improved by removing RLs from the system by coupling a back-extraction as described in Chapter 3.1 to the solvent recirculation. Preliminary results show its feasibility, but it needs to be optimized for application combined with the MPLR.

Table 9 Performance indicators and key characteristics of the cultivation of *P. putida* KT2440 SK4 in different reactor types at current stages of bioprocess and reactor development.

Performance Indicator	Two-liquid phase STR	Multiphase loop reactor
Process time [h]	8.6	12.8
Yield [$\text{g}_{\text{RL}} \text{g}_{\text{GLC}}^{-1}$]	0.12	0.11
Productivity [$\text{g L}^{-1} \text{h}^{-1}$]	0.13	0.08
Phase separation during operation	-	(+)
Potential continuous cultivation	-	(+)

RLs as the product of choice have proven to be challenging due to their strong influence on fluid dynamics, which are crucial for the functionality of the MPLR. To advance the MPLR as a platform technology for a broad range of applications in biotechnology, the suitability of different microorganisms and products needs to be assessed. *In situ* product extraction is advantageous for producing inhibiting compounds [46] or products causing process instabilities, such as foaming during biosurfactant production, as presented here. For a successful transfer to the MPLR, a comprehensive solvent screening needs to be performed, and the organism's ability to endure temporary oxygen limitations needs to be characterized, alike described for *P. putida* KT2440 SK4 and RLs in this thesis, to define an operational window for the cultivation in the MPLR in advance.

3.5.5 Conclusion

A proof of concept for the functionality of the MPLR to simultaneously support the cultivation of microorganisms and the continuous *in situ* extraction of the product was demonstrated. In combination with a distinct bioprocess design, RLs were produced and accumulated in the extractant, ethyl decanoate, avoiding excessive foaming. The cultivation in the MPLR compared well with two-liquid phase cultivations in STRs with the advantage of allowing phase separation and thereby solvent recirculation. In future, next to further optimizations, the application of the MPLR will be expanded to other product-inhibited cultivations.

Chapter 4

General Discussion & Outlook

Contributions

This chapter was written by Philipp Demling and reviewed by Lars M. Blank.

4 General Discussion & Outlook

In this thesis, approaches for a holistic perspective on bioprocess design have been presented at the example of rhamnolipid (RL) production with recombinant *Pseudomonas putida* KT2440. Although many different interdisciplinary aspects have been experimentally and theoretically covered in the previous chapters, further considerations and general aspects of establishing microbial production processes in the industrial landscape are discussed in this chapter.

4.1 Integrated design of holistic bioprocesses

Implementing industrial bioprocesses based on renewable resources is required to transition to a circular bioeconomy [417, 418], eventually contributing to fighting climate change and all its consequences. Although there has been substantial progress in establishing biotechnological processes in industrial settings, many approaches do not excel beyond the level of proof of concept on laboratory scale. While the latter is crucial for exploring and extending the limits of feasibility in biotechnology, transition to an industrial application is challenging due to many reasons. Limitations in scalability and unfavorable economics, lead to non-competitiveness compared to conventional processes. The latter clearly has to be supported by governments, fostering sustainable processes, *e.g.*, by creating incentives to reduce the CO₂-footprint, thereby making process based on renewable carbon resources more favorable. Nevertheless, considerations for a transfer to an industrial application with a strong focus on process integration need to be implemented in early stages of process development.

Bioprocesses need to be designed holistically. There are multiple levels of bioprocess development ranging from molecular pathway and chassis engineering to reaction engineering and, finally, its implementation in an overall process chain. To maximize efficiency and minimize the chance of failure at a certain level due to misaligning prerequisites, all levels have to be integrated [29]. Further, a constantly supervising and coordinating techno-economic assessment (TEA) needs to unveil potential bottlenecks and limitations, thereby identifying required adjustments of the process on a superordinate level (refer to Chapter 1, Figure 1). Detailed elaborations on general interconnections of levels in bioprocess development are given in the Introduction (Chapter 1).

In this thesis, multiple levels of bioprocess design have been pursued to interconnect for gaining a holistic perspective of an exemplary RL production process. Several interactions have been elucidated, and strategies have been developed to achieve integration. An approach for selecting an *in situ* extraction solvent considered the feasibility of an application in an actual fermentation process. Therefore, aspects such as flammability, biocompatibility, phase separation,

and, most prominently, the pH value were considered to define an operational window suiting both extraction and cultivation. However, using strain engineering, the constraints of the operational window imposed by the whole-cell biocatalyst were mitigated by allowing the use of additional extraction solvents (Figure 31). Additionally, approaches for solvent and product recovery were explored, thereby yielding first considerations for integration into an overall process chain. Regarding the multiphase loop reactor (MPLR), heterogeneous conditions in different compartments were mimicked to assess the compatibility with the whole-cell biocatalyst. The findings of the assessment could have resulted in geometrical adaptations of the reactor or further host engineering to either reduce heterogeneities or enhance the robustness of the whole-cell biocatalyst. However, as *P. putida* KT2440 showed sufficient robustness, no adaptation of the reactor or the organism was necessary.

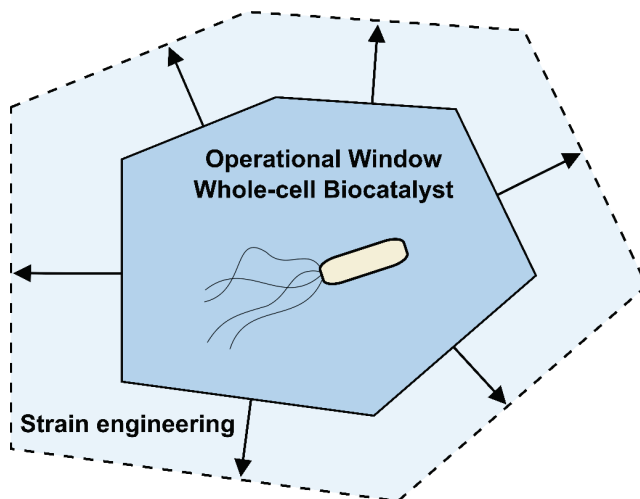


Figure 31 Extending the boundaries of the operational window imposed by the whole-cell biocatalyst *via* strain engineering. In this thesis, the solvent tolerance of *P. putida* KT2440 was enhanced, thereby allowing the use of 1-octanol as an extraction solvent. Other boundaries of the operational window instated by parameters such as pH value and temperature can be shifted within limits *via* strain engineering.

Although several aspects of integrating different stages of bioprocess development have been investigated in this thesis, others were not covered. Pathway and metabolic engineering could be further explored, *e.g.*, to increase the product yield on the consumed carbon or adjusting production rates to extraction rates, thereby fine-tuning the production to the conditions in the MPLR. Further, the advantageousness of integrations has to be critically assessed in a holistic perspective, *e.g.*, by applying techno-economic assessment (TEA) and life-cycle analysis (LCA) on the overall process [61], including the MPLR compared with conventional bioreactors. Although catastrophic phase

inversion (CPI) and back-extraction as methods for solvent and product recovery have been explored, integration and automatization of further continuous downstream processing (DSP) operations are required. Finally, to reach production capacities matching the market demand, a scale-up has to be performed [377]. Considerations for upscaling of microbial bioprocesses are elaborated in the following section.

4.2 Considerations for the scale-up of microbial production processes

Reaching economic viability is essential for microbial bioprocesses to compete with established production based on fossil resources. Therefore, an early TEA is valuable for identifying economic and ecologic advantages in consideration of the market demand, thus requiring production capacities and consequentially scaling the process [26]. In this regard, scaling up microbial production processes bears many challenges [377, 419], potentially hindering efficient production if not identified and solved in early development stages. The primary and recurring challenges during upstream processing (USP) are discussed in the following.

First, the reactions catalyzed by the whole-cell biocatalysts are producing a significant amount of heat [420]. Heat is usually not a substantial issue in small- to laboratory-scale cultivations as efficient cooling systems can be integrated comparably simply, and the amount of cooling water required for cooling is manageable. In fact, most laboratory-scale cultivations require active heating to control the temperature at the set value as the ambient temperature has enough cooling capacity. In contrast, the high number of cells in large-scale cultivations, the increased total power input, and the smaller surface-to-volume ratio of the vessel can cause heating of the cultivation broth to temperatures, which are unfavorable for the whole-cell biocatalyst. Therefore, an efficient cooling system with a high surface area for heat transfer needs to be implemented in large-scale cultivations [421], potentially leading to a decreased economic value of the overall process [422].

Second, inhomogeneities are a known phenomenon in large-scale cultivations. The volumetric power input is smaller in large-scale fermenters than in small-scale fermenters [423]. Due to the resulting limited mixing and mass transfer, distinct non-turbulent zones can develop, exhibiting altered environmental conditions [169, 424], in which, *e.g.*, low amounts of dissolved oxygen and high concentrations of carbon dioxide are present. Particularly in fed-batch cultivations, non-ideal mixing can cause so-called ‘feeding zones’ with high local concentrations of nutrients [329]. Further, with an increasing scale, the hydrostatic pressure influences the solubility of gases supplied at the bottom of the reactor and the size of the sparged air bubbles. In combination with the reduced volumetric power input, the volume-specific surface area of the sparged air bubbles is lower compared to laboratory-scale reactors [169]. These effects can lead to gradients of dissolved gases over the height of the reactor. It is vital in bioprocess development to assess if the whole-

cell biocatalyst can temporarily withstand changing environmental conditions when repeatedly encountering inhomogeneous zones in the reactor [331]. *P. putida* KT2440 can endure temporary oxygen starvation as assessed by scale-down approaches in this thesis. Previous studies elucidated its robust phenotype when encountering carbon starvation [321], emphasizing its suitability for large-scale cultivations.

Third, the overall maximal oxygen transfer rates (OTR_{max}), which can be achieved in large-scale fermenters, are lower than at laboratory scale due to the lower volumetric power input. Therefore, it is essential to assess the required oxygen for efficient processing, especially for highly oxygen-demanding cultivations, and predict if this demand can be met at large scale [425]. Similar to mimicking oxygen oscillations in scale-down cultivations, the OTR can be capped at laboratory scale at the maximal value, which can be achieved in large scale, to predict scalability in early stages of process development.

Regarding the MPLR, which was described in Chapter 3.5, additional considerations for upscaling are required. The geometry of the MPLR, or bubble column and airlift reactors in general, typically have a larger height-to-diameter ratio than stirred-tank reactors (STRs), thus the hydrostatic pressure is higher. This influences aeration, creates stronger gradients of dissolved gases as described above, and can cause high turbulence due to the expansion of the gas bubbles [421]. Besides, the supplied gas needs to be compressed, requiring higher amounts of energy. Due to the enhanced height, the residence time of whole-cell biocatalysts increases at large scale. Thus, the whole-cell biocatalyst needs to be able to cope with longer durations of oxygen starvation. Although *P. putida* KT2440 can endure more extended periods of low oxygen availability as described in Chapter 3.4, the applicability of the MPLR should not be limited only to *P. putida* KT2440 but is envisioned to be established as a platform technology for other pairs of whole-cell biocatalysts and products. Additional measures for transferring oxygen into the cultivation broth in the non-aerated downcomer could be taken, such as attaching aeration membranes on the downcomer-facing side of the cylinder or saturating the extraction solvent with oxygen.

Concluding, to estimate the scalability of the MPLR, the reactor needs to be fully characterized. Dimensional analysis and the definition of dimensional quantities can then be used to mimic large-scale conditions in a scale-down apparatus [27, 419] to assess the feasibility and redefine the operational window for a large-scale MPLR. Subsequently, a functional large-scale MPLR in respective dimensional limits can be designed and implemented in a process chain to enable production in a magnitude suitable for the market.

4.3 Implementation of *in situ* product removal in bioprocesses

The novel feature of the MPLR compared to state-of-the-art airlift reactors is the implemented *in situ* product removal (ISPR) in the form of a counter-current *in situ* liquid-liquid extraction (LLE). ISPR is a promising approach for increasing the efficiency of cultivations in which compounds are produced, which inhibit the growth and production capacity of the whole-cell biocatalyst [69]. Further, a product can cause process instabilities due to its physicochemical properties if accumulating in the cultivation.

Several different methods for ISPR have been applied in bioprocesses. The major criteria for the type and design of the method are the physicochemical properties of the compound, which is targeted for removal. Methods for ISPR in bioprocesses include evaporation, adsorption, liquid-liquid extraction, crystallization, or reactive extraction, *e.g.*, by complexation [46, 69, 70]. In many cases, the mentioned methods are supported by membranes [86], also allowing a size-selective permeation. Besides, the combination of multiple methods for ISPR has been reported to maximize efficiency. However, the applicability of the respective method depends on the product and the technical feasibility of implementation. For biosurfactants, excessive foaming has been utilized as the most prominent method for ISPR by fractionating foam exiting the reactor [41, 122, 123]. Further, foam fractionation has been directly coupled to adsorption to capture and isolate the biosurfactants from other media components and cells present in the foam [117, 123].

Here, an *in situ* LLE has been chosen to recover RLs, thereby preventing excessive foaming. Specific challenges and opportunities of *in situ* LLEs in microbial biotechnology and specifically for RLs produced by recombinant *P. putida* KT2440 are thus described in the following paragraph.

4.3.1 Challenges and opportunities for *in situ* liquid-liquid extractions in biotechnological processes

In situ LLEs have been implemented into fermentation processes previously, allowing the removal of inhibiting or process-hindering products [69]. Different designs, ranging from the simple addition of solvent directly to the fermenter to membrane-supported extractions of products from a cell-free cultivation broth in an external loop [86], have been established in academia. However, little is known about the application of *in situ* LLEs in industrial biotechnology, especially if the cell-enriched cultivation broth is directly contacted by an organic solvent. This is likely due to the formation of crud or interphases, which is regarded as highly problematic in the chemical industry [426]. In microbial bioprocesses, the formation of interphases is greatly enhanced due to the precipitation of proteins in the presence of organic solvents [209] and the attachment of cells to the phase boundary, resulting in loss of product [163]. In particular, protein

precipitation has been identified as the major drawback preventing two-liquid phase cultivations from widely entering industrial processes despite its many benefits [427].

In the presented thesis, *P. putida* KT2440 was used as a whole-cell biocatalyst. Although *P. putida* KT2440 is regarded as solvent-sensitive compared to other strains from the *Pseudomonas* genus, choosing a biocompatible solvent (refer to Chapter 3.1) or engineering its solvent tolerance (refer to Chapter 3.2) can promote its application in two-liquid phase cultivations, particularly due to its robust phenotype regarding large-scale inhomogeneities (refer to Chapter 3.4 and [321]). Its large capacity to produce value-added compounds is due to its metabolic versatility [114, 115, 428], showcased in its use as a whole-cell biocatalyst for various value-added compounds. By applying ISPR, *e.g.*, *via in situ* LLEs [429], this enormous potential can be further exploited if the industrial constraints regarding interphase formation can be abolished. Therefore, further host engineering strategies to reduce the attachment to the organic phase by engineering the hydrophobicity of the cell surface [41] and, if possible, to reduce the amount of secreted proteins and lipids originating from cell lysis, secretion, or outer membrane vesicles [430] need to be explored for tailoring the chassis strain to two-liquid phase cultivations.

In this regard, the *in situ* LLE presented in this thesis was successfully implemented to prevent excessive foaming when producing RLs in different cultivation devices. However, producing a surfactant in a two-liquid phase cultivation is challenging as it highly contributes to emulsification [200], which complicates phase separation. Nevertheless, the MPLR could be operated, and sufficient phase separation was achieved for a major part of the cultivation despite the challenging characteristics of the product. Removal of the RLs from the organic phase, *e.g.*, by implementing an at-line back-extraction in the overall process design, which was shown to be feasible in Chapter 3.1, could alleviate the emulsification caused by the surfactants.

4.4 Concluding remarks and outlook

The presented thesis explores approaches for integrated bioprocessing and advocates the requirement for a holistic view of the entire chain of process development. Strain development needs to be fine-tuned for eventual large-scale production, requiring specialized phenotypes to endure environments in industrial-scale reactors. Simultaneously, process parameters need to be tailored to the whole-cell biocatalyst to ensure optimal conditions for production. Further, bioprocess development does not terminate after upstreaming, but considerations for DSP need to be implemented in early stages of biotechnological approaches. Therefore, mutual understanding and interdisciplinary awareness of biotechnologists, chemical engineers, and economists are essential for establishing biotechnological processes.

Here, interactions have been explored at the exemplary production of RLs with recombinant *P. putida* KT2440. An *in situ* LLE of RLs has been implemented into state-of-the-art cultivations to avoid excessive foaming and to integrate USP and DSP, including the assessment of further product recovery and solvent recycling. To enable functionality, an operational window had to be defined by refining and optimizing cultivation parameters, in turn, influencing the performance of the whole-cell biocatalyst. This demonstrates the crucial interactions of USP and DSP development, especially in the scope of process intensification. Further, different cultivation modes, including batch and fed-batch fermentations, have been assessed to evaluate enhanced production strategies.

However, genuinely integrated bioprocess design is not a one-way road. Therefore, next to designing cultivations and intensifying processes on a macroscopic scale, host strain engineering was approached to enhance the solvent tolerance of *P. putida* KT2440 and thereby enable the utilization of additional extraction solvents. Further, the ability of *P. putida* KT2440 to withstand temporary but repeated oxygen starvation was confirmed, highlighting its outstanding suitability for industrial-scale production processes.

Finally, while defining the operational window by considering all previous findings, the performance of RL producing *P. putida* KT2440 in the novel, custom-designed MPLR was identified to compare well with previously conducted two-liquid phase STR cultivations. This emphasizes the flexibility and robustness of *P. putida* KT2440 and serves as a proof of principle for the novel reactor, which will be developed into a platform cultivation technology for biotechnological processes with whole-cell biocatalyst/product pairs requiring or benefiting from *in situ* LLEs.

Metabolic and bioreaction engineering for an enhanced production, ideally supported by computational approaches, have not been pursued in this thesis but also need to be considered in holistic bioprocess development. Additionally, a continuous and coupled method for subsequent product recovery needs to be implemented. A TEA combined with considerations for scale-up is required to evaluate the economic competitiveness compared to established production processes.

The presented interdisciplinary approaches might initiate further considerations for establishing integrated biotechnological processes in the envisaged circular bioeconomy. While the specific outcomes of this thesis are related to the presented system of producing RLs with recombinant *P. putida* KT2440, basic concepts and proposed solutions can be extrapolated to other challenging cases in bioprocess development. To eventually establish the circular bioeconomy and thus fight climate change, we urgently need to push the limits of biotechnological process development by thinking holistically. The time to act is now ‘to preserve and cherish the pale blue dot, the only home we’ve ever known’ [431].

Appendix

A.1 Appendix for Chapter 2

Table A1.1 Stock solutions for MSM. The concentration of the stock solution in respect to the final concentration in the standard MSM for cultivations in bioreactors is given in brackets.

Name	Concentration
Phosphate buffer stock solution (100x)	
K_2HPO_4	388 g L ⁻¹
$\text{NaH}_2\text{PO}_4 \cdot 2 \text{H}_2\text{O}$	212 g L ⁻¹
Nitrogen source stock solution (100x)	
$(\text{NH}_4)_2\text{SO}_4$	200 g L ⁻¹
Trace element stock solution (100x)	
EDTA	1000 mg L ⁻¹
$\text{MgCl}_2 \cdot 2 \text{H}_2\text{O}$	10 g L ⁻¹
$\text{ZnSO}_4 \cdot 7 \text{H}_2\text{O}$	200 mg L ⁻¹
$\text{CaCl}_2 \cdot 2 \text{H}_2\text{O}$	100 mg L ⁻¹
$\text{FeSO}_4 \cdot 7 \text{H}_2\text{O}$	500 mg L ⁻¹
$\text{Na}_2\text{MoO}_4 \cdot 2 \text{H}_2\text{O}$	20 mg L ⁻¹
$\text{CuSO}_4 \cdot 5 \text{H}_2\text{O}$	20 mg L ⁻¹
$\text{CoCl}_2 \cdot 6 \text{H}_2\text{O}$	40 mg L ⁻¹
$\text{MnCl}_2 \cdot 2 \text{H}_2\text{O}$	100 mg L ⁻¹
Carbon source stock solution	
Glucose monohydrate	550 g L ⁻¹

Table A1.2 Oligonucleotides used in PCRs. Oligonucleotides for diagnostic PCRs and sequencings are omitted.

Name	Direction	Application	Sequence	Combine
PD7	fwd	pBT vector amplification for <i>groEL/groES</i> insertion	AGGAGCATGCGACGTCGG	PD8
PD8	rev	pBT vector amplification for <i>groEL/groES</i> insertion	ACCTCCTACTCGAGGAATTCGGTACCTG	PD7
PD9	fwd	<i>groEL/groES</i> amplification for insertion in pBT	AGGTACCGAATTCCTCGAGTAGGAGGTATC GACAATGAAACTTCGTCC	PD10
PD10	rev	<i>groEL/groES</i> amplification for insertion in pBT	GCCCGACGTCGCATGCTCCTTTACATCATGC CGCCCATG	PD9
PD11	fwd	pBT vector amplification for <i>cspA-II</i> insertion	TCGAGTAGGAGGTATGTCCAATCGCCAACA AG	PD12
PD12	rev	pBT vector amplification for <i>cspA-II</i> insertion	CCCCGACGTCGCATGCTCCTTTACTCCGGAC GAACCTG	PD11
PD13	fwd	<i>cspA-II</i> amplification for insertion in pBT	AGGAGCATGCGACGTCGG	PD14
PD14	rev	<i>cspA-II</i> amplification for insertion in pBT	ACCTCCTACTCGAGGAATTCGGTACCTG	PD13
PD15	fwd	pBNT vector amplification for <i>tigGHI</i> insertion	CGGCCGCGTAGCACTGA	PD16
PD16	rev	pBNT vector amplification for <i>tigGHI</i> insertion	CGCATGCTCCTCTAGACTCGAGG	PD15
PD17	fwd	pBT vector amplification for <i>tigGHI</i> insertion	CGGTATCGAGCGGCCGCC	PD18
PD18	rev	pBT vector amplification for <i>tigGHI</i> insertion	GCAACAAAGCCCGCGTCC	PD17
PD19	fwd	<i>tigGHI</i> amplification for insertion in pBT	CGGGACGGCGCTTGTGTCTCTCCTCGG CGTGCAC	PD20
PD20	rev	<i>tigGHI</i> amplification for insertion in pBT	TGGGCGGCCGCTCGATACCGTGCTAATACT CCCGATTAAAAATTGACGATAATTC	PD19
PD21	fwd	<i>tigGHI</i> amplification for insertion in pBNT	CGAGTCTAGAGGAGCATGCGATGCTGGTGA CCGCCTGT	PD22
PD22	rev	<i>tigGHI</i> amplification for insertion in pBNT	GGTCAGTGCTAGCGCGGCCGTTAGTTTGA CTCACGCTCCAGC	PD21
SK1	fwd	Amplification of promotor of library SPS2.X	AATATGGGTTTGTGGAAGCACCGAACAGG CTTATGTC	SK2
SK2	rev	Amplification of promotor of library SPS2.X	TCACCAGCATTAGAAAACCTCCTTAGCATG	SK1
PD23	fwd	<i>tigGHI</i> amplification for insertion in pBNT + SPS2.X	AGGTTTTCTAATGCTGGTGACCGCCTGT	PD24
PD24	rev	<i>tigGHI</i> amplification for insertion in pBNT + SPS2.X	GTCAGTGCTAGCGCGGCCGCTTAGTTTGA CTCACGCTCCAGC	PD23
PD25	fwd	pBNT backbone amplification for SPS2.X- <i>tigGHI</i> insertion	GCGGCCGCGTAGCACTG	PD26
PD26	rev	pBNT backbone amplification for SPS2.X- <i>tigGHI</i> insertion	GCTTCCAGCAAACCCATATTGACTGCC	PD25
PD27	fwd	Ampl. of promotor of library SPS2.X for ins. in pEMG	CTTTAATTAAGCAAGCTACCGAACAGG CTTATGTC	PD28
PD28	rev	Ampl. of promotor of library SPS2.X for ins. in pEMG	TCACCAGCATTAGAAAACCTCCTTAGCATG	PD27
PD29	fwd	<i>tigGHI</i> amplification for insertion in pEMG	AGGTTTTCTAATGCTGGTGACCGCCTGT	PD30

Name	Direction	Application	Sequence	Combine
PD30	rev	<i>tigGHI</i> amplification for insertion in pEMG	TGAAGTTCCTCTTGCAATTCTTAGTTTTGAC TCACGCTCCAGC	PD29
SK3	fwd	TS ampl. for insertion at various loci	GAATTGCAAGAGGAACCTTCACTAGTCTGGA TTCTCAC	SK4, SK5, SK6
SK4	rev	TS1 amplification for insertion at PP_1738	AGCTTGCTTTTAAATTAAGCAAATGCCAC CGCAGCGG	SK3
SK5	rev	TS1 amplification for insertion at PP_4945	AGCTTGCTTTTAAATTAAGCAGGCAACGC GGTGGATGG	SK3
SK6	rev	TS1 amplification for insertion at PP_3808	AGCTTGCTTTTAAATTAAGCAATCAGGCG GACAGCCG	SK3
PD31	fwd	TS1 ampl. for generating point mutatuion PP_3453 P324R	AGGGATAACAGGGTAATCTGAGAGAGCCTT ACCACCGCGC	PD32
PD32	rev	TS1 ampl. for generating point mutatuion PP_3453 P324R	TTTGTA CTG GACCGCGACTGACGGCGC	PD31
PD33	fwd	TS2 ampl. for generating point mutatuion PP_3453 P324R	AGTCGCCGGTCCAGTACAAAGCGCGGCAAC	PD34
PD34	rev	TS2 ampl. for generating point mutatuion PP_3453 P324R	GAAGCTTGCA TGCCTGCAGGTGTGGGTTTG GCCGCACT	PD33
PD35	fwd	TS1 ampl. for generating point mutatuion PP_3453 P106R	AGGGATAACAGGGTAATCTGCATGAACCGG TCGCGGAACAG	PD36
PD36	rev	TS1 ampl. for generating point mutatuion PP_3454 P106R	CCCTGTGAGCGACGCGTGTCTGGCCC	PD35
PD37	fwd	TS2 ampl. for generating point mutatuion PP_3454 P106R	AGCACGCGTCGCTCACAGGGTTTGTCAC	PD38
PD38	rev	TS2 ampl. for generating point mutatuion PP_3454 P106R	GAAGCTTGCA TGCCTGCAGGTACTGTAGG GCGAGTGTG	PD37
PD39	fwd	TS1 ampl. for generating ΔPP_3453	AGGGATAACAGGGTAATCTGTCGATGCCCT GACCGACATTC	PD40
PD40	rev	TS1 ampl. for generating ΔPP_3453	GAGTGTGATAGCAACCGCGAAGAGACG	PD39
PD41	fwd	TS2 ampl. for generating ΔPP_3453	CGCGGTTGCTATCAGCACTCCCACTCGAC	PD42
PD42	rev	TS2 ampl. for generating ΔPP_3453	GAAGCTTGCA TGCCTGCAAGAGTCGCAGAC CCTGCCAATC	PD41
PD43	fwd	TS1 ampl. for generating ΔPP_3454	AGGGATAACAGGGTAATCTGAAACCCACA GCAGCAGGC	PD44
PD44	rev	TS1 ampl. for generating ΔPP_3454	CGCCCAAGCATCGGCCATGCTCAAGATC	PD43
PD45	fwd	TS2 ampl. for generating ΔPP_3454	GCATGGCCGATGCTTGGGCGTCTGGGTT	PD46
PD46	rev	TS2 ampl. for generating ΔPP_3454	GAAGCTTGCA TGCCTGCAGGTTGCGGTAC ACCCGCTT	PD45
PD47	fwd	TS1 ampl. for generating ΔPP_3453 ΔPP_3454	AGGGATAACAGGGTAATCTGTCGATGCCCT GACCGACATTC	PD48
PD48	rev	TS1 ampl. for generating ΔPP_3453 ΔPP_3454	CGCCCAAGCAAGCAACCGCGAAGAGACG	PD47
PD49	fwd	TS2 ampl. for generating ΔPP_3453 ΔPP_3454	CGCGGTTGCTTGTGGGCGTCTGGGTT	PD50
PD50	rev	TS2 ampl. for generating ΔPP_3453 ΔPP_3454	GAAGCTTGCA TGCCTGCAGGTTGCGGTAC ACCCGCTT	PD49

Empirical equation for the prediction of the OTR_{max} in MTPs dependent on the geometry of wells $Peri$, the shaking frequency n , and the filling volume V_L according to Lattermann *et al.* [150]:

$$OTR_{max} = 2.5 \cdot 10^{-7} \cdot Peri \cdot n^{2.37} \cdot V_L^{-0.64} + 3.3 \cdot 10^{-4} \quad (20)$$

$Peri$ denotes the ratio of the perimeter of a well with a specific geometry to the perimeter of a round well. As the used MTPs are round-well plates, $Peri$ equals 1. Further, the equation is only valid for a shaking diameter of 3 mm, which agrees with the shaking diameter of the BioLector.

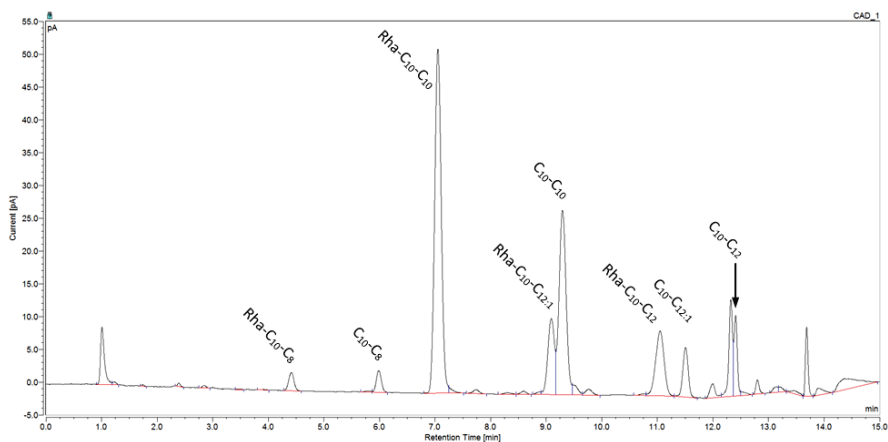


Figure A1.1 Representative HPLC-CAD chromatogram for the separation and quantification of rhamnolipid congeners. Peaks of all eight identified congeners are annotated. This figure was previously published [125] and is reprinted with permission from Green Chemistry. Copyright The Royal Society of Chemistry 2020.

A.2 Appendix for Chapter 3.1

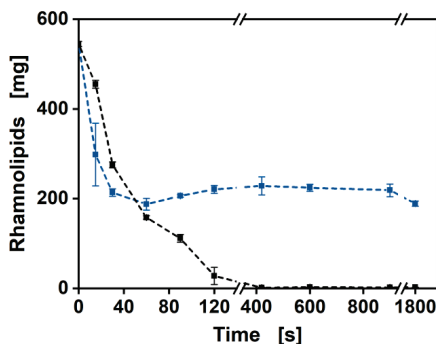


Figure A2.1 Time-resolved depletion of rhamnolipids in the aqueous phases. Extractions were performed with ethyl decanoate (blue squares) and 1-decanol (black squares). Error bars represent standard deviations from the mean of measurements from three independent experiments. This figure was previously published [125] and is reprinted with permission from Green Chemistry. Copyright The Royal Society of Chemistry 2020.

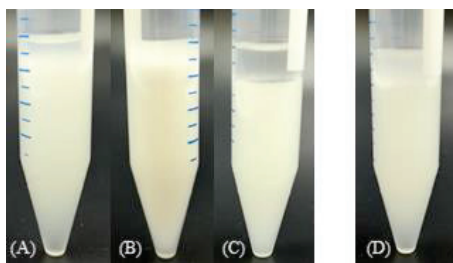


Figure A2.2 Selected solvents after shaking for 4 h before centrifugation. Alkenes (A - 1-octene, B - 1-decene, C - 1-dodecene) and ethyl decanoate (D). This figure was previously published [125] and is reprinted with permission from Green Chemistry. Copyright The Royal Society of Chemistry 2020.

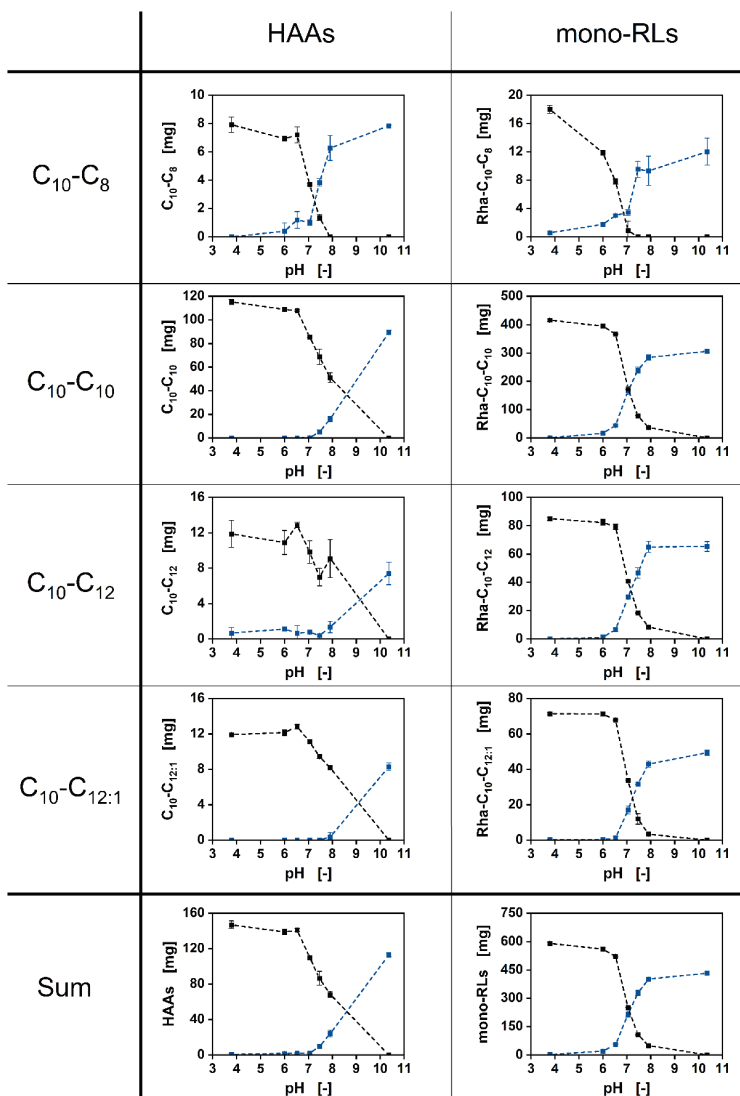


Figure A2.3 pH-dependency of rhamnolipid extraction with ethyl decanoate resolved for measured congeners. Rhamnolipid congeners in the coherent ethyl decanoate phase (black) and the aqueous phase (blue) at different pH values. Columns differentiate between HAAs and mono-rhamnolipids (mono-RLs) and lines differentiate between chain length and saturation of the fatty acid groups. Composite masses of all HAAs and all mono-RLs are given in the bottom line. An overall composite, including both HAAs and mono-RLs, is presented in the main article (refer to Figure 6). Error bars represent standard deviations from the mean of measurements from three independent experiments. This figure was previously published [125] and is reprinted with permission from Green Chemistry. Copyright The Royal Society of Chemistry 2020.

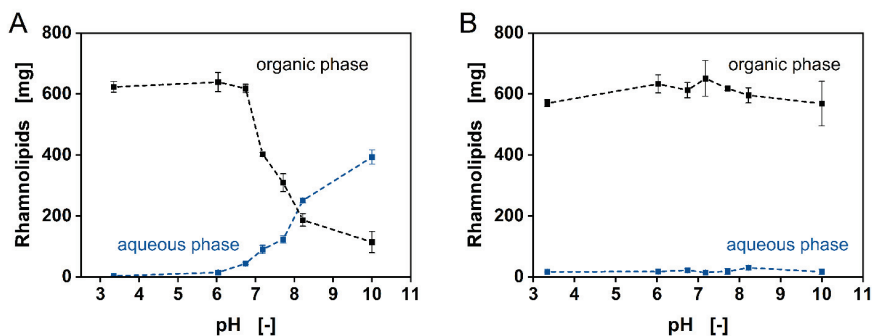


Figure A2.4 Extractions of rhamnolipids at varying pH values. Rhamnolipids in coherent organic (black) and aqueous (blue) phases at different pH values are presented. (A) Methyl decanoate, (B) 1-decanol. Error bars represent standard deviations from the mean of measurements from three independent experiments. Data associated to this figure were partially taken from Carolin Grütering's Master Thesis [211]. This figure was previously published [125] and is reprinted with permission from Green Chemistry. Copyright The Royal Society of Chemistry 2020.

n.a. - not available or only for analytical application available		Solvent properties (20 °C, 113 bar)										Flashpoint			Price			Health Score	
Solvent name (IUPAC)	CAS	Suitable Solvent?	Density [g/L]	source	Solubility [g/L]	source	Boiling point [°C]	source	log K _{ow} -value	source	Flashpoint [°C]	source	[€/100ml]	date	source	[€]	source	[1]	source
			880		0.3		100		4				100						
			920		0.3		80		3.5				120						
ethyl decanoate	110-38-3	unrestricted	862	a)	1.59E-02	b)	241.5	b)	4.29	a)	104	a)	23.00	d)	24.05.2020	1			
ethyl (Z)-octadec-9-enoate	115-62-6	unrestricted	870	a)	5.79E-07	a)	217	a)	8.53	b)	>103	b)	47.67	d)	24.05.2020	1			
ethyl dodecanoate	110-49-9	unrestricted	873	b)	4.40E-03	b)	224	b)	4.41	b)	107	b)	55.96	d)	24.05.2020	1			
diethyl ether	629-82-3	unrestricted	820	b)	1.00E-01	c)	300	b)	5.7	d)	109	d)	83.64	d)	24.05.2020	1			
1-methyl-4-prop-1-en-2-ylcyclohexene	138-86-3	unrestricted	841	b)	1.38E-02	b)	176	b)	4.57	b)	43	b)	5.12	d)	24.05.2020	2			
dec-1-ene	872-05-9	unrestricted	741	b)	1.15E-04	b)	170.6	b)	5.7	b)	44	b)	20.60	d)	24.05.2020	2			
dec-1-ol	112-30-1	unrestricted	830	b)	3.70E-02	b)	230	b)	4.57	b)	108	b)	21.40	d)	24.05.2020	2			
adipic-1-ene	12-24-4	unrestricted	758	b)	1.00E+00	b)	212.8	b)	6.1	b)	77	b)	24.10	d)	24.05.2020	2			
undec-1-ene	112-41-4	unrestricted	768	b)	1.00E+00	b)	218.8	b)	6.1	b)	77	b)	24.10	d)	24.05.2020	2			
undec-1-ol	112-42-1	unrestricted	769	b)	1.00E+00	b)	219.8	b)	6.1	b)	77	b)	24.10	d)	24.05.2020	2			
undec-2-ene	115-66-0	unrestricted	715	b)	4.10E-03	b)	121.2	b)	4.57	b)	8	b)	29.10	d)	24.05.2020	2			
undec-2-ol	114-65-9	unrestricted	699	b)	6.00E-04	b)	126	b)	5.18	b)	13	b)	35.20	d)	24.05.2020	2			
undec-3-ene	124-18-5	unrestricted	730	b)	5.20E-05	b)	174.1	b)	5.01	b)	51	b)	37.20	d)	24.05.2020	2			
undec-3-ol	112-12-9	unrestricted	826	b)	2.00E-02	b)	231.5	b)	4.09	b)	96	b)	38.00	d)	24.05.2020	2			
undec-4-ene	118-84-2	unrestricted	718	b)	2.20E-04	b)	130.5	b)	5.65	b)	31	b)	43.40	d)	24.05.2020	2			
undec-4-ol	544-76-3	unrestricted	770	b)	9.00E-07	b)	287.2	b)	8.2	b)	135	b)	54.50	d)	24.05.2020	2			
undec-5-ene	120-21-4	unrestricted	740	b)	4.40E-06	b)	195.5	b)	5.74	b)	56	b)	55.90	d)	24.05.2020	2			
undec-5-ol	120-22-1	unrestricted	741	b)	4.40E-06	b)	196.5	b)	5.74	b)	56	b)	55.90	d)	24.05.2020	2			
undec-6-ene	108-51-8	unrestricted	860	b)	1.18E-02	b)	183.3	b)	4.38	b)	58	b)	76.00	d)	24.05.2020	2			
methyl nonanoate	1231-84-6	restricted	900	a)	2.29E-02	b)	213.5	b)	4.32	b)	87	b)	4.95	d)	24.05.2020	1			
octyl acetate	112-14-1	restricted	868	a)	4.60E-02	a)	210	b)	3.81	a)	83	b)	31.25	d)	24.05.2020	1			
(Z)-octadec-9-enoic acid	112-80-1	restricted	895	b)	1.15E-05	b)	288	b)	7.64	b)	189	b)	4.56	d)	24.05.2020	1			
1,2,4-trimethylbenzene	95-63-6	restricted	876	b)	5.70E-02	b)	168.9	b)	3.78	b)	50	b)	19.90	d)	24.05.2020	2			
2-phenylpropane	98-82-8	restricted	862	b)	6.13E-02	b)	152.4	b)	3.66	b)	31	b)	20.90	d)	24.05.2020	2			
nonan-1-ol	143-06-8	restricted	827	b)	1.40E-01	b)	213.3	b)	3.77	b)	98.5	b)	23.40	d)	24.05.2020	2			
propylbenzene	123-12-7	restricted	900	a)	2.75E-02	b)	159	b)	4.15	b)	38	a)	56.10	d)	24.05.2020	2			
2,2,4-trimethylpentane	629-06-1	restricted	692	a)	9.91E-03	a)	99.2	b)	4.96	a)	-9	b)	60.20	d)	24.05.2020	2			
heptane	142-82-5	restricted	680	b)	3.40E-03	b)	98.4	b)	4.46	b)	-7	b)	63.00	d)	24.05.2020	2			
(1Z,2Z)-cycloocta-1,5-diene	111-78-4	restricted	882	b)	0.00E+00	b)	150.8	b)	3.67	a)	31	b)	70.50	d)	24.05.2020	2			
methylcyclohexane	108-87-2	restricted	770	b)	1.40E-02	b)	100.9	b)	3.61	b)	-4	b)	79.60	d)	24.05.2020	2			
2-ethylhexyl 2-methylprop-2-enoate	688-84-6	restricted	880	b)	5.92E-03	a)	110	b)	4.54	b)	92	b)	106.80	d)	24.05.2020	2			
2-ethyl-1-methylcyclohexyl benzene-1,2-dicarboxylate	8651-548-0	not suitable	990	a)	2.32E-08	a)	405	a)	9.77	a)	216.3	a)	4.14	d)	24.05.2020	1			
2-ethyl-1-methylcyclohexyl benzene-1,4-dicarboxylate	945-88-2	not suitable	990	a)	2.32E-08	a)	405	a)	9.55	a)	216.3	a)	4.14	d)	24.05.2020	1			
2-ethyl-1-methylcyclohexyl benzene-1,3-dicarboxylate	945-89-1	not suitable	990	a)	2.32E-08	a)	405	a)	9.55	a)	216.3	a)	4.14	d)	24.05.2020	1			
2-ethyl-1-methylcyclohexyl benzene-1,2,4-tricarboxylate	1003-14-1	not suitable	1000	a)	1.83E-02	a)	269	a)	1.83	a)	113	a)	8.30	d)	24.05.2020	1			
2-ethyl-1-methylcyclohexyl benzene-1,2,4,5-tetracarboxylate	104-85-5	not suitable	1000	a)	1.83E-02	a)	269	a)	4.21	a)	130	a)	10.92	d)	24.05.2020	1			
Bulky benzate	136-60-7	not suitable	1010	a)	2.95E-02	a)	249	b)	3.79	a)	106	b)	12.00	d)	24.05.2020	1			
1-methylnaphthalene	90-12-0	not suitable	1020	b)	0.0258	b)	244	b)	3.87	b)	82	b)	17.04	d)	24.05.2020	1			
diethyl benzene-1,2-dicarboxylate	84-66-2	not suitable	1120	a)	n.a.	a)	289	b)	2.7	a)	156	b)	18.90	d)	24.05.2020	1			
Ethyl benzate	93-89-0	not suitable	1050	a)	0.0215	a)	212	c)	2.73	a)	93	b)	18.90	d)	24.05.2020	1			
2-ethyl-1-methylcyclohexyl hexanedioate	9389-0	not suitable	922	b)	7.80E-04	b)	417	b)	8.12	a)	196	b)	19.90	d)	24.05.2020	1			
Propyl benzate	123-15-6	not suitable	1000	a)	1.76E-01	a)	231	b)	3.26	b)	100	b)	20.52	d)	24.05.2020	1			
2-ethyl-1-methylcyclohexyl benzene-1,2,4-tricarboxylate	104-85-5	not suitable	1000	a)	1.83E-02	a)	269	a)	4.21	a)	130	a)	10.92	d)	24.05.2020	1			
2-ethyl-1-methylcyclohexyl benzene-1,2,4,5-tetracarboxylate	104-85-5	not suitable	1000	a)	1.83E-02	a)	269	a)	4.21	a)	130	a)	10.92	d)	24.05.2020	1			
2-ethyl-1-methylcyclohexyl benzene-1,2,4,5-tetracarboxylate	104-85-5	not suitable	1000	a)	1.83E-02	a)	269	a)	4.21	a)	130	a)	10.92	d)	24.05.2020	1			
2-ethyl-1-methylcyclohexyl benzene-1,2,4,5-tetracarboxylate	104-85-5	not suitable	1000	a)	1.83E-02	a)	269	a)	4.21	a)	130	a)	10.92	d)	24.05.2020	1			
2-ethyl-1-methylcyclohexyl benzene-1,2,4,5-tetracarboxylate	104-85-5	not suitable	1000	a)	1.83E-02	a)	269	a)	4.21	a)	130	a)	10.92	d)	24.05.2020	1			
2-ethyl-1-methylcyclohexyl benzene-1,2,4,5-tetracarboxylate	104-85-5	not suitable	1000	a)	1.83E-02	a)	269	a)	4.21	a)	130	a)	10.92	d)	24.05.2020	1			
2-ethyl-1-methylcyclohexyl benzene-1,2,4,5-tetracarboxylate	104-85-5	not suitable	1000	a)	1.83E-02	a)	269	a)	4.21	a)	130	a)	10.92	d)	24.05.2020	1			
2-ethyl-1-methylcyclohexyl benzene-1,2,4,5-tetracarboxylate	104-85-5	not suitable	1000	a)	1.83E-02	a)	269	a)	4.21	a)	130	a)	10.92	d)	24.05.2020	1			
2-ethyl-1-methylcyclohexyl benzene-1,2,4,5-tetracarboxylate	104-85-5	not suitable	1000	a)	1.83E-02	a)	269	a)	4.21	a)	130	a)	10.92	d)	24.05.2020	1			
2-ethyl-1-methylcyclohexyl benzene-1,2,4,5-tetracarboxylate	104-85-5	not suitable	1000	a)	1.83E-02	a)	269	a)	4.21	a)	130	a)	10.92	d)	24.05.2020	1			
2-ethyl-1-methylcyclohexyl benzene-1,2,4,5-tetracarboxylate	104-85-5	not suitable	1000	a)	1.83E-02	a)	269	a)	4.21	a)	130	a)	10.92	d)	24.05.2020	1			
2-ethyl-1-methylcyclohexyl benzene-1,2,4,5-tetracarboxylate	104-85-5	not suitable	1000	a)	1.83E-02	a)	269	a)	4.21	a)	130	a)	10.92	d)	24.05.2020	1			
2-ethyl-1-methylcyclohexyl benzene-1,2,4,5-tetracarboxylate	104-85-5	not suitable	1000	a)	1.83E-02	a)	269	a)	4.21	a)	130	a)	10.92	d)	24.05.2020	1			
2-ethyl-1-methylcyclohexyl benzene-1,2,4,5-tetracarboxylate	104-85-5	not suitable	1000	a)	1.83E-02	a)	269	a)	4.21	a)	130	a)	10.92	d)	24.05.2020	1			
2-ethyl-1-methylcyclohexyl benzene-1,2,4,5-tetracarboxylate	104-85-5	not suitable	1000	a)	1.83E-02	a)	269	a)	4.21	a)	130	a)	10.92	d)	24.05.2020	1			
2-ethyl-1-methylcyclohexyl benzene-1,2,4,5-tetracarboxylate	104-85-5	not suitable	1000	a)	1.83E-02	a)	269	a)	4.21	a)	130	a)	10.92	d)	24.05.2020	1			
2-ethyl-1-methylcyclohexyl benzene-1,2,4,5-tetracarboxylate	104-85-5	not suitable	1000	a)	1.83E-02	a)	269	a)	4.21	a)	130	a)	10.92	d)	24.05.2020	1			
2-ethyl-1-methylcyclohexyl benzene-1,2,4,5-tetracarboxylate	104-85-5	not suitable	1000	a)	1.83E-02	a)	269	a)	4.21	a)	130	a)	10.92	d)	24.05.2020	1			
2-ethyl-1-methylcyclohexyl benzene-1,2,4,5-tetracarboxylate	104-85-5	not suitable	1000	a)	1.83E-02	a)	269	a)	4.21	a)	130	a)	10.92	d)	24.05.2020	1			
2-ethyl-1-methylcyclohexyl benzene-1,2,4,5-tetracarboxylate	104-85-5	not suitable	1000	a)	1.83E-02	a)	269	a)	4.21	a)	130	a)	10.92	d)	24.05.2020	1			
2-ethyl-1-methylcyclohexyl benzene-1,2,4,5-tetracarboxylate	104-85-5	not suitable	1000	a)	1.83E-02	a)	269	a)	4.21	a)	130	a)	10.92	d)	24.05.2020	1			
2-ethyl-1-methylcyclohexyl benzene-1,2,4,5-tetracarboxylate	104-85-5	not suitable	1000	a)	1.83E-02	a)	269	a)	4.21	a)	130	a)	10.92	d)	24.05.2020	1			
2-ethyl-1-methylcyclohexyl benzene-1,2,4,5-tetracarboxylate	104-85-5	not suitable	1000	a)	1.83E-02	a)	269	a)	4.21	a)	130	a)	10.92	d)	24.05.2020	1			
2-ethyl-1-methylcyclohexyl benzene-1,2,4,5-tetracarboxylate	104-85-5	not suitable	1000	a)	1.83E-02	a)	269	a)	4.21	a)	130	a)	10.92	d)	24.05.2020	1			
2-ethyl-1-methylcyclohexyl benzene-1,2,4,5-tetracarboxylate	104-85-5	not suitable	1000	a)	1.83E-02	a)	269	a)	4.21	a)	130	a)	10.92	d)	24.05.2020	1			
2-ethyl-1-methylcyclohexyl benzene-1,2,4,5-tetracarboxylate	104-85-5	not suitable	1000	a)	1.83E-02	a)	269	a)	4.21	a)	130	a)	10.92	d)	24.05.2020	1			
2-ethyl-1-methylcyclohexyl benzene-1,2,4,5-tetracarboxylate	104-85-5	not suitable	1000	a)	1.83E-02	a)	269	a)	4.21	a)	130	a)	10.92	d)	24.05.2020	1			
2-ethyl-1-methylcyclohexyl benzene-1,2,4,5-tetracarboxylate	104-85-5	not suitable	1000	a)	1.83E-02	a)	269	a)	4.21	a)	130	a)	10.92	d)	24.05.2020	1			
2-ethyl-1-methylcyclohexyl benzene-1,2,4,5-tetracarbox																			

[illegible]

[illegible]

Solvent name (IUPAC)										CAS	Suitable Solvent?	Density [g/L]	Solubility [g/L]		Boiling point [°C]		log K _{ow} -value []		Flashpoint [°C]		Price [€/100ml]		Health Score [] source																																																																																																																																																																																																																																																																																																																																																																																																																																																																																																																																																																																																																																																																																																																																																																																																																													
												source	g/L	source	°C	source	g/L	source	°C	source	g/L	source	date [DD.MM.YYYY]	source	date [DD.MM.YYYY]	source																																																																																																																																																																																																																																																																																																																																																																																																																																																																																																																																																																																																																																																																																																																																																																																																																										
												900	0.3	80	3.5	4	100	120	216.61	24.05.2020	4	24.05.2020	5	24.05.2020	5	24.05.2020	5	24.05.2020	5	24.05.2020	5	24.05.2020	5	24.05.2020	5	24.05.2020	5	24.05.2020	5	24.05.2020	5	24.05.2020	5	24.05.2020	5	24.05.2020	5	24.05.2020	5	24.05.2020	5	24.05.2020	5	24.05.2020	5	24.05.2020	5	24.05.2020	5	24.05.2020	5	24.05.2020	5	24.05.2020	5	24.05.2020	5	24.05.2020	5	24.05.2020	5	24.05.2020	5	24.05.2020	5	24.05.2020	5	24.05.2020	5	24.05.2020	5	24.05.2020	5	24.05.2020	5	24.05.2020	5	24.05.2020	5	24.05.2020	5	24.05.2020	5	24.05.2020	5	24.05.2020	5	24.05.2020	5	24.05.2020	5	24.05.2020	5	24.05.2020	5	24.05.2020	5	24.05.2020	5	24.05.2020	5	24.05.2020	5	24.05.2020	5	24.05.2020	5	24.05.2020	5	24.05.2020	5	24.05.2020	5	24.05.2020	5	24.05.2020	5	24.05.2020	5	24.05.2020	5	24.05.2020	5	24.05.2020	5	24.05.2020	5	24.05.2020	5	24.05.2020	5	24.05.2020	5	24.05.2020	5	24.05.2020	5	24.05.2020	5	24.05.2020	5	24.05.2020	5	24.05.2020	5	24.05.2020	5	24.05.2020	5	24.05.2020	5	24.05.2020	5	24.05.2020	5	24.05.2020	5	24.05.2020	5	24.05.2020	5	24.05.2020	5	24.05.2020	5	24.05.2020	5	24.05.2020	5	24.05.2020	5	24.05.2020	5	24.05.2020	5	24.05.2020	5	24.05.2020	5	24.05.2020	5	24.05.2020	5	24.05.2020	5	24.05.2020	5	24.05.2020	5	24.05.2020	5	24.05.2020	5	24.05.2020	5	24.05.2020	5	24.05.2020	5	24.05.2020	5	24.05.2020	5	24.05.2020	5	24.05.2020	5	24.05.2020	5	24.05.2020	5	24.05.2020	5	24.05.2020	5	24.05.2020	5	24.05.2020	5	24.05.2020	5	24.05.2020	5	24.05.2020	5	24.05.2020	5	24.05.2020	5	24.05.2020	5	24.05.2020	5	24.05.2020	5	24.05.2020	5	24.05.2020	5	24.05.2020	5	24.05.2020	5	24.05.2020	5	24.05.2020	5	24.05.2020	5	24.05.2020	5	24.05.2020	5	24.05.2020	5	24.05.2020	5	24.05.2020	5	24.05.2020	5	24.05.2020	5	24.05.2020	5	24.05.2020	5	24.05.2020	5	24.05.2020	5	24.05.2020	5	24.05.2020	5	24.05.2020	5	24.05.2020	5	24.05.2020	5	24.05.2020	5	24.05.2020	5	24.05.2020	5	24.05.2020	5	24.05.2020	5	24.05.2020	5	24.05.2020	5	24.05.2020	5	24.05.2020	5	24.05.2020	5	24.05.2020	5	24.05.2020	5	24.05.2020	5	24.05.2020	5	24.05.2020	5	24.05.2020	5	24.05.2020	5	24.05.2020	5	24.05.2020	5	24.05.2020	5	24.05.2020	5	24.05.2020	5	24.05.2020	5	24.05.2020	5	24.05.2020	5	24.05.2020	5	24.05.2020	5	24.05.2020	5	24.05.2020	5	24.05.2020	5	24.05.2020	5	24.05.2020	5	24.05.2020	5	24.05.2020	5	24.05.2020	5	24.05.2020	5	24.05.2020	5	24.05.2020	5	24.05.2020	5	24.05.2020	5	24.05.2020	5	24.05.2020	5	24.05.2020	5	24.05.2020	5	24.05.2020	5	24.05.2020	5	24.05.2020	5	24.05.2020	5	24.05.2020	5	24.05.2020	5	24.05.2020	5	24.05.2020	5	24.05.2020	5	24.05.2020	5	24.05.2020	5	24.05.2020	5	24.05.2020	5	24.05.2020	5	24.05.2020	5	24.05.2020	5	24.05.2020	5	24.05.2020	5	24.05.2020	5	24.05.2020	5	24.05.2020	5	24.05.2020	5	24.05.2020	5	24.05.2020	5	24.05.2020	5	24.05.2020	5	24.05.2020	5	24.05.2020	5	24.05.2020	5	24.05.2020	5	24.05.2020	5	24.05.2020	5	24.05.2020	5	24.05.2020	5	24.05.2020	5	24.05.2020	5	24.05.2020	5	24.05.2020	5	24.05.2020	5	24.05.2020	5	24.05.2020	5	24.05.2020	5	24.05.2020	5	24.05.2020	5	24.05.2020	5	24.05.2020	5	24.05.2020	5	24.05.2020	5	24.05.2020	5	24.05.2020	5	24.05.2020	5	24.05.2020	5	24.05.2020	5	24.05.2020	5	24.05.2020	5	24.05.2020	5	24.05.2020	5	24.05.2020	5	24.05.2020	5	24.05.2020	5	24.05.2020	5	24.05.2020	5	24.05.2020	5	24.05.2020	5	24.05.2020	5	24.05.2020	5	24.05.2020	5	24.05.2020	5	24.05.2020	5	24.05.2020	5	24.05.2020	5	24.05.2020	5	24.05.2020	5	24.05.2020	5	24.05.2020	5	24.05.2020	5	24.05.2020	5	24.05.2020	5	24.05.2020	5	24.05.2020	5	24.05.2020	5	24.05.2020	5	24.05.2020	5	24.05.2020	5	24.05.2020	5	24.05.2020	5	24.05.2020	5	24.05.2020	5	24.05.2020	5	24.05.2020	5	24.05.2020	5	24.05.2020	5	24.05.2020	5	24.05.2020	5	24.05.2020	5	24.05.2020	5	24.05.2020	5	24.05.2020	5	24.05.2020	5	24.05.2020	5	24.05.2020	5	24.05.2020	5	24.05.2020	5	24.05.2020	5	24.05.2020	5	24.05.2020	5	24.05.2020	5	24.05.2020	5	24.05.2020	5	24.05.2020	5	24.05.2020	5	24.05.2020	5	24.05.2020	5	24.05.2020	5	24.05.2020	5	24.05.2020	5	24.05.2020	5	24.05.2020	5	24.05.2020	5	24.05.2020	5	24.05.2020	5	24.05.2020	5	24.05.2020	5	24.05.2020	5	24.05.2020	5	24.05.2020	5	24.05.2020	5	24.05.2020	5	24.05.2020	5	24.05.2020	5	24.05.2020	5	24.05.2020	5	24.05.2020	5	24.05.2020	5	24.05.2020	5	24.05.2020	5	24.05.2020	5	24.05.2020	5	24.05.2020	5	24.05.2020	5	24.05.2020	5	24.05.2020	5	24.05.2020	5	24.05.2020	5	24.05.2020	5	24.05.2020	5	24.05.2020	5	24.05.2020	5	24.05.2020	5	24.05.2020	5	24.05.2020	5	24.05.2020	5	24.05.2020	5	24.05.2020	5	24.05.2020	5	24.05.2020	5	24.05.2020	5	24.05.2020	5	24.05.2020	5	24.05.2020	5	24.05.2020	5	24.05.2020	5	24.05.2020	5	24.05.2020	5	24.05.2020	5	24.05.2020	5	24.05.2020	5	24.05.2020	5	24.05.2020	5	24.05.2020	5	24.05.2020	5	24.05.2020	5	24.05.2020	5	24.05.2020	5	24.05.2020	5	24.05.2020	5	24.05.2020	5	24.05.2020	5	24.05.2020	5	24.05.2020	5	24.05.2020	5	24.05.2020	5	24.05.2020	5	24.05.2020	5	24.05.2020	5	24.05.2020	5	24.05.2020	5	24.05.2020	5	24.05.2020	5	24.05.2020	5	24.05.2020	5	24.05.2020	5	24.05.2020	5	24.05.2020	5	24.05.2020	5	24.05.2020	5	24.05.2020	5	24.05.2020	5	24.05.2020	5	24.05.2020	5	24.05.2020	5	24.05.2020	5	24.05.2020	5	24.05.2020	5	24.05.2020	5	24.05.2020	5	24.05.2020	5	24.05.2020	5	24.05.2020	5	24.05.2020	5	24.05.2020	5	24.05.2020	5	24.05.2020	5	24.05.2020	5	24.05.2020	5	24.05.2020	5	24.05.2020	5	24.05.2020	5	24.05.2020	5	24.05.2020	5	24.05.2020

Figure A2.5 List of physicochemical properties of solvent candidates. Applied threshold values are chosen according to Table 2. The interactive list with optional adjustment of threshold values is publicly available at <https://git.rwth-aachen.de/campenhausem/list-of-solvents>. White category - suitable, yellow category - restricted, red category - not suitable, a) www.chemspider.com, b) www.pubchem.com, c) pubchem.ncbi.nlm.nih.gov, e) www.vwr.com, f) Deutsche Gesetzliche Unfallversicherung e.V., Berlin, Germany, g) Merck KGaA, Darmstadt, Germany, h) Carl Roth GmbH + Co. KG, Karlsruhe, Germany, i) <https://echa.europa.eu/information-on-chemicals>. This figure was previously published [125] and is reprinted in an adapted form with permission from Green Chemistry. Copyright The Royal Society of Chemistry 2020.

A.3 Appendix for Chapter 3.2

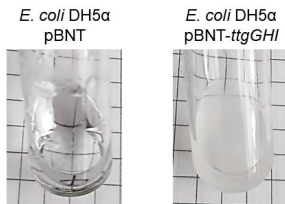


Figure A3.1 Cultivation of *E. coli* DH5 α pBNT (left) and *E. coli* DH5 α pBNT-*ttgGHI* in the presence of 50% (v/v) *n*-hexane. MSM was supplemented with 10 g L⁻¹ glucose. The pictures were taken after 24 h of incubation at 30 °C and 200 rpm.

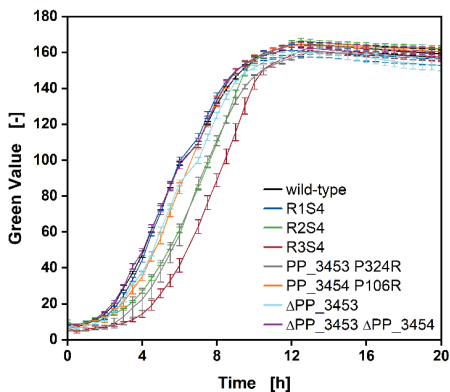


Figure A3.1 Growth of adapted and constructed *P. putida* KT2440 strains in absence of 1-octanol. MSM was supplied with 10 g L⁻¹ glucose. Data for the single-deletion strain *P. putida* KT2440 Δ PP_3454 was not recorded. Data associated to this figure were taken from Greta Kleinert's Bachelor Thesis [271].

A.4 Appendix for Chapter 3.3

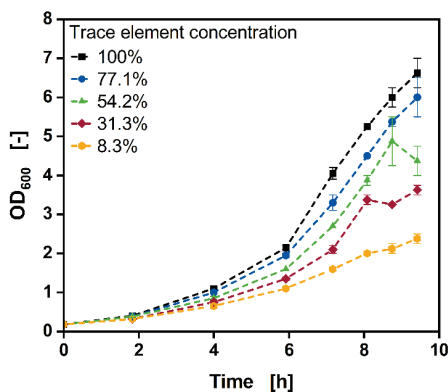


Figure A4.1 Growth of *P. putida* KT2440 at differing supplied trace element concentrations. The trace element concentrations are given as percent of the original MSM. 100% - black squares, 77.1% - blue dots, 54.2% - green triangles, 31.3% - red diamonds, 8.3% - yellow hexagons. The error bars represent minimal and maximal values of two independent experiments. Data associated to this figure are taken from Carolin Grütering's Master Thesis [211].

A.5 Appendix for Chapter 3.4

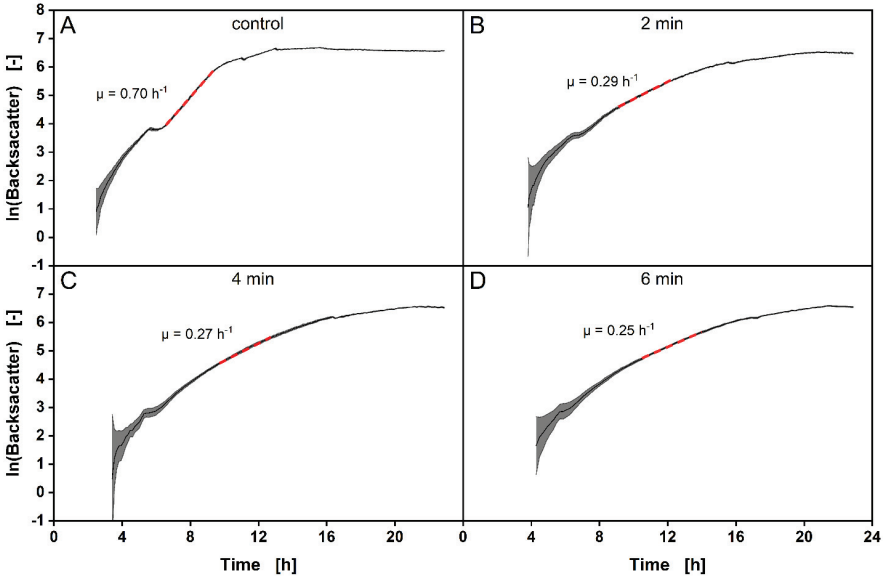


Figure A5.1 Logarithmic backscatter signal over time of cultivations of *P. putida* KT2440 in microtiter plates at different intervals of oscillating agitation. (A) control, (B) 2 min oscillation, (C) 4 min oscillation, (D) 6 min oscillation. The red dashed lines indicate regions used for the determination of the growth rate. Shaded areas represent the standard deviation of measurements from five independent experiments.

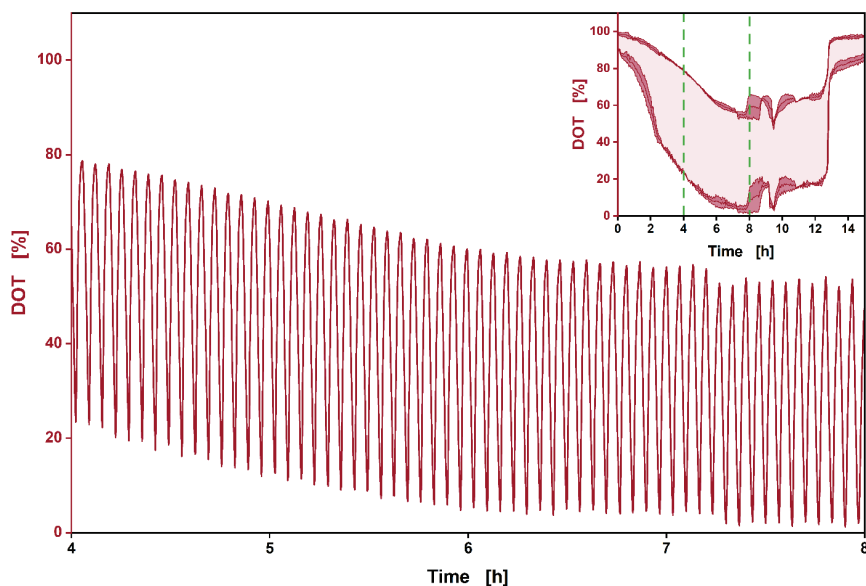


Figure A5.3 Close view of the DOT signal of an STR cultivation of *P. putida* KT2440 subjected to an oscillating agitation and aeration at an interval of 2 min. The depicted section of the cultivation ranges from 4 h to 8 h as illustrated by the green dashed lines in the graph of the entire cultivation in the top right corner. Only one replicate is shown for clarity.

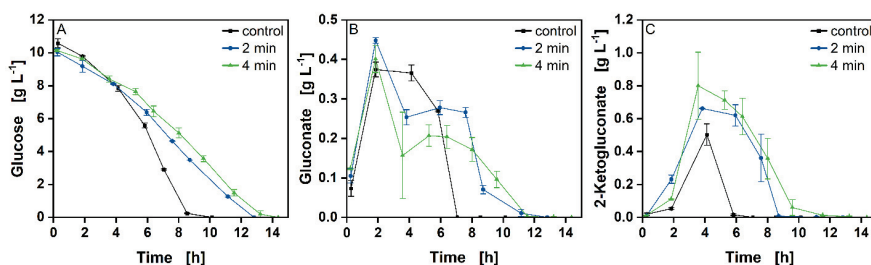


Figure A5.2 Extracellular metabolites measured during cultivations of *P. putida* KT2440 at different intervals of oscillating aeration and agitation. (A) glucose, (B) gluconate, and (C) 2-ketogluconate concentrations for the control cultivations (black squares), 2 min intervals of oscillation (blue circles), and 4 min intervals of oscillation over the duration of the cultivation. Error bars represent errors derived from two independent experiments. Note the different scales of the y-axes.

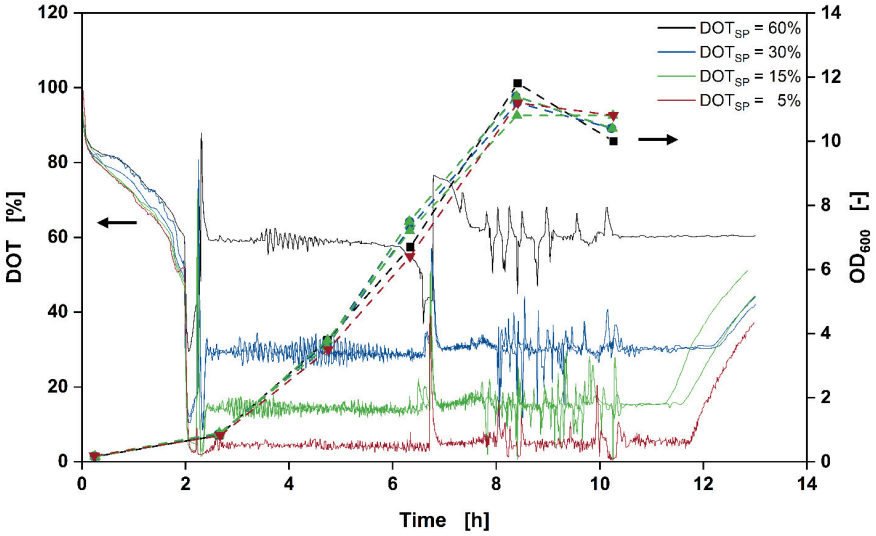


Figure A5.4 Batch cultivations of wild-type *P. putida* KT2440 at differing DOT_{SP} in a parallel cultivation device (DASBox, Eppendorf GmbH, Jülich, Germany). Duplicates for $\text{DOT}_{\text{SP}} = 30\%$ and $\text{DOT}_{\text{SP}} = 15\%$ are shown. Dashed lines and symbols represent OD_{600} , solid lines represent DOT_{PV} .

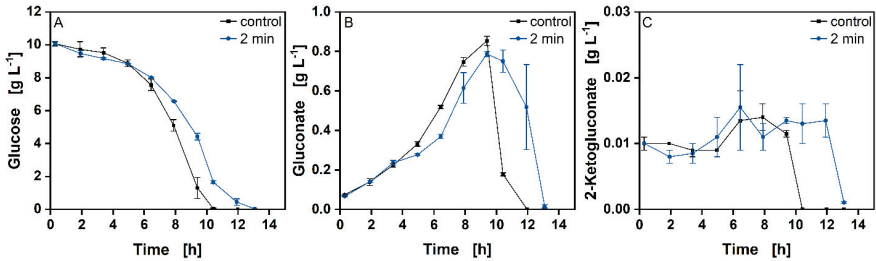


Figure A5.5 Extracellular metabolites measured during cultivations of *P. putida* KT2440 SK4 at different intervals of oscillating aeration and agitation. (A) glucose, (B) gluconate, and (C) 2-ketogluconate concentrations for the control cultivations (black squares) and 2 min intervals of oscillation (blue circles) over the duration of the cultivation. Error bars represent errors derived from two independent experiments. Note the different scales of the y-axes.

Table A5.1 Significantly altered proteins of *P. putida* KT2440 subjected to 2 min intervals of oscillation compared to control cultivations at t_1 and t_2 .

ID ^{a)}	Annotation ^{a)}	fold change	p-value ($\cdot 10^{-2}$)	COG ^{b)}
t_1				
PP_4116	isocitrate lyase AceA	0.228	0.062	C
PP_2679	quinoprotein ethanol dehydrogenase PedH	0.230	0.010	G
PP_4487	acetyl-CoA synthetase AcsA-I	0.230	0.027	I
PP_5365	fatty acid methyltransferase	0.400	2.716	M
PP_2675	cytochrome c-type protein	0.468	0.931	C
PP_2680	aldehyde dehydrogenase AldB-II	0.473	0.001	C
PP_2677	hypothetical protein	0.496	3.697	S
PP_3839	alcohol dehydrogenase AdhP	2.092	0.799	P
PP_3924	hypothetical protein	2.132	0.319	L
PP_5391	hypothetical protein	2.162	0.028	S
PP_0485	single-stranded DNA-binding protein (ssb)	2.395	0.199	L
PP_2132	universal stress protein	2.404	0.005	T
PP_1000	ornithine carbamoyltransferase ArcB	2.437	0.092	E
PP_3420	sensor histidin kinase	2.816	1.354	L
t_2				
PP_4116	isocitrate lyase AceA	0.368	0.987	C
PP_2679	quinoprotein ethanol dehydrogenase PedH	0.437	0.568	G
PP_4487	acetyl-CoA synthetase AcsA-I	0.436	1.131	I
PP_0625	chaperone protein ClpB	2.701	4.893	O

^{a)} According to pseudomonas.com [264]

^{b)} Clusters of orthologous groups (COG). According to the COG database [355] retrieved via eggnog 5.0.0.

COGs: C - Energy production and conversion, E - Amino acid transport and metabolism, G - Carbohydrate transport and metabolism, I - Lipid transport and metabolism, L - Replication, recombination, and repair, M - Cell wall/membrane/envelope biogenesis, O - Post-translational modification, protein turnover, and chaperones, P - Inorganic ion transport and metabolism, S - Unknown function, T - Signal transduction mechanism.

A.6 Appendix for Chapter 3.5

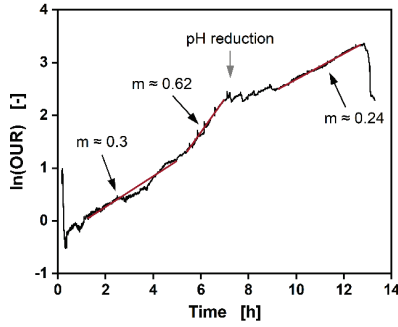


Figure A6.1 Half-logarithmic plot of the OUR of *P. putida* KT2440 SK4 in the MPLR with the second generation of the aeration setup. Linear regression yields the slope (denoted as m), which correlates with the growth rate.

The superficial gas velocity in the riser U_{Gr} is defined as

$$U_{Gr} = \frac{Q_m R T}{h_L A_r \rho_L g} \ln \left(1 + \frac{\rho_L g h_L}{p_h} \right) \quad (21)$$

where Q_m is the molar gas flow rate, R the universal gas constant, T the temperature, h_L the static height of the gas-free liquid, A_r the cross-sectional area of the riser, ρ_L the density of the liquid phase, g the gravitational acceleration constant, and p_h the headspace pressure.

References

References

- [1] von Schuckmann K, Le Traon P-Y, Smith N, Pascual A, Djavidnia S, Gattuso J-P, Grégoire M, Nolan G, *et al.* 2020. Copernicus marine service ocean state report, Issue 4. *Journal of Operational Oceanography* 13:S1-S172. doi: 10.1080/1755876X.2020.1785097.
- [2] Woolway RI, Jennings E, Shatwell T, Golub M, Pierson DC, Maberly SC. 2021. Lake heatwaves under climate change. *Nature* 589(7842):402–407. doi: 10.1038/s41586-020-03119-1.
- [3] Diffenbaugh NS, Singh D, Mankin JS, Horton DE, Swain DL, Touma D, Charland A, Liu Y, *et al.* 2017. Quantifying the influence of global warming on unprecedented extreme climate events. *Proceedings of the National Academy of Sciences* 114(19):4881. doi: 10.1073/pnas.1618082114.
- [4] Cahill AE, Aiello-Lammens ME, Fisher-Reid MC, Hua X, Karanewsky CJ, Yeong Ryu H, Sbeglia GC, Spagnolo F, *et al.* 2013. How does climate change cause extinction? *Proceedings of the Royal Society B: Biological Sciences* 280(1750):20121890. doi: 10.1098/rspb.2012.1890.
- [5] Slater T, Lawrence IR, Otosaka IN, Shepherd A, Gourmelen N, Jakob L, Tepes P, Gilbert L, *et al.* 2021. Review article: Earth's ice imbalance. *The Cryosphere* 15(1):233–246. doi: 10.5194/tc-15-233-2021.
- [6] Gbadamosi AO, Junin R, Manan MA, Agi A, Yusuff AS. 2019. An overview of chemical enhanced oil recovery: Recent advances and prospects. *International Nano Letters* 9(3):171–202. doi: 10.1007/s40089-019-0272-8.
- [7] Geetha SJ, Banat IM, Joshi SJ. 2018. Biosurfactants: Production and potential applications in microbial enhanced oil recovery (MEOR). *Biocatalysis and Agricultural Biotechnology* 14:23–32. doi: 10.1016/j.bcab.2018.01.010.
- [8] Jackson PM, Smith LK. 2014. Exploring the undulating plateau: the future of global oil supply. *Philosophical Transactions of the Royal Society A: Mathematical, Physical and Engineering Sciences* 372(2006):20120491. doi: 10.1098/rsta.2012.0491.
- [9] Betts RA, Alfieri L, Bradshaw C, Caesar J, Feyen L, Friedlingstein P, Gohar L, Koutroulis A, *et al.* 2018. Changes in climate extremes, fresh water availability and vulnerability to food insecurity projected at 1.5°C and 2°C global warming with a higher-resolution global climate model. *Philosophical Transactions of the Royal Society A: Mathematical, Physical and Engineering Sciences* 376(2119):20160452. doi: 10.1098/rsta.2016.0452.
- [10] Haile MG, Wossen T, Tesfaye K, Braun J von. 2017. Impact of climate change, weather extremes, and price risk on global food supply. *Economics of Disasters and Climate Change* 1(1):55–75. doi: 10.1007/s41885-017-0005-2.
- [11] Forster PM, Maycock AC, McKenna CM, Smith CJ. 2020. Latest climate models confirm need for urgent mitigation. *Nature Climate Change* 10(1):7–10. doi: 10.1038/s41558-019-0660-0.
- [12] United Nations, Department of Economic and Social Affairs, Population Division. 2019. World population prospects 2019: Volume II: Demographic profiles.
- [13] Xu Y, Ramanathan V, Victor DG. 2018. Global warming will happen faster than we think. *Nature* 564(7734):30–32. doi: 10.1038/d41586-018-07586-5.
- [14] Federal Ministry for the Environment, Nature Conservation and Nuclear Safety. 2020. Environmental Awareness in Germany 2018 - Results of a Representative Survey.
- [15] Martin R, Preux LB de, Wagner UJ. 2014. The impact of a carbon tax on manufacturing: Evidence from microdata. *Journal of Public Economics* 117:1–14. doi: 10.1016/j.jpubeco.2014.04.016.
- [16] D'Amato D, Korhonen J, Toppinen A. 2019. Circular, Green, and Bio Economy: How do companies in land-use intensive sectors align with sustainability concepts? *Ecological Economics* 158:116–133. doi: 10.1016/j.ecolecon.2018.12.026.

- [17] Penz E, Polsa P. 2018. How do companies reduce their carbon footprint and how do they communicate these measures to stakeholders? *Journal of Cleaner Production* 195:1125–1138. doi: 10.1016/j.jclepro.2018.05.263.
- [18] Liesen A, Hoepner AG, Patten DM, Figge F. 2015. Does stakeholder pressure influence corporate GHG emissions reporting? Empirical evidence from Europe. *Accounting, Auditing & Accountability Journal* 28(7):1047–1074. doi: 10.1108/AAAJ-12-2013-1547.
- [19] Venkata Mohan S, Modestra JA, Amulya K, Butti SK, Velvizhi G. 2016. A circular bioeconomy with biobased products from CO₂ sequestration. *Trends in Biotechnology* 34(6):506–519. doi: 10.1016/j.tibtech.2016.02.012.
- [20] Hatti-Kaul R, Törnvall U, Gustafsson L, Börjesson P. 2007. Industrial biotechnology for the production of bio-based chemicals – A cradle-to-grave perspective. *Trends in Biotechnology* 25(3):119–124. doi: 10.1016/j.tibtech.2007.01.001.
- [21] Communication from the Commission to the European Parliament, the European Council, the Council, the European Economic and Social Committee and the Committee of the Regions. 2019. The European Green Deal, COM/2019/640 final.
- [22] Gasser T, Guivarch C, Tachiiri K, Jones CD, Ciais P. 2015. Negative emissions physically needed to keep global warming below 2 °C. *Nature Communications* 6(1):7958. doi: 10.1038/ncomms8958.
- [23] Voigt CA. 2020. Synthetic biology 2020–2030: Six commercially-available products that are changing our world. *Nature Communications* 11(1):6379. doi: 10.1038/s41467-020-20122-2.
- [24] Basso LC, Basso TO, Rocha SN. 2011. Ethanol production in Brazil: The industrial process and its impact on yeast fermentation. In: Dos Santos Bernades, M. A., Schneidhofer C, Dörr N, Sen S, editors. Biofuel production: Recent developments and prospects: INTECH Open Access Publisher. p 85–100.
- [25] Cheng J, Chen P, Song A, Wang D, Wang Q. 2018. Expanding lysine industry: Industrial biomanufacturing of lysine and its derivatives. *Journal of Industrial Microbiology & Biotechnology* 45(8):719–734. doi: 10.1007/s10295-018-2030-8.
- [26] Ögmundarson Ó, Sukumara S, Herrgård MJ, Fantke P. 2020. Combining environmental and economic performance for bioprocess optimization. *Trends in Biotechnology* 38(11):1203–1214. doi: 10.1016/j.tibtech.2020.04.011.
- [27] Delvigne F, Takors R, Mudde R, van Gulik W, Noorman H. 2017. Bioprocess scale-up/down as integrative enabling technology: From fluid mechanics to systems biology and beyond. *Microbial Biotechnology* 10(5):1267–1274. doi: 10.1111/1751-7915.12803.
- [28] Straathof A. 2011. The proportion of downstream costs in fermentative production processes. In: Moo-Young M, editor. Comprehensive biotechnology. Principles and practices in industry, agriculture, medicine and the environment. Amsterdam: Elsevier. p 811–814.
- [29] Kuhn D, Blank LM, Schmid A, Bühler B. 2010. Systems biotechnology – Rational whole-cell biocatalyst and bioprocess design. *Engineering in Life Sciences* 10(5):384–397. doi: 10.1002/elsc.201000009.
- [30] Kwok R. 2010. Five hard truths for synthetic biology. *Nature* 463(7279):288–290. doi: 10.1038/463288a.
- [31] Willrodt C, Karande R, Schmid A, Julsing MK. 2015. Guiding efficient microbial synthesis of non-natural chemicals by physicochemical properties of reactants. *Current Opinion in Biotechnology* 35:52–62. doi: 10.1016/j.copbio.2015.03.010.
- [32] Nielsen J, Keasling JD. 2016. Engineering cellular metabolism. *Cell* 164(6):1185–1197. doi: 10.1016/j.cell.2016.02.004.
- [33] Chubukov V, Mukhopadhyay A, Petzold CJ, Keasling JD, Martín HG. 2016. Synthetic and systems biology for microbial production of commodity chemicals. *npj Systems Biology and Applications* 2(1):16009. doi: 10.1038/npjbsa.2016.9.

- [34] Lechner A, Brunk E, Keasling JD. 2016. The need for integrated approaches in metabolic engineering. *Cold Spring Harbor Perspectives in Biology* 8(11):a023903. doi: 10.1101/cshperspect.a023903.
- [35] Erb TJ, Jones PR, Bar-Even A. 2017. Synthetic metabolism: metabolic engineering meets enzyme design. *Current Opinion in Chemical Biology* 37:56–62. doi: 10.1016/j.cbpa.2016.12.023.
- [36] Hoynes-O'Connor A, Moon TS. 2015. Programmable genetic circuits for pathway engineering. *Current Opinion in Biotechnology* 36:115–121. doi: 10.1016/j.copbio.2015.08.007.
- [37] Plotkin JB, Kudla G. 2011. Synonymous but not the same: the causes and consequences of codon bias. *Nature Reviews. Genetics* 12(1):32–42. doi: 10.1038/nrg2899.
- [38] Nielsen AAK, Der BS, Shin J, Vaidyanathan P, Paralanov V, Strychalski EA, Ross D, Densmore D, *et al.* 2016. Genetic circuit design automation. *Science* 352(6281):aac7341. doi: 10.1126/science.aac7341.
- [39] Ellis T, Adie T, Baldwin GS. 2011. DNA assembly for synthetic biology: From parts to pathways and beyond. *Integrative Biology* 3(2):109–118. doi: 10.1039/c0ib00070a.
- [40] Mukhopadhyay A. 2015. Tolerance engineering in bacteria for the production of advanced biofuels and chemicals. *Trends in Microbiology* 23(8):498–508. doi: 10.1016/j.tim.2015.04.008.
- [41] Blesken CC, Bator I, Eberlein C, Heipieper HJ, Tiso T, Blank LM. 2020. Genetic cell-surface modification for optimized foam fractionation. *Frontiers in Bioengineering and Biotechnology* 8:572892. doi: 10.3389/fbioe.2020.572892.
- [42] Wynands B, Otto M, Runge N, Preckel S, Polen T, Blank LM, Wierckx N. 2019. Streamlined *Pseudomonas taiwanensis* VLB120 chassis strains with improved bioprocess features. *ACS Synthetic Biology* 8(9):2036–2050. doi: 10.1021/acssynbio.9b00108.
- [43] Blank LM. 2017. Let's talk about flux or the importance of (intracellular) reaction rates. *Microbial Biotechnology* 10(1):28–30. doi: 10.1111/1751-7915.12455.
- [44] Lee SY, Lee D-Y, Kim TY. 2005. Systems biotechnology for strain improvement. *Trends in Biotechnology* 23(7):349–358. doi: 10.1016/j.tibtech.2005.05.003.
- [45] Willrodt C, Hoschek A, Bühler B, Schmid A, Julius MK. 2015. Coupling limonene formation and oxyfunctionalization by mixed-culture resting cell fermentation. *Biotechnology and Bioengineering* 112(9):1738–1750. doi: 10.1002/bit.25592.
- [46] van Hecke W, Kaur G, Wever H de. 2014. Advances in *in-situ* product recovery (ISPR) in whole cell biotechnology during the last decade. *Biotechnology Advances* 32(7):1245–1255. doi: 10.1016/j.biotechadv.2014.07.003.
- [47] Hemmerich J, Noack S, Wiechert W, Oldiges M. 2018. Microbioreactor systems for accelerated bioprocess development. *Biotechnology Journal* 13(4):1700141. doi: 10.1002/biot.201700141.
- [48] Grünberger A, Wiechert W, Kohlheyer D. 2014. Single-cell microfluidics: opportunity for bioprocess development. *Current Opinion in Biotechnology* 29:15–23. doi: 10.1016/j.copbio.2014.02.008.
- [49] Demling P, Westerwalbesloh C, Noack S, Wiechert W, Kohlheyer D. 2018. Quantitative measurements in single-cell analysis: Towards scalability in microbial bioprocess development. *Current Opinion in Biotechnology* 54:121–127. doi: 10.1016/j.copbio.2018.01.024.
- [50] Morschett H, Jansen R, Neuendorf C, Moch M, Wiechert W, Oldiges M. 2020. Parallelized microscale fed-batch cultivation in online-monitored microtiter plates: Implications of media composition and feed strategies for process design and performance. *Journal of Industrial Microbiology & Biotechnology* 47(1):35–47. doi: 10.1007/s10295-019-02243-w.
- [51] Velez-Suberbie ML, Betts JPI, Walker KL, Robinson C, Zoro B, Keshavarz-Moore E. 2018. High throughput automated microbial bioreactor system used for clone selection and

- rapid scale-down process optimization. *Biotechnology Progress* 34(1):58–68. doi: 10.1002/btpr.2534.
- [52] Croughan MS, Konstantinov KB, Cooney C. 2015. The future of industrial bioprocessing: Batch or continuous? *Biotechnology and Bioengineering* 112(4):648–651. doi: 10.1002/bit.25529.
- [53] Kumar A, Udugama IA, Gargalo CL, Gernaey KV. 2020. Why is batch processing still dominating the biologics landscape? Towards an integrated continuous bioprocessing alternative. *Processes* 8(12):1641. doi: 10.3390/pr8121641.
- [54] Bednarz A, Jupke A, Schmidt M, Weber B. 2017. Multi-phase loop reactor and method of operation. WO2017149099A1.
- [55] Bednarz A, Weber B, Jupke A. 2017. Development of a CFD model for the simulation of a novel multiphase counter-current loop reactor. *Chemical Engineering Science* 161:350–359. doi: 10.1016/j.ces.2016.12.048.
- [56] Weber B, von Campenhausen M, Maßmann T, Bednarz A, Jupke A. 2019. CFD based compartment-model for a multiphase loop-reactor. *Chemical Engineering Science: X* 2:100010. doi: 10.1016/j.cesx.2019.100010.
- [57] Clarke KG. 2013. Downstream processing. In: Clarke KG, editor. Bioprocess engineering. An introductory engineering and life science approach. Oxford: Woodhead Publishing. p 209–234.
- [58] López-Garzón CS, Straathof AJJ. 2014. Recovery of carboxylic acids produced by fermentation. *Biotechnology Advances* 32(5):873–904. doi: 10.1016/j.biotechadv.2014.04.002.
- [59] Pedraza-de La Cuesta S, Knopper L, van der Wielen LA, Cuellar MC. 2019. Technoeconomic assessment of the use of solvents in the scale-up of microbial sesquiterpene production for fuels and fine chemicals. *Biofuels, Bioproducts and Biorefining* 13(1):140–152. doi: 10.1002/bbb.1949.
- [60] Hanes RJ, Carpenter A. 2017. Evaluating opportunities to improve material and energy impacts in commodity supply chains. *Environment Systems and Decisions* 37(1):6–12. doi: 10.1007/s10669-016-9622-5.
- [61] Lynch MD. 2021. The bioprocess TEA calculator: An online technoeconomic analysis tool to evaluate the commercial competitiveness of potential bioprocesses. *Metabolic Engineering* 65:42–51. doi: 10.1016/j.ymben.2021.03.004.
- [62] Winter B, Meys R, Bardow A. 2021. Towards aromatics from biomass: Prospective Life Cycle Assessment of bio-based aniline. *Journal of Cleaner Production* 290:125818. doi: 10.1016/j.jclepro.2021.125818.
- [63] van Gerven T, Stankiewicz A. 2009. Structure, energy, synergy, time - The fundamentals of process intensification. *Industrial & Engineering Chemistry Research* 48(5):2465–2474. doi: 10.1021/ie801501y.
- [64] Garg N, Kontogeorgis GM, Woodley JM, Gani R. 2018. A multi-stage and multi-level computer aided framework for sustainable process intensification. In: Friedl A, Klemeš JJ, Radl S, Varbanov PS, Wallek T, editors. Computer Aided Chemical Engineering: 28 European Symposium on Computer Aided Process Engineering: Elsevier. p 875–880.
- [65] Woodley JM. 2017. Bioprocess intensification for the effective production of chemical products. *Computers & Chemical Engineering* 105:297–307. doi: 10.1016/j.compchemeng.2017.01.015.
- [66] Schügerl K, Hubbuch J. 2005. Integrated bioprocesses. *Current Opinion in Microbiology* 8(3):294–300. doi: 10.1016/j.mib.2005.01.002.
- [67] van der Wielen LA, Mussatto SI, van Breugel J. 2021. Bioprocess intensification: Cases that (don't) work. *New Biotechnology* 61:108–115. doi: 10.1016/j.nbt.2020.11.007.
- [68] Woodley JM, Titchener-Hooker NJ. 1996. The use of windows of operation as a bioprocess design tool. *Bioprocess Engineering* 14(5):263–268. doi: 10.1007/BF00369924.

- [69] Freeman A, Woodley JM, Lilly MD. 1993. *In situ* product removal as a tool for bioprocessing. *Nature Biotechnology* 11(9):1007–1012. doi: 10.1038/nbt0993-1007.
- [70] Flores A, Wang X, Nielsen DR. 2019. Recent trends in integrated bioprocesses: Aiding and expanding microbial biofuel/biochemical production. *Current Opinion in Biotechnology* 57:82–87. doi: 10.1016/j.copbio.2019.02.007.
- [71] Hanson C. 1971. Solvent extraction: The current position. In: Hanson C, editor. Recent advances in liquid-liquid extraction. Burlington: Elsevier Science. p 1–13.
- [72] Rosinha Grundtvig IP, Heintz S, Krühne U, Gernaey KV, Adlercreutz P, Hayler JD, Wells AS, Woodley JM. 2018. Screening of organic solvents for bioprocesses using aqueous-organic two-phase systems. *Biotechnology Advances* 36(7):1801–1814. doi: 10.1016/j.biotechadv.2018.05.007.
- [73] Dafoe JT, Daugulis AJ. 2014. *In situ* product removal in fermentation systems: Improved process performance and rational extractant selection. *Biotechnology Letters* 36(3):443–460. doi: 10.1007/s10529-013-1380-6.
- [74] Isken S, de Bont JA. 1998. Bacteria tolerant to organic solvents. *Extremophiles* 2(3):229–238. doi: 10.1007/s007920050065.
- [75] Kuhn D, Julsing MK, Heinzle E, Bühler B. 2012. Systematic optimization of a biocatalytic two-liquid phase oxyfunctionalization process guided by ecological and economic assessment. *Green Chemistry* 14(3):645–653. doi: 10.1039/C2GC15985F.
- [76] Roffler SR, Blanch HW, Wilke CR. 1987. *In-situ* recovery of butanol during fermentation. *Bioprocess Engineering* 2(1):1–12. doi: 10.1007/BF00369221.
- [77] van Sonsbeek HM, Beeffink HH, Tramper J. 1993. Two-liquid-phase bioreactors. *Enzyme and Microbial Technology* 15(9):722–729. doi: 10.1016/0141-0229(93)90001-I.
- [78] Teke GM, Pott RWM. 2021. Design and evaluation of a continuous semipartition bioreactor for *in situ* liquid-liquid extractive fermentation. *Biotechnology and Bioengineering* 118(1):58–71. doi: 10.1002/bit.27550.
- [79] Ezeji TC, Qureshi N, Blaschek HP. 2004. Acetone butanol ethanol (ABE) production from concentrated substrate: Reduction in substrate inhibition by fed-batch technique and product inhibition by gas stripping. *Applied Microbiology and Biotechnology* 63(6):653–658. doi: 10.1007/s00253-003-1400-x.
- [80] Baez A, Cho K-M, Liao JC. 2011. High-flux isobutanol production using engineered *Escherichia coli*: A bioreactor study with *in situ* product removal. *Applied Microbiology and Biotechnology* 90(5):1681–1690. doi: 10.1007/s00253-011-3173-y.
- [81] Diaz VH, Stosch M von, Willis MJ. 2019. Butanol production *via* vacuum fermentation: An economic evaluation of operating strategies. *Chemical Engineering Science* 195:707–719.
- [82] Mariano AP, Costa CBB, Angelis DF de, Maugeri Filho F, Atala DIP, Wolf Maciel MR, Maciel Filho R. 2010. Optimisation of a continuous flash fermentation for butanol production using the response surface methodology. *Chemical Engineering Research & Design: Transactions of the Institution of Chemical Engineers* 88(5):562–571. doi: 10.1016/j.cherd.2009.11.002.
- [83] Ehnstrom L, Frisenfelt J, Danielsson M. 2019. The biostil process. In: Mattiason B, editor. Extractive bioconversions. Boca Raton: CRC Press.
- [84] Levario TJ, Dai M, Yuan W, Vogt BD, Nielsen DR. 2012. Rapid adsorption of alcohol biofuels by high surface area mesoporous carbons. *Microporous and Mesoporous Materials* 148(1):107–114. doi: 10.1016/j.micromeso.2011.08.001.
- [85] Staggs KW, Qiang Z, Madathil K, Gregson C, Xia Y, Vogt B, Nielsen DR. 2017. High efficiency and facile butanol recovery with magnetically responsive micro/mesoporous carbon adsorbents. *ACS Sustainable Chemistry & Engineering* 5(1):885–894. doi: 10.1021/acssuschemeng.6b02204.

- [86] Carstensen F, Apel A, Wessling M. 2012. *In situ* product recovery: Submerged membranes vs. external loop membranes. *Journal of Membrane Science* 394-395:1–36. doi: 10.1016/j.memsci.2011.11.029.
- [87] Buque-Taboada EM, Straathof AJJ, Heijnen JJ, van der Wielen LAM. 2006. *In situ* product recovery (ISPR) by crystallization: Basic principles, design, and potential applications in whole-cell biocatalysis. *Applied Microbiology and Biotechnology* 71(1):1–12. doi: 10.1007/s00253-006-0378-6.
- [88] Saur KM, Brumhard O, Scholz K, Hayen H, Tiso T. 2019. A pH shift induces high-titer liamocin production in *Aureobasidium pullulans*. *Applied Microbiology and Biotechnology* 103(12):4741–4752. doi: 10.1007/s00253-019-09677-3.
- [89] Kocks C, Görtz J, Holtz A, Gausmann M, Jupke A. 2020. Electrochemical crystallization concept for succinic acid reduces waste salt production. *Chemie Ingenieur Technik* 92(3):221–228. doi: 10.1002/cite.201900088.
- [90] Gorden J, Geiser E, Wierckx N, Blank LM, Zeiner T, Brandenbusch C. 2017. Integrated process development of a reactive extraction concept for itaconic acid and application to a real fermentation broth. *Engineering in Life Sciences* 17(7):809–816. doi: 10.1002/else.201600253.
- [91] Hong YK, Hong WH, Han DH. 2001. Application of reactive extraction to recovery of carboxylic acids. *Biotechnology and Bioprocess Engineering* 6(6):386.
- [92] Soberón-Chávez G (editor). 2011. Biosurfactants: From genes to applications. Berlin, Heidelberg: Springer Berlin Heidelberg.
- [93] Fleurackers S. 2015. Biosurfactants versus chemically synthesized surface-active agents. In: Kosaric N, Vardar-Sukan F, editors. Biosurfactants. Production and utilization-processes, technologies, and economics. Boca Raton: CRC Press. p 37–48.
- [94] Banat IM, Franzetti A, Gandolfi I, Bestetti G, Martinotti MG, Fracchia L, Smyth TJ, Marchant R. 2010. Microbial biosurfactants production, applications and future potential. *Applied Microbiology and Biotechnology* 87(2):427–444. doi: 10.1007/s00253-010-2589-0.
- [95] Drakontis CE, Amin S. 2020. Biosurfactants: Formulations, properties, and applications. *Current Opinion in Colloid & Interface Science* 48:77–90. doi: 10.1016/j.cocis.2020.03.013.
- [96] Research and Markets. Biosurfactants - Global Market Trajectory & Analytics. <https://www.researchandmarkets.com/reports/5139450/biosurfactants-global-market-trajectory-and> (accessed 13 April 2021).
- [97] Rosenberg E, Ron EZ. 1999. High- and low-molecular-mass microbial surfactants. *Applied Microbiology and Biotechnology* 52(2):154–162. doi: 10.1007/s002530051502.
- [98] Santos DKF, Rufino RD, Luna JM, Santos VA, Sarubbo LA. 2016. Biosurfactants: Multifunctional biomolecules of the 21st century. *International Journal of Molecular Sciences* 17(3):401. doi: 10.3390/ijms17030401.
- [99] Müller MM, Kügler JH, Henkel M, Gerlitzki M, Hörmann B, Pöhnlein M, Syltatk C, Hausmann R. 2012. Rhamnolipids - Next generation surfactants? *Journal of Biotechnology* 162(4):366–380. doi: 10.1016/j.jbiotec.2012.05.022.
- [100] Abdel-Mawgoud AM, Hausmann R, Lépine F, Müller MM, Déziel E. 2011. Rhamnolipids: Detection, analysis, biosynthesis, genetic regulation, and bioengineering of production. In: Soberón-Chávez G, editor. Biosurfactants: From genes to applications. Berlin, Heidelberg: Springer Berlin Heidelberg. p 13–55.
- [101] Abdel-Mawgoud AM, Lépine F, Déziel E. 2010. Rhamnolipids: Diversity of structures, microbial origins and roles. *Applied Microbiology and Biotechnology* 86(5):1323–1336. doi: 10.1007/s00253-010-2498-2.
- [102] Germer A, Tiso T, Müller C, Behrens B, Vosse C, Scholz K, Froning M, Hayen H, et al. 2020. Exploiting the natural diversity of RhlA acyltransferases for the synthesis of the

- rhamnolipid precursor 3-(3-hydroxyalkanoyloxy)alkanoic acid. *Applied and Environmental Microbiology* 86(6):e02317-19. doi: 10.1128/AEM.02317-19.
- [103] Řezanka T, Siristova L, Sigler K. 2011. Rhamnolipid-producing thermophilic bacteria of species *Thermus* and *Meiothermus*. *Extremophiles* 15(6):697. doi: 10.1007/s00792-011-0400-5.
- [104] Syldatk C, Lang S, Wagner F, Wray V, Witte L. 1985. Chemical and physical characterization of four interfacial-active rhamnolipids from *Pseudomonas* spec. DSM 2874 grown on *n*-alkanes. *Zeitschrift für Naturforschung C* 40(1-2):51–60. doi: 10.1515/znc-1985-1-212.
- [105] Evonik Industries AG. The foam makers. <https://corporate.evonik.de/en/the-foam-makers-1291.html> (accessed 13 April 2021).
- [106] Wittgens A, Tiso T, Arndt TT, Wenk P, Hemmerich J, Müller C, Wichmann R, Küpper B, et al. 2011. Growth independent rhamnolipid production from glucose using the non-pathogenic *Pseudomonas putida* KT2440. *Microbial Cell Factories* 10(1):80. doi: 10.1186/1475-2859-10-80.
- [107] Tiso T, Zauter R, Tulke H, Leuchtle B, Li W-J, Behrens B, Wittgens A, Rosenau F, et al. 2017. Designer rhamnolipids by reduction of congener diversity: production and characterization. *Microbial Cell Factories* 16(1):225. doi: 10.1186/s12934-017-0838-y.
- [108] Belda E, van Heck RGA, José Lopez-Sanchez M, Cruveiller S, Barbe V, Fraser C, Klenk H-P, Petersen J, et al. 2016. The revisited genome of *Pseudomonas putida* KT2440 enlightens its value as a robust metabolic chassis. *Environmental Microbiology* 18(10):3403–3424. doi: 10.1111/1462-2920.13230.
- [109] Sudarsan S, Dethlefsen S, Blank LM, Siemann-Herzberg M, Schmid A, Paraless RE. 2014. The functional structure of central carbon metabolism in *Pseudomonas putida* KT2440. *Applied and Environmental Microbiology* 80(17):5292. doi: 10.1128/AEM.01643-14.
- [110] Blank LM, Ebert BE, Buehler K, Bühler B. 2010. Redox biocatalysis and metabolism: Molecular mechanisms and metabolic network analysis. *Antioxidants & Redox Signaling* 13(3):349–394. doi: 10.1089/ars.2009.2931.
- [111] Ebert BE, Kurth F, Grund M, Blank LM, Schmid A. 2011. Response of *Pseudomonas putida* KT2440 to increased NADH and ATP demand. *Applied and Environmental Microbiology* 77(18):6597–6605. doi: 10.1128/AEM.05588-11.
- [112] Nikel PI, Chavarria M, Danchin A, de Lorenzo V. 2016. From dirt to industrial applications: *Pseudomonas putida* as a synthetic biology chassis for hosting harsh biochemical reactions. *Current Opinion in Chemical Biology* 34:20–29. doi: 10.1016/j.cbpa.2016.05.011.
- [113] Tiso T, Wierckx N, Blank LM. 2014. Non-pathogenic *Pseudomonas* as platform hosts for industrial biocatalysis. In: Grunwald P, editor. *Industrial biocatalysis*. Hoboken: Pan Stanford.
- [114] Weimer A, Kohlstedt M, Volke DC, Nikel PI, Wittmann C. 2020. Industrial biotechnology of *Pseudomonas putida*: Advances and prospects. *Applied Microbiology and Biotechnology* 104(18):7745–7766. doi: 10.1007/s00253-020-10811-9.
- [115] Nikel PI, de Lorenzo V. 2018. *Pseudomonas putida* as a functional chassis for industrial biocatalysis: From native biochemistry to *trans*-metabolism. *Metabolic Engineering* 50:142–155. doi: 10.1016/j.ymben.2018.05.005.
- [116] Gong Z, Yang G, Che C, Liu J, Si M, He Q. 2021. Foaming of rhamnolipids fermentation: Impact factors and fermentation strategies. *Microbial Cell Factories* 20(1):77. doi: 10.1186/s12934-021-01516-3.
- [117] Blesken CC, Strümpfler T, Tiso T, Blank LM. 2020. Uncoupling foam fractionation and foam adsorption for enhanced biosurfactant synthesis and recovery. *Microorganisms* 8(12). doi: 10.3390/microorganisms8122029.

- [118] Beuker J, Barth T, Steier A, Wittgens A, Rosenau F, Henkel M, Hausmann R. 2016. High titer heterologous rhamnolipid production. *AMB Express* 6(1):124. doi: 10.1186/s13568-016-0298-5.
- [119] Routledge SJ. 2012. Beyond de-foaming: The effects of antifoams on bioprocess productivity. *Computational and Structural Biotechnology Journal* 3:e201210014. doi: 10.5936/csbj.201210014.
- [120] McGregor WC, Weaver JF, Tansey SP. 1988. Antifoam effects on ultrafiltration. *Biotechnology and Bioengineering* 31(4):385–389. doi: 10.1002/bit.260310416.
- [121] Gong Z, Peng Y, Wang Q. 2015. Rhamnolipid production, characterization and fermentation scale-up by *Pseudomonas aeruginosa* with plant oils. *Biotechnology Letters* 37(10):2033–2038. doi: 10.1007/s10529-015-1885-2.
- [122] Beuker J, Steier A, Wittgens A, Rosenau F, Henkel M, Hausmann R. 2016. Integrated foam fractionation for heterologous rhamnolipid production with recombinant *Pseudomonas putida* in a bioreactor. *AMB Express* 6(1):11. doi: 10.1186/s13568-016-0183-2.
- [123] Anic I, Apolonia I, Franco P, Wichmann R. 2018. Production of rhamnolipids by integrated foam adsorption in a bioreactor system. *AMB Express* 8(1):122. doi: 10.1186/s13568-018-0651-y.
- [124] Henkel M, Geissler M, Weggenmann F, Hausmann R. 2017. Production of microbial biosurfactants: Status quo of rhamnolipid and surfactin towards large-scale production. *Biotechnology Journal* 12(7):1600561. doi: 10.1002/biot.201600561.
- [125] Demling P, von Campenhausen M, Grütering C, Tiso T, Jupke A, Blank LM. 2020. Selection of a recyclable *in situ* liquid-liquid extraction solvent for foam-free synthesis of rhamnolipids in a two-phase fermentation. *Green Chemistry* 22:8495-8510. doi: 10.1039/D0GC02885A.
- [126] Demling P, Ankenbauer A, Klein B, Noack S, Tiso T, Takors R, Blank LM. 2021 *Pseudomonas putida* KT2440 endures temporary oxygen limitations. *Biotechnology & Bioengineering* 1-16. doi: 10.1002/bit.27938.
- [127] Nakazawa T. 2002. Travels of a *Pseudomonas*, from Japan around the world. *Environmental Microbiology* 4(12):782–786. doi: 10.1046/j.1462-2920.2002.00310.x.
- [128] Bagdasarian M, Lurz R, Rückert B, Franklin F, Bagdasarian MM, Frey J, Timmis KN. 1981. Specific-purpose plasmid cloning vectors II. Broad host range, high copy number, RSF 1010-derived vectors, and a host-vector system for gene cloning in *Pseudomonas*. *Gene* 16(1):237–247. doi: 10.1016/0378-1119(81)90080-9.
- [129] Kampers LFC, Volkers RJM, Martins dos Santos, Vitor A. P. 2019. *Pseudomonas putida* KT2440 is HV1 certified, not GRAS. *Microbial Biotechnology* 12(5):845–848. doi: 10.1111/1751-7915.13443.
- [130] Hartmans S, Smits JP, van der Werf MJ, Volkering F, Bont JAM de. 1989. Metabolism of styrene oxide and 2-phenylethanol in the styrene-degrading *Xanthobacter* Strain 124X. *Applied and Environmental Microbiology* 55(11):2850.
- [131] Gibson DG, Young L, Chuang R-Y, Venter JC, Hutchison CA3, Smith HO. 2009. Enzymatic assembly of DNA molecules up to several hundred kilobases. *Nature Methods* 6(5):343–345. doi: 10.1038/nmeth.1318.
- [132] Koopman F, Wierckx N, Winde JH de, Ruijsenaars HJ. 2010. Identification and characterization of the furfural and 5-(hydroxymethyl)furfural degradation pathways of *Cupriavidus basilensis* HMF14. *Proceedings of the National Academy of Sciences* 107(11):4919–4924. doi: 10.1073/pnas.0913039107.
- [133] Verhoef S, Ballerstedt H, Volkers RJM, Winde JH de, Ruijsenaars HJ. 2010. Comparative transcriptomics and proteomics of *p*-hydroxybenzoate producing *Pseudomonas putida* S12: Novel responses and implications for strain improvement. *Applied Microbiology and Biotechnology* 87(2):679–690. doi: 10.1007/s00253-010-2626-z.

- [134] Hanahan D. 1983. Studies on transformation of *Escherichia coli* with plasmids. *Journal of Molecular Biology* 166(4):557–580. doi: 10.1016/s0022-2836(83)80284-8.
- [135] Chomczynski P, Rymaszewski M. 2006. Alkaline polyethylene glycol-based method for direct PCR from bacteria, eukaryotic tissue samples, and whole blood. *BioTechniques* 40(4):454, 456, 458. doi: 10.2144/000112149.
- [136] Choi K-H, Kumar A, Schweizer HP. 2006. A 10-min method for preparation of highly electrocompetent *Pseudomonas aeruginosa* cells: Application for DNA fragment transfer between chromosomes and plasmid transformation. *Journal of Microbiological Methods* 64(3):391–397. doi: 10.1016/j.mimet.2005.06.001.
- [137] Wynands B, Lenzen C, Otto M, Koch F, Blank LM, Wierckx N. 2018. Metabolic engineering of *Pseudomonas taiwanensis* VLB120 with minimal genomic modifications for high-yield phenol production. *Metabolic Engineering* 47:121–133. doi: 10.1016/j.ymben.2018.03.011.
- [138] Köbbing S. 2020. Development of synthetic biology tools for *Pseudomonas putida*. Aachen: Apprimus Verlag. 188 p.
- [139] Bator I, Wittgens A, Rosenau F, Tiso T, Blank LM. 2020. Comparison of three xylose pathways in *Pseudomonas putida* KT2440 for the synthesis of valuable products. *Frontiers in Bioengineering and Biotechnology* 7:480. doi: 10.3389/fbioe.2019.00480.
- [140] Köbbing S, Blank LM, Wierckx N. 2020. Characterization of context-dependent effects on synthetic promoters. *Frontiers in Bioengineering and Biotechnology* 8:551. doi: 10.3389/fbioe.2020.00551.
- [141] Zobel S, Benedetti I, Eisenbach L, de Lorenzo V, Wierckx N, Blank LM. 2015. Tn7-Based device for calibrated heterologous gene expression in *Pseudomonas putida*. *ACS Synthetic Biology* 4(12):1341–1351. doi: 10.1021/acssynbio.5b00058.
- [142] Hanahan D, Jessee J, Bloom FR. 1991. Plasmid transformation of *Escherichia coli* and other bacteria. *Methods in Enzymology* 204:63–113. doi: 10.1016/0076-6879(91)04006-a.
- [143] de Lorenzo V, Timmis KN. 1994. Analysis and construction of stable phenotypes in Gram-negative bacteria with Tn5- and Tn10-derived minitransposons. *Methods in Enzymology* 235:386–405. doi: 10.1016/0076-6879(94)35157-0.
- [144] Ditta G, Stanfield S, Corbin D, Helinski DR. 1980. Broad host range DNA cloning system for Gram-negative bacteria: Construction of a gene bank of *Rhizobium meliloti*. *Proceedings of the National Academy of Sciences* 77(12):7347. doi: 10.1073/pnas.77.12.7347.
- [145] Martínez-García E, de Lorenzo V. 2011. Engineering multiple genomic deletions in Gram-negative bacteria: Analysis of the multi-resistant antibiotic profile of *Pseudomonas putida* KT2440. *Environmental Microbiology* 13(10):2702–2716. doi: 10.1111/j.1462-2920.2011.02538.x.
- [146] Choi K-H, Gaynor JB, White KG, Lopez C, Bosio CM, Karkhoff-Schweizer RR, Schweizer HP. 2005. A Tn7-based broad-range bacterial cloning and expression system. *Nature Methods* 2(6):443–448. doi: 10.1038/nmeth765.
- [147] Panke S, Witholt B, Schmid A, Wubbolts MG. 1998. Towards a biocatalyst for (S)-styrene oxide production: Characterization of the styrene degradation pathway of *Pseudomonas* sp. strain VLB120. *Applied and Environmental Microbiology* 64(6):2032. doi: 10.1128/AEM.64.6.2032-2043.1998.
- [148] Tiso T, Ihling N, Kubicki S, Biselli A, Schonhoff A, Bator I, Thies S, Karmainski T, et al. 2020. Integration of genetic and process engineering for optimized rhamnolipid production using *Pseudomonas putida*. *Frontiers in Bioengineering and Biotechnology* 8:976. doi: 10.3389/fbioe.2020.00976.
- [149] Kensy F, Zimmermann HF, Knabben I, Anderlei T, Trauthwein H, Dingerdissen U, Büchs J. 2005. Oxygen transfer phenomena in 48-well microtiter plates: Determination by optical monitoring of sulfite oxidation and verification by real-time measurement during microbial growth. *Biotechnology and Bioengineering* 89(6):698–708. doi: 10.1002/bit.20373.

- [150] Lattermann C, Funke M, Hansen S, Diederichs S, Büchs J. 2014. Cross-section perimeter is a suitable parameter to describe the effects of different baffle geometries in shaken microtiter plates. *Journal of Biological Engineering* 8(1):18. doi: 10.1186/1754-1611-8-18.
- [151] Duetz WA, Rüedi L, Hermann R, O'Connor K, Büchs J, Witholt B. 2000. Methods for intense aeration, growth, storage, and replication of bacterial strains in microtiter plates. *Applied and Environmental Microbiology* 66(6):2641. doi: 10.1128/AEM.66.6.2641-2646.2000.
- [152] Eng T, Demling P, Herbert RA, Chen Y, Benites V, Martin J, Lipzen A, Baidoo EEK, *et al.* 2018. Restoration of biofuel production levels and increased tolerance under ionic liquid stress is enabled by a mutation in the essential *Escherichia coli* gene *cydC*. *Microbial Cell Factories* 17(1):159. doi: 10.1186/s12934-018-1006-8.
- [153] Li H, Durbin R. 2009. Fast and accurate short read alignment with Burrows–Wheeler transform. *Bioinformatics* 25(14):1754–1760. doi: 10.1093/bioinformatics/btp324.
- [154] Cingolani P, Platts A, Le Wang L, Coon M, Nguyen T, Wang L, Land SJ, Lu X, *et al.* 2012. A program for annotating and predicting the effects of single nucleotide polymorphisms, SnpEff: SNPs in the genome of *Drosophila melanogaster* strain w1118; iso-2; iso-3. *Fly* 6(2):80–92. doi: 10.4161/fly.19695.
- [155] Sikkema J, de Bont JA, Poolman B. 1995. Mechanisms of membrane toxicity of hydrocarbons. *Microbiological Reviews* 59(2):201–222.
- [156] Prat D, Wells A, Hayler J, Sneddon H, McElroy CR, Abou-Shehadeh S, Dunn PJ. 2016. CHEM21 selection guide of classical- and less classical-solvents. *Green Chemistry* 18(1):288–296. doi: 10.1039/C5GC01008J.
- [157] Fonseca P, Moreno R, Rojo F. 2011. Growth of *Pseudomonas putida* at low temperature: Global transcriptomic and proteomic analyses. *Environmental Microbiology Reports* 3(3):329–339. doi: 10.1111/j.1758-2229.2010.00229.x.
- [158] Hartland S, Jeelani S. 1987. Choice of model for predicting the dispersion height in liquid/liquid gravity settlers from batch settling data. *Chemical Engineering Science* 42(8):1927–1938. doi: 10.1016/0009-2509(87)80139-2.
- [159] Voges R, Noack S. 2012. Quantification of proteome dynamics in *Corynebacterium glutamicum* by (15)N-labeling and selected reaction monitoring. *Journal of Proteomics* 75(9):2660–2669. doi: 10.1016/j.jprot.2012.03.020.
- [160] Salek K, Euston SR. 2019. Sustainable microbial biosurfactants and bioemulsifiers for commercial exploitation. *Process Biochemistry* 85:143–155. doi: 10.1016/j.procbio.2019.06.027.
- [161] Müller MM, Hörmann B, Syltatk C, Hausmann R. 2010. *Pseudomonas aeruginosa* PAO1 as a model for rhamnolipid production in bioreactor systems. *Applied Microbiology and Biotechnology* 87(1):167–174. doi: 10.1007/s00253-010-2513-7.
- [162] Siemann M, Wagner F. 2015. Prospects and limits for the production of biosurfactants using immobilized biocatalysts. In: Kosaric N, Vardar-Sukan F, editors. Biosurfactants. Production and utilization-processes, technologies, and economics. Boca Raton: CRC Press. p 99–133.
- [163] Schilling M, Ruetering M, Dahl V, Cabirol F. 2012. Process for the isolation of rhamnolipids. US20140148588A1.
- [164] Yabannavar VM, Wang DI. 1991. Extractive fermentation for lactic acid production. *Biotechnology and Bioengineering* 37(11):1095–1100. doi: 10.1002/bit.260371115.
- [165] Hollmann D, Switalski J, Geipel S, Onken U. 1995. Extractive fermentation of gibberellic acid by *Gibberella fujikuroi*. *Journal of Fermentation and Bioengineering* 79(6):594–600. doi: 10.1016/0922-338X(95)94754-F.
- [166] Kraemer K, Harwardt A, Bronneberg R, Marquardt W. 2010. Separation of butanol from acetone-butanol-ethanol fermentation by a hybrid extraction-distillation process. In: 20th European Symposium on Computer Aided Process Engineering: Elsevier. p 7–12.

- [167] Kreyenschulte D, Heyman B, Eggert A, Maßmann T, Kalvelage C, Kossack R, Regestein L, Jupke A, *et al.* 2018. *In situ* reactive extraction of itaconic acid during fermentation of *Aspergillus terreus*. *Biochemical Engineering Journal* 135:133–141. doi: 10.1016/j.bej.2018.04.014.
- [168] Takors R. 2004. Ganzzell-ISPR-Prozessentwicklung: Chancen und Risiken. *Chemie Ingenieur Technik* 76(12):1857–1864. doi: 10.1002/cite.200407040.
- [169] Lara AR, Galindo E, Ramirez OT, Palomares LA. 2006. Living with heterogeneities in bioreactors. *Molecular Biotechnology* 34(3):355–381. doi: 10.1385/MB:34:3:355.
- [170] Käß F, Junne S, Neubauer P, Wiechert W, Oldiges M. 2014. Process inhomogeneity leads to rapid side product turnover in cultivation of *Corynebacterium glutamicum*. *Microbial Cell Factories* 13(1):6. doi: 10.1186/1475-2859-13-6.
- [171] Ng HY, Tan TW, Ong SL. 2006. Membrane fouling of submerged membrane bioreactors: Impact of mean cell residence time and the contributing factors. *Environmental Science & Technology* 40(8):2706–2713. doi: 10.1021/es0516155.
- [172] Wierckx NJP, Ballerstedt H, Bont JAM de, Wery J. 2005. Engineering of solvent-tolerant *Pseudomonas putida* S12 for bioproduction of phenol from glucose. *Applied and Environmental Microbiology* 71(12):8221–8227. doi: 10.1128/AEM.71.12.8221-8227.2005.
- [173] Verhoef S, Wierckx N, Westerhof RGM, Winde JH de, Ruijsenaars HJ. 2009. Bioproduction of *p*-hydroxystyrene from glucose by the solvent-tolerant bacterium *Pseudomonas putida* S12 in a two-phase water-decanol fermentation. *Applied and Environmental Microbiology* 75(4):931–936. doi: 10.1128/AEM.02186-08.
- [174] Connor MR, Cann AF, Liao JC. 2010. 3-Methyl-1-butanol production in *Escherichia coli*: Random mutagenesis and two-phase fermentation. *Applied Microbiology and Biotechnology* 86(4):1155–1164. doi: 10.1007/s00253-009-2401-1.
- [175] Ishii S, Taya M, Kobayashi T. 1985. Production of butanol by *Clostridium acetobutylicum* in extractive fermentation system. *Journal Chemical Engineering of Japan* 18(2):125–130. doi: 10.1252/jcej.18.125.
- [176] Minier M, Goma G. 1982. Ethanol production by extractive fermentation. *Biotechnology and Bioengineering* 24(7):1565–1579. doi: 10.1002/bit.260240710.
- [177] Badhwar P, Kumar P, Dubey KK. 2019. Extractive fermentation for process integration and amplified pullulan production by *A. pullulans* in aqueous two phase systems. *Scientific Reports* 9(1):32. doi: 10.1038/s41598-018-37314-y.
- [178] Volmer J, Schmid A, Bühler B. 2017. The application of constitutively solvent-tolerant *P. taiwanensis* VLB120Δ*CattgV* for stereospecific epoxidation of toxic styrene alleviates carrier solvent use. *Biotechnology Journal* 12(7):1600558. doi: 10.1002/biot.201600558.
- [179] Kuhn D, Bühler B, Schmid A. 2012. Production host selection for asymmetric styrene epoxidation: *Escherichia coli* vs. solvent-tolerant *Pseudomonas*. *Journal of Industrial Microbiology & Biotechnology* 39(8):1125–1133. doi: 10.1007/s10295-012-1126-9.
- [180] Janssen ACJM, Kierkels JGT, Lentzen GF. 2013. Two-Phase fermentation process for the production of an organic compound. US20160168595A1.
- [181] Job C, Blass E. 1994. Problems concerning liquid-liquid extraction of extracellular products directly from fermenter broths. *The Chemical Engineering Journal and the Biochemical Engineering Journal* 56(1):B1-B8. doi: 10.1016/0923-0467(94)87025-X.
- [182] Pursell MR, Mendes-Tassis MA, Stuckey DC. 2004. Effect of fermentation broth and biosurfactants on mass transfer during liquid-liquid extraction. *Biotechnology and Bioengineering* 85(2):155–165. doi: 10.1002/bit.10840.
- [183] Anvari M, Pahlavanzadeh H, Vasheghani-Farahani E, Khayati G. 2009. *In situ* recovery of 2,3-butanediol from fermentation by liquid-liquid extraction. *Journal of Industrial Microbiology & Biotechnology* 36(2):313–317. doi: 10.1007/s10295-008-0501-z.

- [184] Eiteman MA, Gainer JL. 1989. *In situ* extraction versus the use of an external column in fermentation. *Applied Microbiology and Biotechnology* 30(6):129–136. doi: 10.1007/BF00255368.
- [185] Prpich GP, Daugulis AJ. 2007. Solvent selection for enhanced bioproduction of 3-methylcatechol in a two-phase partitioning bioreactor. *Biotechnology and Bioengineering* 97(3):536–543. doi: 10.1002/bit.21257.
- [186] Job C, Schertler C, Staudenbauer WL, Blass E. 1989. Selection of organic solvents for *in situ* extraction of fermentation products from *Clostridium thermohydrosulfuricum* cultures. *Biotechnology Techniques* 3(5):315–320. doi: 10.1007/BF01875628.
- [187] Sánchez-Castañeda AK, Moussa M, Ngansop L, Trelea IC, Athès V. 2020. Organic phase screening for in-stream reactive extraction of bio-based 3-hydroxypropionic acid: Biocompatibility and extraction performances. *Journal of Chemical Technology & Biotechnology* 95(4):1046–1056. doi: 10.1002/jctb.6284.
- [188] Domańska U. 2019. Experimental data of fluid phase equilibria- correlation and prediction models: A review. *Processes* 7(5):277. doi: 10.3390/pr7050277.
- [189] Kollerup F, Daugulis AJ. 1985. Screening and identification of extractive fermentation solvents using a database. *The Canadian Journal of Chemical Engineering* 63(6):919–927. doi: 10.1002/cjce.5450630608.
- [190] Prat D, Hayler J, Wells A. 2014. A survey of solvent selection guides. *Green Chemistry* 16(10):4546–4551. doi: 10.1039/C4GC01149J.
- [191] Schmid A, Kollmer A, Mathys RG, Witholt B. 1998. Developments toward large-scale bacterial bioprocesses in the presence of bulk amounts of organic solvents. *Extremophiles* 2(3):249–256. doi: 10.1007/s007920050067.
- [192] Ramos JL, Duque E, Gallegos M-T, Godoy P, Ramos-González MI, Rojas A, Terán W, Segura A. 2002. Mechanisms of solvent tolerance in Gram-negative bacteria. *Annual Review of Microbiology* 56(1):743–768. doi: 10.1146/annurev.micro.56.012302.161038.
- [193] Heipieper HJ, Neumann G, Cornelissen S, Meinhardt F. 2007. Solvent-tolerant bacteria for biotransformations in two-phase fermentation systems. *Applied Microbiology and Biotechnology* 74(5):961–973. doi: 10.1007/s00253-006-0833-4.
- [194] Grütering C. 2019. Solvent selection for *in situ* extraction for rhamnolipid production using *Pseudomonas putida* KT2440 SK4. Internship Report. RWTH Aachen University.
- [195] Jackson RS (editor). 2008. Wine Science (Third Edition): Food science and technology. San Diego: Academic Press.
- [196] Blackford CL, Dennis EG, Keyzers RA, Schueuermann C, Trengove RD, Boss PK. 2018. Fermentation-guided natural products isolation of a grape berry triacylglyceride that enhances ethyl ester production. *Molecules (Basel, Switzerland)* 23(1):152. doi: 10.3390/molecules23010152.
- [197] Joint FAO/WHO Expert Committee on Food Additives. 1997. Evaluation of certain food additives and contaminants. Forty-sixth report of the Joint FAO/WHO expert committee on food additives. Geneva: World Health Organization. 69 p.
- [198] Burdock GA, Fenaroli G (editors). 2005. Fenaroli's handbook of flavor ingredients. Boca Raton: CRC Press. 1864 p.
- [199] Eagleson M. 2011. Concise encyclopedia chemistry. Hawthorne: De Gruyter. 1211 p.
- [200] Lovaglio RB, dos Santos FJ, Jafellicci M, Contiero J. 2011. Rhamnolipid emulsifying activity and emulsion stability: pH rules. *Colloids and Surfaces. B, Biointerfaces* 85(2):301–305. doi: 10.1016/j.colsurfb.2011.03.001.
- [201] Chen HT, Middleman S. 1967. Drop size distribution in agitated liquid-liquid systems. *AIChE Journal. American Institute of Chemical Engineers* 13(5):989–995. doi: 10.1002/aic.690130529.
- [202] Patel RM, Desai AJ. 1997. Surface-active properties of rhamnolipids from *Pseudomonas aeruginosa* GS3. *Journal of Basic Microbiology* 37(4):281–286. doi: 10.1002/jobm.3620370407.

- [203] Maaß S, Kraume M. 2012. Determination of breakage rates using single drop experiments. *Chemical Engineering Science* 70:146–164. doi: 10.1016/j.ces.2011.08.027.
- [204] Weinhhammer C, Blass E. 1994. Continuous fermentation with product recovery by *in-situ* extraction. *Chemical Engineering & Technology* 17(6):365–373. doi: 10.1002/ceat.270170602.
- [205] Kertes AS, King CJ. 1986. Extraction chemistry of fermentation product carboxylic acids. *Biotechnology and Bioengineering* 28(2):269–282. doi: 10.1002/bit.260280217.
- [206] Lebrón-Paler A, Pemberton JE, Becker BA, Otto WH, Larive CK, Maier RM. 2006. Determination of the acid dissociation constant of the biosurfactant monorhamnolipid in aqueous solution by potentiometric and spectroscopic methods. *Analytical Chemistry* 78(22):7649–7658. doi: 10.1021/ac0608826.
- [207] Servis MJ, Clark AE. 2019. Surfactant-enhanced heterogeneity of the aqueous interface drives water extraction into organic solvents. *Physical Chemistry Chemical Physics* 21(6):2866–2874. doi: 10.1039/C8CP06450D.
- [208] Kłosowska-Chomiczewska IE, Mędrzycka K, Hallmann E, Karpenko E, Pokynbroda T, Macierzanka A, Jungnickel C. 2017. Rhamnolipid CMC prediction. *Journal of Colloid and Interface Science* 488:10–19. doi: 10.1016/j.jcis.2016.10.055.
- [209] Biselli A, Willenbrink A-L, Leipnitz M, Jupke A. 2020. Development, evaluation, and optimisation of downstream process concepts for rhamnolipids and 3-(3-hydroxyalkanoyloxy)alkanoic acids. *Separation and Purification Technology* 250:117031. doi: 10.1016/j.seppur.2020.117031.
- [210] Özdemir G, Peker S, Helvacı S. 2004. Effect of pH on the surface and interfacial behavior of rhamnolipids R1 and R2. *Colloids and Surfaces. A, Physicochemical and Engineering Aspects* 234(1):135–143. doi: 10.1016/j.colsurfa.2003.10.024.
- [211] Grütering C. 2020. Bioprocess intensification for rhamnolipid production by implementing liquid-liquid extraction in an innovative multiphase loop reactor. Master Thesis. RWTH Aachen University.
- [212] Nikel PI, Chavarría M, Fuhrer T, Sauer U, de Lorenzo V. 2015. *Pseudomonas putida* KT2440 strain metabolizes glucose through a cycle formed by enzymes of the Entner-Doudoroff, Embden-Meyerhof-Parnas, and Pentose Phosphate Pathways. *Journal of Biological Chemistry* 290(43):25920–25932. doi: 10.1074/jbc.M115.687749.
- [213] Blank LM, Ionidis G, Ebert BE, Bühler B, Schmid A. 2008. Metabolic response of *Pseudomonas putida* during redox biocatalysis in the presence of a second octanol phase. *The FEBS Journal* 275(20):5173–5190. doi: 10.1111/j.1742-4658.2008.06648.x.
- [214] Chan Z, Zhong T, Yi Z, Xiao J, Zeng R. 2015. A pH shift feeding strategy for increased enduracidin production during fed–batch fermentation by a deep–sea bacterium *Streptomyces* sp. MC079. *Biotechnology and Bioengineering* 20(5):908–914. doi: 10.1007/s12257-015-0251-5.
- [215] Hosseinpour Tehrani H, Saur K, Tharmasothirajan A, Blank LM, Wierckx N. 2019. Process engineering of pH tolerant *Ustilago cynodontis* for efficient itaconic acid production. *Microbial Cell Factories* 18(1):213. doi: 10.1186/s12934-019-1266-y.
- [216] Bahl H, Andersch W, Braun K, Gottschalk G. 1982. Effect of pH and butyrate concentration on the production of acetone and butanol by *Clostridium acetobutylicum* grown in continuous culture. *Applied Microbiology and Biotechnology* 14(1):17–20. doi: 10.1007/BF00507998.
- [217] Henderson RK, Jiménez-González C, Constable DJC, Alston SR, Inglis GGA, Fisher G, Sherwood J, Binks SP, *et al.* 2011. Expanding GSK's solvent selection guide – Embedding sustainability into solvent selection starting at medicinal chemistry. *Green Chemistry* 13(4):854. doi: 10.1039/c0gc00918k.
- [218] Mannhold R, Poda GI, Ostermann C, Tetko IV. 2009. Calculation of molecular lipophilicity: State-of-the-art and comparison of Log *P* methods on more than 96,000 compounds. *Journal of Pharmaceutical Sciences* 98(3):861–893. doi: 10.1002/jps.21494.

- [219] Najmi Z, Ebrahimpour G, Franzetti A, Banat IM. 2018. *In situ* downstream strategies for cost-effective bio/surfactant recovery. *Biotechnology and Applied Biochemistry* 65(4):523–532. doi: 10.1002/bab.1641.
- [220] Kampwerth J, Weber B, Rußkamp J, Kaminski S, Jupke A. 2020. Towards a holistic solvent screening: On the importance of fluid dynamics in a rate-based extraction model. *Chemical Engineering Science* 227:115905. doi: 10.1016/j.ces.2020.115905.
- [221] Scheffczyk J, Redepenning C, Jens CM, Winter B, Leonhard K, Marquardt W, Bardow A. 2016. Massive, automated solvent screening for minimum energy demand in hybrid extraction–distillation using COSMO-RS. *Chemical Engineering Research & Design: Transactions of the Institution of Chemical Engineers* 115:433–442. doi: 10.1016/j.cherd.2016.09.029.
- [222] Kruber KF, Scheffczyk J, Leonhard K, Bardow A, Skiborowski M. 2018. A hierarchical approach for solvent selection based on successive model refinement. In: 28th European Symposium on Computer Aided Process Engineering: Elsevier. p 325–330.
- [223] Birajdar SD, Padmanabhan S, Rajagopalan S. 2014. Rapid solvent screening using thermodynamic models for recovery of 2,3-butanediol from fermentation by liquid–liquid extraction. *Journal of Chemical and Engineering Data* 59(8):2456–2463. doi: 10.1021/je500196e.
- [224] Piccione PM, Baumeister J, Salvesen T, Grosjean C, Flores Y, Groelly E, Murudi V, Shyadligeri A, *et al.* 2019. Solvent selection methods and tool. *Organic Process Research & Development* 23(5):998–1016. doi: 10.1021/acs.oprd.9b00065.
- [225] Prat D, Pardigon O, Flemming H-W, Letestu S, Ducandas V, Isnard P, Guntrum E, Senac T, *et al.* 2013. Sanofi's solvent selection guide: A step toward more sustainable processes. *Organic Process Research & Development* 17(12):1517–1525. doi: 10.1021/op4002565.
- [226] Diorazio LJ, Hose DRJ, Adlington NK. 2016. Toward a more holistic framework for solvent selection. *Organic Process Research & Development* 20(4):760–773. doi: 10.1021/acs.oprd.6b00015.
- [227] Alfonsi K, Colberg J, Dunn PJ, Fevig T, Jennings S, Johnson TA, Kleine HP, Knight C, *et al.* 2008. Green chemistry tools to influence a medicinal chemistry and research chemistry based organisation. *Green Chemistry* 10(1):31–36. doi: 10.1039/B711717E.
- [228] Alder CM, Hayler JD, Henderson RK, Redman AM, Shukla L, Shuster LE, Sneddon HF. 2016. Updating and further expanding GSK's solvent sustainability guide. *Green Chemistry* 18(13):3879–3890. doi: 10.1039/C6GC00611F.
- [229] Ringfeil M. 2004. Hydrocarbons and renewable energy. *Nature Biotechnology* 22(9):1077. doi: 10.1038/nbt0904-1077a.
- [230] Shears J. 2019. Is there a role for synthetic biology in addressing the transition to a new low-carbon energy system? *Microbial Biotechnology* 12(5):824–827. doi: 10.1111/1751-7915.13462.
- [231] Adegbeye MF, Ojuederie OB, Talia PM, Babalola OO. 2021. Bioprospecting of microbial strains for biofuel production: Metabolic engineering, applications, and challenges. *Biotechnology for Biofuels* 14(1):5. doi: 10.1186/s13068-020-01853-2.
- [232] Mendez-Perez D, Alonso-Gutierrez J, Hu Q, Molinas M, Baidoo EE, Wang G, Chan LJ, Adams PD, *et al.* 2017. Production of jet fuel precursor monoterpenoids from engineered *Escherichia coli*. *Biotechnology and Bioengineering* 114(8):1703–1712. doi: 10.1002/bit.26296.
- [233] Peralta-Yahya PP, Zhang F, Del Cardayre SB, Keasling JD. 2012. Microbial engineering for the production of advanced biofuels. *Nature* 488(7411):320–328. doi: 10.1038/nature11478.
- [234] Liu Y, Cruz-Morales P, Zargar A, Belcher MS, Pang B, Englund E, Dan Q, Yin K, *et al.* 2021. Biofuels for a sustainable future. *Cell* 184(6):1636–1647. doi: 10.1016/j.cell.2021.01.052.

- [235] Heipieper HJ, Martínez PM. 2010. Toxicity of hydrocarbons to microorganisms. In: Timmis KN, editor. Handbook of hydrocarbon and lipid microbiology. Berlin, Heidelberg: Springer Berlin Heidelberg. p 1563–1573.
- [236] Panke S, de Lorenzo V, Kaiser A, Witholt B, Wubbolts MG. 1999. Engineering of a stable whole-cell biocatalyst capable of (*S*)-styrene oxide formation for continuous two-liquid-phase applications. *Applied and Environmental Microbiology* 65(12):5619–5623. doi: 10.1128/AEM.65.12.5619-5623.1999.
- [237] Gross R, Buehler K, Schmid A. 2013. Engineered catalytic biofilms for continuous large scale production of *n*-octanol and (*S*)-styrene oxide. *Biotechnology and Bioengineering* 110(2):424–436. doi: 10.1002/bit.24629.
- [238] Dunlop MJ. 2011. Engineering microbes for tolerance to next-generation biofuels. *Biotechnology for Biofuels* 4(1):32. doi: 10.1186/1754-6834-4-32.
- [239] Ramos J-L, Sol Cuenca M, Molina-Santiago C, Segura A, Duque E, Gomez-Garcia MR, Udaondo Z, Roca A. 2015. Mechanisms of solvent resistance mediated by interplay of cellular factors in *Pseudomonas putida*. *FEMS Microbiology Reviews* 39(4):555–566. doi: 10.1093/femsre/fuv006.
- [240] Dunlop MJ, Dossani ZY, Szmidi HL, Chu HC, Lee TS, Keasling JD, Hadi MZ, Mukhopadhyay A. 2011. Engineering microbial biofuel tolerance and export using efflux pumps. *Molecular Systems Biology* 7:487. doi: 10.1038/msb.2011.21.
- [241] Basler G, Thompson M, Tullman-Ercek D, Keasling J. 2018. A *Pseudomonas putida* efflux pump acts on short-chain alcohols. *Biotechnology for Biofuels* 11(1):136. doi: 10.1186/s13068-018-1133-9.
- [242] Mezzina MP, Álvarez DS, Egoburo DE, Díaz Peña R, Nikel PI, Pettinari MJ, Müller V. 2017. A new player in the biorefineries field: Phasin PhaP enhances tolerance to solvents and boosts ethanol and 1,3-propanediol synthesis in *Escherichia coli*. *Applied and Environmental Microbiology* 83(14):e00662-17. doi: 10.1128/AEM.00662-17.
- [243] Okochi M, Kanie K, Kurimoto M, Yohda M, Honda H. 2008. Overexpression of prefoldin from the hyperthermophilic archaeum *Pyrococcus horikoshii* OT3 endowed *Escherichia coli* with organic solvent tolerance. *Applied Microbiology and Biotechnology* 79(3):443–449. doi: 10.1007/s00253-008-1450-1.
- [244] Routh MD, Zalucki Y, Su C-C, Zhang Q, Shafer WM, Yu EW. 2011. Efflux pumps of the resistance-nodulation-division family: A perspective of their structure, function, and regulation in Gram-negative bacteria. *Advances in Enzymology and Related Areas of Molecular Biology* 77:109–146. doi: 10.1002/9780470920541.ch3.
- [245] Rojas A, Duque E, Mosqueda G, Golden G, Hurtado A, Ramos JL, Segura A. 2001. Three efflux pumps are required to provide efficient tolerance to toluene in *Pseudomonas putida* DOT-T1E. *Journal of Bacteriology* 183(13):3967–3973. doi: 10.1128/JB.183.13.3967-3973.2001.
- [246] Rodríguez-Herva JJ, García V, Hurtado A, Segura A, Ramos JL. 2007. The *ttgGHI* solvent efflux pump operon of *Pseudomonas putida* DOT-T1E is located on a large self-transmissible plasmid. *Environmental Microbiology* 9(6):1550–1561. doi: 10.1111/j.1462-2920.2007.01276.x.
- [247] Kieboom J, Dennis JJ, de Bont JA, Zylstra GJ. 1998. Identification and molecular characterization of an efflux pump involved in *Pseudomonas putida* S12 solvent tolerance. *The Journal of Biological Chemistry* 273(1):85–91. doi: 10.1074/jbc.273.1.85.
- [248] Domínguez-Cuevas P, González-Pastor J-E, Marqués S, Ramos J-L, de Lorenzo V. 2006. Transcriptional tradeoff between metabolic and stress-response programs in *Pseudomonas putida* KT2440 cells exposed to toluene. *The Journal of Biological Chemistry* 281(17):11981–11991. doi: 10.1074/jbc.M509848200.
- [249] Segura A, Godoy P, van Dillewijn P, Hurtado A, Arroyo N, Santacruz S, Ramos J-L. 2005. Proteomic analysis reveals the participation of energy- and stress-related proteins in the

- response of *Pseudomonas putida* DOT-T1E to toluene. *Journal of Bacteriology* 187(17):5937–5945. doi: 10.1128/JB.187.17.5937-5945.2005.
- [250] Abdelaal AS, Ageez AM, Abd El-Hadi, Abd El-Hadi A, Abdallah NA. 2015. Genetic improvement of *n*-butanol tolerance in *Escherichia coli* by heterologous overexpression of *groESL* operon from *Clostridium acetobutylicum*. *3 Biotech* 5(4):401–410. doi: 10.1007/s13205-014-0235-8.
- [251] Tomas CA, Welker NE, Papoutsakis ET. 2003. Overexpression of *groESL* in *Clostridium acetobutylicum* results in increased solvent production and tolerance, prolonged metabolism, and changes in the cell's transcriptional program. *Applied and Environmental Microbiology* 69(8):4951–4965. doi: 10.1128/aem.69.8.4951-4965.2003.
- [252] Mans R, Daran J-MG, Pronk JT. 2018. Under pressure: Evolutionary engineering of yeast strains for improved performance in fuels and chemicals production. *Current Opinion in Biotechnology* 50:47–56. doi: 10.1016/j.copbio.2017.10.011.
- [253] Dragosits M, Mattanovich D. 2013. Adaptive laboratory evolution – Principles and applications for biotechnology. *Microbial Cell Factories* 12(1):64. doi: 10.1186/1475-2859-12-64.
- [254] Lim HG, Fong B, Alarcon G, Magurudeniya HD, Eng T, Szubin R, Olson CA, Palsson BO, et al. 2020. Generation of ionic liquid tolerant *Pseudomonas putida* KT2440 strains via adaptive laboratory evolution. *Green Chemistry* 22(17):5677–5690. doi: 10.1039/D0GC01663B.
- [255] Reyes LH, Almario MP, Winkler J, Orozco MM, Kao KC. 2012. Visualizing evolution in real time to determine the molecular mechanisms of *n*-butanol tolerance in *Escherichia coli*. *Metabolic Engineering* 14(5):579–590. doi: 10.1016/j.ymben.2012.05.002.
- [256] Horinouchi T, Tamaoka K, Furusawa C, Ono N, Suzuki S, Hirasawa T, Yomo T, Shimizu H. 2010. Transcriptome analysis of parallel-evolved *Escherichia coli* strains under ethanol stress. *BMC Genomics* 11(1):579. doi: 10.1186/1471-2164-11-579.
- [257] Bator I, Karmainski T, Tiso T, Blank LM. 2020. Killing two birds with one stone – Strain engineering facilitates the development of a unique rhamnolipid production process. *Frontiers in Bioengineering and Biotechnology* 8:899. doi: 10.3389/fbioe.2020.00899.
- [258] Qian Y, Huang H-H, Jiménez JI, Del Vecchio D. 2017. Resource competition shapes the response of genetic circuits. *ACS Synthetic Biology* 6(7):1263–1272. doi: 10.1021/acssynbio.6b00361.
- [259] Janardhan Garikipati, S. V. B., Peeples TL. 2015. Solvent resistance pumps of *Pseudomonas putida* S12: Applications in 1-naphthol production and biocatalyst engineering. *Journal of Biotechnology* 210:91–99. doi: 10.1016/j.jbiotec.2015.06.419.
- [260] Lorimer GH, Fei X, Ye X. 2018. The GroEL chaperonin: A protein machine with pistons driven by ATP binding and hydrolysis. *Philosophical Transactions of the Royal Society of London. Series B, Biological Sciences* 373(1749):20170179. doi: 10.1098/rstb.2017.0179.
- [261] Rennella E, Sára T, Juen M, Wunderlich C, Imbert L, Solyom Z, Favier A, Ayala I, et al. 2017. RNA binding and chaperone activity of the *E. coli* cold-shock protein CspA. *Nucleic Acids Research* 45(7):4255–4268. doi: 10.1093/nar/gkx044.
- [262] Mohamed ET, Werner AZ, Salvachúa D, Singer CA, Szostkiewicz K, Rafael Jiménez-Díaz M, Eng T, Radi MS, et al. 2020. Adaptive laboratory evolution of *Pseudomonas putida* KT2440 improves *p*-coumaric and ferulic acid catabolism and tolerance. *Metabolic Engineering Communications* 11:e00143-e00143. doi: 10.1016/j.mec.2020.e00143.
- [263] Zimmermann A. 2021. Improving the solvent tolerance of *Pseudomonas putida* KT2440 using rational strain engineering and adaptive laboratory evolution. Master Thesis. RWTH Aachen University.
- [264] Winsor GL, Griffiths EJ, Lo R, Dhillon BK, Shay JA, Brinkman FSL. 2016. Enhanced annotations and features for comparing thousands of *Pseudomonas* genomes in the

- Pseudomonas* genome database. *Nucleic Acids Research* 44(D1):D646-53. doi: 10.1093/nar/gkv1227.
- [265] Jeannot K, Elsen S, Köhler T, Attree I, van Delden C, Plésiat P. 2008. Resistance and virulence of *Pseudomonas aeruginosa* clinical strains overproducing the MexCD-OprJ efflux pump. *Antimicrobial Agents and Chemotherapy* 52(7):2455–2462. doi: 10.1128/AAC.01107-07.
- [266] Poole K, Gotoh N, Tsujimoto H, Zhao Q, Wada A, Yamasaki T, Neshat S, Yamagishi J, et al. 1996. Overexpression of the *mexC-mexD-oprJ* efflux operon in *nfxB*-type multidrug-resistant strains of *Pseudomonas aeruginosa*. *Molecular Microbiology* 21(4):713–724. doi: 10.1046/j.1365-2958.1996.281397.x.
- [267] Li XZ, Zhang L, Poole K. 1998. Role of the multidrug efflux systems of *Pseudomonas aeruginosa* in organic solvent tolerance. *Journal of Bacteriology* 180(11):2987–2991. doi: 10.1128/JB.180.11.2987-2991.1998.
- [268] Skerker JM, Perchuk BS, Siryaporn A, Lubin EA, Ashenberg O, Goulian M, Laub MT. 2008. Rewiring the specificity of two-component signal transduction systems. *Cell* 133(6):1043–1054. doi: 10.1016/j.cell.2008.04.040.
- [269] Krieger F, Möglich A, Kiefhaber T. 2005. Effect of proline and glycine residues on dynamics and barriers of loop formation in polypeptide chains. *Journal of the American Chemical Society* 127(10):3346–3352. doi: 10.1021/ja042798i.
- [270] Kanehisa M, Goto S, Furumichi M, Tanabe M, Hirakawa M. 2010. KEGG for representation and analysis of molecular networks involving diseases and drugs. *Nucleic Acids Research* 38:D355–D360. doi: 10.1093/nar/gkp896.
- [271] Kleinert G. 2020. Reverse engineering of *P. putida* KT2440 to enable tolerance to 1-octanol. Bachelor Thesis. RWTH Aachen University.
- [272] Nelson KE, Weinel C, Paulsen IT, Dodson RJ, Hilbert H, Martins dos Santos VAP, Fouts DE, Gill SR, et al. 2002. Complete genome sequence and comparative analysis of the metabolically versatile *Pseudomonas putida* KT2440. *Environmental Microbiology* 4(12):799–808. doi: 10.1046/j.1462-2920.2002.00366.x.
- [273] Hume AR, Nikodinovic-Runic J, O'Connor K. 2009. FadD from *Pseudomonas putida* CA-3 is a true long-chain fatty acyl coenzyme A synthetase that activates phenylalkanoic and alkanolic acids. *Journal of Bacteriology* 191(24):7554. doi: 10.1128/JB.01016-09.
- [274] He Q, Bennett GN, San K-Y, Wu H. 2019. Biosynthesis of medium-chain ω -hydroxy fatty acids by AlkBGT of *Pseudomonas putida* GPo1 with native FadL in engineered *Escherichia coli*. *Frontiers in Bioengineering and Biotechnology* 7:273. doi: 10.3389/fbioe.2019.00273.
- [275] Lieder S, Nikel PI, de Lorenzo V, Takors R. 2015. Genome reduction boosts heterologous gene expression in *Pseudomonas putida*. *Microbial Cell Factories* 14(1):23. doi: 10.1186/s12934-015-0207-7.
- [276] Martínez-García E, Nikel PI, Aparicio T, de Lorenzo V. 2014. *Pseudomonas* 2.0: Genetic upgrading of *P. putida* KT2440 as an enhanced host for heterologous gene expression. *Microbial Cell Factories* 13(1):159. doi: 10.1186/s12934-014-0159-3.
- [277] Li Y-C, Chang C, Chang C-F, Cheng Y-H, Fang P-J, Yu T, Chen S-C, Li Y-C, et al. 2014. Structural dynamics of the two-component response regulator RstA in recognition of promoter DNA element. *Nucleic Acids Research* 42(13):8777–8788. doi: 10.1093/nar/gku572.
- [278] Wright MS, Suzuki Y, Jones MB, Marshall SH, Rudin SD, van Duin D, Kaye K, Jacobs MR, et al. 2015. Genomic and transcriptomic analyses of colistin-resistant clinical isolates of *Klebsiella pneumoniae* reveal multiple pathways of resistance. *Antimicrobial Agents and Chemotherapy* 59(1):536. doi: 10.1128/AAC.04037-14.
- [279] Kidd TJ, Mills G, Sá-Pessoa J, Dumigan A, Frank CG, Insua JL, Ingram R, Hobley L, et al. 2017. A *Klebsiella pneumoniae* antibiotic resistance mechanism that subdues host

- defences and promotes virulence. *EMBO Molecular Medicine* 9(4):430–447. doi: 10.15252/emmm.201607336.
- [280] Liu Y, Li S, Li W, Wang P, Ding P, Li L, Wang J, Yang P, *et al.* 2019. RstA, a two-component response regulator, plays important roles in multiple virulence-associated processes in enterohemorrhagic *Escherichia coli* O157:H7. *Gut Pathogens* 11(1):53. doi: 10.1186/s13099-019-0335-4.
- [281] Huang L, Xu W, Su Y, Zhao L, Yan Q. 2018. Regulatory role of the RstB-RstA system in adhesion, biofilm production, motility, and hemolysis. *MicrobiologyOpen* 7(5):e00599. doi: 10.1002/mbo3.599.
- [282] Kusumawardhani H, Furtwängler B, Blommesteijn M, Kalteny  t   A, van der Poel J, Kolk J, Hosseini R, Winde JH de. 2021. Adaptive laboratory evolution restores solvent tolerance in plasmid-cured *Pseudomonas putida* S12; a molecular analysis. *Applied and Environmental Microbiology*. doi: 10.1128/AEM.00041-21.
- [283] Rosenberg M. 2006. Microbial adhesion to hydrocarbons: twenty-five years of doing MATH. *FEMS Microbiology Letters* 262(2):129–134. doi: 10.1111/j.1574-6968.2006.00291.x.
- [284] Brink L, Tramper J, Luyben K, van 't Riet K. 1988. Biocatalysis in organic media. *Enzyme and Microbial Technology* 10(12):736–743. doi: 10.1016/0141-0229(88)90118-4.
- [285] Oda S, Ohta H. 1992. Alleviation of toxicity of poisonous organic compounds on hydrophilic carrier/hydrophobic organic solvent interface. *Bioscience, Biotechnology, and Biochemistry* 56(9):1515–1517. doi: 10.1271/bbb.56.1515.
- [286] Kollmer A, Schmid A, Rohr PR von, Sonnleitner B. 1999. On liquid-liquid mass transfer in two-liquid-phase fermentations. *Bioprocess Engineering* 20(5):441–448. doi: 10.1007/s004490050613.
- [287] Herzog M, Li L, Blesken CC, Welsing G, Tiso T, Blank LM, Winter R. 2021. Impact of the number of rhamnose moieties of rhamnolipids on the structure, lateral organization and morphology of model biomembranes. *Soft Matter*. doi: 10.1039/D0SM01934H.
- [288] Herzog M, Tiso T, Blank LM, Winter R. 2020. Interaction of rhamnolipids with model biomembranes of varying complexity. *Biochimica et Biophysica Acta (BBA) - Biomembranes* 1862(11):183431. doi: 10.1016/j.bbamem.2020.183431.
- [289] Shuler ML, Kargi F, DeLisa M (editors). 2017. Bioprocess engineering. Boston: Prentice Hall.
- [290] Bartholomew WH, Reisman HB. 1979. Economics of fermentation processes. In: Peppler HJ, Perlman D, editors. Microbial technology (Second Edition): Academic Press. p 463–496.
- [291] Modak JM, Lim HC, Tayeb YJ. 1986. General characteristics of optimal feed rate profiles for various fed-batch fermentation processes. *Biotechnology and Bioengineering* 28(9):1396–1407. doi: 10.1002/bit.260280914.
- [292] Lee J, Lee SY, Park S, Middelberg AP. 1999. Control of fed-batch fermentations. *Biotechnology Advances* 17(1):29–48. doi: 10.1016/S0734-9750(98)00015-9.
- [293] Longobardi GP. 1994. Fed-batch versus batch fermentation. *Bioprocess Engineering* 10(5):185–194. doi: 10.1007/BF00369529.
- [294] Yaman   T, Shimizu S. 1984. Fed-batch techniques in microbial processes. In: Fiechter A, Shimizu S, editors. Bioprocess parameter control. Berlin, Heidelberg: Springer Berlin Heidelberg. p 147–194.
- [295] Pollock J, Ho SV, Farid SS. 2013. Fed-batch and perfusion culture processes: Economic, environmental, and operational feasibility under uncertainty. *Biotechnology and Bioengineering* 110(1):206–219. doi: 10.1002/bit.24608.
- [296] Hong J. 1986. Optimal substrate feeding policy for a fed batch fermentation with substrate and product inhibition kinetics. *Biotechnology and Bioengineering* 28(9):1421–1431. doi: 10.1002/bit.260280916.

- [297] Chiou J-P, Wang F-S. 1999. Hybrid method of evolutionary algorithms for static and dynamic optimization problems with application to a fed-batch fermentation process. *Computers & Chemical Engineering* 23(9):1277–1291. doi: 10.1016/S0098-1354(99)00290-2.
- [298] Rocha M, Mendes R, Rocha O, Rocha I, Ferreira EC. 2014. Optimization of fed-batch fermentation processes with bio-inspired algorithms. *Expert Systems with Applications* 41(5):2186–2195. doi: 10.1016/j.eswa.2013.09.017.
- [299] Zuo K, Wu WT. 2000. Semi-realtime optimization and control of a fed-batch fermentation system. *Computers & Chemical Engineering* 24(2):1105–1109. doi: 10.1016/S0098-1354(00)00490-7.
- [300] Bazsefidpar S, Mokhtarani B, Panahi R, Hajfarajollah H. 2019. Overproduction of rhamnolipid by fed-batch cultivation of *Pseudomonas aeruginosa* in a lab-scale fermenter under tight DO control. *Biodegradation* 30(1):59–69. doi: 10.1007/s10532-018-09866-3.
- [301] Yano T, Kurokawa M, Nishizawa Y. 1991. Optimum substrate feed rate in fed-batch culture with the DO-stat method. *Journal of Fermentation and Bioengineering* 71(5):345–349. doi: 10.1016/0922-338X(91)90348-K.
- [302] Davis R, Duane G, Kenny ST, Cerrone F, Guzik MW, Babu RP, Casey E, O'Connor KE. 2015. High cell density cultivation of *Pseudomonas putida* KT2440 using glucose without the need for oxygen enriched air supply. *Biotechnology and Bioengineering* 112(4):725–733. doi: 10.1002/bit.25474.
- [303] Unrean P, Champreda V. 2017. High-throughput screening and dual feeding fed-batch strategy for enhanced single-cell oil accumulation in *Yarrowia lipolytica*. *BioEnergy Research* 10(4):1057–1065. doi: 10.1007/s12155-017-9865-0.
- [304] Chen W, Graham C, Ciccarelli RB. 1997. Automated fed-batch fermentation with feed-back controls based on dissolved oxygen (DO) and pH for production of DNA vaccines. *Journal of Industrial Microbiology & Biotechnology* 18(1):43–48. doi: 10.1038/sj.jim.2900355.
- [305] Heeres AS, Picone CS, van der Wielen LA, Cunha RL, Cuellar MC. 2014. Microbial advanced biofuels production: Overcoming emulsification challenges for large-scale operation. *Trends in Biotechnology* 32(4):221–229. doi: 10.1016/j.tibtech.2014.02.002.
- [306] Strengé K, Seifert A. 1991. Determination of coalescence stability of emulsions by analytical ultracentrifugation under separation of dispersed phase. In: Borchard W, editor. *Progress in analytical ultracentrifugation*. Darmstadt: Steinkopff. p 76–83.
- [307] Shinoda K, Takeda H. 1970. The effect of added salts in water on the hydrophile-lipophile balance of nonionic surfactants: The effect of added salts on the phase inversion temperature of emulsions. *Journal of Colloid and Interface Science* 32(4):642–646. doi: 10.1016/0021-9797(70)90157-8.
- [308] Brandenbusch C, Glonke S, Collins J, Hoffrogge R, Grunwald K, Bühler B, Schmid A, Sadowski G. 2015. Process boundaries of irreversible scCO₂-assisted phase separation in biphasic whole-cell biocatalysis. *Biotechnology and Bioengineering* 112(11):2316–2323. doi: 10.1002/bit.25655.
- [309] Perazzo A, Preziosi V, Guido S. 2015. Phase inversion emulsification: Current understanding and applications. *Advances in Colloid and Interface Science* 222:581–599. doi: 10.1016/j.cis.2015.01.001.
- [310] Bouchama F, van Aken G, Autin A, Koper G. 2003. On the mechanism of catastrophic phase inversion in emulsions. *Colloids and Surfaces. A, Physicochemical and Engineering Aspects* 231(1):11–17. doi: 10.1016/j.colsurfa.2003.08.011.
- [311] Dunstan TS, Fletcher PDI, Mashinchi S. 2012. High internal phase emulsions: Catastrophic phase inversion, stability, and triggered destabilization. *Langmuir* 28(1):339–349. doi: 10.1021/la204104m.
- [312] Glonke S, Sadowski G, Brandenbusch C. 2016. Applied catastrophic phase inversion: A continuous non-centrifugal phase separation step in biphasic whole-cell biocatalysis.

- Journal of Industrial Microbiology & Biotechnology* 43(11):1527–1535. doi: 10.1007/s10295-016-1837-4.
- [313] Brandenbusch C, Sadowski G, Buehler B, Collins JA. 2019. Method for processing of stable emulsions from whole-cell biotransformations by means of phase inversion. US20150125931A1.
- [314] Heyd M, Kohnert A, Tan T-H, Nusser M, Kirschhöfer F, Brenner-Weiss G, Franzreb M, Berensmeier S. 2008. Development and trends of biosurfactant analysis and purification using rhamnolipids as an example. *Analytical and Bioanalytical Chemistry* 391(5):1579–1590. doi: 10.1007/s00216-007-1828-4.
- [315] Schenk T, Schuphan I, Schmidt B. 1995. High-performance liquid chromatographic determination of the rhamnolipids produced by *Pseudomonas aeruginosa*. *Journal of Chromatography. A* 693(1):7–13. doi: 10.1016/0021-9673(94)01127-Z.
- [316] Guerra-Santos L, Käppeli O, Fiechter A. 1984. *Pseudomonas aeruginosa* biosurfactant production in continuous culture with glucose as carbon source. *Applied and Environmental Microbiology* 48(2):301.
- [317] Levermann P, Freiburger F, Katha U, Zaun H, Möller J, Hass VC, Schoop KM, Kuballa J, et al. 2020. NMPC-based workflow for simultaneous process and model development applied to a fed-batch process for recombinant *C. glutamicum*. *Processes* 8(10):1313. doi: 10.3390/pr8101313.
- [318] Fink M, Cserjan-Puschmann M, Reinisch D, Striedner G. 2021. High-throughput microbioreactor provides a capable tool for early stage bioprocess development. *Scientific Reports* 11(1):2056. doi: 10.1038/s41598-021-81633-6.
- [319] Jansen R, Morschett H, Hasenklever D, Moch M, Wiechert W, Oldiges M. 2021. Microbioreactor-assisted cultivation workflows for time-efficient phenotyping of protein producing *Aspergillus niger* in batch and fed-batch mode. *Biotechnology Progress* e3144. doi: 10.1002/btpr.3144.
- [320] Lima-Ramos J, Tufvesson P, Woodley JM. 2014. Application of environmental and economic metrics to guide the development of biocatalytic processes. *Green Processing and Synthesis* 3(3):195–213. doi: 10.1515/gps-2013-0094.
- [321] Ankenbauer A, Schäfer RA, Viegas SC, Pobre V, Voß B, Arraiano CM, Takors R. 2020. *Pseudomonas putida* KT2440 is naturally endowed to withstand industrial-scale stress conditions. *Microbial Biotechnology* 13(4):1145–1161. doi: 10.1111/1751-7915.13571.
- [322] Hintermayer SB, Weuster-Botz D. 2017. Experimental validation of *in silico* estimated biomass yields of *Pseudomonas putida* KT2440. *Biotechnology Journal* 12(6). doi: 10.1002/biot.201600720.
- [323] Blank LM, Narancic T, Mampel J, Tiso T, O'Connor K. 2020. Biotechnological upcycling of plastic waste and other non-conventional feedstocks in a circular economy. *Current Opinion in Biotechnology* 62:212–219. doi: 10.1016/j.copbio.2019.11.011.
- [324] Tiso T, Narancic T, Wei R, Pollet E, Beagan N, Schröder K, Honak A, Jiang M, et al. 2021. Towards bio-upcycling of polyethylene terephthalate. *Metabolic Engineering* 66:167–178. doi: 10.1016/j.mben.2021.03.011.
- [325] Nikel PI, Fuhrer T, Chavarria M, Sánchez-Pascuala A, Sauer U, de Lorenzo V. 2020. Redox stress reshapes carbon fluxes of *Pseudomonas putida* for cytosolic glucose oxidation and NADPH generation. *bioRxiv*:2020.06.13.149542. doi: 10.1101/2020.06.13.149542.
- [326] Nikel PI, de Lorenzo V. 2014. Robustness of *Pseudomonas putida* KT2440 as a host for ethanol biosynthesis. *New Biotechnology* 31(6):562–571. doi: 10.1016/j.nbt.2014.02.006.
- [327] Simon O, Klebensberger J, Mukschel B, Klaiber I, Graf N, Altenbuchner J, Huber A, Hauer B, et al. 2015. Analysis of the molecular response of *Pseudomonas putida* KT2440 to the next-generation biofuel *n*-butanol. *Journal of Proteomics* 122:11–25. doi: 10.1016/j.jpro.2015.03.022.

-
- [328] Enfors S-O, Jahic M, Rozkov A, Xu B, Hecker M, Jürgen B, Krüger E, Schweder T, *et al.* 2001. Physiological responses to mixing in large scale bioreactors. *Journal of Biotechnology* 85(2):175–185. doi: 10.1016/S0168-1656(00)00365-5.
- [329] Kuschel M, Takors R. 2020. Simulated oxygen and glucose gradients as a prerequisite for predicting industrial scale performance *a priori*. *Biotechnology and Bioengineering* 117(9):2760–2770. doi: 10.1002/bit.27457.
- [330] Neubauer P, Haggstrom L, Enfors SO. 1995. Influence of substrate oscillations on acetate formation and growth yield in *Escherichia coli* glucose limited fed-batch cultivations. *Biotechnology and Bioengineering* 47(2):139–146. doi: 10.1002/bit.260470204.
- [331] Neubauer P, Junne S. 2010. Scale-down simulators for metabolic analysis of large-scale bioprocesses. *Current Opinion in Biotechnology* 21(1):114–121. doi: 10.1016/j.copbio.2010.02.001.
- [332] Olugbu W, Deepika G, Hewitt C, Rielly C. 2019. Insight into the large-scale upstream fermentation environment using scaled-down models. *Journal of Chemical Technology & Biotechnology* 94(3):647–657. doi: 10.1002/jctb.5804.
- [333] Nadal-Rey G, McClure DD, Kavanagh JM, Cornelissen S, Fletcher DF, Gernaey KV. 2020. Understanding gradients in industrial bioreactors. *Biotechnology Advances*:107660. doi: 10.1016/j.biotechadv.2020.107660.
- [334] Soini J, Ukkonen K, Neubauer P. 2008. High cell density media for *Escherichia coli* are generally designed for aerobic cultivations – Consequences for large-scale bioprocesses and shake flask cultures. *Microbial Cell Factories* 7(1):26. doi: 10.1186/1475-2859-7-26.
- [335] Limberg MH, Joachim M, Klein B, Wiechert W, Oldiges M. 2017. pH fluctuations imperil the robustness of *C. glutamicum* to short term oxygen limitation. *Journal of Biotechnology* 259:248–260. doi: 10.1016/j.jbiotec.2017.08.018.
- [336] Lange J, Münch E, Müller J, Busche T, Kalinowski J, Takors R, Blombach B. 2018. Deciphering the adaptation of *Corynebacterium glutamicum* in transition from aerobiosis via microaerobiosis to anaerobiosis. *Genes* 9(6):297. doi: 10.3390/genes9060297.
- [337] Lórantfy B, Jazini M, Herwig C. 2013. Investigation of the physiological response to oxygen limited process conditions of *Pichia pastoris* Mut+ strain using a two-compartment scale-down system. *Journal of Bioscience and Bioengineering* 116(3):371–379. doi: 10.1016/j.jbiosc.2013.03.021.
- [338] Kar T, Destain J, Thonart P, Delvigne F. 2012. Scale-down assessment of the sensitivity of *Yarrowia lipolytica* to oxygen transfer and foam management in bioreactors: Investigation of the underlying physiological mechanisms. *Journal of Industrial Microbiology & Biotechnology* 39(2):337–346. doi: 10.1007/s10295-011-1030-8.
- [339] Bellou S, Makri A, Triantaphyllidou I-E, Papanikolaou S, Aggelis G. 2014. Morphological and metabolic shifts of *Yarrowia lipolytica* induced by alteration of the dissolved oxygen concentration in the growth environment. *Microbiology* 160(4):807–817. doi: 10.1099/mic.0.074302-0.
- [340] Timoumi A, Bideaux C, Guillouet SE, Allouche Y, Molina-Jouve C, Fillaudeau L, Gorret N. 2017. Influence of oxygen availability on the metabolism and morphology of *Yarrowia lipolytica*: Insights into the impact of glucose levels on dimorphism. *Applied Microbiology and Biotechnology* 101(19):7317–7333. doi: 10.1007/s00253-017-8446-7.
- [341] Nikel PI, de Lorenzo V. 2013. Engineering an anaerobic metabolic regime in *Pseudomonas putida* KT2440 for the anoxic biodegradation of 1,3-dichloroprop-1-ene. *Metabolic Engineering* 15:98–112. doi: 10.1016/j.mben.2012.09.006.
- [342] Sohn SB, Kim TY, Park JM, Lee SY. 2010. In silico genome-scale metabolic analysis of *Pseudomonas putida* KT2440 for polyhydroxyalkanoate synthesis, degradation of aromatics and anaerobic survival. *Biotechnology Journal* 5(7):739–750. doi: 10.1002/biot.201000124.
- [343] Steen A, Ütkür FÖ, Borrero-de Acuña JM, Bunk B, Roselius L, Bühler B, Jahn D, Schobert M. 2013. Construction and characterization of nitrate and nitrite respiring
-

- Pseudomonas putida* KT2440 strains for anoxic biotechnical applications. *Journal of Biotechnology* 163(2):155–165. doi: 10.1016/j.jbiotec.2012.09.015.
- [344] Lai B, Yu S, Bernhardt PV, Rabaey K, Virdis B, Krömer JO. 2016. Anoxic metabolism and biochemical production in *Pseudomonas putida* F1 driven by a bioelectrochemical system. *Biotechnology for Biofuels* 9(1):39. doi: 10.1186/s13068-016-0452-y.
- [345] Schmitz S, Nies S, Wierckx N, Blank LM, Rosenbaum MA. 2015. Engineering mediator-based electroactivity in the obligate aerobic bacterium *Pseudomonas putida* KT2440. *Frontiers in Microbiology* 6:284. doi: 10.3389/fmicb.2015.00284.
- [346] Yu S, Lai B, Plan MR, Hodson MP, Lestari EA, Song H, Krömer JO. 2018. Improved overperformance of *Pseudomonas putida* in a bioelectrochemical system through overexpression of periplasmic glucose dehydrogenase. *Biotechnology and Bioengineering* 115(1):145–155. doi: 10.1002/bit.26433.
- [347] Askitosari TD, Berger C, Tiso T, Harnisch F, Blank LM, Rosenbaum MA. 2020. Coupling an electroactive *Pseudomonas putida* KT2440 with bioelectrochemical rhamnolipid production. *Microorganisms* 8(12):1959. doi: 10.3390/microorganisms8121959.
- [348] Kampers LFC, van Heck RGA, Donati S, Saccenti E, Volkers RJM, Schaap PJ, Suarez-Diez M, Nikel PI, et al. 2019. *In silico*-guided engineering of *Pseudomonas putida* towards growth under micro-oxic conditions. *Microbial Cell Factories* 18(1):179. doi: 10.1186/s12934-019-1227-5.
- [349] Kampers LFC, Koehorst JJ, van Heck RJA, Suarez-Diez M, Stams AJM, Schaap PJ. 2021. A metabolic and physiological design study of *Pseudomonas putida* KT2440 capable of anaerobic respiration. *BMC Microbiology* 21(1):9. doi: 10.1186/s12866-020-02058-1.
- [350] John GT, Klimant I, Wittmann C, Heinze E. 2003. Integrated optical sensing of dissolved oxygen in microtiter plates: A novel tool for microbial cultivation. *Biotechnology and Bioengineering* 81(7):829–836. doi: 10.1002/bit.10534.
- [351] Marques MPC, Cabral JMS, Fernandes P. 2010. Bioprocess scale-up: Quest for the parameters to be used as criterion to move from microreactors to lab-scale. *Journal of Chemical Technology & Biotechnology* 85(9):1184–1198. doi: 10.1002/jctb.2387.
- [352] Lebrun G, Xu F, Le Men C, Hébrard G, Dietrich N. 2021. Gas–liquid mass transfer around a rising bubble: Combined effect of rheology and surfactant. *Fluids*, 6(2), 84; doi: 10.3390/fluids6020084
- [353] Tiso T, Sabelhaus P, Behrens B, Wittgens A, Rosenau F, Hayen H, Blank LM. 2016. Creating metabolic demand as an engineering strategy in *Pseudomonas putida* - Rhamnolipid synthesis as an example. *Metabolic Engineering Communications* 3:234–244. doi: 10.1016/j.meten.2016.08.002.
- [354] Röck F. 2021. Einfluss von Sauerstoffoszillationen auf die Rhamnolipidproduktion von *Pseudomonas putida* KT2440 SK4. Internship Report. RWTH Aachen University.
- [355] Tatusov RL, Koonin EV, Lipman DJ. 1997. A genomic perspective on protein families. *Science* 278(5338):631. doi: 10.1126/science.278.5338.631.
- [356] Kuschel M, Siebler F, Takors R. 2017. Lagrangian trajectories to predict the formation of population heterogeneity in large-scale bioreactors. *Bioengineering* 4(2):27. doi: 10.3390/bioengineering4020027.
- [357] Haringa C, Tang W, Deshmukh AT, Xia J, Reuss M, Heijnen JJ, Mudde RF, Noorman HJ. 2016. Euler-Lagrange computational fluid dynamics for (bio)reactor scale down: An analysis of organism lifelines. *Engineering in Life Sciences* 16(7):652–663. doi: 10.1002/elsc.201600061.
- [358] Lieder S, Jahn M, Koepff J, Muller S, Takors R. 2016. Environmental stress speeds up DNA replication in *Pseudomonas putida* in chemostat cultivations. *Biotechnology Journal* 11(1):155–163. doi: 10.1002/biot.201500059.
- [359] Escobar S, Rodriguez A, Gomez E, Alcon A, Santos VE, Garcia-Ochoa F. 2016. Influence of oxygen transfer on *Pseudomonas putida* effects on growth rate and biodesulfurization

- capacity. *Bioprocess and Biosystems Engineering* 39(4):545–554. doi: 10.1007/s00449-016-1536-6.
- [360] Rodriguez A, Escobar S, Gomez E, Santos VE, Garcia-Ochoa F. 2018. Behavior of several *Pseudomonas putida* strains growth under different agitation and oxygen supply conditions. *Biotechnology Progress* 34(4):900–909. doi: 10.1002/btpr.2634.
- [361] Chavarría M, Nikel PI, Pérez-Pantoja D, de Lorenzo V. 2013. The Entner–Doudoroff pathway empowers *Pseudomonas putida* KT2440 with a high tolerance to oxidative stress. *Environmental Microbiology* 15(6):1772–1785. doi: 10.1111/1462-2920.12069.
- [362] Chapman AG, Fall L, Atkinson DE. 1971. Adenylate energy charge in *Escherichia coli* during growth and starvation. *Journal of Bacteriology* 108:1072–1086.
- [363] Vallon T, Simon O, Rendgen-Heugle B, Frana S, Mückschel B, Broicher A, Siemann-Herzberg M, Pfannenstiel J, et al. 2015. Applying systems biology tools to study *n*-butanol degradation in *Pseudomonas putida* KT2440. *Engineering in Life Sciences* 15(8):760–771. doi: 10.1002/elsc.201400051.
- [364] Hauryliuk V, Atkinson GC, Murakami KS, Tenson T, Gerdes K. 2015. Recent functional insights into the role of (p)ppGpp in bacterial physiology. *Nature Reviews. Microbiology* 13(5):298–309. doi: 10.1038/nrmicro3448.
- [365] Traxler MF, Zacharia VM, Marquardt S, Summers SM, Nguyen H-T, Stark SE, Conway T. 2011. Discretely calibrated regulatory loops controlled by ppGpp partition gene induction across the ‘feast to famine’ gradient in *Escherichia coli*. *Molecular Microbiology* 79(4):830–845. doi: 10.1111/j.1365-2958.2010.07498.x.
- [366] Löffler M, Simen JD, Jäger G, Schäferhoff K, Freund A, Takors R. 2016. Engineering *E. coli* for large-scale production – Strategies considering ATP expenses and transcriptional responses. *Metabolic Engineering* 38:73–85. doi: 10.1016/j.ymben.2016.06.008.
- [367] Klinke S, Dauner M, Scott G, Kessler B, Witholt B. 2000. Inactivation of isocitrate lyase leads to increased production of medium-chain-length poly(3-hydroxyalkanoates) in *Pseudomonas putida*. *Applied and Environmental Microbiology* 66(3):909–913. doi: 10.1128/aem.66.3.909-913.2000.
- [368] Obruca S, Sedlacek P, Koller M, Kucera D, Pernicova I. 2018. Involvement of polyhydroxyalkanoates in stress resistance of microbial cells: Biotechnological consequences and applications. *Biotechnology Advances* 36(3):856–870. doi: 10.1016/j.biotechadv.2017.12.006.
- [369] Thompson MG, Incha MR, Pearson AN, Schmidt M, Sharpless WA, Eiben CB, Cruz-Morales P, Blake-Hedges JM, et al. 2020. Fatty acid and alcohol metabolism in *Pseudomonas putida*: Functional analysis using random barcode transposon sequencing. *Applied and Environmental Microbiology* 86(21):e01665-20. doi: 10.1128/AEM.01665-20.
- [370] Li W-J, Narancic T, Kenny ST, Niehoff P-J, O'Connor K, Blank LM, Wierckx N. 2020. Unraveling 1,4-butanediol metabolism in *Pseudomonas putida* KT2440. *Frontiers in Microbiology* 11:382. doi: 10.3389/fmicb.2020.00382.
- [371] García-Horsman JA, Barquera B, Rumbley J, Ma J, Gennis RB. 1994. The superfamily of heme-copper respiratory oxidases. *Journal of Bacteriology* 176(18):5587. doi: 10.1128/jb.176.18.5587-5600.1994.
- [372] Wehrmann M, Elsayed EM, Köbbing S, Bendz L, Lepak A, Schwabe J, Wierckx N, Bange G, et al. 2020. Engineered PQQ-dependent alcohol dehydrogenase for the oxidation of 5-(hydroxymethyl)furoic acid. *ACS Catalysis* 10(14):7836–7842. doi: 10.1021/acscatal.0c01789.
- [373] Dewangan NK, Conrad JC. 2020. Bacterial motility enhances adhesion to oil droplets. *Soft Matter* 16(35):8237–8244. doi: 10.1039/D0SM00944J.

- [374] Guieysse B, Quijano G, Muñoz R. 2011. Airlift Bioreactors. In: Moo-Young M, editor. *Comprehensive biotechnology. Principles and practices in industry, agriculture, medicine and the environment*. Amsterdam: Elsevier. p 199–212.
- [375] Chisti Y, Moo-Young M. 1989. On the calculation of shear rate and apparent viscosity in airlift and bubble column bioreactors. *Biotechnology and Bioengineering* 34(11):1391–1392. doi: 10.1002/bit.260341107.
- [376] Gavrilescu M, Roman RV. 1998. Performance of airlift bioreactors in the cultivation of some antibiotic producing microorganisms. *Acta Biotechnologica* 18(3):201–229. doi: 10.1002/abio.370180304.
- [377] Nielsen J, Villadsen J, Lidén G. 2003. Scale-up of bioprocesses. In: Nielsen J, Villadsen J, Lidén G, editors. *Bioreaction engineering principles*. Boston, MA: Springer US. p 477–518.
- [378] Siegel MH, Robinson CW. 1992. Application of airlift gas-liquid-solid reactors in biotechnology. *Chemical Engineering Science* 47(13):3215–3229. doi: 10.1016/0009-2509(92)85030-F.
- [379] Heijnen JJ, Hols J, van der Lans R, van Leeuwen H, Mulder A, Weltevrede R. 1997. A simple hydrodynamic model for the liquid circulation velocity in a full-scale two- and three-phase internal airlift reactor operating in the gas recirculation regime. *Chemical Engineering Science* 52(15):2527–2540. doi: 10.1016/S0009-2509(97)00070-5.
- [380] Chisti MY, Halard B, Moo-Young M. 1988. Liquid circulation in airlift reactors. *Chemical Engineering Science* 43(3):451–457. doi: 10.1016/0009-2509(88)87005-2.
- [381] Chisti Y. 1998. Pneumatically agitated bioreactors in industrial and environmental bioprocessing: Hydrodynamics, hydraulics, and transport phenomena. *Applied Mechanics Reviews* 51(1):33–112. doi: 10.1115/1.3098989.
- [382] Chisti MY, Moo-Young M. 1987. Airlift reactors: Characteristics, applications and design considerations. *Chemical Engineering Communications* 60(1-6):195–242. doi: 10.1080/00986448708912017.
- [383] Chisti MY. 1989. *Airlift bioreactors*. London: Elsevier. 345 p.
- [384] Degen J, Uebele A, Retze A, Schmid-Staiger U, Trösch W. 2001. A novel airlift photobioreactor with baffles for improved light utilization through the flashing light effect. *Journal of Biotechnology* 92(2):89–94. doi: 10.1016/S0168-1656(01)00350-9.
- [385] Ghosh TK, Maiti BR, Bhattacharyya BC. 1993. Studies on mass transfer characteristics of a modified airlift fermenter. *Bioprocess Engineering* 9(6):239–244. doi: 10.1007/BF01061528.
- [386] Wu J-Y, Wu W-T. 1991. Fed-batch culture of *Saccharomyces cerevisiae* in an airlift reactor with net draft tube. *Biotechnology Progress* 7(3):230–233. doi: 10.1021/bp00009a005.
- [387] Karamanev DG, Chavarie C, Samson R. 1996. Hydrodynamics and mass transfer in an airlift reactor with a semipermeable draft tube. *Chemical Engineering Science* 51(7):1173–1176. doi: 10.1016/S0009-2509(96)80016-9.
- [388] Särkelä R, Eerikäinen T, Pitkänen J-P, Bankar S. 2019. Mixing efficiency studies in an airlift bioreactor with helical flow promoters for improved reactor performance. *Chemical Engineering and Processing - Process Intensification* 137:80–86. doi: 10.1016/j.cep.2019.02.006.
- [389] Gavrilescu M, Roman RV, Tudose RZ. 1997. Hydrodynamics in external-loop airlift bioreactors with static mixers. *Bioprocess Engineering* 16(2):93–99. doi: 10.1007/s004490050294.
- [390] Chisti Y, Jauregui-Haza UJ. 2002. Oxygen transfer and mixing in mechanically agitated airlift bioreactors. *Biochemical Engineering Journal* 10(2):143–153. doi: 10.1016/S1369-703X(01)00174-7.

-
- [391] Nikakhtari H, Hill GA. 2005. Hydrodynamic and oxygen mass transfer in an external loop airlift bioreactor with a packed bed. *Biochemical Engineering Journal* 27(2):138–145. doi: 10.1016/j.bej.2005.08.014.
 - [392] Pirsahab M, Hossaini H, Nabizadeh R, Azizi N. 2020. Zeolite-intermittent cycle moving bed air-lift bioreactor (Zeo-ICMBABR) for composting leachate treatment; simultaneous COD, nitrogen and phosphorous compounds removal. *Journal of Environmental Health Science and Engineering* 18(2):933–945. doi: 10.1007/s40201-020-00517-5.
 - [393] Campani G, Ribeiro MPA, Horta ACL, Giordano RC, Badino AC, Zangirolami TC. 2015. Oxygen transfer in a pressurized airlift bioreactor. *Bioprocess Engineering* 38(8):1559–1567. doi: 10.1007/s00449-015-1397-4.
 - [394] Bakker WA, Kers P, Beeftink HH, Tramper J, Gooijer CD de. 1996. Nitrite conversion by immobilized *Nitrobacter agilis* cells in an air-lift loop bioreactor cascade: Effects of combined substrate and product inhibition. *Journal of Fermentation and Bioengineering* 81(5):390–393. doi: 10.1016/0922-338X(96)85138-5.
 - [395] Bakker WA, Overdevest PE, Beeftink HH, Tramper J, Gooijer CD de. 1997. Serial air-lift bioreactors for the approximation of aerated plug flow. *Trends in Biotechnology* 15(7):264–269. doi: 10.1016/S0167-7799(97)01053-6.
 - [396] Wang IC, Hatch RT, Cuevas C. 1971. Engineering aspects of single-cell protein production from hydrocarbon substrates: The airlift fermentor. In: 8th World Petroleum Congress. Moscow.
 - [397] Chen NY. 1990. The design of airlift fermenters for use in biotechnology. *Biotechnology and Genetic Engineering Reviews* 8(1):379–396. doi: 10.1080/02648725.1990.10647875.
 - [398] Kracke-Helm HA, Rinas U, Hitzmann B, Schügerl K. 1991. Cultivation of recombinant *E. coli* and production of fusion protein in 60 L bubble column and airlift tower loop reactors. *Enzyme and Microbial Technology* 13(7):554–564. doi: 10.1016/0141-0229(91)90091-N.
 - [399] Mihai M, Gavin SP, Markoš J. 2013. Airlift reactor-membrane extraction hybrid system for aroma production. *Chemical Papers* 67(12):1485–1494. doi: 10.2478/s11696-012-0261-0.
 - [400] Bakker WAM, Knitel JT, Tramper J, Gooijer CD de. 1994. Sucrose conversion by immobilized invertase in a multiple air-lift loop bioreactor. *Biotechnology Progress* 10(3):277–283. doi: 10.1021/bp00027a007.
 - [401] Mirghorayshi M, Zinatizadeh AA, van Loosdrecht M. 2021. Simultaneous biodegradability enhancement and high-efficient nitrogen removal in an innovative single stage anaerobic/anoxic/aerobic hybrid airlift bioreactor (HALBR) for composting leachate treatment: Process modeling and optimization. *Chemical Engineering Journal* 407:127019. doi: 10.1016/j.cej.2020.127019.
 - [402] Sun Y, Li Y-L, Bai S, Hu Z-D. 1999. Modeling and simulation of an *in situ* product removal process for lactic acid production in an airlift bioreactor. *Industrial & Engineering Chemistry Research* 38(9):3290–3295. doi: 10.1021/ie990090k.
 - [403] Millitzer M, Wenzig E, Peukert W. 2005. Process modeling of *in situ*-adsorption of a bacterial lipase. *Biotechnology and Bioengineering* 92(6):789–801. doi: 10.1002/bit.20661.
 - [404] Dietz S. 2021. Experimental investigation of the oxygen transfer in the MPLR. Internship Report. RWTH Aachen University.
 - [405] Rols JL, Condoret JS, Fonade C, Goma G. 1990. Mechanism of enhanced oxygen transfer in fermentation using emulsified oxygen-vectors. *Biotechnology and Bioengineering* 35(4):427–435. doi: 10.1002/bit.260350410.
 - [406] Quijano G, Revah S, Gutiérrez-Rojas M, Flores-Cotera LB, Thalasso F. 2009. Oxygen transfer in three-phase airlift and stirred tank reactors using silicone oil as transfer vector. *Process Biochemistry* 44(6):619–624. doi: 10.1016/j.procbio.2009.01.015.
 - [407] Clift R, Grace JR, Weber ME. 2005. Bubbles, drops, and particles. Mineola, New York: Dover Publications Inc. 381 p.
-

- [408] Jamialahmadi M, Müller-Steinhagen H. 1993. Effect of superficial gas velocity on bubble size, terminal bubble rise velocity and gas hold-up in bubble columns. *Developments in Chemical Engineering and Mineral Processing* 1(1):16–31. doi: 10.1002/apj.5500010103.
- [409] Alves SS, Orvalho SP, Vasconcelos J. 2005. Effect of bubble contamination on rise velocity and mass transfer. *Chemical Engineering Science* 60(1):1–9. doi: 10.1016/j.ces.2004.07.053.
- [410] Sánchez Mirón A, Cerón García M-C, García Camacho F, Molina Grima E, Chisti Y. 2004. Mixing in bubble column and airlift reactors. *Chemical Engineering Research & Design: Transactions of the Institution of Chemical Engineers* 82(10):1367–1374. doi: 10.1205/cerd.82.10.1367.46742.
- [411] Marangoni C. 1865. Sull'espansione delle gocce d'un liquido galleggianti sulla superficie di altro liquido: Fratelli Fusi.
- [412] Gibbs JW. 1878. On the equilibrium of heterogeneous substances. *American Journal of Science* s3-16(96):441–458. doi: 10.2475/ajs.s3-16.96.441.
- [413] Tomiyama A, Celata GP, Hosokawa S, Yoshida S. 2002. Terminal velocity of single bubbles in surface tension force dominant regime. *International Journal of Multiphase Flow* 28(9):1497–1519. doi: 10.1016/S0301-9322(02)00032-0.
- [414] Luhede L, Wollborn T, Fritsching U. 2020. Stability of multiple emulsions under shear stress. *The Canadian Journal of Chemical Engineering* 98(1):186–193. doi: 10.1002/cjce.23578.
- [415] Heeres AS, Schroën K, Heijnen JJ, van der Wielen LAM, Cuellar MC. 2015. Fermentation broth components influence droplet coalescence and hinder advanced biofuel recovery during fermentation. *Biotechnology Journal* 10(8):1206–1215. doi: 10.1002/biot.201400570.
- [416] Kulkarni PS, Patel SU, Chase GG. 2012. Layered hydrophilic/hydrophobic fiber media for water-in-oil coalescence. *Separation and Purification Technology* 85:157–164. doi: 10.1016/j.seppur.2011.10.004.
- [417] Wohlgemuth R, Twardowski T, Aguilar A. 2021. Bioeconomy moving forward step by step – A global journey. *New Biotechnology* 61:22–28. doi: 10.1016/j.nbt.2020.11.006.
- [418] Lokko Y, Heijde M, Schebesta K, Scholtès P, van Montagu M, Giacca M. 2018. Biotechnology and the bioeconomy - Towards inclusive and sustainable industrial development. *New Biotechnology* 40:5–10. doi: 10.1016/j.nbt.2017.06.005.
- [419] Noorman H. 2011. An industrial perspective on bioreactor scale-down: What we can learn from combined large-scale bioprocess and model fluid studies. *Biotechnology Journal* 6(8):934–943. doi: 10.1002/biot.201000406.
- [420] Türker M. 2003. Measurement of metabolic heat in a production-scale bioreactor by continuous and dynamic calorimetry. *Chemical Engineering Communications* 190(5-8):573–598. doi: 10.1080/00986440302130.
- [421] Shaikh A, Al-Dahhan M. 2013. Scale-up of bubble column reactors: A review of current state-of-the-art. *Industrial & Engineering Chemistry Research* 52(24):8091–8108. doi: 10.1021/ie302080m.
- [422] Anastasovski A, Rašković P, Guzović Z. 2015. Design and analysis of heat recovery system in bioprocess plant. *Energy Conversion and Management* 104:32–43. doi: 10.1016/j.enconman.2015.06.081.
- [423] Junker BH. 2004. Scale-up methodologies for *Escherichia coli* and yeast fermentation processes. *Journal of Bioscience and Bioengineering* 97(6):347–364. doi: 10.1016/S1389-1723(04)70218-2.
- [424] Heins A-L, Weuster-Botz D. 2018. Population heterogeneity in microbial bioprocesses: Origin, analysis, mechanisms, and future perspectives. *Bioprocess Engineering* 41(7):889–916. doi: 10.1007/s00449-018-1922-3.

-
- [425] Garcia-Ochoa F, Gomez E. 2009. Bioreactor scale-up and oxygen transfer rate in microbial processes: An overview. *Biotechnology Advances* 27(2):153–176. doi: 10.1016/j.biotechadv.2008.10.006.
- [426] Ritcey GM. 1980. Crud in solvent extraction processing - A review of causes and treatment. *Hydrometallurgy* 5(2):97–107. doi: 10.1016/0304-386X(80)90031-6.
- [427] Kopf M-H. *In situ* Extraktionen in Bioprozessen. Call. von Campenhausen, Maximilian, Demling, Philipp. 06.08.2020.
- [428] Loeschcke A, Thies S. 2015. *Pseudomonas putida* - A versatile host for the production of natural products. *Applied Microbiology and Biotechnology* 99(15):6197–6214. doi: 10.1007/s00253-015-6745-4.
- [429] Schwanemann T, Otto M, Wierckx N, Wynands B. 2020. *Pseudomonas* as versatile aromatics cell factory. *Biotechnology Journal* 15(11):1900569. doi: 10.1002/biot.201900569.
- [430] Salvachúa D, Werner AZ, Pardo I, Michalska M, Black BA, Donohoe BS, Haugen SJ, Katahira R, *et al.* 2020. Outer membrane vesicles catabolize lignin-derived aromatic compounds in *Pseudomonas putida* KT2440. *Proceedings of the National Academy of Sciences* 117(17):9302. doi: 10.1073/pnas.1921073117.
- [431] Sagan C. 1997. Pale blue dot: A vision of the human future in space: Random House Digital, Inc.

Curriculum Vitae

Personal Data

Name	Philipp Demling
Born	August 12 th , 1992 in Münster, Germany
Nationality	German
Mobile	+491758420826
Email	philipp.demling@rwth-aachen.de

Education

2017 - 2021	Doctoral studies at the Institute of Applied Microbiology, RWTH Aachen University, Aachen, Germany
2018	Summer School: Biosystems Engineering Course, Braunwald, Switzerland
2014 - 2016	Master of Science in Molecular and Applied Biotechnology at RWTH Aachen University, Aachen, Germany Focus: Chemical Engineering and Industrial Biotechnology Overall grade: 1.1 (excellent)
2016	Master thesis “Strain engineering and growth optimization for improved biofuel production” at the Joint BioEnergy Institute, Lawrence Berkeley National Laboratory / University of California, Berkeley; Emeryville, CA, USA
2011 - 2014	Bachelor of Science in Molecular and Applied Biotechnology at RWTH Aachen University, Aachen, Germany Overall grade: 1.2 (very good) Bachelor thesis “Influence of different carbon sources on the virulence of <i>Pseudomonas aeruginosa</i> ” at the Institute of Applied Microbiology, RWTH Aachen University, Aachen, Germany
2002 - 2011	Ratsgymnasium Münster, Münster, Germany for the acquisition of the Abitur (higher education entrance qualification)
2008/2009	Salisbury Christian School, Salisbury, MD, USA as part of a student exchange program

Work experience

since 2017	Scientific employee and doctoral candidate at the Institute of Applied Microbiology, RWTH Aachen University, Aachen, Germany
2017	Research Assistant at Bayer Pharmaceuticals, Division of Upstream Development, Wuppertal, Germany
2017	Research Assistant at the Institute of Bio- and Geosciences (IBG-1), Forschungszentrum Jülich, Jülich, Germany
2015/2016	Student Research Assistant at the Institute of Applied Microbiology, RWTH Aachen University, Aachen Germany

Awards and Grants

2021	Fermentation Travel Award 2021, MDPI
2019	DAAD scholarship (Kongressreisenprogramm) for presenting at the Recent Advances in Fermentation Technology (RAFT) 13 in Bonita Springs, FL, USA
2017	Springorium Commemorative Coin, RWTH Aachen University
2017	DAAD travel grant to participate in the ACalNet Workshop 2017 in Santa Barbara, CA, USA
2016	DAAD scholarship <i>via</i> the ACalNet for research at the Joint BioEnergy Institute, Berkeley, CA, USA
2015 - 2017	Dean's List Award for excellent academic performances during the Master of Science studies in Molecular and Applied Biotechnology
2015 - 2016	Deutschlandstipendium <i>via</i> proRWTH and Bayer AG

Publications

Journal articles

Demling P, Ankenbauer A, Klein B, Noack S, Tiso T, Takors R, Blank LM. *Pseudomonas putida* KT2440 endures temporary oxygen limitations. *Biotechnology & Bioengineering* 2021, 1-16. DOI: 10.1002/bit.27938.

Demling P[§], von Campenhausen M[§], Grütering C, Tiso T, Jupke A, Blank LM. Selection of a recyclable *in situ* liquid-liquid extraction solvent for foam-free synthesis of rhamnolipids in a two-phase fermentation. *Green Chemistry* 2020, 22:8495-8510. DOI: 10.1039/D0GC02885A.

Rockenbach A, Sudarsan S, Behrens J, Kosubek M, Lazar J, Demling P, Hanke R, Mennicken P, Ebert BE, Blank LM, Schnakenberg U. Microfluidic irreversible electroporation - A versatile tool to extract intracellular contents in cultures of bacteria and yeast. *Metabolites* 2019, 9(10):211. DOI: 10.3390/metabo9100211.

Demling P[§], Westerwalbesloh C[§], Noack S, Wiechert W, Kohlheyer D. Quantitative measurements in single-cell analysis: Towards scalability in microbial bioprocess development. *Current Opinion in Biotechnology* 2018, 54:121-127. DOI: 10.1016/j.copbio.2018.01.024.

Eng T, Demling P, Herbert RA, Chen Y, Benitez V, Blank LM, Martin J, Lipzen A, Baidoo EEK, Petzold CJ, Mukhopadhyay A. Restoration of biofuel production levels and increased tolerance under ionic liquid stress is enabled by a mutation in the essential *Escherichia coli* gene *cydC*. *Microbial Cell Factories* 2018, 17:159. DOI: 10.1186/s12934-018-1006-8.

Demling P, Kleinert G, Zimmermann A, Tiso T, Blank LM. Adaptive laboratory evolution reveals point mutations in a two-component system for enabling tolerance of *P. putida* KT2440 to 1-octanol. *In preparation*.

von Campenhausen M[§], Demling P[§], Dietz S, Scheele A, Bongartz P, Tiso T, Wessling M, Blank LM, Jupke A. Design and operation of a novel multiphase loop reactor. *In preparation*.

Sudarsan S[§], Demling P[§], Oezdemir E, Mennicken P, Buescher JM, Meurer G, Ebert BE, Blank LM. NADPH recycling is enabled *via* acetol biosynthesis under nitrogen limitation in engineered *Escherichia coli*. *In preparation*.

Book Chapters

Hanke R[§], Bailly N[§], Demling P[§], Gohr FN[§], Opdensteine P[§], Osthege MJ[§], Joppich M, Sudarsan S, Schwaneberg U, Wiechert W, Blank LM. Development of a Modular Biosensor System for Rapid Pathogen Detection in Rinken T (Ed.), *Biosensing Technologies for the Detection of Pathogens*. InTechOpen 2018, 89-110. DOI: 10.5772/intechopen.72457.

Oral presentations

Demling P, von Campenhausen M, Tiso T, Jupke A, Blank LM. Bioprocess intensification in a novel multiphase loop reactor. 13th European Congress of Chemical Engineering & 6th European Congress of Applied Biotechnology (ECCE 13 & ECAB 6). online. September 20-23, 2021.

von Campenhausen M[§], Demling P[§], Tiso T, Blank LM, Jupke A. Bioprocess intensification in a novel multiphase loop reactor. DECHEMA Himmelfahrtstagung 2021. online. May 10-12, 2021.

Demling P[§], von Campenhausen M[§], Tiso T, Jupke A, Blank LM. Bioprocess intensification in a novel multiphase loop reactor. Recent Advances in Fermentation Technology (RAFT) 13. Bonita Springs, FL, USA. October 27-30, 2019

Poster presentations

Demling P, von Campenhausen M, Tiso T, Jupke A, Blank LM. Bioprocess intensification in a novel multiphase loop reactor. ProcessNet. online. September 21-24, 2020.

Grütering C, Demling P, von Campenhausen M, Tiso T, Jupke A, Blank LM. Bioprocess intensification of surfactant production by implementing liquid-liquid extraction for *in situ* product removal. BioProcessingDays 2020. Recklinghausen, Germany. February 17-19, 2020.

Demling P, von Campenhausen M, Ankenbauer A, Tiso T, Takors R, Jupke A, Blank LM. Bioprocess intensification for surfactant production with *Pseudomonas putida* KT2440 in an innovative multiphase loop reactor. Biosurfactants International Conference. Hohenheim, Germany. September 25-27, 2019.

Demling P, von Campenhausen M, Ankenbauer A, Grütering C, Tiso T, Takors R, Jupke A, Blank LM. Bioprocess design for surfactant production with *Pseudomonas putida* KT2440 in an innovative multiphase loop reactor. DECHEMA Himmelfahrtstagung 2019. Hamburg, Germany. May 27-29, 2019.

von Campenhausen M, Demling P, Tiso T, Jupke A, Blank LM. Novel multiphase loop reactor (MPLR) for in situ extraction of biotechnological products. DECHEMA Himmelfahrtstagung 2019. Hamburg, Germany. May 27-29, 2019.

Demling P, von Campenhausen M, Ankenbauer A, Tiso T, Takors R, Jupke A, Blank LM. Bioprocess design for surfactant production with *Pseudomonas putida* KT2440 in an innovative multiphase loop reactor. BioProcessingDays 2019. Recklinghausen, Germany. February 18-20, 2019.

Demling P, Eng T, Herbert RA, Chen Y, Benitez V, Blank LM, Martin J, Lipzen A, Baidoo EEK, Petzold CJ, Mukhopadhyay A. Adaptive laboratory evolution provides a route to improve biofuel production under ionic liquid stress. ACalNet & ACalIRES Workshop 2018: Chemistry at Interfaces: Academia, Industry & Student Exchange. Aachen, Germany. June 18-19, 2018.

Demling P, Eng T, Mukhopadhyay A. Strain engineering and growth optimization for improved biofuel production. ACalNet Workshop 2017 on Sustainable Chemical Manufacturing. Santa Barbara, CA, USA. March 22-23, 2017.

§ Authors contributed equally to this work or were co-presenters

- Additional co-authorship of several conference presentations (oral and poster).
- Co-authorship of three grant proposals.